MARTIN MARIETTA ENERGY SYSTEMS LIBRARIES
3 4456 0361383 7

CRL
CENTRAL RESEARCH LIBRARY
DOCUMENT COLLECTION

ORNL-2739
Physics and Mathematics

Cy. 4

PROCEEDINGS OF THE NEUTRON THERMALIZATION CONFERENCE, APRIL 28-30, 1958 GATLINBURG, TENNESSEE

CENTRAL RESEARCH LIBRARY
DOCUMENT COLLECTION
LIBRARY LOAN COPY
DO NOT TRANSFER TO ANOTHER PERSON
If you wish someone else to see this document, send in name with document and the library will arrange a loan.

OAK RIDGE NATIONAL LABORATORY
operated by
UNION CARBIDE CORPORATION
for the
U.S. ATOMIC ENERGY COMMISSION

Printed in USA. Price $4.00. Available from the

Office of Technical Services
Department of Commerce
Washington 25, D.C.

LEGAL NOTICE

This report was prepared as an account of Government sponsored work. Neither the United States, nor the Commission, nor any person acting on behalf of the Commission:

A. Makes any warranty or representation, expressed or implied, with respect to the accuracy, completeness, or usefulness of the information contained in this report, or that the use of any information, apparatus, method, or process disclosed in this report may not infringe privately owned rights; or

B. Assumes any liabilities with respect to the use of, or for damages resulting from the use of any information, apparatus, method, or process disclosed in this report.

As used in the above, "person acting on behalf of the Commission" includes any employee or contractor of the Commission, or employee of such contractor, to the extent that such employee or contractor of the Commission, or employee of such contractor prepares, disseminates, or provides access to, any information pursuant to his employment or contract with the Commission, or his employment with such contractor.

UNCLASSIFIED

ORNL-2739

Copy 4

Contract No. W-7405-eng-26

PROCEEDINGS OF THE NEUTRON THERMALIZATION CONFERENCE,

April 28-30, 1958
Gatlinburg, Tennessee

Sponsored by
Advisory Committee on Reactor Physics
and
Oak Ridge National Laboratory

Date Issued

SEP 2 1959

Oak Ridge National Laboratory
Oak Ridge, Tennessee
operated by
UNION CARBIDE CORPORATION
for the
U.S. ATOMIC ENERGY COMMISSION

MARTIN MARIETTA ENERGY SYSTEMS LIBRARIES

3 4456 0361383 7

TABLE OF CONTENTS

	Paper No.
Session I. THE EPITHERMAL RANGE	
Calculation of Wigner-Wilkins Spectra with M = 18 Kernel and M = 1 Source - T. J. Kreiger, P. F. Zweifel, and D. M. Keaveney	I-A
Thermal Neutron Spectrum in Harmonically Bound Hydrogen Moderators - E. R. Cohen, E. U. Vaughan	I-B
Neutron Moderation by Chemically Bound Hydrogen - E. U. Vaughan and E. R. Cohen	I-C
Session II: THE THERMAL RANGE	
Neutron Scattering Properties of Liquid Moderators - B. N. Brockhouse	II-A
Chemical Binding Effects in Hydrogen Moderated Reactors - M. S. Nelkin	II-B
Thermalization of Neutrons at Very Low Temperatures - C. N. Kelber	II-C
Neutron Thermalization in Infinite Homogeneous Systems - N. Corngold	II-D
A Remark on Neutron Thermalization Theory - G. Liebfried	II-E
Thermal Neutron Flux in a Nonabsorbing Heavy Gas Medium with a Temperature Discontinuity - D. A. Kottwitz	II-F
Session III: CRYSTALLINE EFFECTS	
Inelastic Scattering of Slow Neutrons in Moderators - D. J. Hughes, A. M. Ghose, H. Palevsky, and P. Kienle	III-A
Neutron Thermal Inelastic Scattering by Bound Atoms - A. W. McReynolds	III-B
A Study Using Time-of-Flight Techniques of the Thermal Inelastic Scattering of Neutrons - W. L. Whittemore	III-C

Paper No.

Session IV: LOW ENERGY SPECTRA IN HETEROGENEOUS MEDIA

Neutron Thermalization Calculations for a Heterogeneous Lattice Consisting of Rods of Uranium and Plutonium Fuel in Water - P. Greebler	IV-A
The Influence of Non-1/v Absorbers on Reactor Parameters - T. J. Kreiger, M. L. Storm, P. F. Zweifel, and D. M. Keaveney	IV-B
Measurement of Neutron Spectra in Reactors - M. J. Poole	IV-C
Low Energy Spectra Measurements - R. E. Slovacek R. S. Stone	IV-D
Measurement of Low Energy Neutron Spectra Using a Pulsed Neutron Source - J. R. Beyster	IV-E

Session I: THE EPITHERMAL RANGE

Paper I-A

CALCULATION OF WIGNER-WILKINS SPECTRA WITH M = 18 KERNEL AND M = 1 SOURCE

T. J. Kreiger P. F. Zweifel
D. M. Keaveney
Knolls Atomic Power Laboratory

Calculation of Wigner-Wilkins Spectra With M = 18 Kernel and M = 1 Source

T. J. Krieger* P. F. Zweifel
D. M. Keaveney
Knolls Atomic Power Laboratory
Schenectady, New York

Abstract

In an attempt to explain the excellent agreement of measured thermal spectra in water with calculations based on a free monatomic moderator of mass M = 1, a conjecture has been advanced that the calculated spectrum is insensitive to the value of the moderator mass used in the energy change kernel $\Sigma(E_1 \rightarrow E_f)$ of the Wigner-Wilkins integral equation. The truth of this conjecture has been investigated by assigning to the protons a mass equal to 18 neutron masses in evaluating the energy change kernel and also in establishing a distribution of initial proton velocities. The source term in the Wigner-Wilkins equation, which represents the neutrons fed into the thermal group from the epithermal region, is, however, calculated with the true proton mass, since the chemical binding is negligible for epithermal neutrons. The integral equation has been solved on an IBM-650 computer and the resulting spectra compared with the usual M = 1 spectra. The comparisons indicate that the spectrum is indeed sensitive to the value of the moderator mass used in the energy change kernel. The effect of thermal-cutoff choice and Doppler effect is also shown.

---

*Speaker.

CALCULATION OF WIGNER-WILKINS SPECTRA WITH M = 18 KERNEL AND M = 1 SOURCE

T. J. Krieger
P. F. Zweifel
D. M. Keaveney

The very good agreement between measured thermal neutron spectra in water and theoretical spectra calculated neglecting chemical binding effects has led to a good deal of speculation concerning the origin of the apparent lack of sensitivity of the spectrum on the form of the energy change kernel $\sigma(E \rightarrow E')$, at least when the absorbers are of the 1/v type. Experiments in which both energy and angular distributions of monoenergetic slow neutrons scattered by water are measured seem to indicate that the scattering law is simply that corresponding to a mass 18 proton. This result is plausible, since owing to the large electric dipole moment of the H_2O molecule, the rotations in the liquid state are probably strongly inhibited, so that the molecule recoils without rotation when struck by a slow neutron. In view of these considerations, a conjecture has been advanced that the calculated spectrum is insensitive to the details of the scattering kernel $\sigma(E \rightarrow E')$ (provided, of course, that detailed balance and neutron conservation are obeyed), and in particular, that spectra calculated with M = 18 and with M = 1 kernels should not differ appreciably. Now, it is already known from work on the heavy mass approximation ($M \rightarrow \infty$) that the spectral hardening factor is given by the ratio $\Sigma_a(kT)/\xi\,\Sigma_s$, implying that an increase in the mass from M = 1 to M = 18 yields a spectrum which is hardened roughly in the ratio $\xi\Sigma_s(M=1)$: $\xi\Sigma_s(M=18) \approx 2.5$. Thus, a straight forward M = 18 calculation could not possibly give results similar to those for an M = 1 scatterer with the same absorption and scattering properties. However, if, instead, we assume that an M = 1 scattering

law is operative at neutron energies above some thermal cut-off energy $E_c \gg kT$, while for neutron energies less than E_c an M = 18 law applies, there is some hope that the calculated spectrum will not differ from a straight M = 1 solution. The essential difference is that with M = 1 epithermal moderation, many more neutrons are fed into the thermal group at lower energies than with M = 18 moderation. The resulting spectrum is, therefore, expected to be softer than that due to a straight M = 18 moderation and thermalization. Of course, when differing proton masses are assumed for thermal and epithermal neutron energies, the spectra calculated are bound to be somewhat dependent on the cut-off energy E_c chosen.

Another feature of the "two mass value" method is concerned with the Doppler effect, i.e., the influence of the target thermal motion on the scattering. Although the Doppler effect is automatically included in the scattering kernel $\sigma(E \rightarrow E')$, since the latter contains the temperature, it must also be taken into account in a correct formulation of S(E), the energy distribution of neutrons feeding into the thermal group from epithermal energies. Thus in the case of monatomic hydrogen moderation, if the protons were assumed to be initially at rest, the distribution of neutrons fed into the thermal group would be uniform down to zero energy. However, owing to thermal motion, S(E) is proportional to erf $\sqrt{\frac{E}{kT}}$, i.e., it is constant down to $\sim kT$ and then drops to zero. In the present problem, it is assumed that the Doppler effect is characterized by M = 18 rather than M = 1 (See Fig. 1) so that S(E) is constant down to a somewhat lower energy than for a M = 1 Doppler before dropping to zero. In any event, the variation in the value of M entering the initial distribution of proton velocities is a minor effect.(See Fig.2

To test the conjecture that the calculated spectrum is insensitive to the details of the thermal scattering law, the Wigner-Wilkins integral equation for

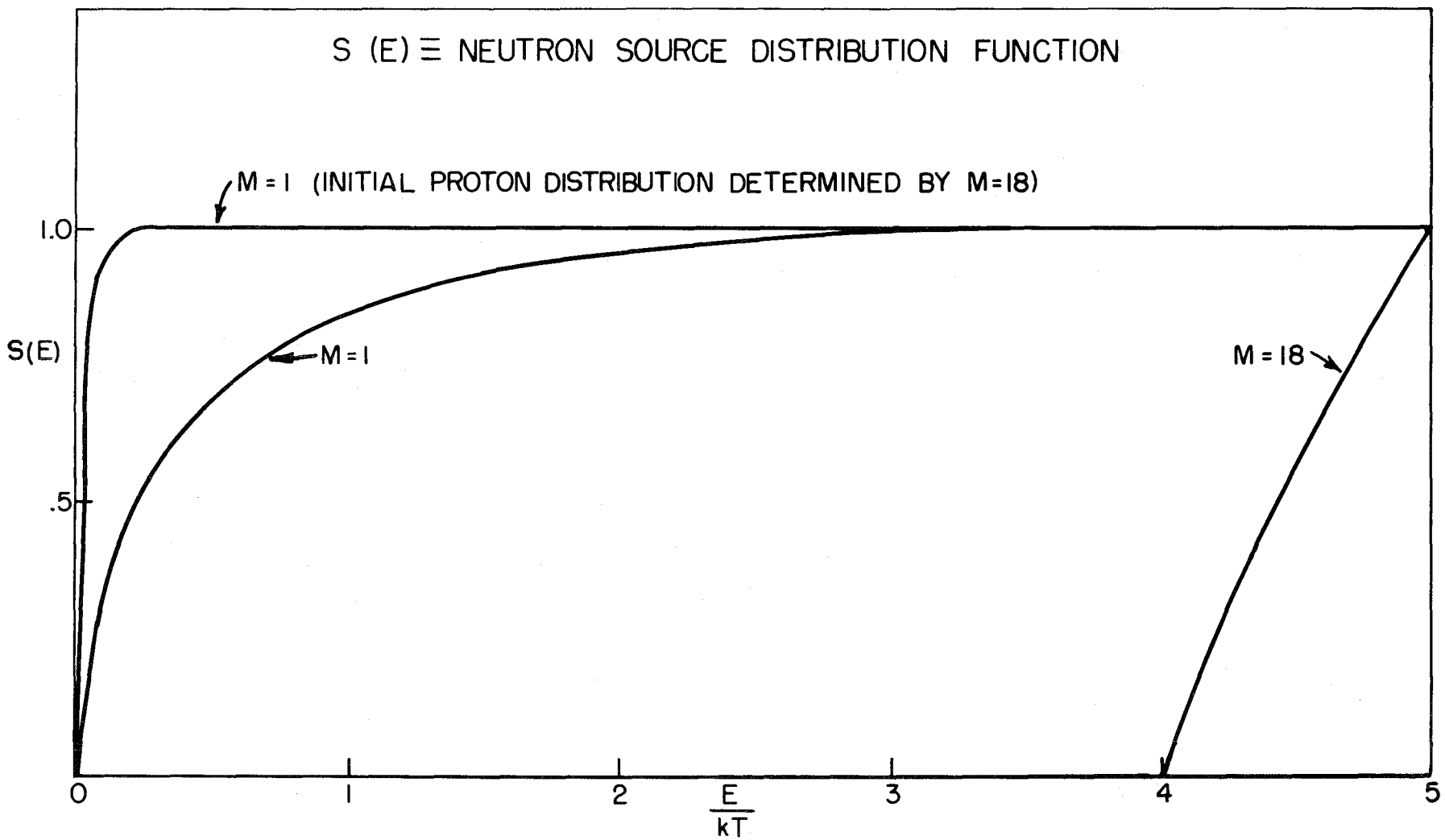
S (E) ≡ NEUTRON SOURCE DISTRIBUTION FUNCTION
M = 1 (INITIAL PROTON DISTRIBUTION DETERMINED BY M=18)
1.0
S(E)
.5
M = 1
M = 18
0
1
2
3
4
5
E/kT

Fig. 1

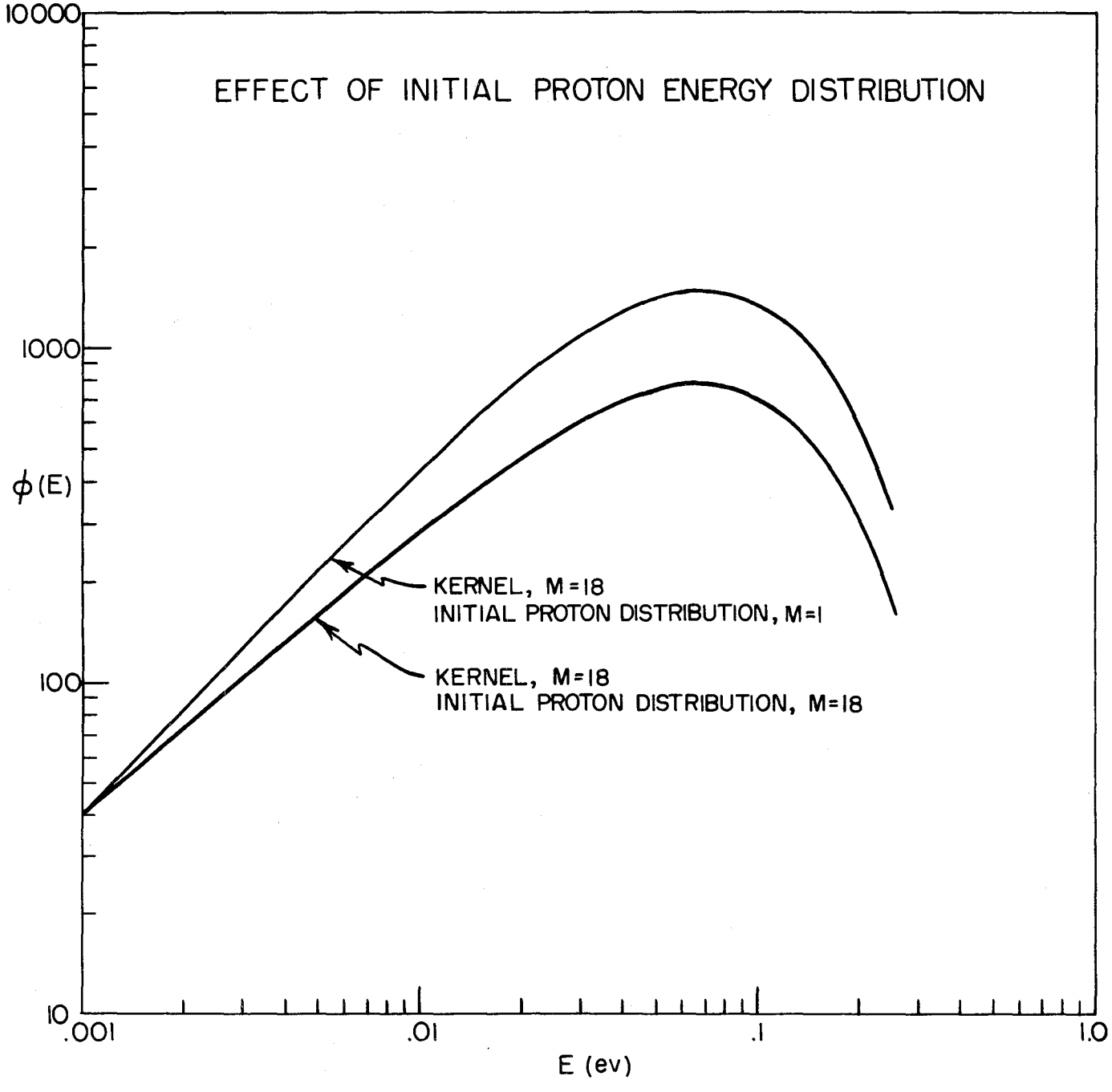
EFFECT OF INITIAL PROTON ENERGY DISTRIBUTION
10000
1000
100
10
ϕ(E)
KERNEL, M=18
INITIAL PROTON DISTRIBUTION, M=1
KERNEL, M=18
INITIAL PROTON DISTRIBUTION, M=18
.001
.01
.1
1.0
E (ev)

Fig. 2

the thermal flux has been solved on an IBM-650 digital computer. The source function S(E) was taken to correspond to M = 1 with an M = 18 initial proton velocity distribution, while the Wigner-Wilkins kernel $\sigma(E' \rightarrow E)$ was calculated with M = 18; the spectral hardening was $\beta\gamma$ = .226. The resulting flux is shown in Fig. 3, in which for comparison, strict M = 1 and M = 18 solutions are also shown. We observe that the (M = 1, M = 18) solution is significantly different from the strict M = 1 solution, which demonstrates the falsity of the conjecture.*

In Fig. 4, the effect of thermal cut-off energy on the (M = 1, M = 18) solution is shown. The two curves correspond to 10 kT and 1 ev cut-offs, respectively.

*** Note added following conference: A preliminary calculation with a $\sim$4 kt cut-off in which the upscattering is included rigorously as an effective absorption, has shown that the M=1 and M=18 solutions are much more similar than the earlier calculations with higher cut-offs indicate.**

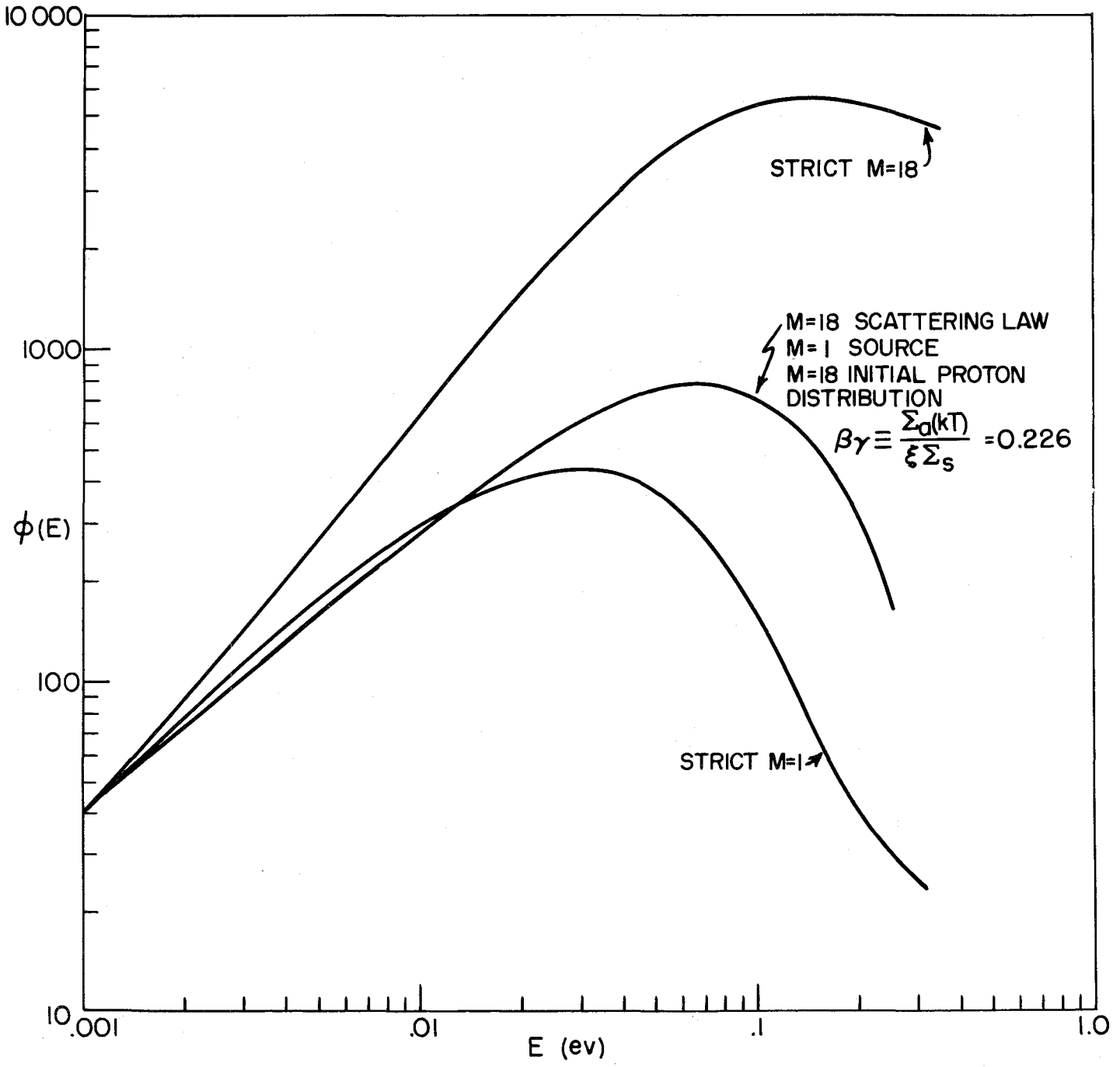
10 000
1000
100
10
ϕ(E)
.001
.01
.1
1.0
E (ev)
STRICT M=18
M=18 SCATTERING LAW
M=1 SOURCE
M=18 INITIAL PROTON DISTRIBUTION
$\beta\gamma \equiv \frac{\Sigma_a(kT)}{\xi \Sigma_s} = 0.226$
STRICT M=1

Fig. 3

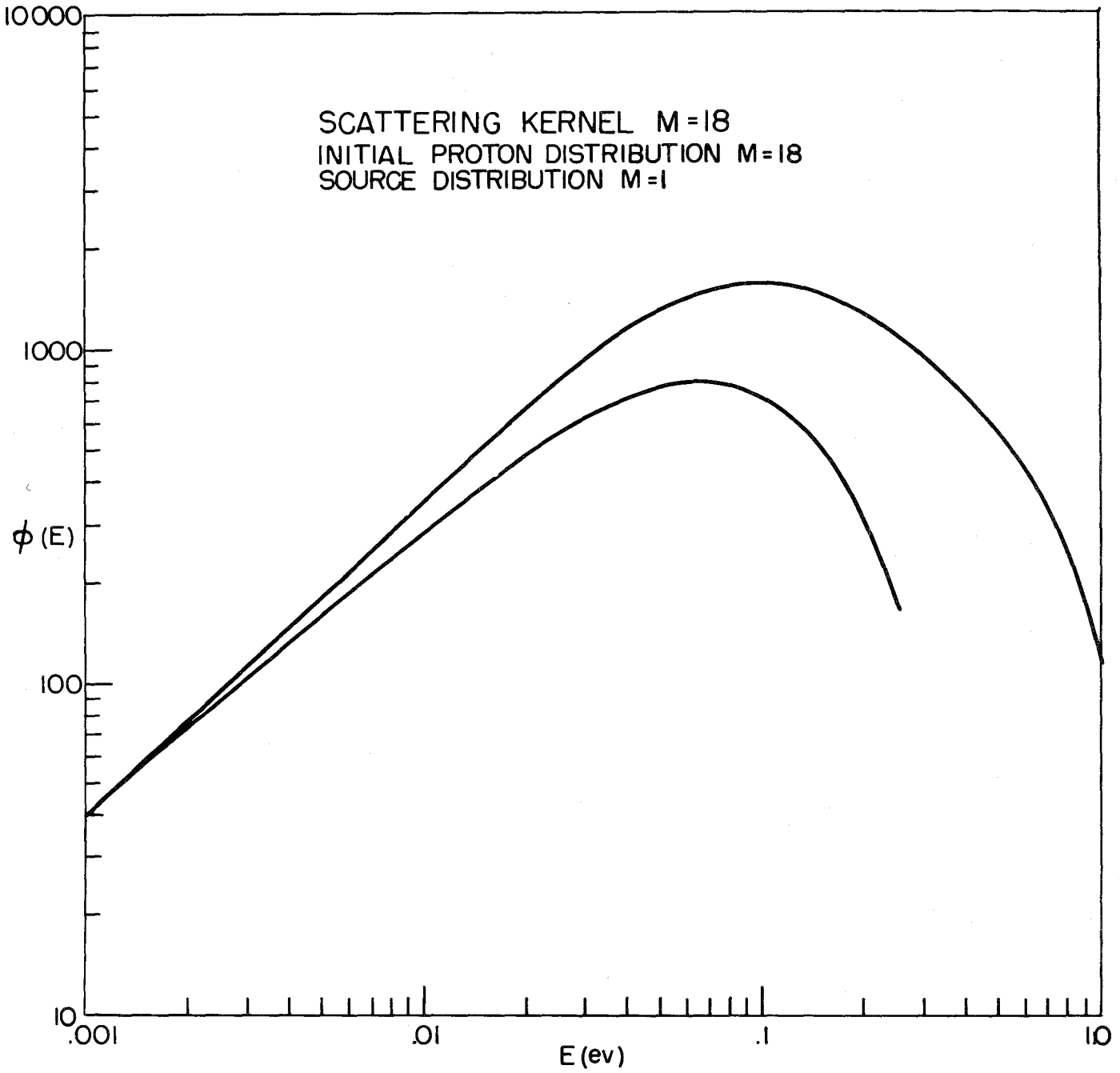
SCATTERING KERNEL M=18
INITIAL PROTON DISTRIBUTION M=18
SOURCE DISTRIBUTION M=1
10000
1000
100
10
φ (E)
.001
.01
.1
1.0
E (ev)

Fig. 4

Paper I-B

THERMAL NEUTRON SPECTRUM IN HARMONICALLY BOUND HYDROGEN MODERATORS

E. R. Cohen E. U. Vaughan
Atomics International

Thermal Neutron Spectrum in Harmonically Bount Hydrogen Moderators

E. Richard Cohen and Edward U. Vaughan
Atomics International
Canoga Park, California

Abstract

The description of hydrogen moderation by chemically bound hydrogen as described by Bethe[1] has been extended to include the Boltzmann distribution of initial hydrogen oscillator states. Because of the discrete energy transfers allowed in the system, the Boltzmann equation for the neutrons can be reduced to independent sets of difference equations. The adjoint equation, which gives the neutron importance is also formulated and is used to provide a simple and easily understood formula for the reactivity change with temperature (population of oscillator initial states). The neutron importance is equal to the number of neutrons produced per absorption averaged over the energy at which the neutron is ultimately absorbed. The change in reactivity produced by a change in the population distribution of the hydrogen arises from the differing importance of neutrons with energy. Thus if the neutron production per neutron absorbed (ηf) is independent of energy, or if there is absorption only in the interval of $0 < E < h\nu$ ($h\nu =$ oscillator level), there is no change in reactivity with temperature even though the neutron spectrum changes radically. The neutron spectrum and the reactivity have been calculated for several cases of interest.

---

1. H. A. Bethe, Rev. Mod. Phys., April 1937, p. 122.

by **E. Richard Cohen and Edward U. Vaughan**

Thermal Neutron Spectrum in Harmonically Bound Hydrogen Moderators

Introduction

Within the last few years there has been an increasing awareness of the importance of chemical binding of the moderator atoms in the determination of the thermal neutron spectrum in a reactor. The free atom (monatomic gas) moderator has been extensively calculated, and several partial attacks have been made on the problem of the chemically bound moderator. A case which represents perhaps the opposite extreme to the monatomic gaseous hydrogen moderator is the harmonically bound hydrogen oscillator. This model represents the moderation of neutrons in a crystalline hydride moderator in which the motion of the hydrogen is severly restricted by the chemical bonds which tie it to an essentially infinite crystal matrix. With an appropriate choice of oscillator frequencies, this model may perhaps also yield approximate representations of the effects of chemical binding in other systems where the vibrational states are predominant (water or hydrocarbons at sufficiently low temperatures).

We shall therefore consider the following system:

Hydrogen is bound in an isotropic harmonic oscillator potential well. The possible energy levels are uniformly spaced with separation $h\nu$. No energy transfers will be considered other than those associated with hydrogen-neutron collisions (collisions with any other elements are either purely elastic or lead to absorption). The neutron can therefore only gain or lose energy in discrete multiples of the quantum $h\nu$. The neutron flux is assumed to be low enough that the population of hydrogen in the various quantum states shall be adequately given by the Boltzman factor just as if there were no neutrons present (the Boltzmann equation for the neutron spectrum is linear.)

Formulation

We can quite generally write down as our starting point, the time independent Boltzmann equation.

$$\vec{\Omega}\cdot\vec{\nabla}\psi(\vec{r},\vec{\Omega},x) + \sigma(x)\psi(\vec{r},\vec{\Omega},x)$$
$$= \iint \sigma(x',x;\mu_o)\psi(\vec{r},\vec{\Omega}',x')d\Omega' dx' + S(\vec{r},x) \qquad (1)$$

The medium is assumed to be homogeneous so that the cross sections are independent of position. The function ψ represents the detailed neutron flux density in angle and energy. The neutron energy is measured in units of $h\nu$, $(E=xh\nu)$. The scattering cross section $\sigma(x',x;\mu_o)$ represents the probability of a neutron at energy x' scattering through angle $\arccos\mu_o$ to energy x. This will be specialized below to exhibit explicitly the restriction that x'-x must be an integer (positive or negative).

In order to reduce this equation to more tractable form we shall consider only a single fourier component of Eq (1) and assume furthermore that ψ can be adequately described in terms of only the first two spherical harmonics, and we shall be ultimately interested only in the total flux or total collision density. Eq (1) can therefore be rewritten:

$$i\kappa\mu\psi + \sigma(x)\psi(x,\mu) = \iint \sigma(x',x;\mu_o)\psi(x',\mu')dx'd\Omega' + S(x)$$
$$\psi(x,\mu) = \phi_o(x) + 3\mu\phi_1(x) \qquad (1.1)$$

This gives two coupled equations

$$i\kappa\phi_1 + \sigma(x)\phi_o(x) = \int\phi_o(x')\int\sigma(x',x;\mu_o)d\mu_o dx' + S(x) \qquad (2.1)$$

$$i\kappa\phi_o + 3\sigma(x)\phi_1(x) = 3\int\phi_1(x')\int\mu_o\sigma(x',x;\mu_o)d\mu_o dx' \qquad (2.2)$$

We now introduce the collision density $K(x) = \sigma(x)\phi_o(x)$ since this function

is more smoothly varying than $\phi_o(x)$ itself, and an auxiliary function J(x) related to the current

$$\frac{i\kappa}{3} J(x) = \sigma(x)\phi_1(x)$$

With these substitutions Eq (2) takes the form

$$K(x) = \int K(x')A(x',x)dx' + S(x) + \frac{\kappa^2 J(x)}{3\sigma(x)} \tag{3.1}$$

$$J(x) = \int J(x')B(x',x)dx' - \frac{K(x)}{\sigma(x)} \tag{3.2}$$

where $$A(x',x) = \int \frac{\sigma(x',x;\mu_o)}{\sigma(x')} d\mu_o \tag{3.3}$$

$$B(x',x) = \int \mu_o \frac{\sigma(x',x;\mu_o)}{\sigma(x')} d\mu_o \tag{3.4}$$

Eqs (3.1) and (3.2) can be solved as soon as the kernels A and B are known. We must now look in more detail at the scattering of neutrons by harmonically bound hydrogen.

Determination of Cross Sections

The first thing that we see with respect to the kernels A and B is that they are not continuous, but are actually sums of delta-functions since the energy of the hydrogen (and hence of the neutron) may change only by integral amounts. Hence we can write

$$\int K(x')A(x',x)dx' = \sum_s K(x+s)A_s(x+s) \tag{4.1}$$

$$\int J(x')B(x',x)dx' = \sum_s J(x+s)B_s(x+s) \tag{4.2}$$

where s ranges over integral values ($s > -x$). In order to evaluate these elements A_s and B_s we must look at the quantum mechanics of the scattering

process. This was first developed by Fermi[1] in connection with the moderation of neutrons by paraffin, and has been summarized by Bethe.[2]

The hydrogen atom may be in any oscillator level before the collision. Hence, we must calculate the transition cross section $\sigma_{m \to n}(x)$ for the hydrogen making a transition from state m to state n in a collision with a neutron of energy x. (In this collision, the hydrogen gains energy n-m, and the neutron loses energy n-m). For a three dimensional oscillator at temperature T the probability that the hydrogen will be in state m is given by $\frac{1}{2}(m+1)(m+2)\epsilon^{m}$ where ϵ is the Boltzmann factor $\epsilon = \exp(-h\nu/kT)$. Hence the cross section per hydrogen atom for energy loss s at initial neutron energy x is given by

$$\sigma_s(x) = \frac{1}{(1-\epsilon)^3} \sum_m \frac{(m+1)(m+2)\epsilon^{m}}{2} \sigma_{m \to m+s}(x) \qquad (5)$$

The total cross section of the reactor is given by

$$\sigma(x) = \sum_s \sigma_s(x) + \sigma_{el}(x) + \sigma_{abs}(x) \qquad (6)$$

where $\sigma_{abs}(x)$ is the total absorption cross section (per hydrogen atom) and σ_{el} is the elastic scattering cross section for all of the non-hydrogen atoms (per hydrogen atom).

The scattering cross section per unit solid angle for the hydrogen oscillator is given (according to Bethe) in the Born approximation as

$$\sigma_{m \to n}(x)dw = \frac{v_f}{v} \frac{\sigma_o}{\pi} \left| \int \exp\left[i(k-k_f).x\right] \psi_i(x) \psi_f^*(x)dx \right|^2 d\omega \qquad (7)$$

v,k are the initial speed and momentum of the neutron and v_f, k_f, are the final values: σ_o is the free atom scattering cross section.

The initial and final hydrogen states are given by the usual harmonic oscillator wave functions:

$$\psi_i = \frac{1}{\sqrt{m!\ \sqrt{2}}} \qquad H_m(\xi)\exp(-\tfrac{1}{4}\xi^2)$$

$$\psi_f = \frac{1}{\sqrt{n!\ \sqrt{2}}} \qquad H_n(\xi)\exp(-\tfrac{1}{4}\xi^2)$$

$$\xi = (2\nu/h)^{\frac{1}{2}} x$$

$H_m(\xi)$ is the Hermite polynomial. The oscillator can be described in terms of three imdependent oscillators at right angles. For each of these three independent directions the oscillator can make a transition from state m_i to state n_i with a corresponding change in the neutron momentum component q_i. The momentum transfer is not uniquely defined by the energy transfer because the crystal (to which the hydrogen is bound) can absorb arbitrary momentum. The unit of momentum is $(2\pi\nu)^{-\frac{1}{2}}$.

The matrix element is

$$A_{n_i}^{(m_i)}(q_i) = \sqrt{m_i!n_i!}\ e^{-\frac{1}{2}q_i^2} \sum \frac{(iq_i)^{m_i+n_i-2p}}{p!(m_i-p)!(n_i-p)!} \tag{8}$$

We must now average over all the initial states such that $m=m_1+m_2+m_3$ and sum over all final states such that $n=n_1+n_2+n_3$. With these restrictions c the sums we have

$$\sigma_{m\to n}(x)d\omega = \frac{2}{(m+1)(m+2)} \cdot \frac{\sigma_0}{\pi}\frac{v_f}{v}\sum_{n_i m_i} \left| A_{n_1}^{(m_1)}(q_1)A_{n_2}^{(m_2)}(q_2)A_{n_3}^{(m_3)}(q_3)\right|^2 dq_1dq_2dq_3 \quad ($$

The summation over initial and final states can be simplified if the coordinate system is properly oriented. If the z-axis is taken to be the direction of momentum transfer in the collision. q_1 and q_2 are zero. All of the matrix elements are then zero except for $n_1=m_1$ and $n_2= m_2$. We see a point which is perhaps physically obvious.

The independent oscillators cannot make an energy transition unless there is a momentum transfer also. This is of course not a trivial statement since the momentum transfer is not uniquely correlated with energy transitions because of the recoil momentum which can be given to the crystal as a whole. We can then reduce Eq (9) to the much simpler summation

$$\sigma_{m\to n}(x')d\omega = \frac{2\sigma_o}{(m+1)(m+2)\pi}\sqrt{\frac{x}{x'}}\sum_{r=0}^{m}(r+1)\left|A^{(m-r)}_{n-r}(u)\right|^2 \cdot d\omega \qquad (10)$$

where $u=q^2$ is the square of the momentum transfer. Eq (10) gives the differential scattering cross section per unit solid angle $d\omega$ from an initial energy x' to a final energy x. The relationship between initial and final energies, momentum transfer and angle of scattering is

$$u = x+x'-2\sqrt{xx'}\,\mu_o \qquad (11)$$

$$\mu_o = \frac{x+x'-u}{2\sqrt{xx'}} \qquad (11.1)$$

$$d\omega = 2\pi d\mu_o = \frac{-\pi du}{\sqrt{xx'}} \qquad (11.2)$$

The integrated cross section for energy transfer from state m to state n is

$$\sigma_{m\to n}(x') = \frac{2\sigma_o}{(m+1)(m+2)x'}\int\sum_r (r+1)\left|A^{(m-r)}_{n-r}(u)\right|^2 du \qquad (12)$$

the limits on the integral are determined from the limits $\mu_o = \pm 1$ in Eq (11.1)

$$u_{\pm} = 2x'-s\pm 2\sqrt{x'(x'-s)} \qquad s=n-m,\ x=x'-s$$

The integrals involved are all elementary but tedious, they are given in more detail in an Appendix. Results are presented in Figures 1, 2, and 3. If the Boltzmann factor, ϵ, is specified, one is now in a position to calculate the transition coefficients $\Lambda_s(x)$

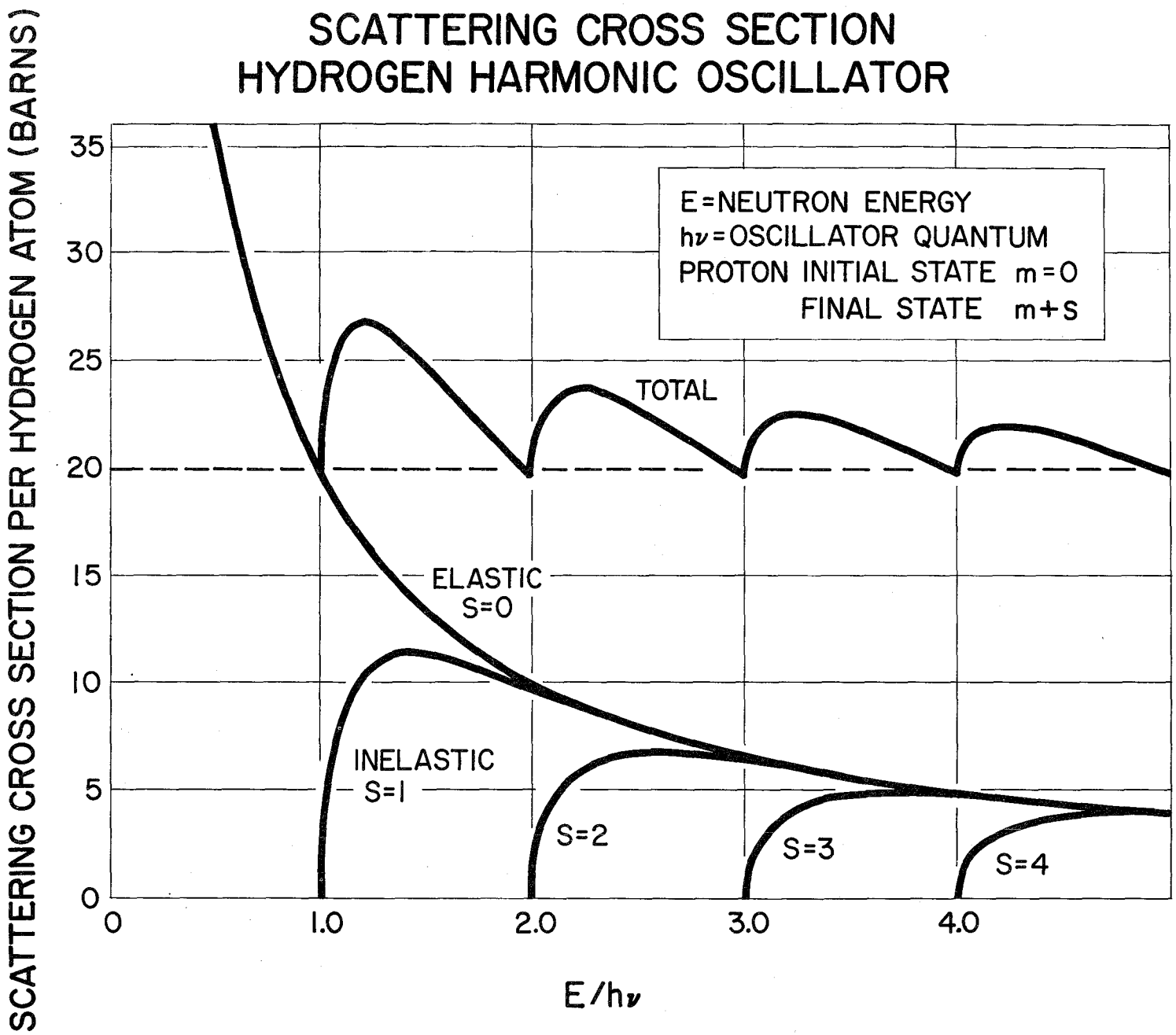

Fig. 1. Scattering by Protons Initially in the Ground State

4 / 22 / 58

00-13157

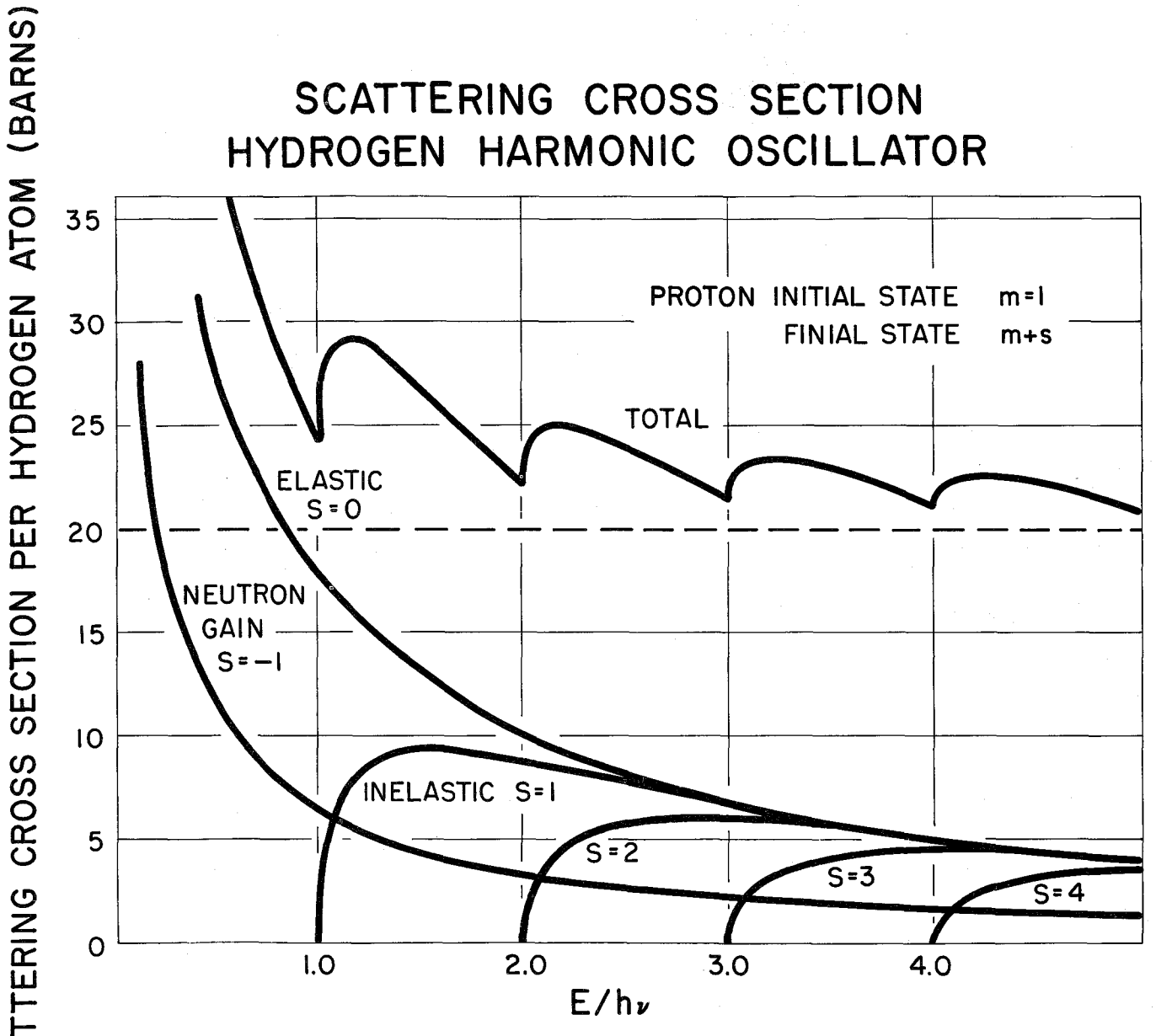

Fig. 2. Scattering by Protons Initially in the First Excited State

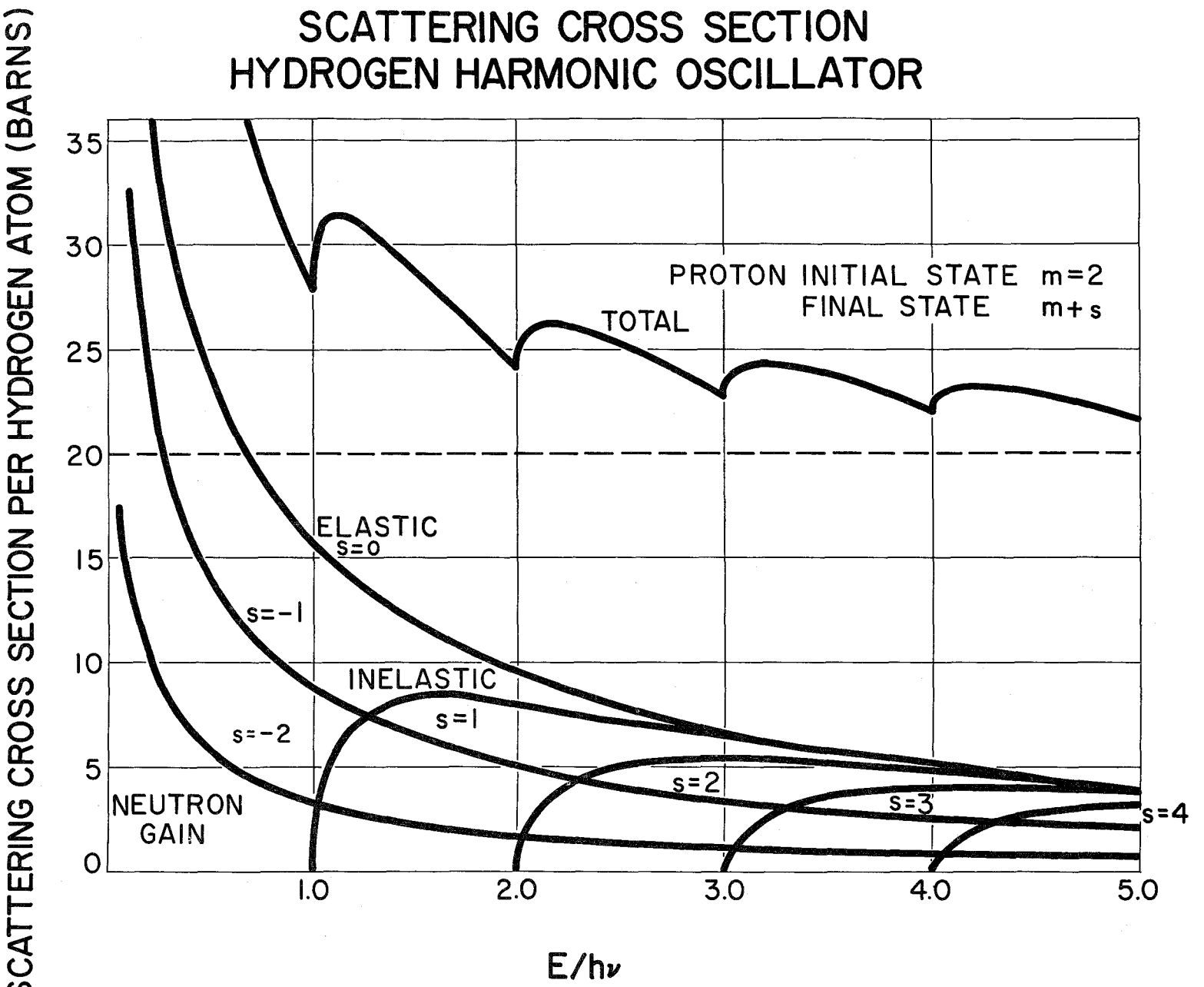

Fig. 3. Scattering by Protons Initially in the Second Excited State

4 / 22 / 58

00-13159

and $B_s(x)$ of Eq (4).

Solution of the Boltzmann Equation

The Boltzmann equation, Eq (1) has been reduced to the approximation

$$K(x) = \sum_s A_s(x+s)K(x+s)+S(x) + \frac{\kappa^2 J(x)}{3\sigma(x)} \tag{13}$$

$$J(x) = \sum_s B_s(x+s)J(x+s) - \frac{K(x)}{\sigma(x)}$$

and we have outlined the evaluation of $\sigma(x)$, $A_s(x)$ and $B_s(x)$ in the previous section. We must now establish a method for solving Eq (13) for the collision density $K(x)$. We see first of all that the solution breaks up into an infinite set of independent systems. If we write $x=k+\xi$ where k is an integer and ξ is a fraction $0 \leq \xi < 1$, we see that equations for different values of ξ are completely independent of each other.

We specialize our problem by considering our solution to apply for neutron energies less than X. For $x > X$ we assume a known flux which scatters neutrons down into the region $o < x < X$ at a known rate, $S(x)$. We have implicitly assumed that this source is isotropic and if we postulate the slowing down to come exclusively from hydrogen collisions, $S(x)$ will be a constant.

Equation (13) can be written as a set of simultaneous equations

$$K(k+\xi) = \sum_{j=o}^{x-1} A_{j-k}(j+\xi)K(j+\xi) + S + \frac{\kappa^2 J(k+\xi)}{3\sigma(k+\xi)}$$

$$J(k+\xi) = \sum_{j=o}^{x-1} B_{j-k}(j+\xi)\, J(j+\xi) - \frac{K(k+\xi)}{\sigma(k+\xi)} \tag{14}$$

These equations can be solved iteratively as they stand but a few observations which can improve the rate of convergence are in order.

1. Since $(\kappa/\sigma)^2$ is small a first approximation is to omit the term in $J(k+\xi)$ from the first equations of Eq (14), giving a first approximation for K. These values of K are then used in the second equations of Eq (14) to obtain the first estimate for J, which are then used in the K equation to improve the approximation; the iteration proceeds until the successive approximants have converged.

2. The equations for K and J are themselves solved by iteration. In the Appendix we show that $A_s(x)$ and $B_s(x)$ are of order $\epsilon^{|s|}$ for negative values of s. The matrices A and B are therefore approximately triangular and we can write

$$[1-A_o(k+\xi)]K(k+\xi) = \sum_{j=k+1}^{x-1} A_{j-k}(j+\xi)K(j+\xi) + S + \frac{\kappa^2 J(k+\xi)}{3\sigma(k+\xi)} + \sum_{j=o}^{k-1} A_{j-k}(j+\xi)K(j+\xi) \tag{15}$$

with a similar equation for $J(k+\xi)$.

The first summation of Eq (15) contains "large" terms, the second summation contains only "small" terms; for k=X-1 the first sum vanishes. Hence we solve the equations successively in the order k=X-1,X-2,X-3,...1,0 using at each step the latest approximants for $K(j+\xi)$. (We can start with $K(j+\xi) = 0$ or with any better guess that may be available). This procedure corresponds to neglecting in the first approximation the collisions in which neutrons gain energy. The resulting approximate collision density can then be used as a "source" of energy gain collisions with which to improve the approximations.

Typical results of the above procedure, as executed on the IBM 704, are presented in Fig. 4.

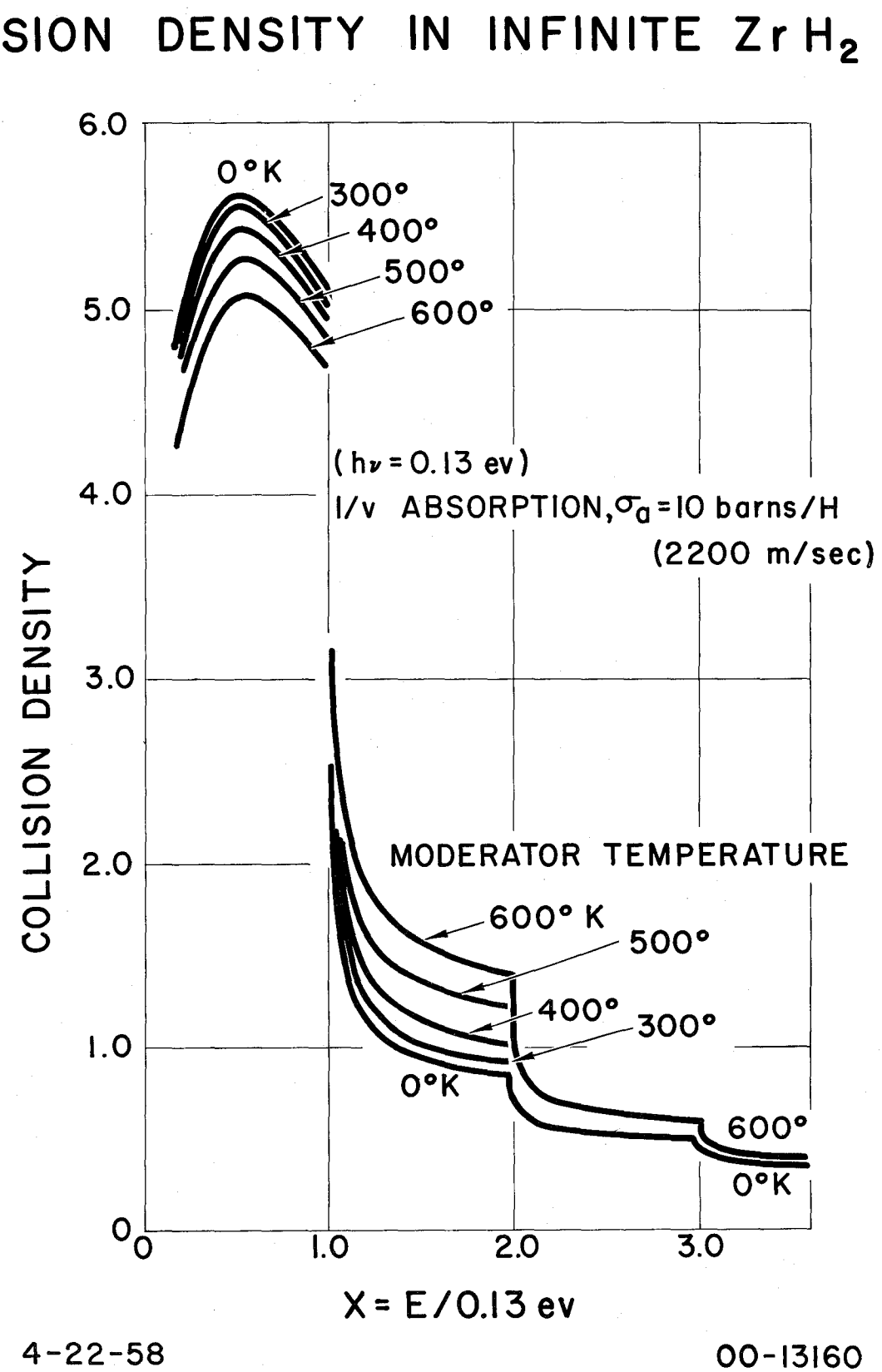

Fig. 4. Neutron Collision Density in Infinite Zr H_2

Appendix

Details of Cross Section Calculation

The fundamental scattering cross section of a neutron of energy x colliding with a hydrogen atom in state m to leave the hydrogen in state n and the neutron with energy $x_f = x+m-n$ is

$$\sigma_{m\to n}(x)\, d\omega = \frac{\sigma_o}{(m+1)(m+2)\pi} \sqrt{\frac{x_f}{x}} \sum_{r=o}^{m} (r+1) \left| A^{m-r}_{n-r}(u) \right|^2 d\omega \qquad (A.1)$$

σ_o = free atom total scattering cross section

u = square of the momentum transfer

$$u = x+x_f - 2\mu_o \sqrt{xx_f} \qquad (A.2)$$

$$d\omega = 2\pi\, d\mu_o = -\frac{\pi\, du}{\sqrt{xx_f}} \qquad (A.3)$$

μ_o = cosine of the angle of scattering of the neutron.

$$\left| A^{(m)}_n(u) \right|^2 = m!n!u^{m+n} \left[\sum_p \frac{(-u)^{-p}}{(m-p)!(n-p)!p!} \right]^2 e^{-u} \qquad (A.4)$$

The population of initial states in the hydrogen is determined by the Boltzmann factor $\epsilon = \exp(-h\nu/kT)$. The total cross section for energy loss is given by an averaging over the contributions of the various population levels

$$\langle \sigma_s(x) \rangle = \int \sigma_s(x)\, d\omega = \frac{1}{D(\epsilon)} \left[\sum_m \frac{(m+1)(m+2)}{2} \sigma_{m\to m+s}(x) . \epsilon^{\,m} \right] \qquad (A.5)$$

where $D(\epsilon) = \sum_{m=o} \frac{(m+1)(m+2)}{2} \epsilon^{\,m}$

The scattering cross sections $\sigma_{m\to n}(x)$ are given by

$$\frac{(m+1)(m+2)}{2}\,\sigma_{m\to n}(x) = \frac{\sigma_o}{x}\left[h_{m,n}(a)e^{-a} - h_{m,n}(b)e^{-b}\right]$$

$$a = 2x+m-n-2\sqrt{x(x+m-n)}$$
$$b = 2x+m-n+2\sqrt{x(x+m-n)} \qquad (A.6)$$

The functions $h_{m,n}(u)$ are symmetric in the subscripts ($h_{m,n} = h_{n,m}$) so that we shall, in the calculation of $h_{m,n}$ assume that $n \geq m$. The functions $h_{m,n}$ are defined in terms of the auxiliary functions $p_r(u)$

$$p_r(u) = 1 \qquad r = o$$
$$= 1 + \sum_{t=1}^{r} \frac{u^t}{t!} \qquad r > o \qquad (A.7)$$
$$h_{m,n}(u) = \sum_{r=n-m}^{n+m} C_r p_r(u)$$

for $m = o$ $\qquad C_n = 1$ $\qquad$ (A.8.0)

for $m = 1$ $\qquad C_{n-1} = n+2$ $\qquad$ (A.8.1)

$$C_n = -2n$$
$$C_{n+1} = n+1$$

for $m = 2$ $\qquad C_{n-2} = \frac{1}{2}(n+1)(n+2)$ $\qquad$ (A.8.2)

$$C_{n-1} = -2(n-1)(n+2)$$
$$C_n = n(3n+1)$$
$$C_{n+1} = -2n(n+1)$$
$$C_{n+2} = \frac{1}{2}(n+1)(n+2)$$

for $m = 3$

$$C_{n-3} = \frac{1}{6}n(n+1)(n+2) \tag{A.8.3}$$

$$C_{n-2} = -(n-2)(n+1)(n+2)$$

$$C_{n-1} = \frac{5}{2}(n-1)^2(n+2)$$

$$C_n = -\frac{10}{3}(n-1)n(n+1)$$

$$C_{n+1} = \frac{5}{2}n^2(n+1)$$

$$C_{n+2} = -n(n+1)(n+2)$$

$$C_{n+3} = \frac{1}{6}(n+1)(n+2)(n+3)$$

In addition to the scattering cross section we are also interested in the "cosine averaged" cross sections

$$\langle \mu \sigma_s(x) \rangle = \int \mu_o \sigma_s(x) d\omega = \frac{1}{D(\epsilon)} \left[\sum_m \frac{(m+1)(m+2)}{2} \langle \mu \sigma_{m \to m+s}(x) \rangle \epsilon^m \right] \tag{A.9}$$

where

$$\frac{(m+1)(m+2)}{2} \langle \mu \sigma_{m \to n}(x) \rangle = \frac{\sigma_o}{x} \left[g_{m,n}(a) e^{-a} - g_{m,n}(b) e^{-b} \right] \tag{A.10}$$

and $$g_{m,n}(u) = \sum_{r=n-m}^{n+m} C_r \left\{ (b+a) p_r(u) - 2(r+1) p_{r+1}(u) \right\} / (b-a)$$

The total cross section is the sum of the absorption cross section, the elastic (non-hydrogen) cross section and the sum of all of the energy transfer and elastic hydrogen cross sections.

$$\sigma_{total}(x) = \sum_s \langle \sigma_s(x) \rangle + \sigma_{el} + \sigma_{abs} \tag{A.11}$$

and the elements of the transfer matrix are

$$A_s(x) = \frac{\langle \sigma_s(x) \rangle}{\sigma_{total}}$$

$$B_s(x) = \frac{\langle \mu \sigma_s(x) \rangle}{\sigma_{total}} \tag{A.12}$$

The actual iteration is best achieved, however, by using the formulas

$$K(k+\xi) = \sum_j M_{kj} K(j+\xi) + P(k+\xi)$$

$$J(k+\xi) = \sum_j N_{kj} J(j+\xi) + Q(k+\xi) \tag{A.13}$$

$$M_{kj} = \frac{A_{j-k}(j+\xi)}{1-A_o(k+\xi)} \qquad k \neq j$$

$$M_{kk} = 0$$

$$N_{kj} = \frac{B_{j-k}(j+\xi)}{1-B_o(k+\xi)} \qquad k \neq j$$

$$N_{kk} = 0$$

$$P(k+\xi) = \frac{\dfrac{\hbar^2}{3\sigma_{total}} J(k+\xi) + S(k+\xi)}{1-A_o(k+\xi)}$$

$$Q(k+\xi) = \frac{-K(k+\xi)}{\sigma_{total}\left[1-B_o(k+\xi)\right]}$$

The matrices M_{kj} and N_{kj} are quasi-triangular in the sense that $A_s(x)$ and $B_s(x)$ are of order $\epsilon^{|s|}$ for $s < 0$; hence M_{kj} and N_{kj} are each composed of a triangular matrix of order unity (and with zeros on the main diagonal), bordered by subdiagonals of order ϵ^s for the subdiagonal which is displaced s rows from the main diagonal. To see this we return to the expressions for $\sigma_{m\to m+s}$. It is readily apparent from equation (A.6) that

$$\frac{(m+1)(m+2)}{2} x\sigma_{m\to m-s}(x) = \frac{(m-s+1)(m-s+2)}{2}(x+s)\sigma_{m+s\to m}(x+s) \tag{A.14}$$

hence $$\sum_{m=o} \frac{(m+1)(m+2)}{2} \sigma_{m\to m-s}(x)\epsilon^m = \frac{x+s}{x} \sum_{m=s} \frac{(m-s+1)(m-s+2)}{2} \sigma_{m-s\to m}(x+s)\epsilon^m$$

$$= \frac{x+s}{x} \sum_{m'} \frac{(m'+1)(m'+2)\epsilon^{m'+s}}{2} \sigma_{m'\to m'+s)}(x+s) \tag{A.15}$$

whence

$$< \sigma_{-s}(x) > \quad = \frac{\epsilon^{s}(x+s)}{x} < \sigma_{s}(x+s) > \quad . \qquad s > o \qquad (A.16$$

The calculation of the cross sections need be carried out only for $\sigma_{m \rightarrow n}$ with $n \geq m$ and we can then use Equation (A.16), (which is a result of the microscopic reversibility or the statistical mechanical detailed balancing of the collision process) in order to calculate the cross section for neutron energy gain from those for neutron energy loss.

References

1. E. Fermi, Ric. Sci. 7, 13 (1936).

2. H. A. Bethe, Rev. Mod. Phys. 9, 124-5 (1937).

Paper I-C

NEUTRON MODERATION BY CHEMICALLY BOUND HYDROGEN

E. U. Vaughan E. R. Cohen
Atomics International

Neutron Moderation by Chemically Bound Hydrogen

Edward U. Vaughan and E. Richard Cohen
Atomics International
Canoga Park, California

Abstract

When the moderator is hydrogen with isotropic harmonic oscillator binding, the neutron balance condition and its adjoint, which determine the neutron flux and importance spectra, respectively, take the form of difference equations because of the discreteness and uniform spacing of the harmonic oscillator energy levels. These equations can be reduced to first order difference equations -- homogeneous in the case of the flux, inhomogeneous in the case of the importance -- provided the hydrogen atoms are all in their ground states (corresponding to absolute zero temperature). By using suitable approximations to the scattering cross sections, the equations can be simplified and solved. The solutions are sufficiently tractable to permit approximate reduction to single sums of the double sums arising in a perturbational treatment of the effect of temperature (through excited states of hydrogen) on reactivity. It can be shown in this way that at room temperature, and for typical hydrogen frequencies, the temperature-dependent part of the reactivity is insensitive to the behavior of the flux and importance for energies more than twice the quantum energy of the hydrogen oscillators. With this simplification, the effect of temperature on reactivity has been evaluated for a number of conditions.

Neutron Moderation by Chemically Bound Hydrogen

By - E. U. Vaughan and E. R. Cohen

The fact that typical level spacings of chemically bound protons are considerably larger than thermal energies kT at typical reactor temperatures necessitates including effects of binding in treating neutron thermalization by hydrogenous moderators. Following Fermi[1] effects of the binding have been studied by treating the proton states as those of an isotropic harmonic oscillator. This model is excellent for zirconium hydride[2], and may give useful insight into other hydrogenous moderators.

Consider first the simplified problem of an infinite homogeneous system, having no significant moderator other than the harmonically bound hydrogen, and no other significant material present except an absorber. At zero absolute temperature, the Boltzmann equation for the neutrons has the form

$$\sigma_{in}(m+\xi)\phi(m+\xi) = \sum_{n=m+1}^{M-1} \sigma_{n-m}(n+\xi)\phi(n+\xi),$$

where

$(m+\xi)h\nu$ = neutron energy ($0<\xi<1$, m an integer),

ν = frequency of proton vibrations,

ϕ = neutron flux,

$$\sigma_{in}(m+\xi) = \sigma_a(m+\xi) + \sum_{n=0}^{m-1} \sigma_{m-n}(m+\xi),$$

$\sigma_a(m+\xi)$ = absorption cross section,

$\sigma_{m-n}(m+\xi)$ = scattering cross sections of neutron from $m+\xi$ to $n+\xi$ by a proton initially in its ground state,

M = suitable upper limit for the energy-parameter m.

It has been known[1] for many years that the cross section is

$$\sigma_{m-n}(m+\xi) = \frac{\sigma_o}{m+\xi}\int_{x_-}^{x_+} \frac{x^{m-n}e^{-x}}{(m-n)!}\,dx,$$

where

$$x_{\pm} = (\sqrt{m+\xi} \pm \sqrt{n+\xi})^2 ,$$

and

σ_o = free-atom hydrogen cross section

= 20b.

Numerical evaluation shows that the integral in the above expression is near unity for $m >> m - n$, but approaches zero rapidly (with vertical tangent) as n approaches zero. The approach to zero being qualitatively similar for various values of m, an attempt has been made to show that the integral is quantitatively insensitive to m.

The integrand of the integral, which is a Poisson distribution, can be approximately replaced by the Gaussian

$$(2\pi)^{-1/2}(m-n+1)^{-1/2} \exp\left[-(1/2)\,(x-m+n-1)^2(m-n+1)^{-1}\right]$$

This is a good approximation if $m-n>>1$. If, moreover, $n+\xi << m+\xi$, another good approximation is

$$x_{\pm} \approx m + \xi \pm 2\sqrt{(m+\xi)(n+\xi)}$$

$$\approx m - n + 1 \pm \sqrt{2(m-n+1)}\;\sqrt{2(n+\xi)}$$

TABLE I

Test of $(n+\epsilon)\sigma_{o\to n}(n+\epsilon)/\sigma_o \approx \mathrm{erf}\sqrt{2\epsilon}$

ϵ	erf $\sqrt{2\epsilon}$	$(n+\epsilon)\sigma_{o\to n}(n+\epsilon)/\sigma_o$					
		n = 1		n = 2		n = 3	
		value	error	value	error	value	error
0.01	0.158	0.147	0.011	0.152	0.006	0.154	0.004
0.20	0.628	0.620	0.008	0.625	0.003	0.625	0.003
0.40	0.792	0.805	-0.013	0.799	-0.007	0.798	-0.006
0.60	0.878	0.893	-0.015	0.890	-0.012	0.883	-0.005
0.80	0.925	0.942	-0.017	0.937	-0.012	0.932	-0.007
1.00	0.954	0.967	-0.013	0.961	-0.007	0.960	-0.006
1.20	0.972	0.980	-0.008	0.977	-0.005	0.975	-0.003
1.40	0.982	0.987	-0.005	0.985	-0.003	0.982	0.0000
1.60	0.989	0.990	-0.001	0.990	-0.001	0.990	-0.001

These approximations yield for the integral the approximate form

$$(m+\xi)\,\sigma_{m-n}(m+\xi)/\sigma_o \approx \mathrm{erf}\sqrt{2(n+\xi)}\ .$$

This expression should be valid for large m and small n, and also for large m and large n where it properly approaches unity. If it is true that the integral is insensitive to m, the approximation will hold more generally. This possibility has been examined by numerical evaluation of the correct expression. The results, shown in Table I, indicate that the approximation is sufficiently accurate for the present purpose.

The Boltzmann equation is actually a set of difference equations, coupling different values of the integer part of $E/h\nu$, but with no coupling between different values of the fractional part ξ. The solution accordingly contains an aribitrary function of ξ as a factor. This factor can be determined by imposing as a boundary condition that for large values of $m + \xi$ the solution should approach the solution for the corresponding problem with free hydrogen. This solution is

$$\phi_f(E) = C[E\sigma_{in}(E)]^{-1} \exp\left\{-\int_E^{E_o} dE'\sigma_a(E')/[E'\sigma_{in}(E')]\right\},$$

which may be written, by using the relation $\sigma_{in}(E) = \sigma_a(E) + \sigma_o$, in the form

$$\phi_f(E) = CE[E\sigma_{in}(E)]^{-2} \exp\left\{-\int_E^{E_o} d[E'\sigma_a(E')]/[E'\sigma_{in}(E')]\right\}.$$

The solution in the bound case is analogous to the second form above, making the evaluation of the arbitrary factor simple. The solution is obtained in a somewhat similar manner, as well; just as the first step in getting the above solution is to reduce the Boltzmann integral equation to a first-order differential equation by differentiation, so in the present problem the first step is to reduce the Boltzmann equation to the first-order difference equation

$$\frac{S_\xi(m)\phi(m+\xi)}{(m+\xi)\,\mathrm{erf}\sqrt{2(m+\xi)}} = \frac{[S_\xi(m+1)+\mathrm{erf}\sqrt{2(m+1+\xi)}]\phi(m+1+\xi)}{(m+1+\xi)\,\mathrm{erf}\sqrt{2(m+1+\xi)}} ,$$

where

$$S_\xi(m) = (m+\xi)\sigma_{in}(m+\xi)/\sigma_o$$

$$= (m+\xi)\sigma_a(m+\xi)/\sigma_o + \sum_{n=0}^{m-1} \mathrm{erf}\sqrt{2(n+\xi)}$$

The solution, obtained by evaluating the periodic factor, and dropping the arbitrary constant factor C, is

$$\phi(m+\xi) = \frac{(m+\xi)\,\mathrm{erf}\sqrt{2(m+\xi)}}{S_\xi(m)S_\xi(m+1)} \prod_{n=m+1}^{M-1} \left[1 - \frac{J_\xi(n)}{S_\xi(n+1)}\right] ,$$

where

$$J_\xi(n) = [(m+1+\xi)\sigma_a(m+1+\xi) - (m+\xi)\sigma_a(m+\xi)]/\sigma_o .$$

The analogy with the free-proton case consists of relating E with $m+\xi$, $E\sigma_{in}(E)$ with $S_\xi(m)$, $d[E'\sigma_a(E')]$ with $J_\xi(n)$ and the exponential of an integral with a product, together with a certain amount of confusion between m and m + 1.

The most important feature of this solution is the large value of ϕ when m = 0, which arises from the small value of $S_{\xi}(0) = \xi \sigma_a(\xi)/\sigma_0$, provided the amount of absorber is relatively small. The flux is shown in figure 1 for the case of 140 atoms of hydrogen per atom of U^{235}, corresponding to a thermal absorption cross section of about 5b per proton.

If the temperature is raised from absolute zero, some of the protons are excited out of the ground state. The changes in the cross sections which result from this excitation produce changes in the neutron flux spectrum. In a thermal reactor, this will result in a change in k_∞, because some neutrons are absorbed at different energies from before, where the ratio α of parasitic captures to fissions is different. This effect can be treated by perturbation theory, provided the temperature is low enough for $\exp(-h\nu/kT)$ to be considered small. In this approximation, all higher powers of $\exp(-h\nu/kT)$ should be ignored. In particular, only the lowest exicted state of the protons is significant.

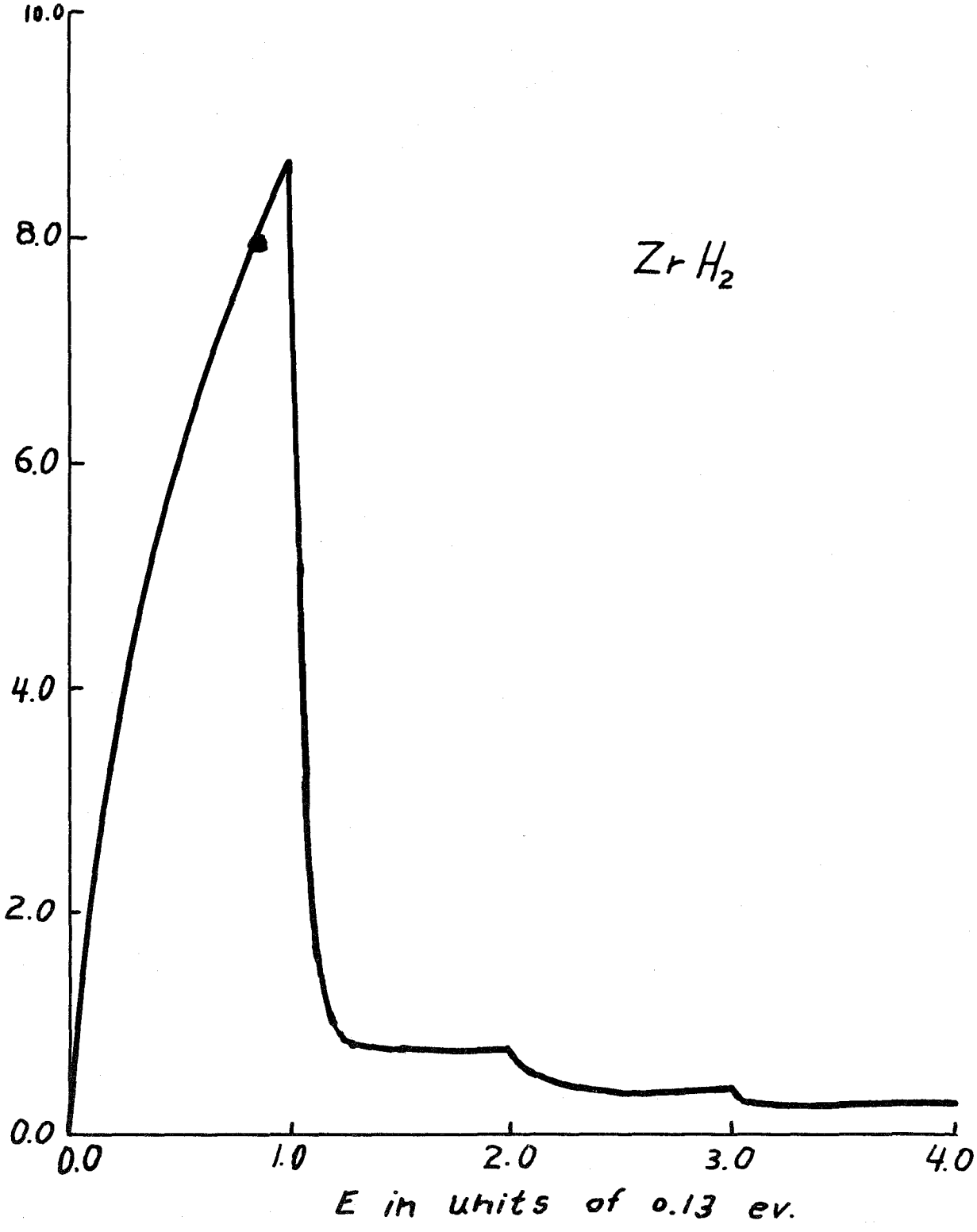

Fig. 1. Neutron Flux in an Infinite Homogeneous Mixture of Zr H_2 and U^{235} Having 140 Hydrogen Atoms per U^{235} Atom

The general expression given by perturbation theory for the reactivity introduced in an infinite homogeneous medium, constituted of harmonically and isotropically bound hydrogen together with fissionable material, by a change of the scattering cross sections is

$$\rho = - \frac{\int_0^1 d\xi \sum_{m=0}^{M-1} \phi(m+\xi) \sum_{n=0}^{M-1} \delta\sigma_{m-n}(m+\xi)[F(m+\xi) - F(n+\xi)]}{\int_0^1 d\xi \sum_{m=0}^{M-1} \sigma_f(m+\xi)\phi(m+\xi)} ,$$

where the importance function $F(m+\xi)$ satisfies the equation

$$\sigma_{in}(m+\xi)F(m+\xi) = \sum_{n=0}^{m-1} \sigma_{m-n}(m+\xi)F(n+\xi) + \sigma_f(n+\xi).$$

Here

$\sigma_f(m+\xi)$ = fission cross section,

$\sigma_{m-n}(m+\xi)$ = unperturbed cross section for scattering of a neutron from $m+\xi$ to $n+\xi$,

$\delta\sigma_{m-n}(m+\xi)$ = change in scattering cross section.

Raising the temperature from zero absolute perturbs the cross sections in two ways:

1) The cross section $\sigma_{-1}(m+\xi)$ no longer vanishes. The approximation used before leads to the expression

$$\delta\sigma_{-1}(m+\xi) \approx \exp(-h\nu/kT)[\sigma_0/(m+\xi)] \operatorname{erf}\sqrt{2(m+\xi)} .$$

Since larger negative-subscript cross sections correspond to higher excited states with higher powers of $\exp(-h\nu/kT)$ in their Boltzmann factors, the sum over n in the expression for ρ can be cut off at m+1 instead of m-1.

2) There is a change in $\sigma_{m-n}(m+\xi)$. This change can be treated by approximations similar to those employed previously, but they must be applied to the <u>change</u> of cross section because this quantity is small, and might be masked by small errors in the separate cross sections. The result is

$$\delta\sigma_{m-n}(m+\xi) \approx -\exp(-h\nu/kT)\left[\sigma_0/(m+\xi)\right]\left[8(n+\xi)/\pi\right]^{1/2}\exp\left[-2(n+\xi)\right] .$$

This approximation is compared in Table II with the exact values computed numerically. The principal result is that the largest error is 18% of the largest value. It will appear later that this entire contribution is small, and hence that this accuracy is adequate. Because of the rapid decrease of $\exp\left[-2(n+\xi)\right]$, it has been deemed sufficient to make this correction for the case n=0 only.

Because of its inhomogenity, the equation for the importance is more complicated than the equation for the flux. Nevertheless, the use of the error-function approximation for the scattering cross section permits its reduction to the first-order difference equation

$$S_\xi(m+1)F(m+1+\xi) - \left[S_\xi(m)+\mathrm{erf}\sqrt{2(m+\xi)}\right]F(m+\xi) = K_\xi(m),$$

where

$$K_\xi(m) = \left[(m+1+\xi)\sigma_f(m+1+\xi)-(m+\xi)\sigma_f(m+\xi)\right]/\sigma_0 .$$

Table II

Test of $(n+\epsilon)[\sigma_{0\to n}(n+\epsilon) - \sigma_{1\to n+1}(n+\epsilon)]/(3\sigma_0) \approx (8\epsilon)^{1/2}(9\pi)^{-1/2}\exp(-2\epsilon)$

ϵ	0.010	0.200	0.600	1.000	1.400
$\sqrt{\frac{8\epsilon}{9\pi}}\, e^{-2\epsilon}$	0.0531	0.159	0.124	0.072	0.038
correct value for n=1	0.0250	0.132	0.148	0.084	0.037
error	+0.0281	+0.027	-0.024	-0.012	+0.001

The arbitrary factor in the solution of this equation is determined, not by a boundary condition for large $m+\xi$, but by the original equation for the case m=0:

$$F(\xi) = \sigma_f(\xi)/\sigma_a(\xi).$$

It may be verified that the solution of this problem is

$$F(m+\xi) = \frac{\sigma_f(\xi)}{\sigma_a(\xi)} + \sum_{\ell=0}^{m-1} L_\xi(\ell) \left\{ 1 - \prod_{n=\ell}^{m-1} \left[1 - \frac{J_\xi(n)}{S_\xi(n+1)} \right] \right\},$$

where $$L_\xi(\ell) = \frac{K_\xi(0)}{J_\xi(0)} - \frac{\sigma_f(\xi)}{\sigma_a(\xi)} \qquad \text{if } \ell = 0$$

$$= \frac{K_\xi(\ell)}{J_\xi(\ell)} - \frac{K_\xi(\ell-1)}{J_\xi(\ell-1)} \qquad \text{if } \ell > 0.$$

The expressions for ϕ and F, especially the latter, are somewhat intricate, and lead to intractable expressions when substituted into the expression for ρ. Consequently, further approximations have been introduced, based on the smallness of the ratio $J_\xi(n)/S_\xi(n+1)$. There is a difficulty when this approximation is made in a product of the form

$$P_\xi(m) = \prod_{n=1}^{m-1} \left[1 - J_\xi(n)/S_\xi(n+1) \right]$$

because of the compounding of errors from several factors.

If the absorption is 10b per proton (thermal average), and $h\nu = 5.2$ kT (corresponding to kT = 0.025 ev., and $h\nu = 0.130$ ev as for zircomium hydride[2], then

$$J_o(1)/S_o(2) = 0.070,$$

$$J_1(1)/S_1(2) = 0.024,$$

$$P_o(2) = 0.930.$$

If the product in $P_\xi(M)$ is written as the exponential of a sum of logarithms, and the sum is approximated by an integral and the logarithm by the first term of a power series, there results

$$P_o(2) \approx 0.94,$$

$$P_o(4) \approx 0.92,$$

$$P_o(\infty) \approx 0.87.$$

The first of these, comparing with the last of the preceding set of numbers, shows the adequacy of the approximation, while the others show that the product is never far from unity.

If n=0 and ξ is small, $J_\xi(n)/S_\xi(n)$ is not small. It appears, however, that if U^{235} is the fissionable material and also the only absorber, then the capture-to-fission ratio α is the same for $1+\xi$ as for ξ for small ξ, provided $h\nu \leq 0.130$ ev. Consequently, the range where $J_\xi(n)/S_\xi(n)$ is not small cannot contribute to ρ, and there is no error in treating $J_\xi(n)/S_\xi(n)$ as being small everywhere.

With these approximations, an explicit expression for ρ can be written. Introducing the notation

$$\rho = -\exp(-h\nu/kT) \quad [\bar{A}_{-1} + A_o]$$

where A_{-1} represents the contribution from $\delta\sigma_{-1}(m+\xi)$, and A_o that from $\delta\sigma_m(m+\xi)$, the expressions for the A's are

$$A_{-1} \approx \frac{\displaystyle\int_o^1 \frac{d\xi}{1+\alpha(\xi)} \sum_{m=0}^{M-1} \frac{\mathrm{erf}^2\sqrt{2(m+\xi)}\,[W(m+1+\xi) - W(m+\xi)]}{S_\xi(m)[S_\xi(m+1)]^2}}{\displaystyle\int_o^1 d\xi \sum_{m=0}^{M-1} \sigma_f(m+\xi)\,\frac{(m+\xi)\,\mathrm{erf}\sqrt{2(m+\xi)}}{S_\xi(m)S_\xi(m+1)}},$$

$$A_o \approx \frac{\displaystyle\int_o^1 \frac{d\xi}{1+\alpha(\xi)} \sqrt{\frac{8\xi}{\pi}}\, e^{-2\xi} \sum_{m=0}^{M-2} \left[1 - \frac{S_\xi(m+1)}{S_\xi(M)}\right] \frac{W(m+1+\xi) - W(m+\xi)}{[S_\xi(m+1)]^2}}{\displaystyle\int_o^1 d\xi \sum_{m=0}^{M-1} \sigma_f(m+\xi)\,\frac{(m+\xi)\,\mathrm{erf}\sqrt{2(m+\xi)}}{S_\xi(m)S_\xi(m+1)}},$$

where

$$W(m+\xi) = (m+\xi)\,\sigma_f(m+\xi)\,[\alpha(m+\xi) - \alpha(\xi)],$$

$$\alpha(m+\xi) = [\sigma_a(m+\xi)/\sigma_f(m+\xi)] - 1.$$

These expressions have been evaluated for the case of zirconium hydride with 70 protons per U^{235} atom (which gives approximately 10b per proton as the thermal-average absorption cross section). The range $0 \leq \xi \leq 1$ was divided into quarters, the integrands evaluated at the five division and bounding points, and the integrations performed by Simpson's rule.

Absorption in H and Zr was ignored. The coefficient A_{-1} was separated into a contribution from $m+\xi < 1.25$ and another from $m+\xi > 1.25$. The results were

$$A_o = 0.002$$

$$A_{-1}(< 1.25) = 0.044 \pm 0.020$$

$$A_{-1}(> 1.25) = 0.000$$

$$A_{-1} + A_o = 0.046 \pm 0.020$$

It is visible that the contributions other than $A_{-1}(< 1.25)$ are not significant compared to the probable error. This error arises from the uncertainty in the values of α, which were taken from BNL 325, Supplement 1. Large as it is, this spread appears to be underestimated, because of the probable positive correlations between the experimental errors at neighboring values of ξ.

Using only $A_{-1}(< 1.25)$, the dependence on composition has been examined. Absorption in the moderator has now been included because it contributes significantly to α for compositions poorer in U^{235} than that used above.

H/U	70	140	210
$A_{-1}(< 1.25)$	0.045 ± 0.020	0.057 ± 0.024	$0.062 + 0.025$

References

1. E. Fermi, Ric. Sci. 7, 13 (1936).
   H. A. Bethe, Rev. Mod. Phys. 9, 124-5 (1937).

2. Pelah et al., Phys. Rev. 108, 1091 (1957).
   Andresen et al., Phys. Rev. 108, 1092 (1957).

Session II: THE THERMAL RANGE

Paper II-A

NEUTRON SCATTERING PROPERTIES OF LIQUID MODERATORS

B. N. Brockhouse
Atomic Energy of Canada, Ltd.

Neutron Scattering Properties of Liquid Moderators

B. N. Brockhouse
Atomic Energy of Canada, Limited
Chalk River, Ontario

Abstract

The neutron scattering properties of a liquid at a given temperature and pressure are described by a scattering function[1] $S(Q,\omega)$, where $Q = \left| \underline{k}_o - \underline{k}' \right|$, $\omega = \hbar^{-1} (E_o - E')$, $\underline{k}_o$ and k' being the initial and final neutron wave vectors, and E_o and E' the initial final neutron energies. The current state of knowledge of the function S for light and heavy water will be discussed. Experiments using neutrons with $E_o \sim 0.005$ ev and in the range 0.03 to 0.07 ev have been performed.[2] These experiments have yielded much qualitative information about S for light water at room temperature in the range of values at $Q \gtrsim 10A^{-1}$ and $|\hbar\omega| \gtrsim 0.07$ ev. Some features of S have also been studied for water at other temperatures and for heavy water. The relationship of the neutron scattering function to self-diffusion, to vibrational and hindered rotational Raman and Infra-red bands, and to models of the liquid state will be indicated.

---

1. L. Van Hove, Phys. Rev. 95, 249 (1954).

2. B. N. Brockhouse, Supplemento del Nuovo Cimento (1957) (Proceedings of the Varenna Conference on the Condensed State of Simple Systems). Acta Cryst. 10, 827 (1957), also unpublished material.

Paper II-B

CHEMICAL BINDING EFFECTS IN HYDROGEN MODERATED REACTORS

M. S. Nelkin
General Atomic

Chemical Binding Effects in Hydrogen Moderated Reactors *

Mark S. Nelkin
General Atomic
San Diego, California

Abstract

A discussion will be given of the effects of chemical binding in reactors moderated by zirconium hydride and/or water. The first portion of the paper will deal with theoretical models describing the inelastic scattering of slow neutrons in these materials. These models will then be applied to calculations of neutron spectra and temperature coefficients. In particular, the effect of the quantized energy transfer on the temperature coefficient of a zirconium hydride moderated reactor will be discussed and illustrated with experimental data from the General Atomic critical assembly. Finally, a discussion will be given of our understanding of the thermalization process in water with emphasis on information attainable with pulsed neutron experiments.

*The text on the following pages is a 1958 Geneva Paper (P/1839) by M. S. Nelkin and E. R. Cohen. It includes a summary of the report given by M. S. Nelkin at the conference, the abstract of which is reproduced above.

RECENT WORK IN NEUTRON THERMALIZATION

M. S. Nelkin and E. R. Cohen*

I. INTRODUCTION

For neutron energies below 1 ev, the energy interchange between neutrons and moderating materials is dependent not only on the nuclear mass and scattering amplitude but also on the state of chemical binding and on the moderator temperature. The moderation of neutrons in this energy region, and the approach to thermal equilibrium between neutrons and moderator, fall under the subject we choose to call "neutron thermalization." This paper covers selected recent developments in this field, including experimental and theoretical investigations of thermal neutron energy distributions and of the fundamental inelastic processes leading to the establishment of these distributions. Detailed discussions will be confined to work which has been completed too late for inclusion in two recent review articles.(1,2) A comprehensive coverage of the field has not been attempted, since this paper is being written prior to the Gatlinburg Conference on Neutron Thermalization(3) and we do not find it either appropriate or possible to give the coverage that will be available in the proceedings of that conference.

The focal point of the present paper is the rapidly increasing amount of information that is becoming available on the inelastic scattering of slow neutrons by materials of interest for neutron moderation in reactors. An experimental basis is becoming available for a fundamental understanding of neutron moderation in the region below 1 ev, where chemical binding effects are important. The interpretation of this data is greatly facilitated by the development of powerful formal techniques for calculation in the Fermi pseudopotential approximation.(4) These techniques reduce the theoretical problem

*John Jay Hopkins Laboratory for Pure and Applied Science, General Atomic Division of General Dynamics Corporation, San Diego, California; and Atomics International, A Division of North American Aviation, Canoga Park, California.
Including discussions of unpublished work by E. Vaughan, Atomics International; N. Corngold, Brookhaven National Laboratory; D.J. Hughes and H. Palevsky, Brookhaven; B. Dunne, M. N. Rosenbluth, R. H. Stahl, M. Stearns, and M. O. Stern, General Atomic; D. A. Kottwitz, Hanford Atomic Products Operation; P. A. Egelstaff, Atomic Energy Research Establishment, Harwell, Berks.; T. J. Krieger, M. L. Storm, P. F. Zweifel, and D. M. Keaveney, Knolls Atomic Power Laboratory; R. S. Stone and R. E. Slovacek, Knolls Atomic Power Laboratory; and J. Griffin, Los Alamos Scientific Laboratory.

to the determination of well-defined time-dependent correlation functions[5] expressing the dynamics of the motion of the scattering nuclei as it is influenced by the interatomic forces.

These experimental and theoretical developments have concentrated on the fundamental problem of investigating the dynamics of lattice vibrations and of atomic motions in a liquid, using slow-neutron inelastic scattering. In this paper we will take a complementary point of view and focus on the effects of interatomic binding on the thermalization of neutrons by moderating materials. To reduce the complexity of the problem to where some understanding can be obtained without the use of high-speed computers, we will first attempt, in Section II, to characterize the moderating properties of importance in the chemical binding region by a few integral parameters of the scattering distribution. This can be done only rather crudely, but it makes possible a semiquantitative identification of those features of the inelastic scattering which are of dominant importance in determining the energy distribution of neutrons in a reactor. The experimental and theoretical evidence on moderation by zirconium hydride, water, graphite, and beryllium in the chemical binding region will be discussed in Section III. Section IV will present recent experimental data on the spectra of close-packed water-moderated lattices, and the temperature coefficient of a zirconium-hydride-moderated reactor will be discussed. These experiments do not conflict with the considerations of Section III.

Section V will discuss recent developments in methods of solving the energy-dependent transport equation in the thermal region. These include analytic results on the asymptotic behavior of the spectrum as the energy increases to the region of free atom scattering, and on the behavior of the spectrum in a region with a plane temperature discontinuity. Finally, we discuss numerical techniques for including neutron speeding up in multigroup calculations and for determining the spectrum in a hydrogenous moderator when the hydrogen atoms are bound in an isotropic harmonic oscillator potential.

II. FACTORS AFFECTING THE SPECTRUM IN A REACTOR

The neutron spectrum in a reactor deviates from an equilibrium Maxwellian distribution for several reasons. The first is the finite time required for fission neutrons to slow down and reach equilibrium with the moderator. In the presence of an appreciable amount of absorption this time can be comparable to the lifetime of thermal neutrons. In the frequently studied case of an infinite homogeneous medium with a 1/v absorption cross section, this is the only cause of deviation from thermal equilibrium. This fact is easily understood by recalling that the neutron distribution at sufficiently long times after the introduction of a pulse of fast neutrons will be an equilibrium Maxwellian which decays exponentially in time. This case has been the subject of considerable calculation and has been investigated experimentally by Poole[6] for solutions of boric acid in water. There have been indications from these studies that the spectrum is very insensitive to the effects of chemical binding on the inelastic scattering of slow neutrons. These indications can be misleading, as they are due largely to the idealization of the problem to an infinite homogeneous medium with 1/v absorption and to the peculiar combination of effects which makes water behave very much like free hydrogen in its thermalization properties.

Before elaborating on these points, we will attempt to define some parameters of the moderator which determine the deviation from equilibrium in this idealized problem. For small deviations from equilibrium we should be able to characterize the hardening of the spectrum by a parameter which is the ratio of the thermalization time to the thermal lifetime. For the special case of a heavy gaseous moderator,[7,8] this parameter is proportional to $(\Sigma_a v/\xi \Sigma_s v_0)$. For the general case, it is convenient to divide the energy spectrum into two regions. The first is from fission energies down to about 10 kT. In this region, the possibility of energy gain in a collision need not be explicitly considered. The effects of temperature and binding can be included approximately in a modified value for the slowing-down cross section, $\xi\sigma_s$, as a function of neutron energy, and the spectrum calculated by the usual techniques of neutron-slowing-down theory. The solution in this energy region, then, determines a source for the "thermal energy group" between zero energy and 10 kT.

An accurate calculation of the spectrum within the thermal energy group requires the explicit consideration of at least the first two moments of the energy transfer kernel $\sigma(E_0, E)$, and preferably of the entire kernel. This cannot be done without extensive numerical computation and can only be done well with the aid of high-speed computers. One can hope, however, to obtain a crude description of the spectrum near its maximum value in terms of a Maxwellian distribution with a neutron temperature, T_n, greater than the moderator temperature, T. To estimate this neutron temperature, we note that if neutrons are inserted at t = 0 in a Maxwellian distribution, with a temperature differing only slightly from the moderator temperature, the neutron temperature will approach the moderator temperature as[9]

$$T_n = T(1 + e^{-\gamma t}) ,$$

where

$$\gamma = (2/3\sqrt{\pi})v_0 M_2 \tag{1}$$

and

$$M_2 = (kT)^{-2} \iint dE\, dE_0\, (E_0 - E)^2\, \sigma(E_0, E)\, \phi_M(E_0) \quad . \tag{2}$$

The factor $\phi_M(E_0)$ is the equilibrium Maxwellian distribution. In the steady state problem one would therefore expect the fractional increase in neutron temperature over moderator temperature to be proportional to the ratio of thermalization time to thermal lifetime, or $(4\Sigma_a v/v_0 M_2)$. In the heavy gas model, $M_2 = 4\xi\Sigma_s$.

The concept of a neutron temperature differing from the moderator temperature is of very limited utility in a quantitative description of the spectrum, but the parameter M_2 as defined by Equation 2 is a useful integral parameter of the slowing down kernel $\sigma(E_0, E)$ in giving a rough estimate of the deviations from equilibrium, and particularly in assessing the adequacy of a sim-

plifying approximation such as the heavy gas model. In general, M_2 will depend quite sensitively on interatomic binding and will be discussed further in connection with moderation by water, graphite, and beryllium.

In addition to the effect of finite slowing-down time, deviations from thermal equilibrium will arise from non-1/v absorption, and from diffusion of neutrons between moderating regions of different temperatures. Non-1/v absorption can arise from the intrinsic energy dependence of the cross sections or from the spatial dependence of neutron loss in a heterogeneous system. These deviations are associated with intrinsically nonequilibrium situations. An equilibrium Maxwellian distribution would not be obtained for any energy spectrum of the neutron source. This differs from the infinite homogeneous medium with 1/v absorption, in which an initial equilibrium distribution would remain in equilibrium, and deviations from equilibrium occur only in the presence of a nonequilibrium source.

The diffusion of neutrons between moderating regions of different temperatures is becoming of greater interest as higher-temperature reactor systems are developed in which the reflector and core are at very different temperatures, with a large portion of the thermalization taking place in the reflector. These problems of spatially dependent spectra are generally too complicated for the semianalytic type of treatment that has been fruitful for the infinite homogeneous medium spectrum, and will have to be attacked by high-speed computer techniques in which the thermal energy region is divided into several energy groups. Developments in this direction are discussed in Section V. The theoretical problem then becomes one of determining the cross sections for energy transfer between the various thermal energy groups from the available experimental data on the inelastic cross sections, and of discovering which cross sections need to be known accurately and which only crudely. Little work along these lines has been done as yet, but it is clear that these effects will depend rather directly on the effects of chemical binding on the inelastic scattering of thermal neutrons. The related problem of the "diffusion cooling" of the equilibrium spectrum in a finite moderator due to the preferential leakage of faster neutrons has been studied,[9] and this investigation indicate that the relevant parameter is M_2 as defined in Equation 2. For example, for room-temperature graphite this parameter is reduced by a factor of 3.5 from the value for an ideal gas of carbon atoms of the same density. This indicates that spatially dependent spectra in graphite-moderated reactors will be quite sensitive to chemical binding effects.

The discussion in the following section will focus on the energy dependence of the slowing down cross section, $\xi\sigma_s$, and on the values of the mean square energy transfer per collision for thermal neutrons as determined by M_2. This is a very crude characterization of the moderating properties of importance for determining neutron spectra, but it helps to define the kinds of variations in scattering properties which are of greatest interest in considerations of neutron thermalization.

III. MODERATION IN THE CHEMICAL BINDING REGION

The most direct demonstration of the effects of interatomic binding on neutron moderation is in various hydrogenous compounds.

A detailed experimental and theoretical consideration of this problem is given in another paper for this conference.[10] We will outline the principal results reported in the above paper and elsewhere, and discuss their implications for reactor performance. The effects of binding on thermalization in beryllium and graphite will also be discussed.

A. Zirconium Hydride

It is for zirconium hydride that interatomic binding has the largest effect on the thermalization process, and this effect may be quantitatively described. Experiments by McReynolds, Whittemore, and co-workers[10] are in excellent agreement with a model in which the hydrogen atom moves in an isotropic harmonic oscillator potential with energy levels $E_n = nh\nu$, where $h\nu = 0.13$ ev. This model is consistent with the position of the hydrogen atom in the lattice, i.e., at the center of a regular tetrahedron of zirconium atoms. A detailed justification of the model and a comparison of theory and experiment are given elsewhere.[10]

The basic result of importance for thermalization is the quantization of the energy transfer in multiples of $h\nu$, which is large compared with kT. This implies that the spectrum in a zirconium-hydride-moderated reactor will have no resemblance to an equilibrium Maxwellian and that the dependence of reactivity on moderator temperature cannot be described in terms of a neutron temperature which follows the moderator temperature, even when the absorption is relatively weak. Theoretical work on the temperature coefficient of a hydride-moderated reactor has been done by Rosenbluth and Stern at General Atomic.[11] They considered only temperatures low enough that terms in second order in $\exp(-h\nu/kT)$ could be neglected, and worked in terms of multigroup diffusion theory. The basic process involved is the speeding up of neutrons by their gaining an energy $h\nu$ from an oscillator in the first excited state. The population of speeded-up neutrons will be proportional to $\exp(-h\nu/kT)$, as will the reactivity. The magnitude of the temperature coefficient depends on the relative importance of speeded-up neutrons and therefore involves a knowledge of the energy dependence of the adjoint flux in the thermal energy region. This cannot be accurately obtained from diffusion theory. Recent work by Cohen and Vaughan, which is discussed in Section V, removes the limitations both of low temperature and of diffusion theory and should make possible more accurate calculations of temperature coefficients for zirconium-hydride-moderated reactors. Critical assembly experiments at General Atomic, discussed in Section IV, agree with a reactivity which goes with hydride temperature as $\exp(-h\nu/kT)$, with $h\nu = 0.13$ ev, but the magnitude of the temperature coefficient could only be calculated to within about $\pm$ 50%.

B. Water

The moderating properties of water for slow neutrons much more nearly resemble those of an ideal gas of monatomic hydrogen than they do those of a strongly bound system such as zirconium hydride. This fact is reflected in the measured spectra for water-moderated systems. Spectra have been measured for solutions of boric acid in water by Poole[6] and for close-packed, highly enriched water lattices by Stone and Slovacek.[2,12] Recent results of Stone

and Slovacek are reported in Section IV. Both of these measurements agree very well with theoretical spectra calculated on a free hydrogen model from Amster's SOFOCATE code for the IBM 704.[13] Both measurements correspond essentially to an infinite homogeneous medium with 1/v absorption of up to 7 barns per hydrogen atom at kT.

This close agreement between a free hydrogen model and experiment is very surprising in light of the experimental information on the energy-change cross sections for slow neutrons in water. Brockhouse[14] has measured the energy distribution of initially monoenergetic neutrons with energies from 0.03 to 0.06 ev after scattering at various angles from a thin water sample. The results are consistent with the scattering from an ideal monatomic gas with the mass of the H_2O molecule, or 18 times the free hydrogen mass. This would indicate that only the translational modes of the molecule have sufficiently low frequencies to transfer energy effectively with thermal neutrons. Calculations have been performed by Krieger of the spectrum of neutrons which enter the thermal region with a distribution characteristic of free hydrogen and are then thermalized by an ideal gas of mass 18. These calculations show noticeable deviations from the spectrum characteristic of free hydrogen.[15]

To understand the agreement between the free hydrogen model and the experimental spectra, it is necessary to consider in more detail the energy transfer between slow neutrons and the translations, hindered rotations, and vibrations of the water molecule. The previously mentioned data obtained by Brockhouse indicate that the translations can be considered as free. Brockhouse has also measured the energy distribution of cold incident neutrons after scattering through 90° by water, and he finds a fairly well defined peak at about 0.06 ev corresponding to energy gain from the hindered rotations. The molecular vibrations for water will have approximately the same characteristic energies (0.20, 0.40, and 0.43 ev) as those for the free molecule. As the neutron energy decreases to 0.20 ev, the effective scattering unit changes from a free proton to an almost rigid H_2O molecule. This change is associated with an increase in the cross section and a decrease in the energy transfer per collision. The net result is a value for $\xi\sigma_s$ which is almost identical for free hydrogen and for hydrogen in water. This is illustrated by calculations[10] at energies of 0.086, 0.117, and 0.20 ev. The water calculations take into account the hindered rotation, free translation, and zero-point vibration of the H_2O molecule. The dynamics of the hindered rotations are replaced by those of an isotropic harmonic oscillator of mass 2.3 (from the trace of the mass tensor) and energy of 0.06 ev The calculated values of $\xi\sigma_s$ for water are somewhat lower than the values measured by McReynolds and Whittemore,[10] and the source of this discrepancy has not been identified. The point we choose to emphasize here is the near equivalence of water and free hydrogen in the calculated value of $\xi\sigma_s$. This near equivalence does not arise from any fundamental similarity in the systems but is due to an accidental cancellation between the increase in σ_s and the decrease in ξ. It is only in the product of ξ and σ_s that the scattering from water and that from free hydrogen have any similarity.

For energies below about 0.10 ev the distinction between $\xi\sigma_s$, which is determined by the average energy loss, and M_2, which is determined by the mean square energy loss, is important. The parameter of greatest importance for the establishment of the thermal spectrum is M_2 as it is defined in Equation 2.

The value of M_2 can be determined experimentally from the diffusion cooling effect[9] to be 48 ± 7 barns per hydrogen atom. This is consistent with a thermal cross section that is chiefly associated with energy transfer to the molecular translations, with a few barns associated with energy transfer to the hindered rotations. M_2 is slightly less than the 60 barns per hydrogen atom that would apply for free hydrogen. The application of the concept of neutron temperature, and the definition of M_2 as the parameter of interest, is probably not very accurate if the quantized energy transfer to the hindered rotations is of importance. We would expect the deviations from equilibrium in the region from zero energy to about 4 kT to be described roughly by a free hydrogen model but to be given rather accurately above 4 kT. The largest differences would be expected between water and a free hydrogen model at energies below kT. This energy region has not been readily available for experimental investigation. Between kT and 4 kT the measured deviations from equilibrium have not been very large but are consistent with a free hydrogen model.

C. Graphite

Experimental information on graphite is considerably more limited than that on zirconium hydride or water, but there is sufficient evidence to indicate that the effects of interatomic binding strongly reduce the energy transfer between slow neutrons and moderator. Experiments on the effective value of $\xi\sigma_s$ for graphite are discussed in detail elsewhere.[10] They show a value significantly below that expected for an ideal monatomic gas of carbon atoms. No theoretical analysis of these data in terms of a model for the lattice vibrations of graphite has yet been made.

A second piece of experimental information concerns the mean square energy transfer between thermal neutrons and the lattice vibrations described by the parameter M_2 of Equation 2. The diffusion cooling effect on the thermal lifetime in a graphite block has been measured by Antonov, et al.,[16] and by Beckurts.[17] Beckurts has also determined the relaxation time of the neutron temperature by measuring the time dependence of foil transmission after a pulse of fast neutrons. All of these measurements agree with a value of M_2 which is smaller by a factor of 3.5 than would obtain for an ideal carbon gas. This value is in agreement with a calculation[9] based on a model which assigns a Debye temperature of 900°K to lattice vibrations perpendicular to the planes and of 2500°K to vibrations parallel to the planes. This model was originally used by Krumhansl and Brooks[18] to explain the specific heat of graphite at low temperatures.

The spectrum in a graphite-moderated reactor at low temperatures would therefore be expected to be considerably more hardened than would be calculated from a heavy gas model The effects of binding would be particularly large under conditions of spatially dependent spectra. For example, neutrons diffusing back into a hot core from a cold reflector would require a large number of collisions to heat-up to the core temperature. Preliminary experimental information on this point has been obtained by Stone and Slovacek.[19] They heated a graphite cube 14 inches on a side to a temperature of 550°K and thermally insulated it from a surrounding graphite thermal column at 300°K.

The spectrum at the center of the cube was found to be approximately Maxwellian with a neutron temperature of 450°K. This corresponds to a minimum distance from the cold graphite of about seven mean free paths and, therefore, to an average of about twenty-five collisions in the hot graphite before a neutron reached the center of the cube.

D. Beryllium

The only available experimental information for beryllium is the diffusion cooling as measured by Antonov, et al.[16] This measurement indicates a value of M_2 lower by a factor of 4.5 than the free atom value. A calculation[9] based on a Debye model with a Debye temperature of 930°K predicts that this factor should be 1.7. Since a similar calculation gives agreement with a more accurate measurement for graphite, and since beryllium is more loosely bound than graphite, it is probable that the diffusion cooling in beryllium is smaller than the quoted experimental value.

If we discount the diffusion cooling measurement, we would expect the effects of interatomic binding on the spectrum in beryllium to be less than those in graphite but to lead to definitely more hardened spectra than would be obtained from a free gas model. This appears to conflict with the results obtained by Nelkin for the spectra in beryllium,[20] which showed negligible deviations between the crystal and the free gas. The model used there for the crystal was the one used in Reference 9. A re-examination of Nelkin's calculations shows that the crystalline effects are not at all negligible, but appeared so because of the misleading way in which the calculated spectra were plotted. To illustrate this, we plot in Fig. 1 the spectra for $(\Sigma_a v/\xi\Sigma_s v_0) = 0.25$, as obtained from the free gas model and from the crystal model with a Debye temperature of 1000°K. $\xi\Sigma_s$ is the free atom value applying at high energy, and the moderator temperature is 294°K. The two curves are normalized to same total neutron density from zero to 0.4 ev. The spectrum for the crystal model is noticeably more hardened than is the free gas spectrum. In the free gas case, the region near the peak can be well fitted by a Maxwellian at 395°K. For the crystal case, the spectrum below the peak drops off much more sharply than does a Maxwellian but can be fitted just above the peak by a Maxwellian at 465°K. For an absorption-to-scattering ratio which is four times greater, similar differences are obtained, although here the concept of neutron temperature has no significance.

We have summarized our understanding of neutron moderation in the chemical binding region on the basis of fragmentary experimental information. The experimental knowledge of the differential-energy-change cross section $\sigma(E_0, E, \theta)$ will be greatly increased by the systematic experimental investigation of scattering laws for moderators in progress at Chalk River under the direction of P. A. Egelstaff of Harwell.[21]

By means of velocity selectors, a neutron beam from a reactor is made to give neutrons of a prescribed energy. The primary energy range from 0.005 ev to 1 ev is covered in 50 steps. The scattered neutrons are measured in 20 equally spaced angular positions located around the sample material. For each angular position the energy distribution is measured in 200 channels. At present, the materials considered are graphite, light water, and heavy water at several temperatures.

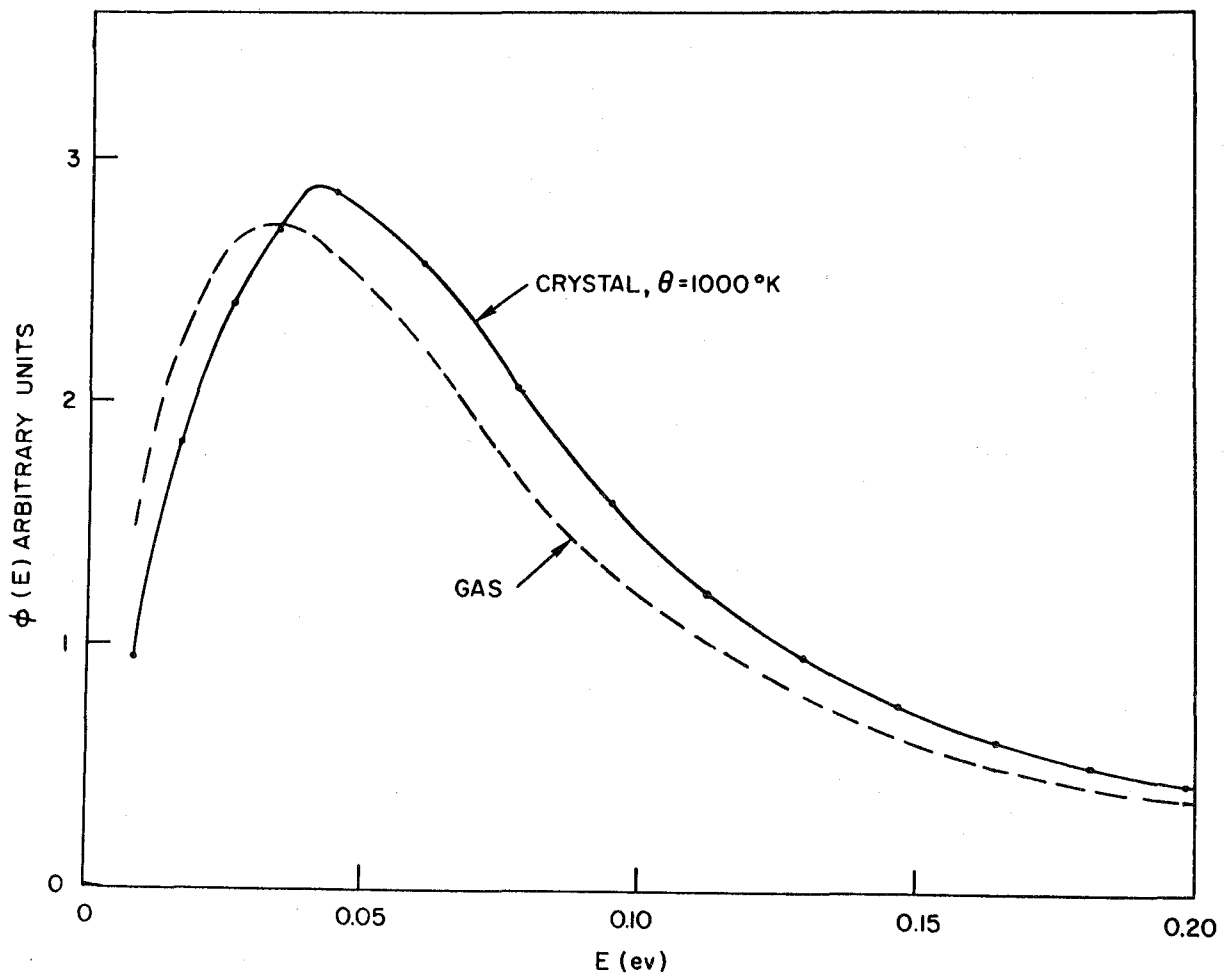

Fig. 1--Calculated spectra for heavy gas and heavy crystal at 294°K with $(\sum_a v/\xi \sum_s v_0) = 0.25$

The development of a systematic program for the measurement of $\sigma(E_0, E, \theta)$ follows many earlier experimental developments. We note the development of the cold neutron time-of-flight technique by Hughes, Palevsky, and collaborators. The work of Brockhouse[14] and of McReynolds and Whittemore[10] in this field has already been mentioned.

IV. RELATED REACTOR EXPERIMENTS

Considerable experimental work has recently been done on the measurement of spectra in reactors and in subcritical assemblies. Most of this work is discussed by Poole and Stone in the experimental section of a recent review article.[2] Two interesting experimental results, however, were too recent for inclusion in that review.

The first stems from the measurement of the spectra of several close-packed, highly enriched water lattices using the chopper technique[2] developed by Stone and Slovacek at the Knolls Atomic Power Laboratory. The lattices consisted of 1-mil uranium foils clad with zircalloy, and approximately equal volumes of zirconium and light water. The new measurements reported here were for a uranium-to-water ratio such that the absorption at 0.025 ev per hydrogen atom was 5.9 barns at 298°K and about 8 barns at 586°K. Calculations were performed using the SOFOCATE code developed by Amster for the Wigner-Wilkins equation for free hydrogen.[13] Corrections were made for the reduced density of water at the higher temperature, for leakage from the assembly, and for self-shielding of the uranium foils. The experimental and theoretical spectra are shown in Figs. 2 and 3. The agreement between the free hydrogen model and experiment is even better than was obtained by Poole for boric acid solutions with approximately the same absorption per hydrogen atom.

The second experiment of interest is the determination of the dependence of reactivity on hydride temperature for a critical assembly moderated by zirconium hydride and water. This experiment was performed by Dunne, Stahl, Stearns, and Stern at General Atomic,[23] and is discussed in more detail in another paper in the proceedings of this conference.[10] This experiment was consistent with a temperature dependence of reactivity which went as exp $(-T_0/T)$, where $T_0 = 1500°K$ is the Einstein temperature for the optical lattice vibrations of zirconium hydride as measured by McReynolds, et al.[10] This gives direct experimental confirmation of the importance of chemical binding in determining the temperature coefficient of a zirconium hydride reactor, and indicates that the Einstein model discussed in Section III is essentially correct.

V. NEW CALCULATIONAL METHODS

The increased interest in the details of the thermalization process and the recognition of the importance of the neutron spectrum in determining the behavior of advanced reactor types has stimulated the development of improved calculational methods. These may be either completely analytical or partly numerical in nature. Although these calculations are related in a broad sense, they represent individual facets of the problem. Several of these

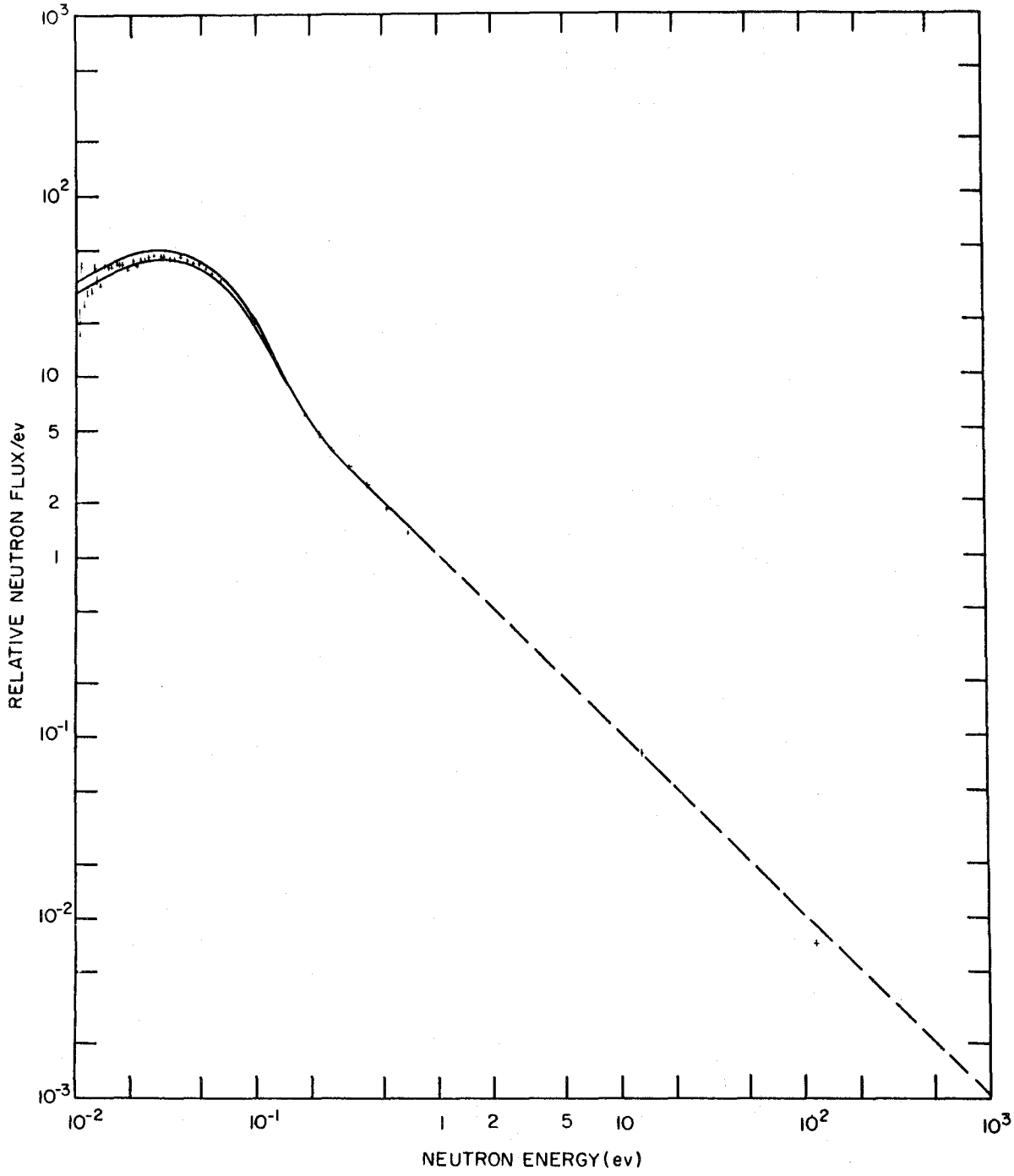

Fig. 2--Neutron flux spectra in highly enriched, water-moderated assembly at 298°K. The solid curves are the calculated spectra for a free hydrogen model. For the upper curve $B^2 = 0$ and thermal self-shielding = 0.898. For the lower curve $B^2 = 0.0055$ cm^{-2} and thermal self-shielding = 1.0.

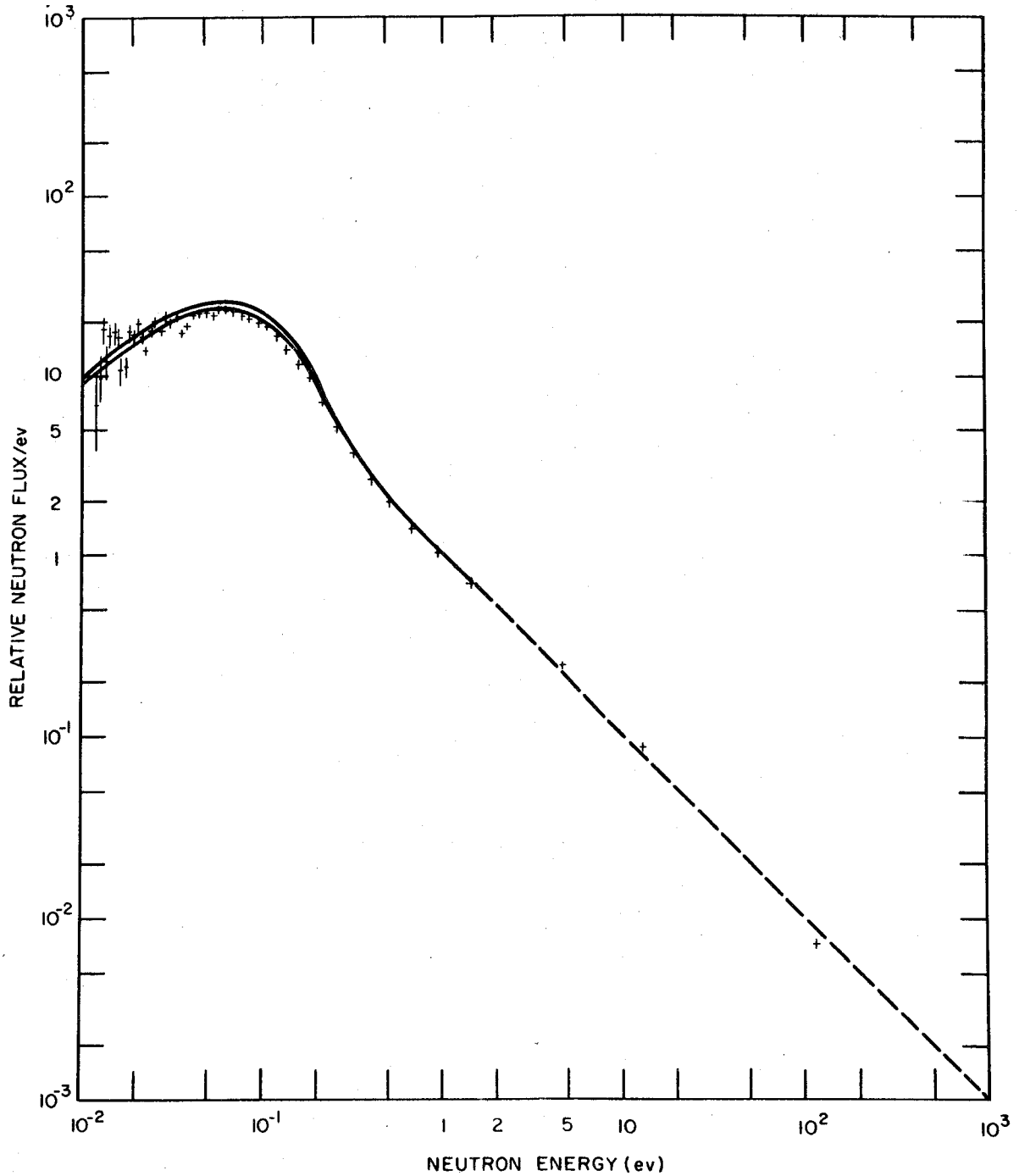

Fig. 3--Neutron flux spectra in the assembly of Fig. 2 at 586°K. Solid curves are again the free hydrogen calculations. For the upper curve $B^2 = 0$ and thermal self-shielding = 0.924. For the lower curve $B^2 = 0.0018\ cm^{-2}$ and thermal self-shielding = 1.0

topics will be separately described as examples of fields in which work is in progress and in which additional effort would appear to be fruitful. We shall not discuss those calculations which are not new in principle but are merely extensions of methods previously reported.[1,2,24] In particular, extensive use has been made of the free hydrogen and the heavy atom gas models for the calculation of thermal spectra and flux average cross sections.[13,25] These calculations are useful for reactor design purposes but are not well suited to condensation for inclusion in a review of this type. The availability of high-speed computing machines has made such spectral calculations almost routine.

Corngold[26] at Brookhaven has considered the problem of neutron thermalization in an infinite homogeneous medium from the standpoint of deriving the maximum of information from an analytical treatment of the Boltzmann equation. The guiding idea is to carry the study of the Boltzmann equation for the neutron spectrum as far as possible without resorting to numerical methods or restricting considerations to very heavy moderators. The results to date have concerned the asymptotic expansion of the flux in inverse powers of the energy. The methods suggested by Placzek[27] and Wick[28] for treating the scattering cross section in the asymptotic region are extended to the collision integral $\int \sigma(E_0, E)\, \Phi(E_0)\, dE_0$. An expansion of the integral equation for the flux in terms of nth-order differential operators is also obtained. For the special case of an ideal monatomic gas, an expansion in powers of the mass ratio yields the Wilkins equation[7,8] as the first approximation and explicitly yields a more accurate differential equation when terms of higher order in the mass ratio are included.

The spatial dependence of the thermalization process is beginning to yield to attack also, and the problem will achieve increased importance as reactors in which there are strong temperature gradients become more common. In small reactors the major thermalization process may occur in a reflector which is at a different temperature from the core; in such a situation there arise additional distortions from an equilibrium Maxwellian neutron distribution. Recently Kottwitz[29] at Hanford has obtained an analytic solution to an idealization of this problem. The energy and spatial dependence of the steady-state neutron flux has been derived for a nonabsorbing infinite medium consisting of a heavy monatomic gas, the temperature of which has a constant value in one half-space and a different constant value in the other. The heavy-gas and P_1 approximations lead to a partial differential equation which is separable for each region. Each resulting energy eigenfunction is a product of a Maxwellian distribution and a Laguerre polynomial of order one. The series expansion coefficients are evaluated by requiring flux and current to be continuous at the boundary plane.

Although the problem considered by Kottwitz is too idealized to be of direct use in reactor applications, the availability of an analytic solution for a spatially dependent spectrum will be of great utility in checking out numerical methods developed for use in more complicated problems. In particular, it will be possible to determine the accuracy of multigroup methods developed for calculating spatially dependent thermal spectra reactors.

A complementary approach to the problem of space-dependent thermalization has been taken by Griffin[30] at Los Alamos. The multigroup SNG (transport

approximation) technique of Carlson[31] is used to calculate the spectrum in a semi-infinite medium as a function of distance from the boundary plane. The source of neutrons is taken as monoenergetic and incident at the boundary. Multigroup scattering cross sections have been calculated for both speeding-up and slowing-down in the thermal region. Two distinct assumptions are made about the moderator: (1) that it is a Maxwellian gas of atoms of mass M at a temperature T; (2) that it is a Debye crystal of atoms of mass M at a temperature T and characterized by a Debye temperature Θ. The first case is treated exactly and the second case in the first-order (1/M) incoherent approximation.[20] From the numerical results for the spatial dependence of the spectrum, it is possible to define a relaxation length for the thermalization of neutrons in a given moderator.

The description of the energy-transfer cross section in terms of hydrogen harmonically bound in an isotropic potential was used by Fermi twenty years ago[4] as an approximate model for the slowing-down of neutrons in paraffin. In a metal hydride moderator such a description becomes much more nearly exact, and it is reasonable to consider this model in more detail.

Preliminary calculations on the neutron spectrum where made by Rosenbluth and Stern,[11] who pointed out that the reactivity in a reactor moderated by a metal hydride would have a Boltzmann-factor temperature dependence $[\exp(-h\nu/kT)]$. More extensive calculations have been carried out by Cohen and Vaughan.[32]

In the approximation that the only energy transfers to the neutrons are associated with changes in the quantum states of the hydrogen, the neutron can gain or lose energy only in discrete amounts. It is then convenient to express the neutron energy as multiples of the quantum energy $h\nu$ of the oscillator levels, i.e., $E = (m + \xi)h\nu$, where m is an integer and $0 \leq \xi < 1$. The scattering can change m but not ξ, and, hence, the integral equation for the neutron spectrum is reduced without further approximation to a difference equation in which ξ is a simple parameter.

The probability that a neutron will change its energy by an amount $sh\nu$ is determined by the cross section for a proton transition from state n to state n - s, weighted by the population of protons in state n. These cross sections can be evaluated in a straightforward manner from a direct extension of Fermi's results.[4] The cross sections for energy transfer approach the free gas values as the initial neutron energy becomes large, and hence it is permissible to consider only a finite number of oscillator states in combination with a free gas model at higher energies. Physically, also, there is justification for this approximation, since the protons are bound in a well of finite depth.

The time-independent Boltzmann equation can be reduced to a set of coupled difference equations by introducing the P_1 approximation and a Fourier transform.

Then $\Phi_0 + 3\mu\Phi_1$ is the Fourier transform of the neutron flux spectrum, and we obtain

$$iK\Phi_1(x) + \sigma(x)\Phi_0(x) = \sum_s \sigma_s(x + s)\Phi_0(x + s) + S(x)\, iK\Phi_0(x)$$

$$+ 3\sigma(x)\Phi_1(x) + \sum_s \tau_s(x + s)\Phi_1(x + s) ,$$

where $x = m + \xi$ = neutron energy measured in units of $h\nu$.

$\sigma(x)$ = total cross section,

$\sigma_s(x)$ = cross section for neutron energy loss, $\Delta E = sh\nu$,

$$\sigma_s(x) = \int_{-1}^{1} \sigma_s(x, \mu)\, d\mu ,$$

$$\tau_s(x) = \int_{-1}^{1} \mu\sigma_s(x, \mu)\, d\mu .$$

$S(x)$ is the source term for neutrons making transitions from the "free proton" to the "bound proton" region.

The equations which are adjoint to these equations give the neutron importance function, $F(x)$, which provides a formula for the reactivity change with temperature of the moderator (and hence with change in the population density of the various oscillator states). The neutron importance is equal to the number of neutrons produced per absorption, averaged over the energy at which the neutron is ultimately absorbed. The change in reactivity produced by a change in moderator temperature arises from the differing importance of neutrons with energy.

The change in reactivity is given by

$$\delta\rho = -\int \Phi_0(x) \sum_s \delta\sigma_s(x) \left[F(x) - F(x - s)\right] dx ,$$

where $\delta\sigma_s$ is the change in transfer cross section produced by the change in temperature.

In an infinite moderator (no leakage) there will be no temperature coefficient of reactivity in two important cases: (1) if the number of neutrons produced per neutron absorbed (ηf) is independent of x (even though the absorption cross section may not be); and (2) if there is absorption only in the energy interval $0 < E < h\nu$, since in both of these cases $F(x)$ is a constant.

If zero excess reactivity is taken to correspond to the moderator temperature at absolute zero, there will be, in the standard state, no possibility of neutron energy-gain collisions. At finite temperature the energy-gain cross section is nonzero and contains a Boltzmann factor. Thus, although at low temperatures ($kT < h\nu$) the temperature coefficient of reactivity is small, it has a strong temperature dependence. In a finite moderator the change in leakage with temperature can have a much larger effect on the reactivity than the change in absorption.

We have indicated some of the directions in which progress in the calculation of neutron spectra has been made. These consist largely in the development of physical understanding of situations which are simpler than typical reactor configurations but are sufficiently realistic that one can obtain considerable insight into the behavior of the energy distributions in reactors. Such investigations will be very useful to check the general-purpose computer programs that will be developed for the calculation of spectra in complex reactor configurations.

REFERENCES

1. Amaldi, E., "Neutron Diffusion and Slowing Down in the Chemical Binding Region," to be published in Handbuch der Physik, Vol. XXXVIII.

2. Poole, M. J., Nelkin, M. S., and Stone, R. S., The Measurement and Theory of Reactor Spectra, Progress in Nuclear Energy Series I, Vol. II, Pergammon Press, 1958.

3. Conference on Neutron Thermalization, Gatlinburg, Tennessee, U.S.A., April 28-30, 1958.

4. Fermi, E., Ricerca sci. 1:13 (1936).

5. Van Hove, L., Phys. Rev., 95:249 (1954); Zemach, A. C., and Glauber, R. J., Phys. Rev., 101:118 (1956).

6. Poole, M. J., Journal of Nuclear Energy, 5:325 (1957).

7. Wilkins, J. E., Jr., Report CP-2481 (1944) (unpublished).

8. Cohen, E. R., Nuclear Science and Eng. 2:227, (1957); Hurwitz, Nelkin, and Habetler, Nuclear Science and Eng., 1:280 (1956).

9. Nelkin, M. S., General Atomic Report GA-248, The Diffusion Cooling of Neutrons in a Finite Medium.

10. McReynolds, A. W., Nelkin, M., Rosenbluth, M. N., and Whittemore, W. L., "Neutron Thermalization by Chemically Bound Hydrogen and Carbon," Geneva Conference, 1958; Andresen, A., McReynolds, A. W., Nelkin, M., Rosenbluth, M. N., and Whittemore, W. L., Phys. Rev., 108:1092 (L) (1957).

11. Rosenbluth, M. N., and Stern, M. O., unpublished internal General Atomic reports, 1957.

12. Stone, R. S., and Slovacek, R. E., Report KAPL-1499 and KAPL report to be issued.

13. Amster, H., Nuclear Science and Eng., 2:394 (1957).

14. Brockhouse, B. N., Supplemento del Nuovo Cimento (1957), Proceedings of the Varenna Conference of the Condensed State of Simple Systems, Acta. Cryst., 10:827 (1957).

15. Krieger, T. J., Zweifel, P. F., and Keaveney, D. M., "Calculation of Wigner-Wilkins Spectra with M = 18 kernel and M = 1 source," Gatlinburg Conference on Neutron Thermalization, April 28-30, 1958.

16. Antonov, A. V., et al., Geneva Conference, P/661, 1955.

17. Beckurts, K. H., Nuclear Science and Eng., 2:516 (1957).

18. Krumhansl, J. A., and Brooks, H., J. Chem. Phys., 21:1663 (1953).

19. Stone, R. S., and Slovacek, R. E., unpublished results obtained at the Knolls Atomic Power Laboratory.

20. Nelkin, M., Nuclear Science and Eng., 2:199 (1957).

21. Egelstaff, P. A. (unpublished).

22. Carter, Palevsky, H., and Hughes, D. J., Phys. Rev., 106:1168 (1957); Eisenhauer, Pelah, Hughes, D. J., and Palevsky, H., Phys. Rev., 109:1046 (1958); Pelah, Eisenhauer, Hughes, D. J., and Palevsky, H., Phys. Rev., 108:1091 (L) (1957); Hughes, D. J., and Palevsky, H., Gatlinburg Conference on Neutron Thermalization.

23. Dunne, B., Stahl, R. H., Stearns, M., and Stern, M. O., unpublished internal General Atomic reports.

24. Cohen, E. R., Geneva Conference P/611, 1955.

25. Krieger, T. J., Storm, M. L., Zweifel, P. F., and Keaveney, D. M., Gatlinburg Conference on Neutron Thermalization.

26. Corngold, N., Bull. Am. Phys. Soc., Series II, Vol. 3, No. 1 (1958), Abstract A8; also Gatlinburg Conference on Neutron Thermalization.

27. Placzek, G., Phys. Rev., 86:377 (1952).

28. Wick, G. C., Phys. Rev., 94:1228 (1954).

29. Kottwitz, D. A., Bull. Am. Phys. Soc., Series II, Vol. 3, No. 1 (1958), Abstract A7.

30. Griffin, J., private communication.

31. Carlson, B., "Recent Developments in the Transport Equation by High Speed Digital Computers," Geneva Conference, 1958.

32. Cohen, E. R., and Vaughan, E. V., Gatlinburg Conference on Neutron Thermalization.

Paper II-C

THERMALIZATION OF NEUTRONS AT VERY LOW TEMPERATURES

C. N. Kelber
Argonne National Laboratory

Thermalization of Neutrons at Very Low Temperatures

C. N. Kelber
Argonne National Laboratory
Lemont, Illinois

Abstract

The slowing down of neutrons in cold moderators to produce neutron beams of low effective temperature has been reconsidered. The early analysis by Pomerantschuk in 1938 pointed out one principal difficulty, namely the increase in capture rate attendant upon a decrease in neutron velocity. This limits the attainable temperature in H_2 to about $30^{\circ}K$. In the case of D_2 or D_2O, however, the capture rate is so low that leakage represents the major sink for neutrons. In typical D_2O moderated reactors the capture rate does not become appreciable in a cold, pure sample of D_2 or D_2O until temperatures of the order of $3^{\circ}K$ are reached. The principal remaining difficulty is that the cross section for exchange of energy with the crystalline lattice becomes exceedingly difficult at very low temperatures. A greatly simplified model of D_2O has been adopted which enables one to compute the inelastic scattering cross section (for one phonon exchange) and, using the methods of Kothari and Singwi [Journal of Nuclear Energy, 5, 3, pp 347-56 (1957)] the age of thermal equilibrium of neutrons in the cold sample can be computed with the assumption that these neutrons originally had a Maxwellian spectrum characterized by a temperature of $300^{\circ}K$. The age is very large for D_2O at $4^{\circ}K$ but should be reasonable for D_2 at the same temperature. The hazards associated with handling D_2 have led us to start a series of experiments with D_2O. The experimental apparatus and design will be discussed, as well as preliminary results. A Monte Carlo calculation of the spectrum expected in the exit beam from a finite block of moderator is also being made.

Thermalization of Neutrons at Very Low Temperatures

The material presented here is in the nature of a progress report on an experiment to be performed at Argonne late this summer.

We propose to construct a graphite thermal column fed by an Sb-Be source and into which a cylinder of D_2O at a few degrees absolute is inserted. Then by foil activations and by slow chopper measurements we aim to determine the neutron spectrum and mean temperature.

D_2O is used as a moderating medium, since it is less hazardous than D_2, while H_2O or H_2 both capture at too great a rate.

THEORY

The moderation of neutrons in cold samples to produce neutron beams of low effective temperature has been considered many times. An early analysis was presented by Pomerantschuk[1] in 1938.

---

(1) Scattering of Slow Neutrons in a Crystal Lattice: I. Pomerantschuk, Phys. Zeits. d. Sovietunion, 13, 1, pp. 65-83 (1938).

The chief conclusion is that moderation in hydrogen will not produce effective temperatures below 30^0K, since the mean free path for capture becomes smaller than the mean free path for scattering at this temperature. This conclusion is no longer valid in the case of moderators such as deuterium or heavy water, since the capture cross section is much lower for these materials. In this case the limiting temperature is likely to be provided by the effective cross section due to leakage - the $D B^2$ term. Apart from enabling one to produce a high intensity beam of cold neutrons, it is also apparent that the reaction rate in a small $1/v$ absorber in a cold region would also be enhanced as the square root of the effective neutron temperature. For this reason a facility has been suggested in connection with the Mighty Mouse reactor design which will amplify the already high flux to higher effective values for work with small samples.

Recent work by Butterworth, Egelstaff, London and Webb[2]

(2) I. Butterworth, P. A. Egelstaff, H. London and F. J. Webb: The Production of Intense Cold Neutron Beams, Phil. Mag. 2, 19, pp. 917-927 (1957).

at Harwell has shown that there is a marked increase in the number of neutrons at low energies (~ 10 A^0) when the volume of moderator (liquid H_2) is only 200 c.c.

To gain some indication of the sample size needed, calculations have been made of the age for neutrons to slow down to the temperature of the cold sample. The calculation is necessarily approximate in nature; since orders of magnitude and scale factors were the sought after quantities it is felt that an analytic presentation is most useful.

The technique is that of Kothari and Singwi[3,4] and consists

(3) Kothari, L. S. and Singwi, K. S.: Thermal Inelastic Scattering of Cold Neutrons in Polycrystals, Proc. Roy. Soc. A, 231, 293-307 (1955).

(4) : Slowing Down of Neutrons in Be from 1.4 ev to Thermal Energy (to be published). (We are indebted to the authors for receipt of their manuscript prior to publication.)

of two steps.

First, develope a multi-phonon expansion of the inelastic scattering cross section of the solid considered as a simple Debye lattice, and consider only incoherent scattering. The fact that the lattice is near absolute zero allows several approximations. Chief among these is the neglect of all collisions wherein the lattice loses energy. Next one neglects processes which involve more than one phonon. The cases considered by

Kothari and Singwi do not allow these approximations. At this point the elastic and inelastic cross sections can be written in terms of tabulated functions. For D_2O, however, the molecular mass of 20 is high enough to allow an expansion of the Debye-Waller factor in powers of $1/M$ (M is the mass). This yields $\sigma_1(E) = 2/7\ (\sigma/M)\ E^3$ where σ is the free atom cross section, M the mass, and E the incident neutron energy in units of $k\ \Theta_D$, Θ_D being the Debye temperature. If E is greater than one, then $\sigma_1(E) = 2/7\ (\sigma/M)\ E^3 - \sigma_1(E-1)$. For $E \gg 1$ this formula is no longer valid.

Similarly the rate of energy loss can be calculated in the same approximation and the result obtained that the mean energy loss $\overline{\Delta E} = .15/\sigma_s\ (\sigma/M)\ E^4$ if $E < 1$, $= .15/\sigma_s\ (\sigma/M)\ (E^4 - (E-1)^4)$ if $E > 1$. Here σ_s is the total scattering cross section. At this point it is advantageous to recall that Weinstock[5] has shown that under these conditions

(5) Weinstock, R.: Inelastic Scattering of Slow Neutrons, Phys. Rev. 65, 1, 1-20 (1944) see esp. eq. 59.

σ_s is nearly constant over the range of incident energies. Then the age can be readily calculated if one takes the second step advocated by Kothari and Singwi.

That is, to assume that the neutrons always have a Maxwellian distribution, and the decrease of temperature of the distribution is caused solely by the loss of energy through collisions. Then

$$d E_n/dt = 3/2\ d T_n/dt = N \int_0^\infty v\, \sigma_s\, \overline{\Delta E}\, M(E, T_n)\, dE.$$

Here E_n is the mean energy of the neutrons; T_n the characteristic temperature of the neutrons in units of Θ_D (the Boltzman constant is suppressed); N the number of scattering centers per unit volume; $Nv\sigma_s$ is the number of collisions per unit of time, $M(E, T_n)\ dE$ the proportion of neutrons in an interval dE about E; t the time. Since

$\tau = \int D \frac{dE}{E\xi\Sigma_s} = \int D\, v\, dt$ the age can now be computed.

D, the diffusion coefficient depends on the total cross section and this is assumed constant over the interval, since we neglect coherent scattering. Then $dt = (dt/dE_n)\ d\,E_n$ and the integral can be performed analytically. When this is done, and small correctiong arising from the change in cross sections for $E > 1$ are neglected, one obtains $\tau = (DM/36\ N\sigma)\ 1/T^3_{nf}$. One can see from this highly approximate formula that the age in D_2O will be of the order of a few hundred square centimeters, even with temperatures of the order of .1 ($\Theta_D \sim 170^0K$). Since the experimental volume should have a radius of roughly $2\sqrt{\tau}$ this implies rather large volumes. A considerable amount can be saved by using D_2. H_2 suffers from the difficulties previously mentioned while He has too low an atomic density. CD_4 (deuterated methane) or CD_2 (deuterated polyethelene) are other possibilities, but processing these materials is a problem.

The neglect of coherent scattering is another serious error which will increase the age considerably. The total effect of coherent scattering is hard to determine, however, since it is certain that, if the D_2O is to be cooled to liquid He temperatures, a large proportion of metallic impurity (e.g., Mg) will have to be included to promote good heat conduction.

A diffusion theory calculation utilizing a modified NICK-II code has been made to determine the effect of the cold sample on the neutron spectrum in the sample. This calculation predicts a mean temperature of 100^0K which is probably not representative of the exit beam. The calculation suffers from a number of defects: scattering into only the next five energy groups can be considered in any one group, so that neutrons which might go all the way down in temperature in one collision are neglected; the sample is small in terms of mean free paths, so that diffusion theory itself is only of the most limited validity; and the albedo

of the surrounding graphite for slow neutrons is not correctly included.

A Monte Carlo calculation of the exit spectrum to be expected is being made at present.

EXPERIMENT

The major experimental problem is the design of the cryostat. In this we have received the generous help of D. W. Osborn and B. Abraham of the Chemistry Division, ANL. The sample size is a square circular cylinder 18" by 18". This is not adequate to slow the neutrons down much below 30^0K, but is a practical maximum for our present purposes.

The cryostat is constructed of stainless steel except for the radiation shield which is 2S Al. We expect to lose an average of 1 liter of He per ~~barn~~ hour. The inner shell of the cryostat is a tube sheet. The D_2O will be frozen by circulating N_2 through the tube sheet and then pre-cooled with H_2. Finally, liquid He will be put through the tube sheet and some poured directly on top of the D_2O to promote cracking and good heat conduction. When the D_2O reaches 4. 2^0K, He will be maintained on ~~cap~~ top of the D_2O.

Figure 1 is a cutaway view of the cryostat. The various parts are:

A	Inner tank
B	Radiation shield
C	Outer tank
D	Nitrogen resevoir
E	Electrical outlet
F	Transfer slide for H_2 and He
G	Vacuum gauge
H	Line to vacuum system

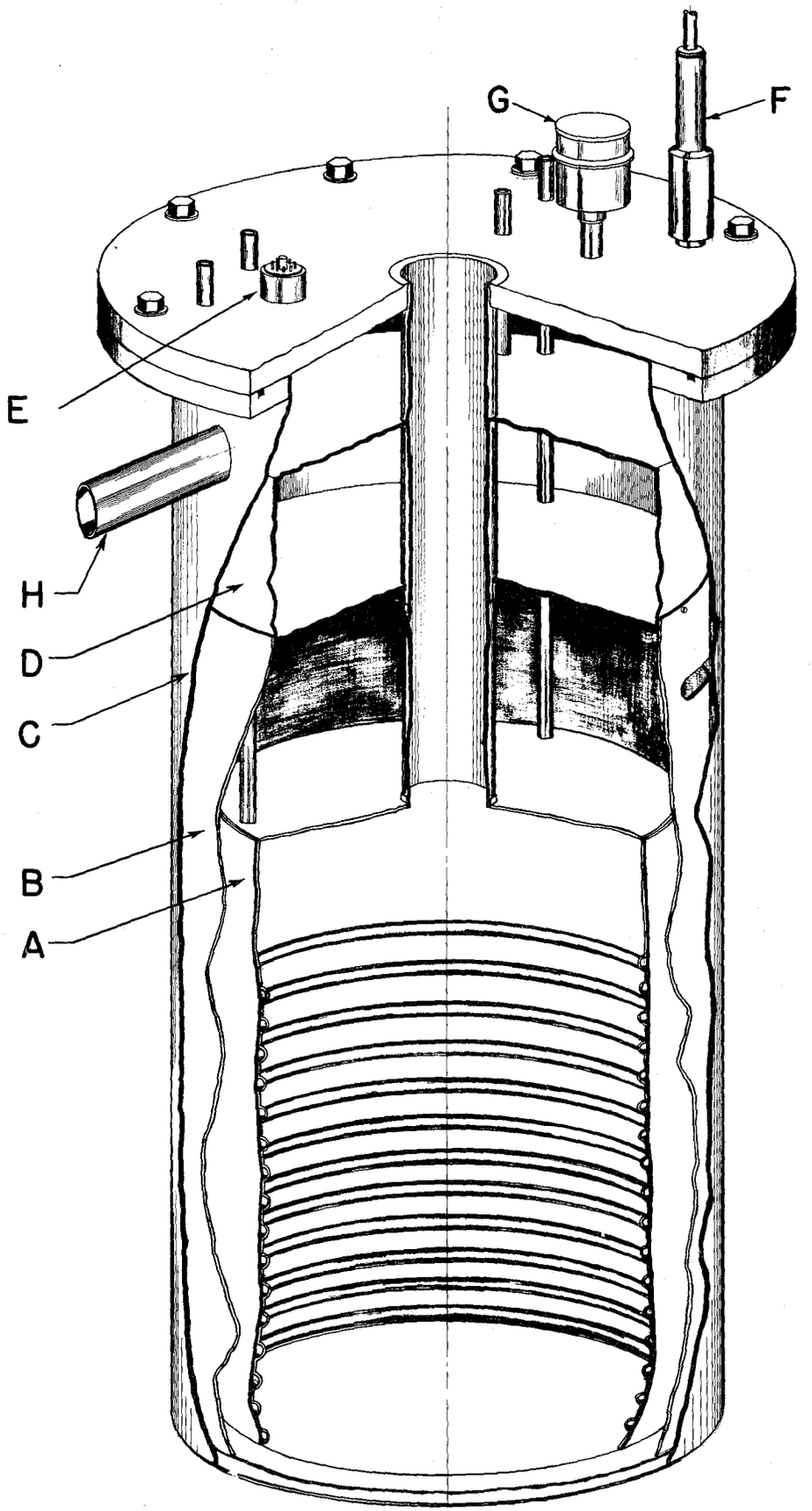
G
F
E
H
D
C
B
A

Paper II-D

NEUTRON THERMALIZATION IN INFINITE HOMOGENEOUS SYSTEMS

N. Corngold
Brookhaven National Laboratory

Neutron Thermalization in Infinite Homogeneous Systems

Noel Corngold
Brookhaven National Laboratory
Upton, Long Island, New York

Abstract

In this talk we shall present some of the latest results of a study of neutron thermalization now in progress at BNL. Our guiding idea is to carry the study of the Boltzmann equation for the neutron flux as far as possible without resorting to numerical methods or restricting our considerations to very heavy moderators. With the Boltzmann equation:

$$\sigma(E)\,\phi(E) = \int_0^\infty dE'\,\sigma_s(E' \to E)\,\phi(E') + S(E) \tag{1}$$

and the physical model of a system of non-interfering scatterers possessing " $\frac{1}{v}$ " absorption we first seek information about the manner in which the " $1/\xi E$ " spectrum joins the thermal spectrum. The methods suggested by Placzek[1] and Wick[2] for treating $\sigma_s(E)$ in the asymptotic region are extended to the collision term in Eq. 1. $\sigma_s(E)$ is expressed as a series in inverse powers of E, while the collision term becomes

$$\frac{\pi}{\mu}\sum_{n=0}^{\infty}\frac{(1-\mu)^n}{n!}\frac{\partial^n}{\partial y^n}\left[\int_{\left(\frac{\sqrt{y}-\mu}{1-\mu}\right)^2 E}^{\left(\frac{\sqrt{y}+\mu}{1-\mu}\right)^2 E}\frac{dE'}{E'}\,\phi(E')\,S_n\left(2M\left[E' - \frac{y-\mu}{1-\mu}E\right]\right)\right]_{y=1} \tag{2}$$

In Eq. 2 μ is the neutron-scattering atom mass ratio and the S_n functions are simply related to the nth moments of energy transfer to the scatterer when a

1. G. Placzek, Phys. Rev. 86, 377 (1952).
2. G. C. Wick, Phys. Rev. 94, 1228 (1954).

given amount of momentum is imparted. They contain the physical characteristics of the system. With these expansions, Eq. 1 may be attacked via a Mellin transform and a series solution expressing the flux in terms of inverse powers of E is obtained. It is:

$$\xi \sigma_o E \phi(E) = \sum_{m=o}^{\infty} \left(\frac{T}{E}\right)^{\frac{m}{2}} \cdot \sum_{k=o}^{\left[\frac{m}{2}\right]} \tau^{k}_{\frac{m}{2}} \left(\frac{\delta}{2}\right)^{m-2k} \tag{3}$$

Here, ξ has its usual meaning, σ_o is σ_s at high energy, T is the moderator temperature and $\frac{1}{2}\delta = \sigma_a(T)\mu\sigma_o$ is the absorption parameter. $\left[\frac{m}{2}\right]$ stands for $\frac{m}{2}$ if m is even and $\frac{m-1}{2}$ if m is odd. The quantities τ^{r}_{n} are given recursively by

$$\tau^{r}_{n} = \frac{1}{\Delta(n+1)}\left[\mu^{r} b_r(n+1)\, \tau^{o}_{n-r} + \mu^{r-1} b_{r-1}(n+1)\tau^{1}_{n-r+1} + \ldots + \mu \cdot b_1(n+1)\tau^{n-1}_{r-1} + \mu\tau^{r}_{n-1/2}\right] \tag{4}$$

and $b_r(s) = -a_r(s)/r!$ with $\Delta(s) = 1 - \frac{1-\alpha^{s}}{(1-\alpha)s}$ and

$$a^{(G)}_{r}(s) = 1/2\left[\delta_{r1} - \frac{4}{1-\alpha}\frac{(1-\mu)^{2(s-r)}}{\mu^{r}}\left(\frac{\partial}{\partial y}\right)^{2r}\int_{-1}^{1} dx \frac{\left[(\sqrt{y}+x)^2-(1-\mu)(y-\mu)\right]^{P}}{(\sqrt{y}+x)^{2(s-P)+1}}\right]_{y=1} \tag{5}$$

in the special case of a gas of "point-particles." For a general system $a_r(s)$ is composed of a group of terms of structure quite similar to Eq. 5. If we take the lowest order in μ, Eqs. 3, 4, and 5 lead to the Wilkins equation[3] and its asymptotic solution. The next order in μ leads to a more accurate differential equation for the flux. If time permits, comparison of Eq. 3 with exact (machine) calculations will be made, and effects of chemical binding will be considered.

---

3. J. E. Wilkins, Jr., CP-2481 (1944).

SUMMARY OF TALK GIVEN AT GATLINBURG

CONFERENCE ON NEUTRON THERMALIZATION

This paper describes a study of neutron thermalization now in progress at BNL. The guiding idea is to carry the study of the Boltzmann equation for the neutron flux in infinite, homogeneous media as far as possible without resorting to numerical methods or restricting our considerations to heavy gaseous moderators. The mathematical problem, that of obtaining a solution to the integral equation

$$(\sigma_a(E) + \sigma_s(E))\ \phi(E) = \int_0^\infty dE'\ \sigma_s(E' \to E)\ \phi(E') + s(E) \qquad (1)$$

has two aspects; one must find appropriate expressions for the cross-sections and one must then extract a solution from (1).

The cross-section $\sigma_a(E)$ in (1) may be taken as proportional to $\frac{1}{v}$, i.e. $\frac{1}{E^{1/2}}$ with reasonable accuracy; the cross-sections $\sigma_s(E)$ and $\sigma(E' \to E)$ are much more complicated since they depend upon the structure of the scattering system. However, a method for calculating the high-energy ($E \gg kT$) behaviour of the scattering from quite general physical systems has been developed by Placzek[1] and by Wick[2]. We shall use these methods to obtain the principal result of this paper, which is an asymptotic series representation of the neutron flux, of the form

$$\phi(E) \sim \frac{1}{\xi\sigma_s E} \sum_{n=0}^{\infty} a_n \left(\frac{kT}{E}\right)^n \qquad (2)$$

In this expansion the important physical characteristics of the system (ratio of neutron to scattering atom mass, character of binding, etc.) are contained in the a_n.

The method of Placzek and Wick is based upon the fact that the differential cross-section $\sigma(\vec{k}_o \rightarrow \vec{k}_f)$ for the scattering of slow neutrons by a system may be expressed as the Fourier transform of the space-time correlation function for the motion of the scattering centers[3]. The correlation function in a classical system would be described as the average proabability of finding at the time, t, a scattering center in the volume element d^3r about $\vec{r}$, if one knows that at time zero some scattering center was present in element d^3r at the origin of coordinates. Wick has shown how an expansion of the correlation function in powers of t leads to an expansion of the total scattering cross-section $\sigma_s(E)$ in $\frac{1}{E}$. We have used this result and have used the same time-expansion to show that the integral term in (1) may be written as an infinite sum of integrals, each having the form of a convolution integral in the context of a Mellin transformation.

When the expansions are inserted into (1) the resulting expression cries out for treatment by Mellin transformation, which converts the integral equation into a difference equation of infinite order. A formal solution to the difference equation may be generated through iteration; this solution has a double infinity of poles in the complex plane, with residues of exceedingly complicated form. Fortunately, the analysis can be simplified by recognizing that most of the poles are connected with source-transient effects and give contributions which vanish as the source energy is removed to infinity. Further, one can find an important recursion formula connecting the residues of significant poles so that general statements may be made regarding the behaviour of the co-efficients a_n in (2). Explicitly,

$$a_n = \sum_{p=0,1,\cdots}^{[n]} \tau_n^p \left(\frac{\Delta}{2}\right)^{2(n-p)} \qquad n = 0, \tfrac{1}{2}, 1, \tfrac{3}{2}, \cdots$$

with

$$\tau_n^p = \frac{1}{a_o(n+1)}\left[-\mu\tau^p_{n-\frac{1}{2}} + \mu b_1(n+1)\tau^{p-1}_{n-1} + \mu^2 b_2(n+1)\tau^{p-2}_{n-2} + \cdots + \mu^p b_p(n+1)\tau^o_{n-p}\right] . \quad (3)$$

In equation (3), [n] signifies the largest integer less than or equal to n , $\frac{\Delta}{2} = \frac{\sigma_a(kT)}{\mu\sigma_s(\infty)}$ and μ is the mass-ratio mentioned above. The quantities $b_p(n+1) = -\frac{1}{p!}\, a_p(n+1)$ are complicated. In the case of scattering by a gas of mass-point particles we find: $(p \geq 1)$

$$a_p^{(G)}(s) = \left[\frac{1}{2}\delta_{p1} - \frac{2}{1-\alpha} \cdot \left(\frac{\mu}{\mu^*}\right) \frac{(\mu^*)^{2(s-p)+1}}{\mu^p} \left(\frac{\partial}{\partial y}\right)^{2p} \int_{-1}^{1} dx \, \frac{\left[(\sqrt{y}+\mu x)^2 - \mu^*(y-\mu)\right]^p}{(\sqrt{y}+\mu x)^{2(s-p)+1}}\right]_{y=1} \quad (4)$$

When the scattering center is bound by a potential, the corresponding $a_p(s)$ functions are linear combinations of integrals quite similar to (4).

The technique of mass-expansion - i.e., the expansion $\phi(E,\mu) = \phi_o(E) + \mu\,\phi_1(E) + \cdots$ in (1) - has been found by other workers[4] to be quite useful in the study of thermalization. In our work, it is most convenient to perform it upon recursion relation (3). A mass expansion of $a_p^{(G)}(s)$, for example, is easy to obtain, and when only the lowest order terms in μ are retained in (3), that equation becomes a three-term recursion formula. Indeed in the case of thermalization by a gas, the recursion

formula becomes a three-term (inhomogeneous) difference equation to all orders of μ. In all of these cases the asymptotic series may be associated with a simple second-order differential equation and the "physical" solution to the equation regarded as the proper sum of the series. We are led, in the gas case, to:

$$x N_o'' + (2x^2 - 1) N_o' + (4x - \Delta) N_o = 0$$

$$x N_1'' + (2x^2 - 1) N_1' + (4x - \Delta) N_1 = \tag{5}$$

$$(2x^{-2} + \tfrac{2}{3}\Delta x^{-1}) N_o' - [4x^{-3} + 2\Delta x^{-2} + (\tfrac{\Delta^2}{3} - 4)x^{-1} - \tfrac{4}{3}\Delta] N_o$$

in the lowest orders of μ. The first equation was first proposed by Wilkins[5]. The "physical" solution to the second equation is identical with that of a fourth-order equation suggested by Wilkins as an improvement over the first. Some curves comparing solutions $x^2 N_o$ and $x^2 N_1$ follow.

REFERENCES

1. G. Placzek, Phys. Rev. 86, 377 (1952).
2. G. C. Wick, Phys. Rev. 94, 1228 (1954).
3. L. van Hove, Phys. Rev. 95, 249 (1954).
4. H. Hurwitz, Jr., M. S. Nelkin, G. J. Habetler, Nuc. Sci. and Eng. 1, 280 (1956); E. R. Cohen, Nuc. Sci. and Eng. 2, 227 (1957).
5. J. E. Wilkins, Jr., CP 2481 (1944); Annals of Math. 49, 189 (1948).

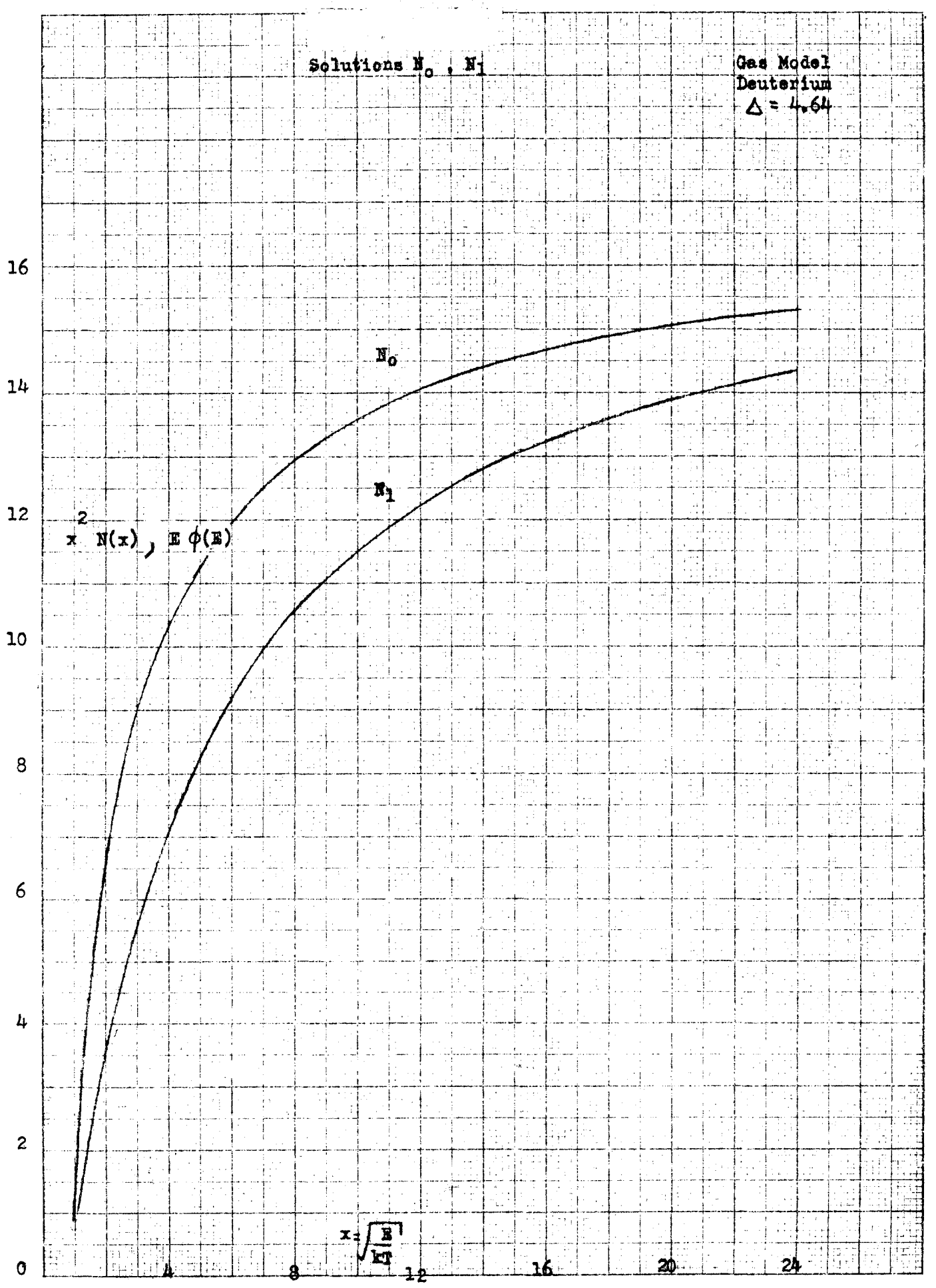
Solutions N_o , N_1
Gas Model
Deuterium
$\Delta = 4.64$
N_o
N_1
$x^2 N(x)$, $E\,\phi(E)$
$x = \sqrt{\frac{E}{kT}}$
0
2
4
6
8
10
12
14
16
4
8
12
16
20
24

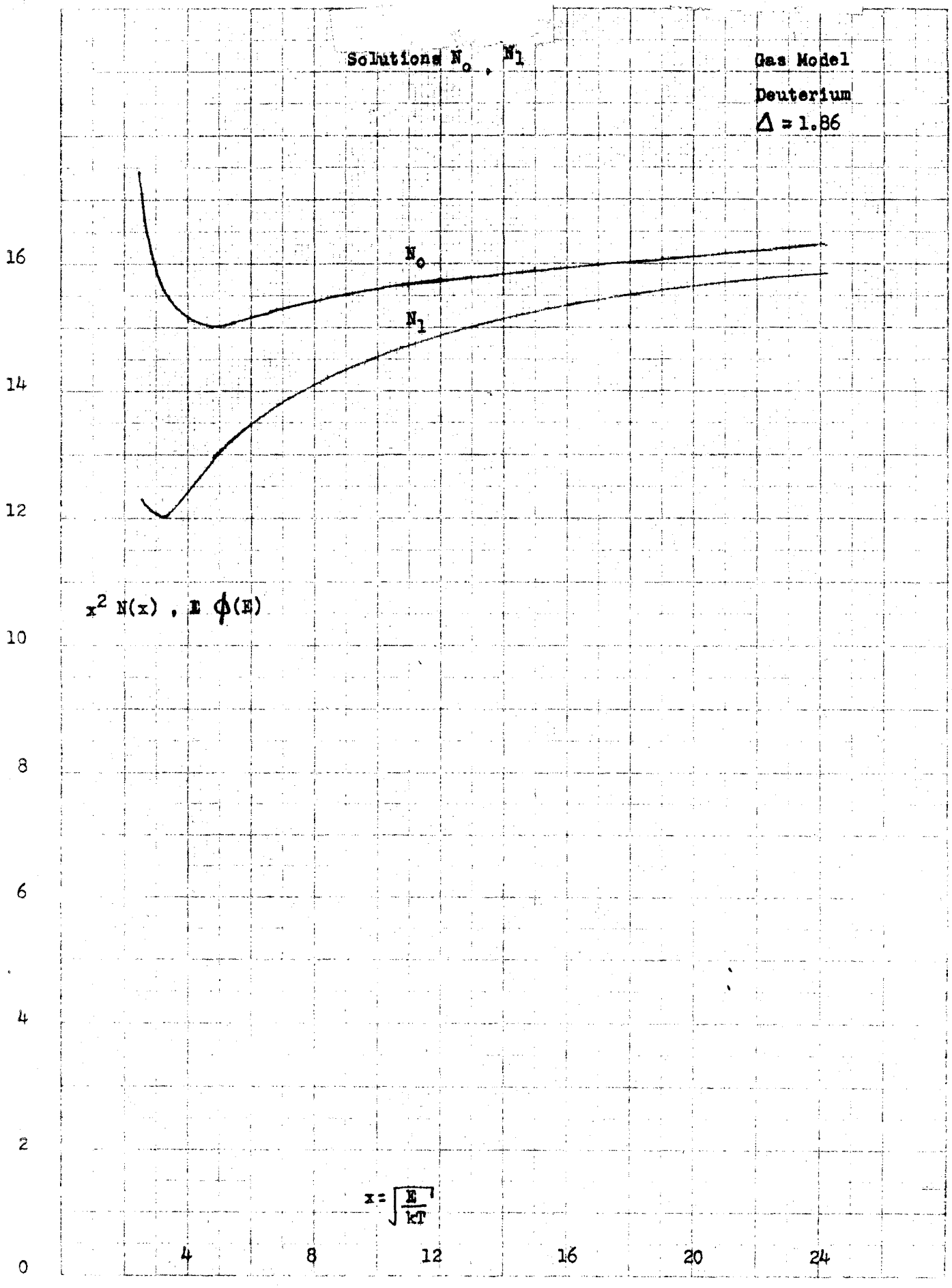
Solutions N_o , N_1
Gas Model
Deuterium
$\Delta = 1.86$
N_o
N_1
$x^2 N(x)$, $E\,\phi(E)$
$x = \sqrt{\frac{E}{kT}}$
0
2
4
6
8
10
12
14
16
4
8
12
16
20
24

Paper II-E

A REMARK ON NEUTRON THERMALIZATION THEORY

G. Liebfried
Aachen, Germany

A Remark on Neutron Thermalization Theory

G.Leibfried, Aachen

The slowing down of neutrons by a monoatomic moderator gas with temperature can be expressed by a variational formalism. Using a suitable trial solution one can calculate the effective neutron temperature and the upper limit of the thermal region by variation. Results are given for large moderator masses and small absorption.

Variational principle for the slowing down equation

The slowing down equation for neutrons in a monoatomic gas with 1/v-absorption and temperature T is generally a complicated integral-equation[1]. It can be shown however that the kernel of this equation may be symmetrized. This means that one can set up a variational principle for the slowing down equation. The treatment becomes especially simple for large atomic weights A.

The slowing down equation for the flux ϕ (E) per unit energy is then a differential equation[2]

$$(1) \qquad \frac{d}{dE}\left\{\xi \Sigma_s \left\{(E-kT)\phi + EkT\frac{d\phi}{dE}\right\}\right. - \Sigma_a(E)\phi + S(E) = 0$$

$\xi = \frac{2}{A}$ is the mean logarithmic energy loss for large A, Σ_s denotes the energyindependent macroscopic cross-section for scattering, Σ_a is the macroscopic cross-section for capture, assumed to be proportional to $1/E^{1/2}$, k is Boltzmanns constant and S (E) is the source density per unit energy and time. The first term in (1) is the derivative of the slowing down density.

Equation (1) is equivalent to the variational principle

$$(2) \qquad \delta J = \delta \int L\, dE = 0 \qquad \text{with}$$

(3) $$L = -e^{-\beta E}\left\{\phi'^2 + \phi^2[\gamma\beta^{1/2}E^{-3/2} - \beta E^{-1}] - \phi\, 2s\beta/(\xi\Sigma_s E)\right\}$$

where $\beta = 1/kT$ and $\gamma = \Sigma_a(kT)/\xi\Sigma_s$ (the ratio of absorption to slowing down power at $E=kT$, $\Sigma_a(E) = \Sigma_a(kT)/(\beta^{1/2}E^{1/2})$)
The ' stands for d/dE. The variational conditions are as usual: vanishing variation at the limits of the integral in (2). The variational equation

(2a) $$-\frac{d}{dE}\frac{\partial L}{\partial \phi'} + \frac{\partial L}{\partial \phi} = 0$$

is identical with equation (1),

It is convenient to introduce a new function $\psi(E)$ by

(4) $$\phi = \psi E e^{-\beta E}$$ together with

(3a) $$L = -e^{-\beta E}\left\{E^2\psi'^2 + \gamma\beta^{1/2}E^{1/2}\psi^2\right\} + \psi\, 2s\beta/\xi\Sigma_s$$

ψ measures the deviation of the flux distribution from the Maxwellian distribution $Ee^{-\beta E}$ at temperature T. The expressions (3) and (3a) are not quite identical. When passing from (3) to (3a) a perfect differential has been omitted since this does not change the validity of the variational principle.

Trial solutions

If one assumes a source term $S(E) = C\,\delta(E-E_0)$, which means C neutrons per sec created at energy E_0 (E_0 large as compared with kT), and if γ is small one expects a nearly thermal distribution of neutrons with a slight change of neutrons temperature in the thermal energy region and for higher energies the normal slowing down distribution uneffected by

the moderating temperature. The problem is how to define the "neutron temperature" and the "thermal region". This can be done by using the variational principle (2) with suitable trial functions e.g.:

$$\psi_1 = C_1 e^{\alpha E} \quad ; \qquad 0 \leq E \leq \varepsilon \qquad \text{"thermal region"}$$

$$(5)\ \psi = \psi_2 = C_2 e^{\beta E}/E^2 \; ; \qquad \varepsilon \leq E \leq E_0 \qquad \text{"fast region"}$$

In the thermal region this corresponds to a Maxwellian - distribution with neutron temperature T_n $\left(\phi = C_1 E e^{(\alpha-\beta)E}; \alpha = 1/kT - 1/kT_n\right)$. In the fast region one has $\phi = C_2/E$, where C_2 is determined by the ratio of the production of neutrons C to the slowing down power $\xi\Sigma_s$ $(C_2 = C/\xi\Sigma_s)$. This is the usual solution neglecting absorption[3]. This solution may be expected to hold if γ is small and ε/kT turns out to be large.

It is convenient and essential to use a fixed as well as a good solution in the fast region because the Lagrangian according to (3) and (5) contains an exponential increasing term in the fast region. Then one has adjustable parameters referring to the thermal region only. One may remember the fact that with zero-temperature the variational principle breaks down which is clearly seen in (3). Symmetrization of the basic integral equation is no longer possible. So it is reasonable to confine the variation to the thermal region only. C_1 is determinded by a continuity condition as will be seen in the next section. The integral $\mathcal{F}$ in (2) then depends on the variational parameters ε, α.

The best choice of ε, α is given by equation (2) which means that for the right values of ε, α the integral $\mathcal{J}$ is stationary. The expression (3a) for the Lagrangian L shows that $\mathcal{J}$ is a maximum because the second variation

$$\delta_2 \mathcal{J} = \int -e^{-\beta E} \left\{ E^2 (\delta\psi')^2 + \gamma \beta^{1/2} E^{1/2} (\delta\psi)^2 \right\} dE$$

is negative definite. So all variations lower the stationary value of $\mathcal{J}$. Hence when one has approximate solutions the one with the largest value of $\mathcal{J}$ is the best approximation.

Determinations of the parameters C_1, ε, α

a) In equation (2) L and therefore ψ' must exist, so it is necessary that ψ be continuous at $E = \varepsilon$

(6) $\quad \psi_1(\varepsilon) = \psi_2(\varepsilon) \quad ; \qquad C_1 e^{\alpha\varepsilon} = C_2 e^{\beta\varepsilon} / \varepsilon^2$

This defines C_1 as a function of ε and α.

b) Variation of ε leads to

(7) $\quad \left(\frac{\partial \mathcal{J}}{\partial \varepsilon} \right)_\alpha = 0$, where $\mathcal{J}$ is given by

(8) $$\mathcal{J} = \int_0^\varepsilon L(\psi_1)\, dE + \int_\varepsilon^\infty L(\psi_2)\, dE$$

So one gets with

$$\frac{\partial \mathcal{J}}{\partial \varepsilon} = L(\psi_1(\varepsilon)) - L(\psi_2(\varepsilon)) + \int_0^\varepsilon \frac{\partial}{\partial \varepsilon} L(\psi_1)\, dE$$

$$\int_0^{\varepsilon} \frac{\partial}{\partial \varepsilon} L(\psi_1)\, dE = \frac{\partial \ln C_1^2}{\partial \varepsilon} \int_0^{\varepsilon} L(\psi_1)\, dE = \frac{\partial \ln C_1^2}{\partial \varepsilon} \cdot \mathcal{J}_1$$

$$\frac{\partial \ln C_1^2}{\partial \varepsilon} = 2(\beta - \alpha) - 4/\varepsilon = 2\left\{\psi_2'(\varepsilon) - \psi_1'(\varepsilon)\right\} / \psi_1(\varepsilon)$$

$$\left\{L(\psi_1) - L(\psi_2)\right\}_{E=\varepsilon} = e^{-\beta\varepsilon} \varepsilon^2 \left\{\psi_2'^2(\varepsilon) - \psi_1'^2(\varepsilon)\right\}$$

the condition

(7a) $$\frac{\partial \mathcal{J}}{\partial \varepsilon} = \left\{\psi_2'(\varepsilon) - \psi_1'(\varepsilon)\right\}\left\{2\mathcal{J}_1 / \psi_1(\varepsilon) + \varepsilon^2 e^{-\beta\varepsilon}\left(\psi_2'(\varepsilon) + \psi_1'(\varepsilon)\right)\right\} = 0$$

One may convince oneself that only the vanishing of the second factor gives a reasonable condition:

(7b) $$2\mathcal{J}_1 + \varepsilon^2 e^{-\beta\varepsilon} \psi_1(\varepsilon)\left(\psi_2'(\varepsilon) + \psi_1'(\varepsilon)\right) = 0$$

Since $\psi_2'(\varepsilon) + \psi_1'(\varepsilon) = (\beta - 2/\varepsilon)\psi_2(\varepsilon) + \alpha\psi_1(\varepsilon) = (\alpha + \beta - 2/\varepsilon)\psi_1(\varepsilon)$

one has

(7c) $$2\mathcal{J}_1 + \varepsilon^2 e^{-\beta\varepsilon}(\alpha + \beta - 2/\varepsilon)\psi_1^2(\varepsilon) = 0$$

Using (5) and dividing (7c) by C_1^2 one gets eventually

(7d) $$2\bar{\mathcal{J}}_1 + \varepsilon^2(\alpha + \beta - 2/\varepsilon)\, e^{-\beta\varepsilon + 2\alpha\varepsilon} = 0$$

where $$\bar{\mathcal{J}}_1 = \mathcal{J}_1 / C_1^2 = -\int_0^{\varepsilon} e^{-\beta E + 2\alpha E}\left\{\alpha^2 E^2 + \gamma\beta^{1/2} E^{1/2}\right\} dE$$

c) Variation of α leads to

(9) $$\left(\frac{\partial \mathcal{F}}{\partial \alpha}\right)_{\varepsilon} = 0$$

Since $$\frac{\partial \mathcal{F}}{\partial \alpha} = \frac{\partial}{\partial \alpha}\left(C_1^2 \cdot \bar{\mathcal{F}}_1\right) = C_1^2 \frac{\partial \bar{\mathcal{F}}_1}{\partial \alpha} + \bar{\mathcal{F}}_1 \cdot \frac{\partial C_1^2}{\partial \alpha}$$

one has with $\frac{\partial \ln C_1^2}{\partial \alpha} = -2\varepsilon$ according to (6)

(9a) $$\frac{\partial \bar{\mathcal{F}}_1}{\partial \alpha} = 2\varepsilon \bar{\mathcal{F}}_1$$

d) Conservation of neutrons

Integrating (1) one gets

(10) $$\int \Sigma_a(E)\, \phi(E)\, dE = C = C_2 \xi \Sigma_s$$

because the slowing down term does not contribute to the integral.

This equation describes the conservation of neutrons i.e. the number of absorbed neutrons equals the number of neutrons emitted by the source in a stationary state. One can use (1b) as an additive useful constraint to the variational conditions. This means that only one parameter would remain for the variational procedure. On the other hand it is not necessary to use (10) whereas the constraint (6) is necessary for the existence of the Lagrangian L. Equation (10) is not contained in the condition (6), (7) and (9). One would have to impose it additively. We will drop the condition (10) for sake of simplicity since one can assume that the variational procedure alone gives reasonable results already. One might even guess that additive conditions which do not arise out of the variational procedure would disprove the result. One can decide this

question by comparing the numerical value of $\mathcal{F}$ for the two methods: the larger the value of $\mathcal{F}$ the better the approximation.

Evalution of the variational conditions for small absorption.

For small absorption γ one expects $\eta = \beta\varepsilon$ to be large $e^{-\eta}$, α/β and $\varepsilon\alpha$ to be small. Hence one can try to expand $\bar{\mathcal{F}}_1$ in the equations (7d) and (9a) in powers of α

(11) $$\bar{\mathcal{F}}_1 = A_0 + A_1\alpha + A_2\alpha^2 \quad \text{with}$$

(11a) $$A_0 = -\int_0^\varepsilon e^{-\beta E}\gamma\beta^{1/2}E^{1/2}\,dE$$

(11b) $$A_1 = -2\int_0^\varepsilon e^{-\beta E}\gamma\beta^{1/2}E^{3/2}\,dE$$

(11c) $$A_2 = -\int_0^\varepsilon e^{-\beta E}(E^2 + 2\gamma\beta^{1/2}E^{3/2})\,dE$$

The integrals may be evaluated asymptotically.

(11a') $$A_0 \approx -\gamma\sqrt{\pi}/2\beta$$

(11b') $$A_1 \approx -\gamma 3\sqrt{\pi}/\beta^2$$

(11c') $$A_2 \approx -2/\beta^3$$

where only the largest terms have been taken into regard.

Now (7d) reads asymptotically

(7e) $$2A_0 + \varepsilon^2\beta e^{-\beta\varepsilon} = 0$$

omitting terms with powers of α and neglecting $2/\varepsilon$ as compared with β.

Using (11a') one gets

$$(12) \qquad \gamma\sqrt{\pi} = \eta^2 e^{-\eta}$$

and for small γ approximately

$$(13) \qquad \eta = \ln 1/\gamma\sqrt{\pi}$$

Equation (9) passes to

$$(14) \qquad A_1 + 2A_2\alpha = 2\varepsilon(A_0 + A_1\alpha + A_2\alpha^2)$$

Since $\varepsilon\alpha$ is supposed to be small one can drop the terms containing α right hand and neglect A_1 as compared with $2\varepsilon A_0$

$$(15) \qquad \alpha = \gamma\sqrt{\pi}\,\varepsilon\beta^2/4 = \gamma\eta\beta\sqrt{\pi}/4$$

So one has eventually

$$(16) \qquad \alpha = \gamma\beta \ln 1/\gamma\sqrt{\pi} \cdot \sqrt{\pi}/4$$

which shows $\alpha\varepsilon$ to be small in accordance with the assumption.

The temperature difference $\delta T = T_n - T$ turns out to be

$$(17) \qquad \delta T/T = \alpha/\beta = \gamma \ln 1/\gamma\sqrt{\pi} \cdot \sqrt{\pi}/4$$

$$(17') \qquad \delta T/T = \frac{A\sqrt{\pi}\,\sigma_a(kT)}{8\,\sigma_s} \cdot \ln \frac{2\sigma_s}{A\sigma_a(kT)\sqrt{\pi}} ,$$

where σ_s and σ_a denote the microscopic scattering and absorption cross-section.

This result should be valid for small γ only, say $\gamma \lesssim 0.1$

Apart of the $\ln 1/\gamma$ dependence of δT corresponding to (17) is in accordance with Cohen's [1] results. Take for instance $A\sigma_a/\sigma_s = 0.1$ one gets for the second factor in (17')

the value 0,5 whereas Cohen gives 0,6. The deviations are of course more serious for very small values of γ, but here the deviations δT are insignificant. It seems however that the neutron temperature defined by the trial solution varies indeed as $\gamma \ln 1/\gamma$ rather than γ for small absorption.

Conclusion

In problems where the concept of neutron temperature and thermal region turns out to be useful at all [1] the variational formalism shows an easy way how to define and to calculate these quantities. The variational principle can as well be applied to larger values of γ and to the case of smaller moderator masses, here the formalism seems to be especially adapted for numerical work.

Acknowledgements

I wish to thank Dr.A.M.Weinberg who stimulated this paper by sending the manuscript of his and E.P.Wigner's new book on reactor physics.

References

[1] E.R.Cohen: A surview of neutron thermalization theory. PICG Vol 5, p 405 (1955); Nuclear Science and Engineering 2, 227 (1957).

Footnotes

1) For the basic principles of thermalization theory the reader may be referred to the article of E.R.Cohen [1].

2) One gets this equation by expanding the exact integral equation in powers of $1/A$, neglecting higher powers than $1/A$.

3) Of course one can find better solutions in the fast region e.g.

$$\psi = e^{\beta E - 2\Sigma_a(E)/\xi\Sigma_s} \cdot C/\xi\Sigma_s E(E-2kT)$$

or

$$\phi = e^{-2\Sigma_a(E)/\xi\Sigma_s} \cdot C/\xi\Sigma_s(E-2kT)$$

which corresponds to a more refined slowing down theory [1]. However in the case of small γ or large ε/kT there is no essential difference as compared with (5).

Paper II-F

THERMAL NEUTRON FLUX IN A NONABSORBING HEAVY GAS MEDIUM WITH A TEMPERATURE DISCONTINUITY

D. A. Kottwitz
Hanford Laboratories Operation

Thermal-Neutron Flux in a Medium With a Temperature Discontinuity

D. A. Kottwitz
Hanford Laboratories Operation
Hanford, Washington

Abstract

The energy and spatial dependence of the steady state neutron flux has been derived for a nonabsorbing infinite gaseous medium in which the medium temperature is a step function of position. In the heavy gas and diffusion approximations, the energy dependent transport equation reduces to a second order partial differential equation which is separable in each region of constant temperature. The solution is a series of eigenfunctions, the leading term of which is Maxwellian in form. From general properties of the differential equation, it can be shown that the total flux (integrated over all energies) is independent of position. This latter result is in agreement with the theory of irreversible processes.

THERMAL NEUTRON FLUX IN A NONABSORBING HEAVY GAS MEDIUM WITH A TEMPERATURE DISCONTINUITY

INTRODUCTION

A question that has aroused some interest of late is the nature of the energy spectrum of neutrons which are in the thermal energy range but which are not in thermal equilibrium, that is, not in a pure Maxwellian distribution. For example, it is of interest to know the "thermal" energy spectrum of neutrons in a moderator which has a nonuniform temperature. This paper describes work on a simple particular case of the latter problem.

In order to obtain analytical results, both geometry and physical system are assumed as simple as possible. Thus, we not only employ slab geometry in an infinite medium, but also assume that the medium temperature is an abrupt step function of position. We assume no sources or sinks of neutrons, and seek only the steady state solution. The scattering medium is assumed to be a heavy gas; this means that scattering is nearly isotropic in the laboratory system and that the average energy change in a scattering event is small. Furthermore, the P_1 (or diffusion) approximation is made, thus assuming that the angular distribution of the flux is represented reasonably well by the zeroth and first spherical harmonics.

DIFFERENTIAL EQUATION AND BOUNDARY CONDITIONS

The result of the assumptions and approximations mentioned above is that the integro - differential equation of transport theory reduces to the second order partial differential equation[1]

$$\frac{\delta^2 F}{\delta x^2} + 6\mu\sigma_o^2 \left(1 + E\frac{\delta}{\delta E} + ET\frac{\delta^2}{\delta E^2}\right) F = 0, \qquad (1)$$

where $F(x, E)$ = spherically symmetric component of the flux.

μ = ratio of neutron mass to gas nuclear mass.

σ_o = bound macroscopic scattering cross section of medium

$T(x)$ = temperature of medium

Boltzmann's constant = 1.

This equation is correct to first order in the mass parameter μ. The spatial dependence of T is given by

$$T(x) = \begin{cases} T_1 & x < 0 \\ T_2 & x > 0. \end{cases} \tag{2}$$

In order to obtain a unique physical solution, we have the following boundary conditions at our disposal. The flux must remain finite at infinite distances, and both flux and current must be continuous at the interface between the two temperature regions. For zero energy, the flux must vanish, and for large energy, it must approach zero rapidly enough to make all moments of the flux finite. These conditions on the energy dependence hold because the flux must be intermediate between two Maxwellian functions, each of which has these characteristics. Analytically, these conditions on F (x, E) are

$$F(\pm \infty, E) = \text{finite function} \tag{3}$$

$$F(0+, E) = F(0-, E) \tag{4}$$

$$\left.\frac{\delta F(x,E)}{\delta x}\right|_{x = 0+} = \left.\frac{\delta F(x,E)}{\delta x}\right|_{x = 0-} \tag{5}$$

$$F(x,0) = 0 \tag{6}$$

$$F(x,\infty) = 0 \tag{7}$$

It should be noted that (5) is only the zeroth order (in μ) approximation to the exact equation expressing continuity of neutron current across the interface.

The derivation of (1) implies that (1) and (5) go together in a consistent approximation.[1] However, for completeness, we shall subsequently prove that only the zeroth approximation of the boundary condition, represented by (5), is physically consistent with the differential equation (1).

AN INTEGRAL CONDITION

Before beginning the detailed solution of (1), let us establish a result for the flux as a whole. Integrating (1) over all energies, while noting the presence of a perfect differential, we get

$$\frac{d^2\phi(x)}{dx^2} + 6\mu\sigma_0^2 \left[ET \frac{\delta F}{\delta E} + (E - T) F \right]_0^\infty = 0 , \tag{8}$$

where

$$\phi(x) \equiv \int_0^\infty F(x,E)\, dE .$$

Since the boundary conditions require that F be regular and vanish at $E = 0$ and vanish strongly at $E = \infty$, the expression in brackets vanishes. The result is

$$\phi(x) = A + Bx \tag{9}$$

The boundary conditions at $|x| = \infty$ require that B vanish. Thus the conclusion is that the physically valid solution of (1) which is finite at $|x| = \infty$ must satisfy the condition [2]

$$\int_0^\infty F(x,E)\, dE = \text{constant}. \tag{10}$$

In Appendix I, it will be shown that (10) can be related to well known results in the theory of irreversible processes. At this point we shall use (10) only to verify that (5) is the proper version of the condition of neutron current continuity.

The steady state condition in the problem, together with the absence of sources and sinks, means that the net flow of neutrons is zero everywhere. It does not mean that the current density, $j(x,E)$, vanishes identically but only that the integral of j over all energy vanishes. The weaker condition not only conserves neutrons but allows "hot" neutrons to flow from the high temperature region to the low temperature region, while "cold" neutrons drift in the opposite direction. Thus, our solution must satisfy

$$\int_0^\infty dE\ j(x,E) = 0 \tag{11}$$

where

$$j(x,E) = -D(x,E)\ \frac{\delta F(x,E)}{\delta x}.$$

From the work of Nelkin and Hurwitz[1], one finds that to first order in μ the diffusion coefficient is

$$\begin{aligned} D(x,E) &\equiv \left[3\ (1 - \overline{\cos\theta})\ \sigma(E,x)\right]^{-1} \\ &= \left[3\ \sigma_0(1 + \mu\ \left\{T/2E - 8/3\right\})\right]^{-1} \end{aligned} \tag{12}$$

Now differentiating (10) with respect to x, we find that

$$\int_0^\infty \frac{\delta F(x,E)}{\delta x}\ dE = 0 \tag{13}$$

Equations (11) and (12) furnish a condition on F similar to (13), but differing from it on account of the presence of the first order term in (12). It is clear from diffusion theory that (13) ought to be identical with (11) and (12). Thus, we conclude that consistent results can be obtained only if the first order term is dropped from (12). Thus, the current density becomes

$$j(x,E) = -(3\sigma_o)^{-1} \frac{\delta F(x,E)}{\delta E} \tag{14}$$

and (5) correctly expresses the desired condition at the interface.

SOLUTION OF THE DIFFERENTIAL EQUATION

The form of (1) and (2) and the boundary conditions (3)---(7) suggests the following method: (a) obtaining a solution in each halfspace of constant temperature by separation of variables, and (b) connecting these solutions at the interface by means of (4) and (5). It is convenient to write (1) in dimensionless form by introducing reduced energy and position variables, as follows

$$\begin{cases} y \equiv \frac{x}{\lambda} \equiv \sigma_o \sqrt{6\mu}\, x \\ \epsilon \equiv \frac{E}{T} \end{cases} \tag{16}$$

The differential equation becomes

$$\frac{\delta^2 F}{\delta y^2} + \left(1 + \epsilon \frac{\delta}{\delta \epsilon} + \epsilon \frac{\delta^2}{\delta \epsilon^2}\right) F = 0. \tag{17}$$

Assuming product solutions of the form $f(\epsilon)\, h(y)$ and introducing the separation constant k, we get the ordinary differential equations

$$h'' - kh = 0 \tag{18}$$

$$\epsilon f'' + \epsilon f' + (1 + k) f = 0 \tag{19}$$

Acceptable solutions of (18) have the form

$$h(y) = \exp\left(-\sqrt{k}\, |y|\right) \tag{20}$$

It is convenient to define a new function $g(\epsilon)$ by factoring a Maxwellian function out of $f(\epsilon)$. Thus,

$$f(\epsilon) \equiv \epsilon \exp(-\epsilon)\, g(\epsilon) \tag{21}$$

then (19) becomes another confluent hypergeometric equation for $g(\epsilon)$

$$\epsilon\, g'' + (2 - \epsilon)\, g' + kg = 0 \tag{22}$$

The general solution of (22) is

$$g(\epsilon) = C_1\, \Phi\,(-k|2|\epsilon) + C_2\, G(-k|2|\epsilon), \tag{23}$$

where $\Phi\,(-k|2|\epsilon)$ is a confluent hypergeometric function and $G(-k|2|\epsilon)$ is a Gordon function[3].

The Gordon functions would lead to a finite flux at $\epsilon = 0$ and thus can be omitted from further consideration. The confluent hypergeometric functions are satisfactory at $\epsilon = 0$, and must be inspected as $\epsilon \to \infty$. Consideration of the asymptotic form of $\Phi\,(-k|2|\epsilon)$ shows that, except for a discrete set of values of k, the flux would vary asymptotically as an inverse power of ϵ and thus would not vanish fast enough to make all energy moments finite. However, for k = 0,1,2,----etc., $\Phi\,(-k|2|\epsilon)$ is a polynomial, which leads to a satisfactory behavior of the flux at large energies. The infinite set of polynomials is in fact one of the families of Laguerre polynomials,[3,4] as follows*

$$\Phi\,(-k|2|\epsilon) \equiv \frac{1}{k+1}\, L_k^1(\epsilon), \quad k = 0,1,2,---- \tag{24}$$

Collecting the results of this section, we conclude that the solution of (17) is

---

* The normalization of reference (4) has been used here. Note the superscript 1 in equation (24); for notational simplicity it will be omitted henceforth.

$$F(y,\epsilon) = \epsilon \exp(-\epsilon) \sum_{m=o}^{\infty} K_m L_m(\epsilon) \exp(-\sqrt{m}\,|y|), \tag{25}$$

where the K_m are expansion coefficients to be determined by the continuity conditions (4) and (5) at the interface.

MATCHING SOLUTION AT THE INTERFACE

In each temperature region the flux can be expressed as a series of the form (25). Thus, we have

$$F(y,E) = \epsilon_1 \exp(-\epsilon_1) \sum_{m=o}^{\infty} \frac{A_m}{T_1} L_m(\epsilon_1) \exp(\sqrt{m}\, y), \qquad (y \leq 0)$$

$$F(y,E) = \epsilon_2 \exp(-\epsilon_2) \sum_{m=o}^{\infty} \frac{B_m}{T_2} L_m(\epsilon_2) \exp(-\sqrt{m}\, y), \qquad (y \geq 0) \tag{26}$$

where

$$\epsilon_1 = E/T_1$$

$$\epsilon_2 = E/T_2$$

Application of (4) and (5) to (26) gives

$$\epsilon_1 \exp(-\epsilon_1) \sum_{m=o}^{\infty} \frac{A_m}{T_1} L_m(\epsilon_1) = \epsilon_2 \exp(-\epsilon_2) \sum_{m=o}^{\infty} \frac{B_m}{T_2} L_m(\epsilon_2)$$

$$\epsilon_1 \exp(-\epsilon_1) \sum_{m=o}^{\infty} \frac{\sqrt{m}A_m}{T_1} L_m(\epsilon_1) = -\epsilon_2 \exp(-\epsilon_2) \sum_{m=o}^{\infty} \frac{\sqrt{m}A_m}{T_2} L_m(\epsilon_2) \tag{27}$$

To obtain the set of equations satisfied by the constants A_m and B_m, we multiply each of equations (27) by $L_m(\epsilon_2)$. Then use the change of scale formula (II-3) in Appendix II to express $L(\epsilon_2)$ on the left hand sides as a linear combination of

$L(\epsilon_1)$ and integrate over E. Application of the orthornormalization integral (II-2) gives

$$B_n = \sum_{q=o}^{n} \binom{n}{q} \left(\frac{T_1}{T_2}\right)^q \left(1 - \frac{T_1}{T_2}\right)^{n-q} A_q$$

$$-\sqrt{n}\, B_n = \sum_{q=o}^{n} \binom{n}{q} \left(\frac{T_1}{T_2}\right)^q \left(1 - \frac{T_1}{T_2}\right)^{n-q} \sqrt{q}\, A_q \tag{28}$$

where $\binom{n}{q}$ is a binomial coefficient.

Elimination of the B_n results in an infinite triangular array of equations for the A_n, which can be solved successively for A_1, A_2, etc., in terms of the arbitrary coefficient A_o. This array is

$$\sum_{q=o}^{m} \binom{m}{q} \left(\frac{T_1}{T_2}\right)^q \left(1 - \frac{T_1}{T_2}\right)^{m-q} \left(\left[\frac{q}{m}\right]^{1/2} + 1\right) A_q = 0 \,. \tag{29}$$

The temperature dependence of the A's is easily seen to be

$$A_n = C_n \left(\frac{T_1}{T_2} - 1\right)^n \left(\frac{T_1}{T_2}\right)^{-n}$$

$$= C_n \left(1 - \frac{T_2}{T_1}\right)^n, \tag{30}$$

where the C's are universal constants which satisfy

$$\sum_{q=o}^{m} \binom{m}{q} \left(\left[\frac{q}{m}\right]^{1/2} + 1\right) (-1)^q C_q = 0 \tag{31}$$

Setting $A_o = C_o = 1$, we find for the first few values of C_n

$$\begin{aligned} C_o &= 1 \\ C_1 &= 0.5 \\ C_2 &= 0.353553 \\ C_3 &= 0.280330 \\ C_4 &= 0.235546 \\ C_5 &= 0.204981 \\ C_6 &= 0.182621 \end{aligned} \tag{32}$$

So far we have solved (28) only for A_n. However, the symmetry of equations (27) shows that B_n can be obtained from A_n by interchanging T_1 and T_2. Thus,

$$B_n = Cn \left(1 - \frac{T_1}{T_2}\right)^n \tag{33}$$

Now combining (26), (30), and (33), we can write the final result as

$$F(y,E) = \frac{E}{T^2} \exp\left(-\frac{E}{T}\right) \sum_{n=o}^{\infty} C_n \left(1 - \frac{T_o}{T}\right)^n L_n\left(\frac{E}{T}\right) \exp\left(-\sqrt{n}\,|y|\right), \tag{34}$$

where T is the local medium temperature and T_o is the medium temperature across the interface.

DISCUSSION

The flux given by (34) is a Maxwellian function modulated by an infinite series of functions each of which, except the first, decays exponentially with distance from the interface. As expected, it reduces to a simple Maxwellian asymptotically at large distances from the plane of temperature discontinuity. It also satisfies the integral condition (10).

An important question is the nature of the transition from one Maxwellian flux to the other in the vicinity of the discontinuity. Unfortunately, each term of the energy spectrum has a different relaxation length. The longest of these, however, occurs in the first correction term and might well be called the fundamental relaxation length. In fact, it is just the length λ defined in (16). The relaxation length for the n-th mode is

$$\lambda_n = \frac{\lambda}{\sqrt{n}} = \frac{1}{\sigma_o \sqrt{6\mu n}} \tag{35}$$

To study the question of the transition in somewhat more detail, let us attempt to find an "effective temperature" of the flux spectrum as a function of position. The simplest way to define a temperature is in terms of the average energy of the

flux. Remembering that the (flux) average of the energy for a Maxwellian flux is 2T, let us take

$$T_{eff} = (1/2)\bar{E} \tag{36}$$

Using the flux given by (34) and the orthornormalization integral (II-2), we find

$$\begin{aligned} T_{eff} &= (1/2)(T_1 + T_2) + (1/2)(T_1 - T_2)(1 - \exp[x/\lambda]), \quad x \leq 0 \\ &= (1/2)(T_1 + T_2) - (1/2)(T_1 - T_2)(1 - \exp[-x/\lambda]), \quad x \geq 0 \end{aligned} \tag{37}$$

Thus, the effective temperature, as measured by the average energy, requires a distance of about 2λ to change from T_1 to T_2. Assuming, for example, that graphite is a heavy gas with $\mu = 1/12$, we get a relaxation distance

$$d \simeq 2\lambda = 2\sqrt{2}\ \lambda_s ,$$

where λ_s is the scattering mean free path.

An additional interesting feature of (34) is the particularly simple dependence of the expansion coefficients on the two temperatures in the system. Essentially, the flux is obtained as a power series in the temperature difference. This property allows us to draw conclusions about the convergence of the series in (34). Assuming that C_{n+1}/C_n approaches unity for large n and using (II-5), it is easy to show that the series converges in both temperature regions if

$$1/2 < T_1/T_2 < 2$$

and that it converges in the high temperature region if the temperature ratio is outside these limits. However, it has not yet been possible to prove convergence in the low temperature region when the temperature ratio is outside the above limits.

APPENDIX I

RELATION TO THE THEORY OF IRREVERSIBLE PROCESSES

The purpose of this appendix is to indicate briefly the connection between the integral condition (10) and the theory of irreversible processes.[5] First, let us note that the essence of the physical situation discussed here is just the type of process considered in the theory, i.e., a pair of coupled steady state transport phenomena. In our particular case, these phenomena are the transport of heat and the transport of particles in a neutron gas.

The theory of irreversible processes has been applied[5] to the so-called Knudsen gas, a system in which two containers of a gas are held at different temperatures by heat baths and in which the containers are thermally insulated from each other but connected by a small opening through which the gas particles may percolate. In the steady state situation, heat is carried by the gas from the hot reservoir to the cold but there is no net flow of matter. The thermodynamic parameters, such as pressure and density as well as temperature, are different in the containers. The theory gives the following relation between these quantities

$$\frac{\rho_1}{\rho_2} = \left(\frac{T_2}{T_1}\right)^{1/2} , \qquad \text{(I-1)}$$

where ρ_i = gas density in the i-th container

T_i = gas temperature in the i-th container.

It is a simple matter to verify that the neutron gas satisfies (I-1) far from the temperature discontinuity. Taking the asymptotic flux to be Maxwellian on each side and normalizing it to satisfy condition (10), one finds the desired result by integrating the number density over energy.

As a final remark, it should be mentioned that there must be a deeper connection between (1) and the theory of irreversible processes. It is well known[5] that the steady state processes covered by the theory are just those which minimize the time rate of production of entropy, subject to the constraints of the problem. Thus, it is reasonable to expect that (1) can be obtained from a variational principle which minimizes the rate of production of entropy. Such a demonstration would be quite instructive.

APPENDIX II

SOME USEFUL PROPERTIES OF THE LAGUERRE POLYNOMIALS $L_m^1(x)$.*

$$L_m(x) = \sum_{n=0}^{m} \binom{m+1}{n+1} \frac{(-x)^n}{n!} \tag{II-1}$$

$$\int_0^\infty dx\, x \exp(-x)\, L_m(x)\, L_n(x) = (m+1)\, \delta_{nm} \tag{II-2}$$

$$L_m\left(\frac{x}{a}\right) = \sum_{n=0}^{m} \binom{m+1}{n+1} \left(\frac{b}{a}\right)^n \left(1 - \frac{b}{a}\right)^{m-n} L_n\left(\frac{x}{b}\right) \tag{II-3}$$

$$(m+1)\, L_{m+1}(x) - (2m+2-x)\, L_m(x) + (m+1)\, L_{m-1}(x) = 0 \tag{II-4}$$

$$\left|L_m(x)\right| \leq (m+1) \exp(x/2) \tag{II-5}$$

* Note again that normalization is the one of reference (4) and that, as in the text of this paper, the superscript 1 has been omitted from the Laguerre function symbols.

REFERENCES

1. H. Hurwitz, Jr., M. S. Nelkin, and G. J. Habetler, Nuclear Science and Engineering 1, 280 (1950).

2. J. L. Powell, Unpublished Notes.

3. P. M. Morse and H. Feshbach, Methods of Theoretical Physics, McGraw-Hill (1953), p. 615 ff.

4. A. Erdélyi, et al., Higher Transcendental Functions, Vol. II, McGraw-Hill (1953).

5. S. R. de Groot, Thermodynamics of Irreversible Processes, Interscience (1951).

DAK:dgl

Session III: CRYSTALLINE EFFECTS

Paper III-A

INELASTIC SCATTERING OF SLOW NEUTRONS IN MODERATORS

D. J. Hughes A. M. Ghose
H. Palevsky P. Kienle
Brookhaven National Laboratory

Inelastic Scattering of Slow Neutrons in Moderators

D. J. Hughes A. M. Ghose
H. Palevsky P. Kienle

Brookhaven National Laboratory
Upton, Long Island, New York

Abstract

The details of the energy exchanges between slow neutrons and lattice vibrations are important in determining the manner in which moderation occurs and the neutron energy spectrum in different geometries. Measurements have been in progress for several years at Brookhaven in which the lattice vibrations are studied by means of the energy gain of incident cold neutrons. The cold neutrons, of energy 0.004 ev, are produced by filtration in cooled polycrystalline beryllium and the velocity of the scattered neutrons is determined by time of flight. For a single crystal of a coherent scattering material, the frequency of the phonons as a function of their wave number, i.e., the dispersion law, may be measured for both acoustical and optical vibrations. For incoherent scatterers the lattice vibration spectrum is obtained directly but not the detailed dispersion law. Measurements have been made for a number of moderators, among which ZrH exhibits[1] an intense optical lattice vibration at an energy of 0.134 ev.

---

1. Pelah, Eisenhauer, Hughes, and Palevsky, Phys. Rev. 108, 1091 (1957).

Gatlinburg Conference

Inelastic Scattering of Slow Neutrons in Moderators

D. J. Hughes

In listening to the papers and the discussion on the thermalization of neutrons it seems to me that people are going in various directions. I don't mean this in a derogatory way at all; I think they should. For example, suppose we start with the cross sections for inelastic scattering. If we knew these as functions of angle and energy change, we could probably then compute the neutron spectrum, which, I take it, is what most of you are interested in doing. Now we don't know this inelastic scattering in all its details. As we have discussed already, for neutrons of sufficiently high energy, i.e., an energy of a few volts at least, there isn't much difficulty. At these energies the atom acts as if it is free in the scattering process. But when the neutron energy drops below the order of a few tenths of a volt things become difficult, and it is extremely hard to calculate or even to measure the cross sections.

Now, although we can't measure the inelastic scattering cross section in every detail, if we were very very good we could compute it from the known details of the materials in which we are interested. For example, we have many energy levels, which represent the specific properties of various solids and liquids. These things have phonons in them, and one way to express properties of the materials is to give the frequency of the phonons as a function of the momentum, or the wave number, of the phonons. These dispersion curves are the fundamental information we need about, say, a crystal. If we had this information and again if we could do the complicated mathematics, we could calculate the cross sections

for the crystal and then the neutron spectrum. However, if we want to build reactors, or if we want to calculate the spectrum in reactors in the next 50 to 100 years, it is probably best not to wait until we measure all the dispersion curves of the materials involved. Nevertheless, in principle we could get all of these desired properties.

The information comes, of course, from various fields. We can measure the elastic properties of materials, and we can measure their specific heats, for example. The results give some information on the dynamics of the lattice. One of the most recent ways of getting information on the dynamics of the lattice is by inference from the measured inelastic scattering cross sections. That will be my subject for this evening, something about the methods in which the observed inelastic scattering cross sections are used to get these fundamental properties. So, in a way, we're going away from our goal, the neutron spectrum, but in principle we will arrive there eventually because from these fundamental dynamical properties of lattices, we can calculate everything we need. The interest of my group at Brookhaven is just this: getting the fundamental information from the observed inelastic scattering.

Another approach is to measure the inelastic cross sections at all desired energies and go from there to the spectrum by direct calculation. This is the type of work that is being started at Chalk River where Egelstaff is starting a very ambitious program of measuring the inelastic scattering as a function of energy and angle for various materials. It is the so-called scattering law experiment and its results can be used to get the spectrum. There is another method now being used for measuring the spectrum directly by time-of-flight

techniques. This is still another approach in which we go in the direction of the desired result, with little regard to basic theory.

Now what we want to learn in the approach followed at Brookhaven is the relationship between the wave number, that is, the inverse of the wavelength, and the frequency, that is, the energy of the phonons, in the lattice. Let us talk about a crystal in which there are phonons, that is, sound waves. They have a wave number vector $\vec{q}$, so that the momentum is equal to $\hbar \vec{q}$, and they have an angular frequency w, so the energy of a phonon is $\hbar$ w. The relationship between w and $\vec{q}$ is what we are trying to find. If we have this relationship, the dispersion curve, we have all the properties we want. Now a simple assumed form of this relationship, of course, is the Debye assumption. The Debye assumption is simply that w = cq, where c is the velocity of sound. This relationship leads to a distribution of vibrations in the crystal in which the number of vibrations of a certain frequency vs frequency, that is, g (w) vs w, rises rapidly then suddenly drops to zero. This is ~~a~~ the familiar Debye frequency spectrum, which follows directly from this assumption. Now this is an approximation; we will find out wherein it fails in our experiments.

The reason that we can learn a lot about the dispersion from the scattering of neutrons is that neutrons change both their momentum and their energy by a large amount in scattering. There is inelastic scattering of x-rays, but in that case, though the momentum changes a lot, the energy changes by an insignificant amount. Neutron scattering is much different, in fact, for a low enough incident energy the gain in the energy of the neutron is much larger than its incident energy, so that the relative gain in energy can be tremendous. These effects become more pronounced the lower the neutron energy

becomes.

In Figure 1 we see an example of the way in which the scattering changes with energy. Much of this material is very, very simple, but it is fundamental so I hope you don't mind my taking up your time with it. The total cross section of Figure 1 is for a material in which capture is small. At a neutron energy of several $e\surd$, the atom acts as if it's free, which in one sense means the scattering is all inelastic; as far as the crystal is concerned it <u>is</u> inelastic scattering. At somewhat lower energy we have the coherent elastic plus the inelastic scattering, and at very low energy there is scattering in which the neutron is moving so slowly it can only gain energy from the lattice.

Now the behavior of these "cold neutrons" is very different from the scattering of x-rays and it is in this region that we have been doing our work at Brookhaven. I will speak of this so-called "energy gain scattering" of cold neutrons, which have temperatures of the order of $30^{\circ}K$, so they actually are very cold. A property of any nuclear reaction in which the outgoing particle is fast compared to the incident particle is that it will have a cross section that is inversely proportional to velocity. So in this energy region we expect the cross section to be $1/v$ if the phonon that is absorbed has energy large compared to the energy of the neutron; and whenever we see an experimental cross section in this region that is $1/v$, we have a direct demonstration that the neutron is gaining energy large compared to its incident energy. Elastic scattering of neutrons, could it occur, would be constant with energy because the outgoing velocity is not large.

The elastic scattering, however, disappears for cold neutrons in most

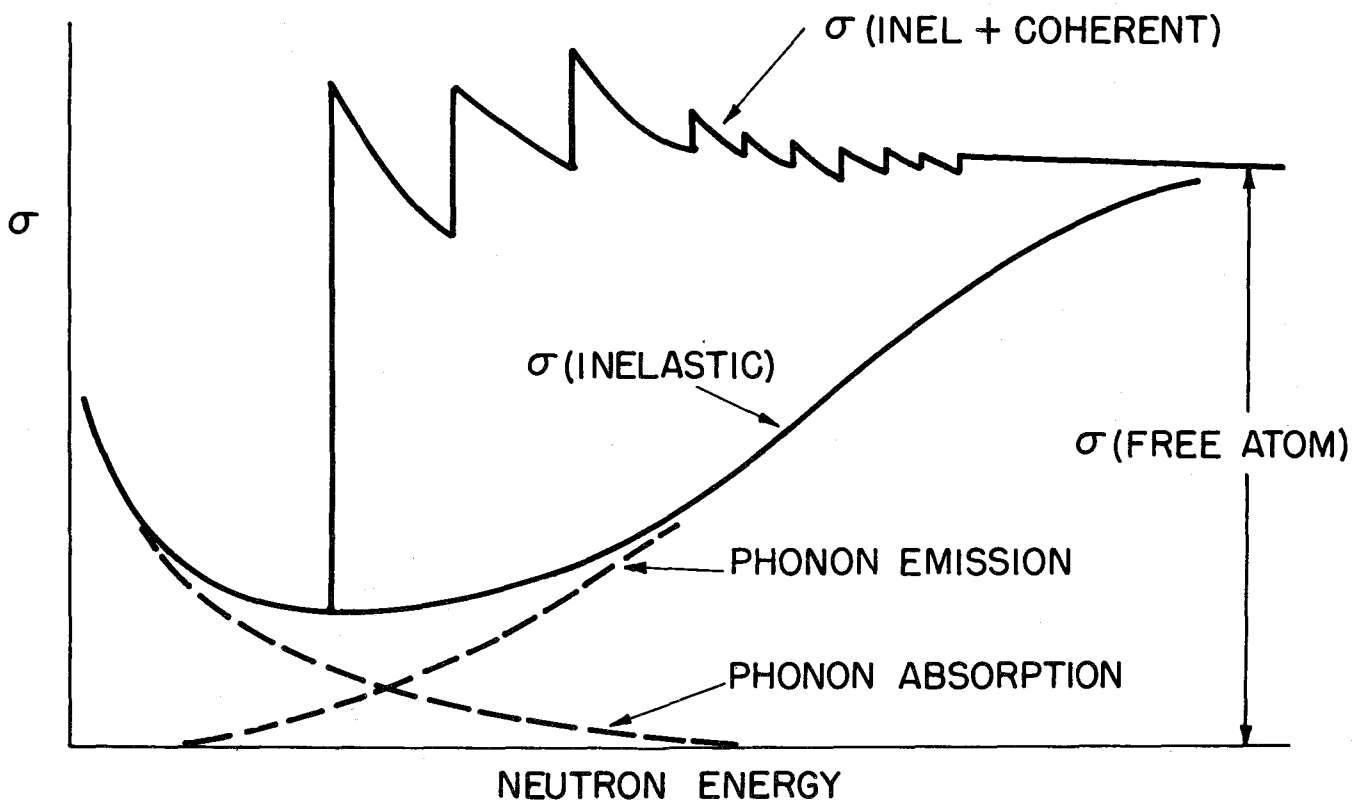

Fig. 1. The Variation of the Different Types of Scattering with Energy in a Material of Low Capture Cross Section

materials because the wavelength is so long that no Bragg scattering is possible. Some materials are very transparent to cold neutrons. For instance, in a piece of graphite for neutrons of wavelengths of, say, 8 A^{o}, the mean free path is about a meter!

Figure 2 is an experimental curve for beryllium, showing that these things really happen. We see the free atom cross section, the crystal cutoff, and the low cross section for slow neutrons with wavelength about 6 A^{o}. The cross section increases rapidly with temperature simply because there are more phonons in the crystal to hit the neutrons. The neutron is moving so much more slowly than the atoms that it really drifts through the crystal and is hit by the atoms, leaving the crystal rapidly. It must be moving rapidly because the cross section is seen to be 1/v. The cross section of beryllium, for sufficiently high temperature, actually becomes higher than the free atom cross section. You see that the cross section for cold neutrons in hot beryllium is quite high; it changes in this wavelength region from about a hundredth of a barn to, say, 10 barns, so the cross section can be changed by a factor of a thousand by merely changing the temperature of the material.

The total cross section we have been talking about doesn't really give much information about the lattice vibrations. In some cases it is valuable, however in particular for iron. Figure 3 is the total cross section of iron and copper with capture subtracted. The cross section here is not plotted against wavelength or neutron energy; it is the cross section at a particular wavelength out in the 1/v region as a function of sample temperature in degrees absolute. Now the cross section for copper rises with temperature and the

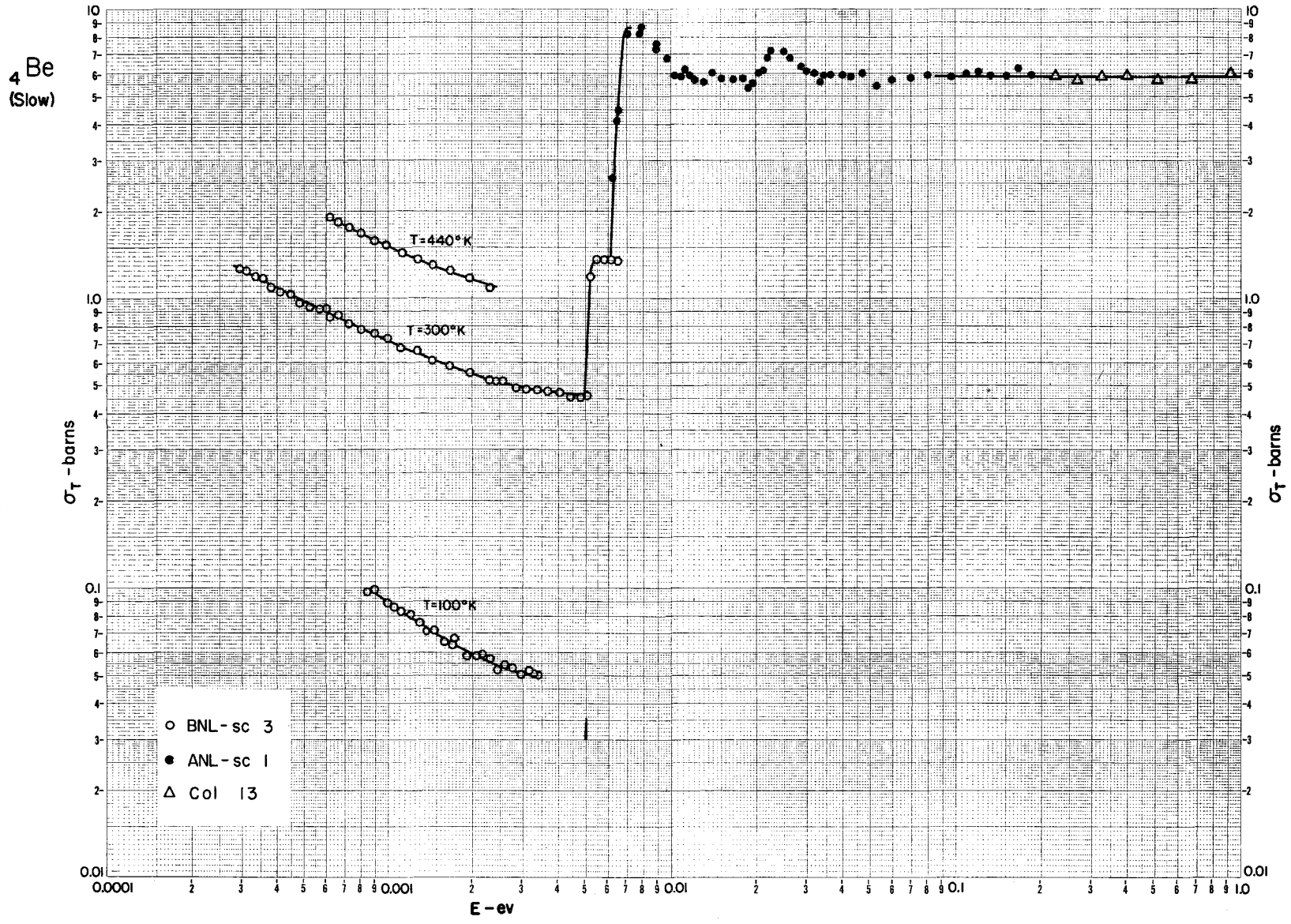

Fig. 2. Cross Section of Beryllium for Low Energy Neutrons, Showing the Rapid Change of Inelastic Scattering with Temperature

points agree so well with theory you can hardly see the points. The theory is based on a few simple parameters: the free atom cross section of copper, and the Debye temperature. Conversely, because so few parameters are needed we don't learn much about the lattice vibrations from this type of work. The total cross section is really analogous to the specific heat, and we don't learn much more than we do from specific heat measurements. It was interesting, however, that in the case of iron the points climbed above the theory quite rapidly and reached a maximum at the Curie point. Because the scattering is 1/v, it must be an interaction in which a large amount of energy is gained. Further, because of the difference between iron and copper and the peaking at the Curie point, it obviously is magnetic inelastic scattering. Actually it was this work that really spurred Van Hove on when he was developing his theory of the time-dependent correlation function, which he invoked to explain this scattering. It is really a type of critical scattering, like critical opalescence for light, ~~which occurs~~ and it is a maximum right at the Curie point.

However, we don't learn much about the details of the lattice dynamics by studying the total cross section alone. What we really want to do is to have neutrons come in, pick up just one phonon, and come out with relatively high energy. In the case where the neutron coming in has essentially zero energy we can say that since momentum and energy must be conserved, the energy of the neutron must be equal to the energy of the phonon, and the momentum of the neutron must be equal to the momentum of the phonon. But if the energy and momentum are conserved in this simple way, then it's easy to show - and I won't take the time to do it - that there is only one possible energy with

which a neutron can emerge from a crystal. This energy, assuming the Debye theory holds, is simply $2\ mc^2$. To a nuclear physicist $2\ mc^2$ is 2 bev, but we must remember that here c is the velocity of sound not light. So if we take 2 bev and multiply by the square of the ratio of the velocity of sound, say in beryllium, to the velocity of light ~~squared~~ we find that for beryllium this energy is 0.8 ev. But this is something like 8,000 degrees and there just aren't any phonons in beryllium of this temperature.

Fortunately, this calculation doesn't really apply, so forget about it. The reason it doesn't apply is that while it is true that we've got to conserve energy and momentum, we can play with momentum exchanges with the crystal itself. So the conservation of momentum is not just that the $\vec{k}$ of the outgoing neutron is equal to $\vec{q}$ of a phonon, it's equal to $\vec{q} + 2\pi\vec{\tau}$ where $\vec{\tau}$ is any vector in reciprocal lattice space. Now it isn't really surprising that the neutron can exchange momentum with the whole crystal. For if we take the case where $\vec{q}$ is zero, that is, no phonons gained, we have $\vec{k} = 2\pi\vec{\tau}$; if you think a bit you will realize that this is just the condition for Bragg scattering, $n\lambda = 2d \sin\theta$, in which momentum is exchanged with the crystal alone. Because of the fact that the reciprocal lattice vector is involved, the scattered neutrons coming out will not have a continuous distribution of energies but will have a few discrete energy peaks in a given direction. In another direction it will have another set of discrete energies.

Now it sounds simple but the experiment is not very easy to do. Various people have been doing experiments like this now for four or five years. The reason the results aren't very good is simply that the counting rates are low in an experiment of this type. The work that has been done at Brookhaven at

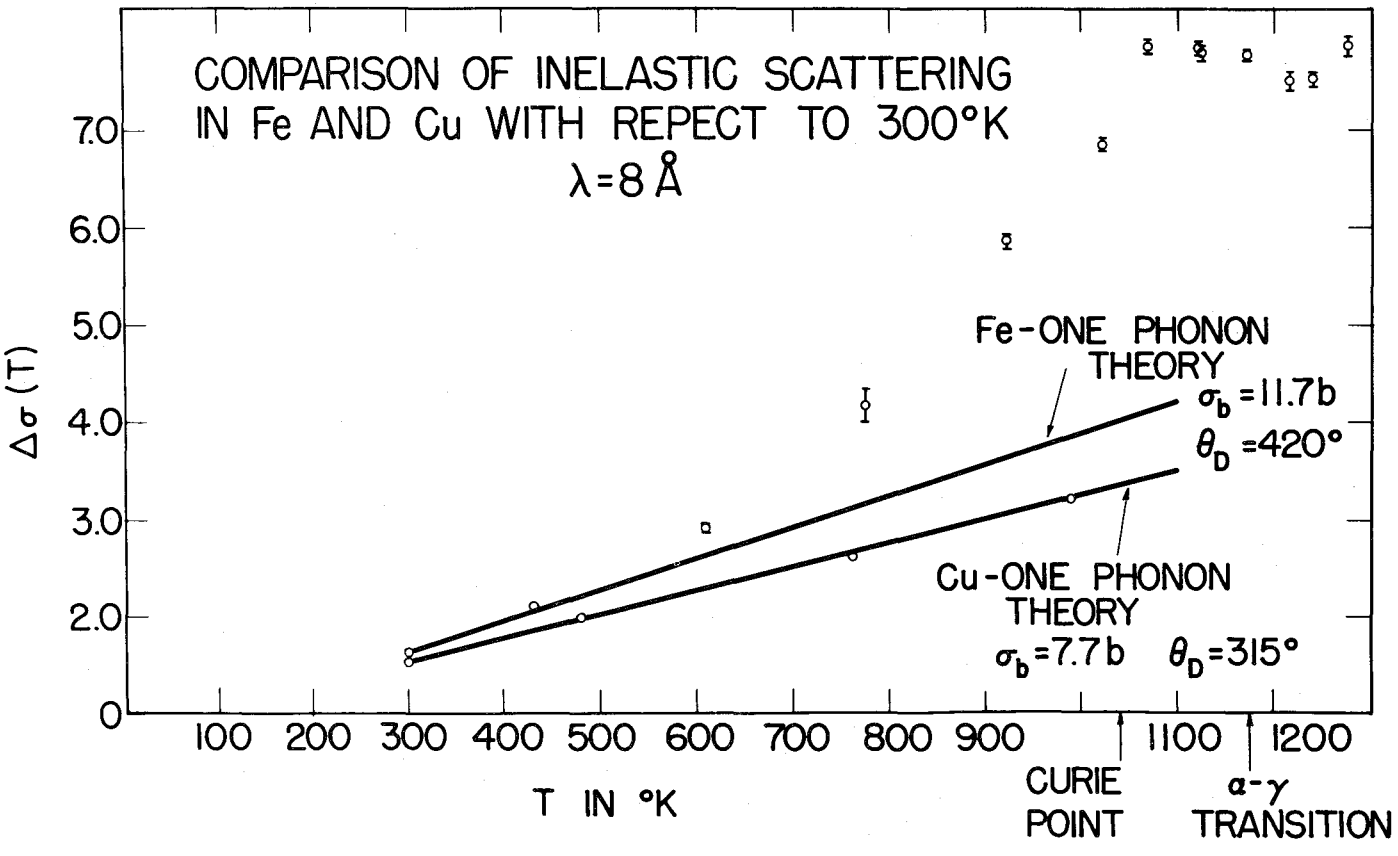

Fig. 3. Cross Sections of Iron and Copper as Functions of Temperature; the Difference in Behavior is Evidence for Magnetic Inelastic Scattering

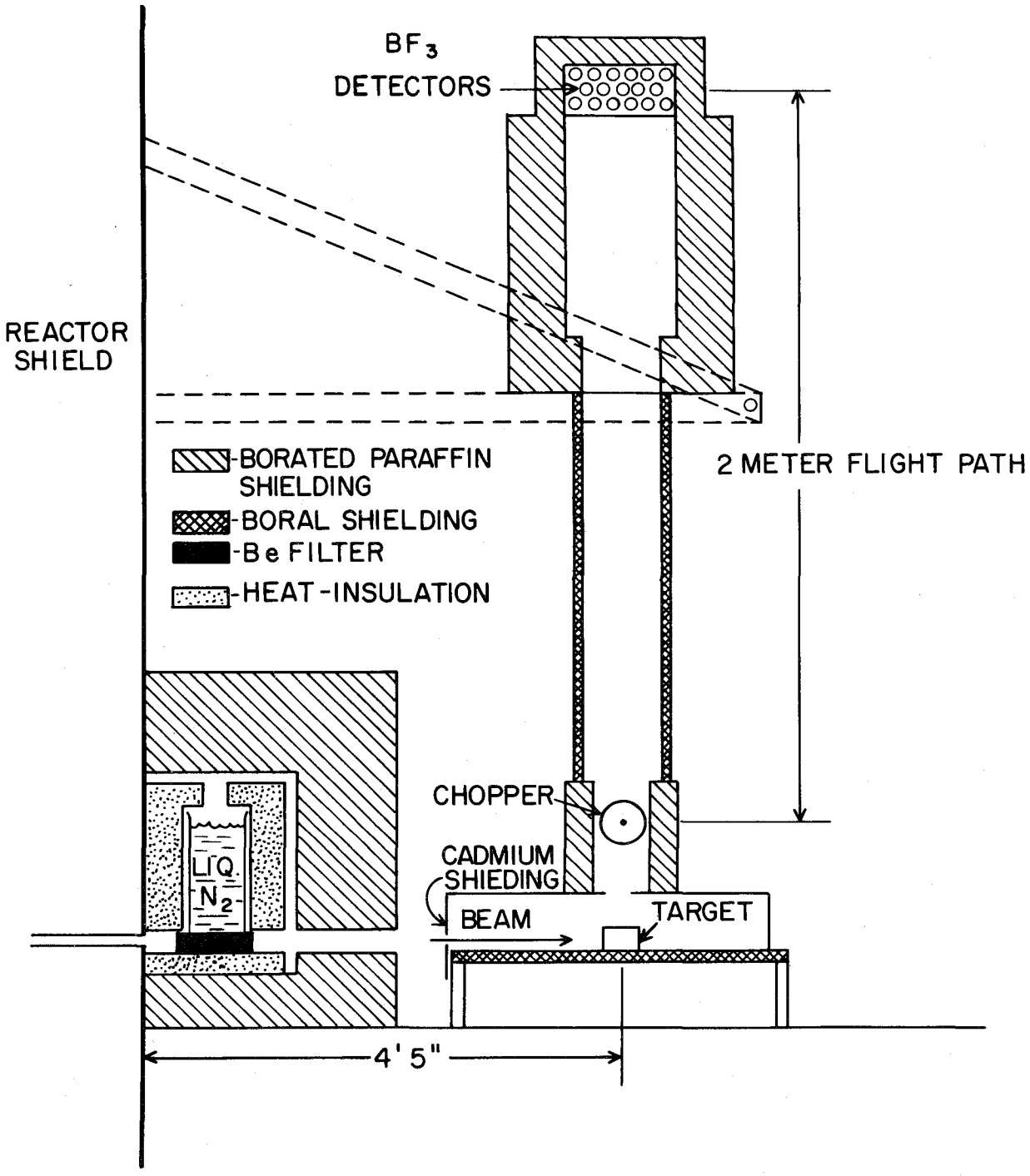

Fig. 4. Equipment for Measurement of Scattering of Cold Neutrons

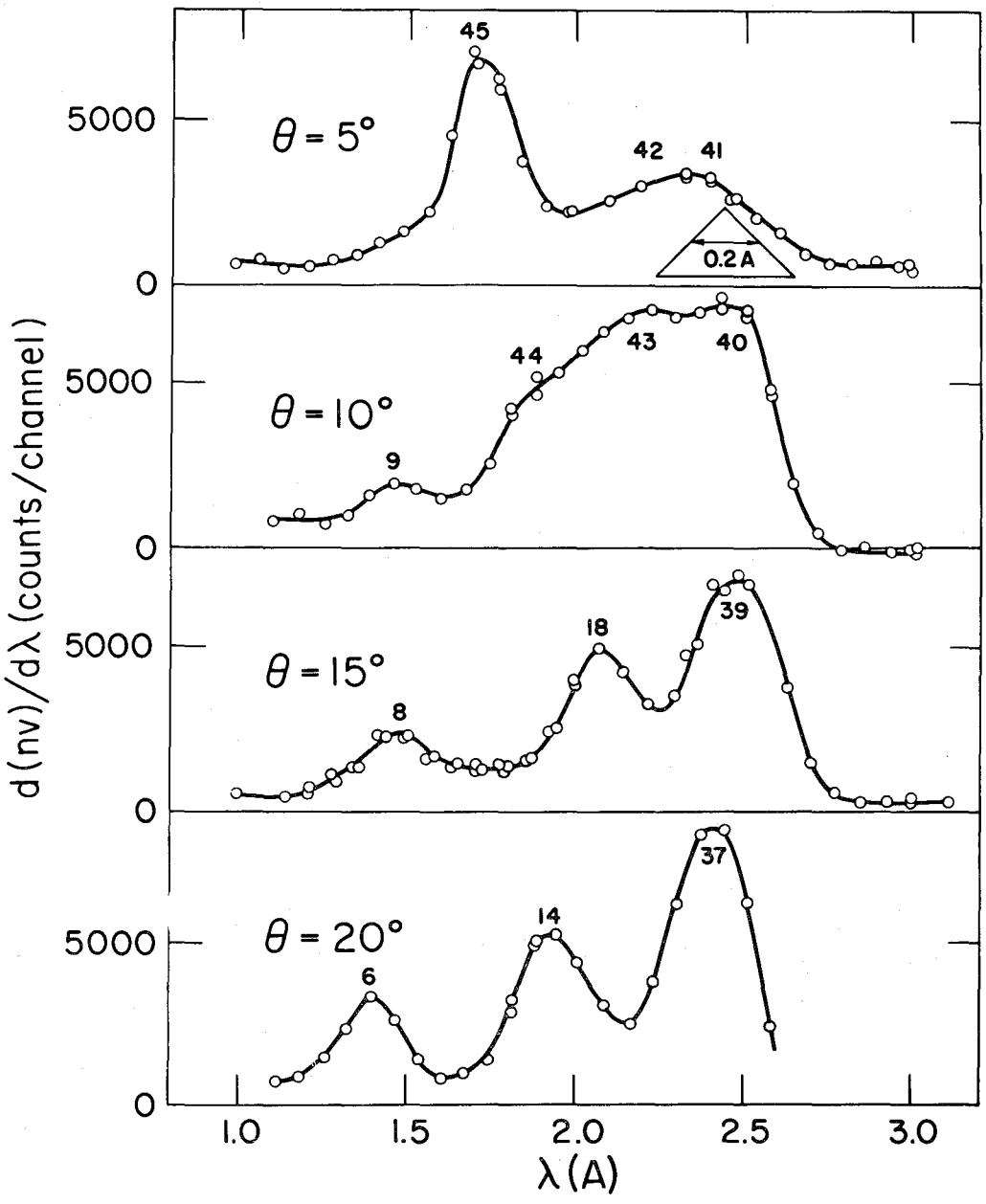

Fig. 5. Distribution of Scattered Neutrons from a Single Crystal of Aluminum, Showing the Characteristic Peaks for a Coherent Scatterer

ALUMINUM
SCATTERING CURVE (100) PLANE

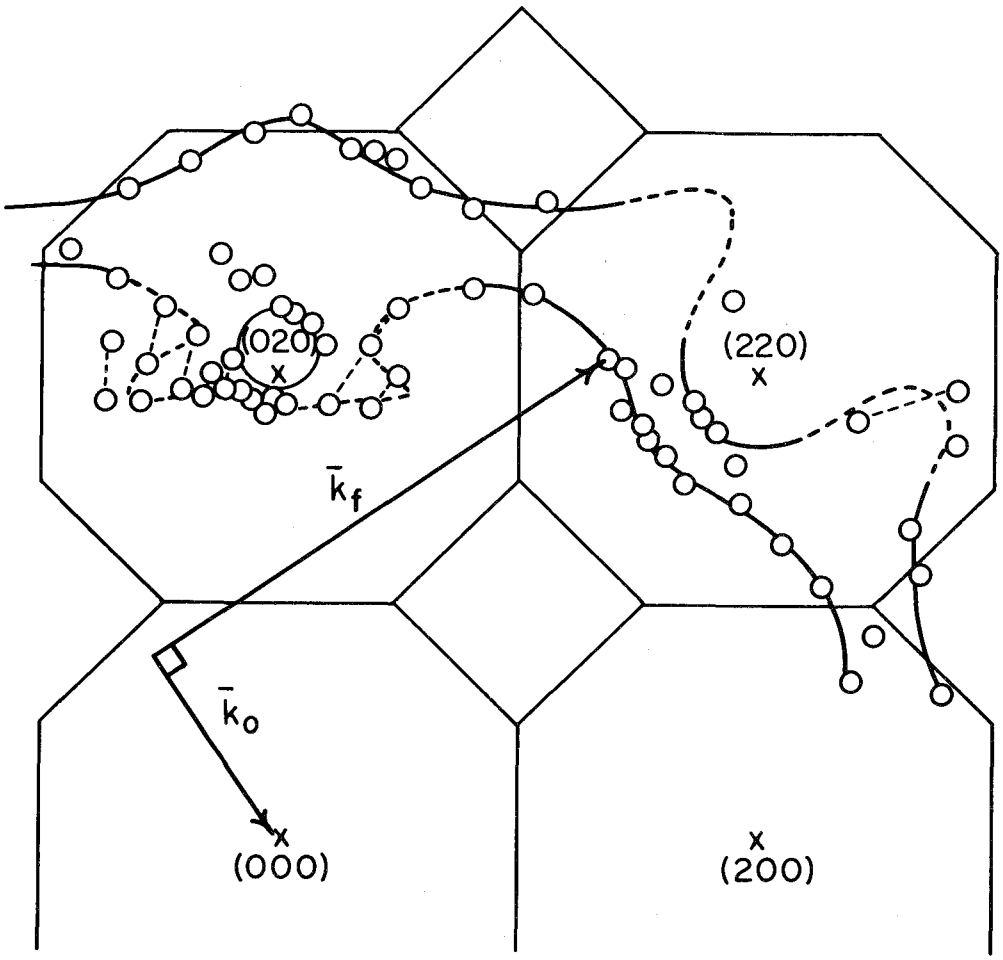

Fig. 6. The Scattering Surfaces for Aluminum in the (100) Plane; the Wave Vectors for the Incident and Scattered Neutrons for a Single Crystal Orientation Are Shown

first used the equipment shown in Figure 4. A beam of neutrons comes from the reactor, goes through a piece of polycrystalline beryllium, and the neutrons that get through the beryllium are those of long wavelength only, about 30° K in temperature. Unfortunately, only a few of them scatter because the inelastic scattering cross section is low, and of those that scatter at 90°, some pass through a "chopper" and emerge as bursts of neutrons. By the flight time to a detector a few meters distant we are able to measure the velocity, hence that is the wave number $\vec{k}$, of the outgoing neutron.

In the first experiments of this type performed at Brookhaven, aluminum was the scattering sample. Figure 5 shows the type of results obtained. These are typical curves giving the counting rate as a function of neutron wavelength for different orientations of the single crystal of aluminum. The incoming neutrons have a wavelength of about 5 Å, and the scattered neutrons are much warmer; in fact, they are at about room temperature, room temperature being at about 1.8 Å. As we would expect, discrete peaks are observed and as the crystal is rotated, the peaks move around, change in height, and often merge so that we can't tell one from another.

The analysis of the results in reciprocal lattice space is shown in Figure 6. It's a little more complicated than we have considered already because the incident neutrons don't have zero momentum; they do have finite momentum. So where I said k, I really should have said the $\vec{k}_f - \vec{k}_o$, the momentum change. Each experimental point gives us the relationship between the energy ($\hbar\omega$) and the momentum ($\vec{q}$) of a single phonon. You see that the points do follow surfaces, which in some regions get very complicated and are hard to follow. Also this is just one plane of the aluminum crystal, and many, many orientations are needed to depict the entire relationship ~~between~~ ω ($\vec{q}$).

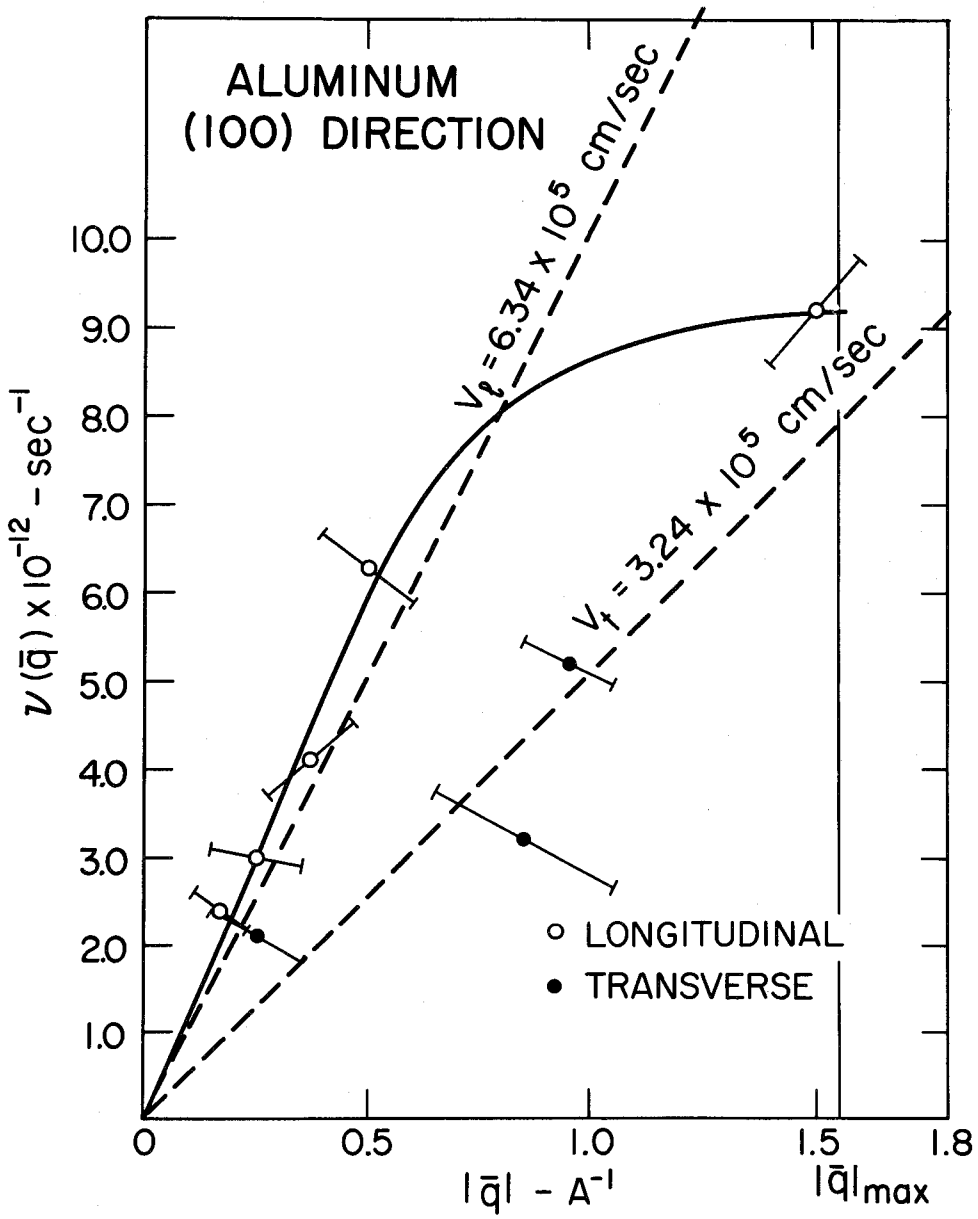

Fig. 7. Dispersion Curves for Aluminum in the (100) Direction

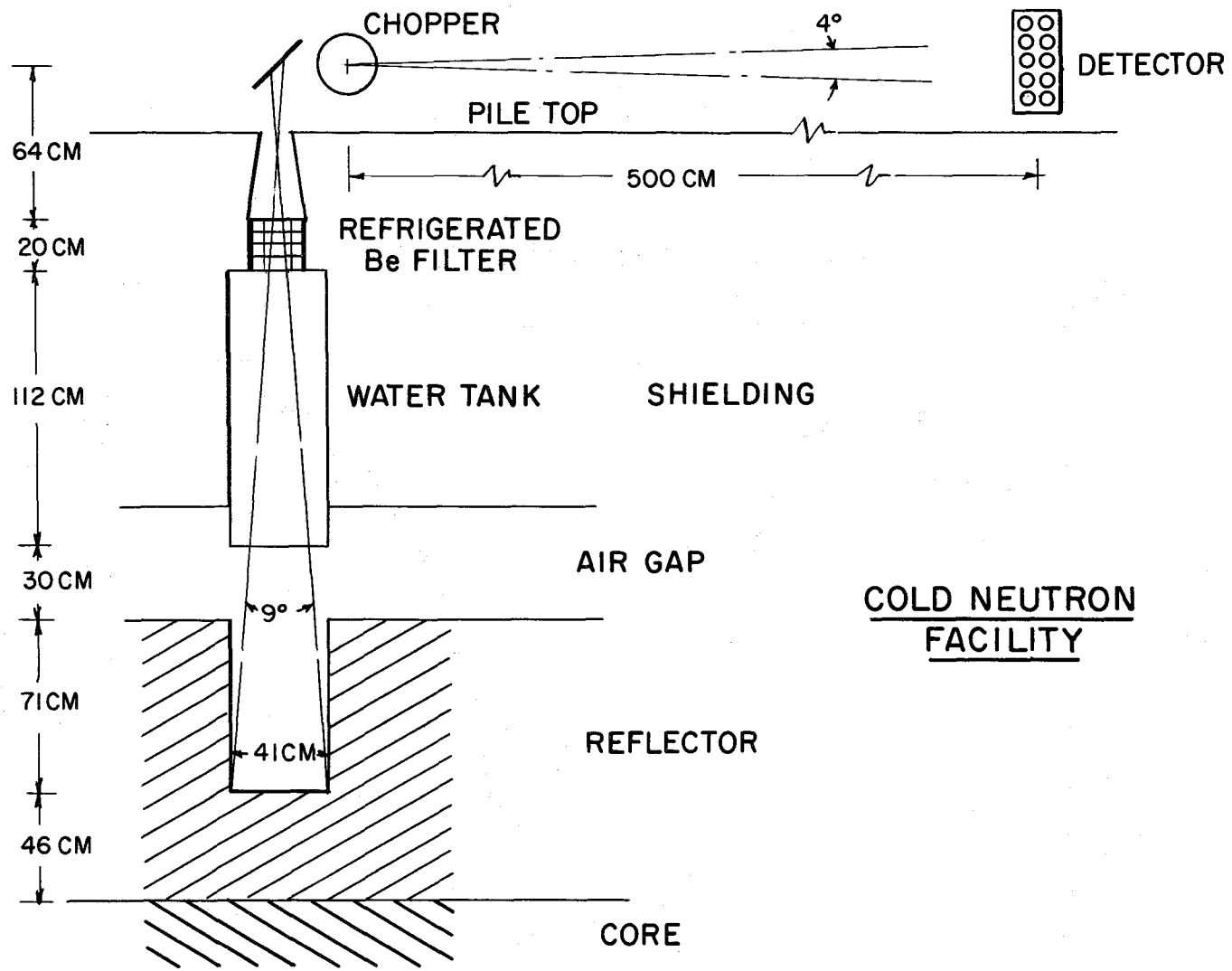

Fig. 8. Cold Neutron Equipment in the Top Shield of the BNL Reactor

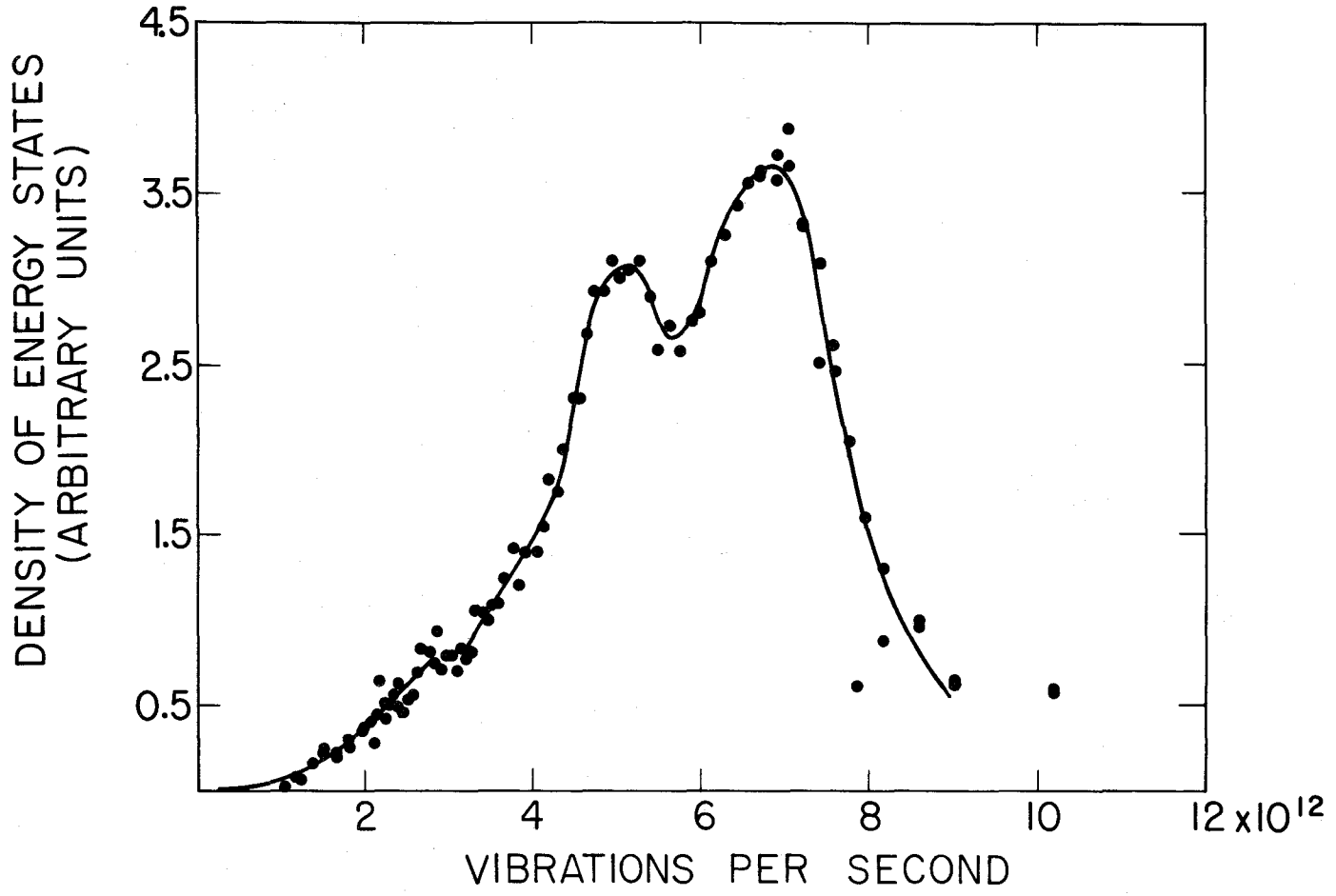

Fig. 9. The distribution of Lattice Vibrations in Vanadium, as Measured with Cold Neutrons

In Figure 7 is plotted the relationship between the frequency and $\vec{q}$ for $\vec{q}$'s in a single direction only. There are two branches; one corresponds to longitudinal vibrations and the other to transverse vibrations. According to the Debye assumption, the frequency-momentum relationship would be just a straight line with a slope given by the velocity of sound, $\omega = cq$. The slope of the dashed line represents the measured velocity of sound, measured of course at very low frequencies. The points start off with a slope that agrees, within the rather poor experimental error, with the measured velocity of sound. You see that at high frequencies the simple Debye assumption is wrong and there is dispersion; the linear relationship $\omega = cq$ no longer holds.

I will now show you some improved equipment, and then report very briefly some results without going into details. In order to get more intensity, what we have done at the Brookhaven reactor is to dig a big hole into the top graphite reflector, Figure 8. The beryllium filter is refrigerated with liquid air so its transmission for cold neutrons will be greater. With this new equipment we get a much increased flux at the scattering sample, some 50 times what we had before, and this increase is utilized to obtain higher resolution.

Some recent results with vanadium are shown in Figure 9. Now vanadium is a rather unusual element in which it is not necessary to conserve momentum, because the nuclear scattering of vanadium is incoherent. This means we need to worry about the conservation of energy only. It follows that the scattered neutrons have an energy distribution that is a direct representation of the lattice vibration spectrum in the vanadium. In other words, we see the distribution directly, instead of discrete energies, as for aluminum. We don't need to use a single crystal because we don't need to conserve momentum. The

observed frequency spectrum starts off like the Debye spectrum, but has a complicated structure at high frequency. It definitely has discrete peaks. Now these are not unexpected, because even though there have not been calculations specifically for vanadium there have been calculations of the expected frequency distribution for body-centered lattices in general, and they predict peaks and valleys. The force constants of the crystal are closely related to the frequency spectrum, and actually from the ratio of these peak heights and their positions it's possible to say something about the ratio of the force constants in the crystal. These results do not give us the complete $\omega(\vec{q})$ relationship that we want, but it is rather pretty in that we see the lattice vibration distribution so directly.

Figure 10 shows the results for zirconium hydride, which was investigated at the request of General Atomics. This material, as Nelkin had predicted, shows a very strong energy gain. Because hydrogen scatters incoherently, we don't need to use a single crystal. Furthermore, we expect rather a smear in the thermal region; it is peaked roughly at room temperature. In addition to that continuous distribution there is a tremendously intense peak here roughly at 0.14 ev. This represents a different type of vibration. It is not an acoustic vibration but an optical vibration in which the frequency is relatively independent of the wave number $\vec{q}$.

This optical vibration, incidentally, was sought for but not found by infrared absorption. It turns out that the cold neutron method is an extremely good one for finding these optical lattice vibrations. Since these first experiments we have, as has Brockhouse at Chalk River, worked on germanium in

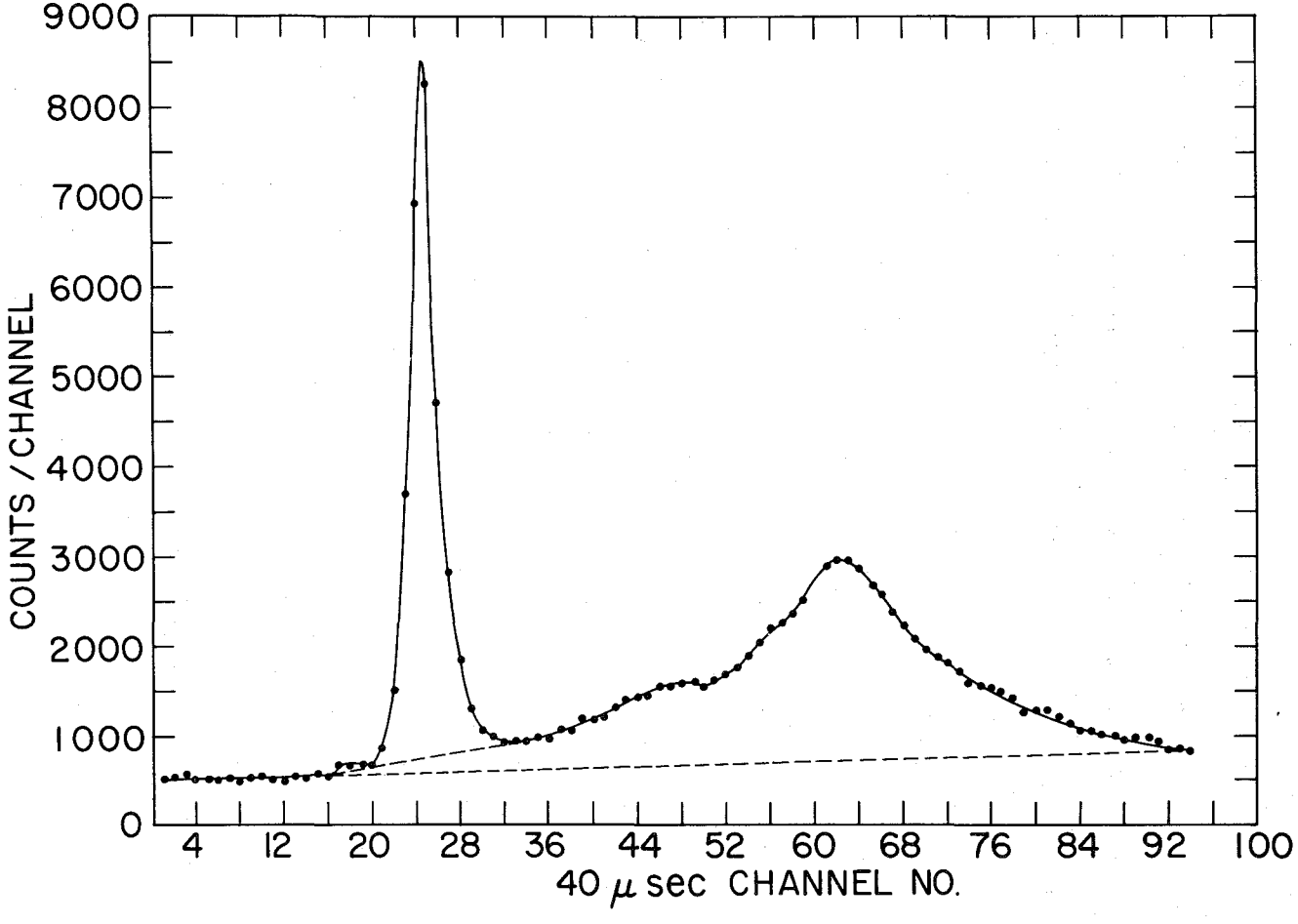

Fig. 10. The Prominent Optical Line in Zirconium Hydride

which almost everything happens, because the scattering is coherent (like aluminum) and optical lines are present as well. We ourselves have not done much more with zirconium hydride, though we intend to study a series of hydrides because it's so easy to find these optical lines. However, McReynolds and Whittemore have done more work on zirconium hydride, checking the temperature variation and so on, which they will report in the next papers.

Paper III-B

NEUTRON THERMAL INELASTIC SCATTERING BY BOUND ATOMS

A. W. McReynolds
John Jay Hopkins Laboratory

Neutron Thermal Inelastic Scattering by Bound Atoms

A. W. McReynolds
John Jay Hopkins Laboratory
San Diego, California

Abstract

In the energy range below about 1 ev, the cross-section $\sigma(\vec{k}, \vec{k}', T)$ for scattering of a neutron with propagation vector k, relative to the scatterer at temperature T, to k' is no longer characteristic of free atoms but dependent on interatomic binding forces. Using monoenergetic neutron beams, ranging from 0.05 to 0.3 ev, from crystal spectrometers at Brookhaven National Laboratory, this dependence has been studied by measurements of total cross-section, the angular distribution, and the average scattered energy, for H in various chemical bonding states and for C and Be. H in H_2O behaves qualitatively as if free, with smooth variation of both total cross-section and energy loss. The tighter binding of H in $ZrH_{1.5}$ gives discrete energy states, .13 ev, characteristic of an isotropic harmonic oscillator. Energy loss per collision is negligible for neutrons of lower energy, but has maxima at the 0.13, 0.26, etc. levels. There are corresponding peaks in total cross section above these energy thresholds in agreement with Fermi's theoretical curve. For carbon the predominance of elastic diffraction scattering over inelastic necessitates higher resolution techniques. These show the product of cross-section and energy loss per collision ($\xi\sigma$) lower by about a factor of 3 than the values for free carbon.

NEUTRON THERMAL INELASTIC SCATTERING BY BOUND ATOMS*

A. W. McReynolds†

The experimental work reported here has been carried out at Brookhaven Laboratory by W. L. Whittemore and myself of the General Atomic staff, with the successive participation of Tormod Riste and Arne Andresen of JENER in Norway and Israel Pelah of the Weizmann Institute, Rehovot, Israel. Referring to the comments and sketch of the previous speaker, thermalization research has clearly proceeded in rather different directions. Reactor physicists are interested in finding neutron spectra after multiple scattering, while neutron and solid state physicists are interested in finding out more about solids by detailed study of single scattering events. By the latter approach one can eventually arrive at a determination of spectra. From the solid-state viewpoint, however, interest is directed toward the simpler cases, such as aluminum or germanium, to elucidate fundamental principles, thus information about spectra of interest to the reactor physicist comes only at the end of a long road. We have therefore undertaken to make basic scattering measurements on several materials which are of dual interest because of the nature of the fundamental scattering processes and their potential use as reactor moderators. These included water, hydrogenous plastics, metallic hydrides, and graphite.

Since very little experimental information was available in the near-thermal energy range, it was necessary to do several different types of experiments. It would be desirable to measure directly the scattering kernel $\sigma(E_0,E,\theta,T)$ for scattering a neutron of initial energy E_0, in moderator at temperature T, to a new energy E, with change θ in direction.

Although limitations in available beam intensity preclude accomplishing this directly, four different types of partial measurement, on each of which there was little available experimental information, have been made. These are illustrated schematically in Figure 1.

Figure 1a shows apparatus for measurement of total cross section, using a crystal spectrometer for selection of a monoenergetic beam. In all of the cases studied, transmission through the sample is determined almost entirely by scattering, with negligible effect of the absorption cross section. In Figure 1b, a crystal spectrometer is also used for selection of the monoenergetic incident beam but with measurements on the neutrons scattered from a sample chosen to be suitably thin so that only a negligible number of neutrons are multiply scattered. Moving the counter to different angles, the angular distribution of scattering is first measured. Whereas it would be desirable to measure also the complete energy distribution at each angle, intensity limitations permit only the measurement of the average energy of the beam at each position. This was accomplished by the determination of transmission through a gold foil, for which the cross section is proportional to 1/v. Measurements of the types 1a and 1b are described in more detail later. Figure 1c illustrates time-of-flight analysis of the energy spectrum of neutrons filtered through beryllium to select those of low energy, then singly scattered from thin

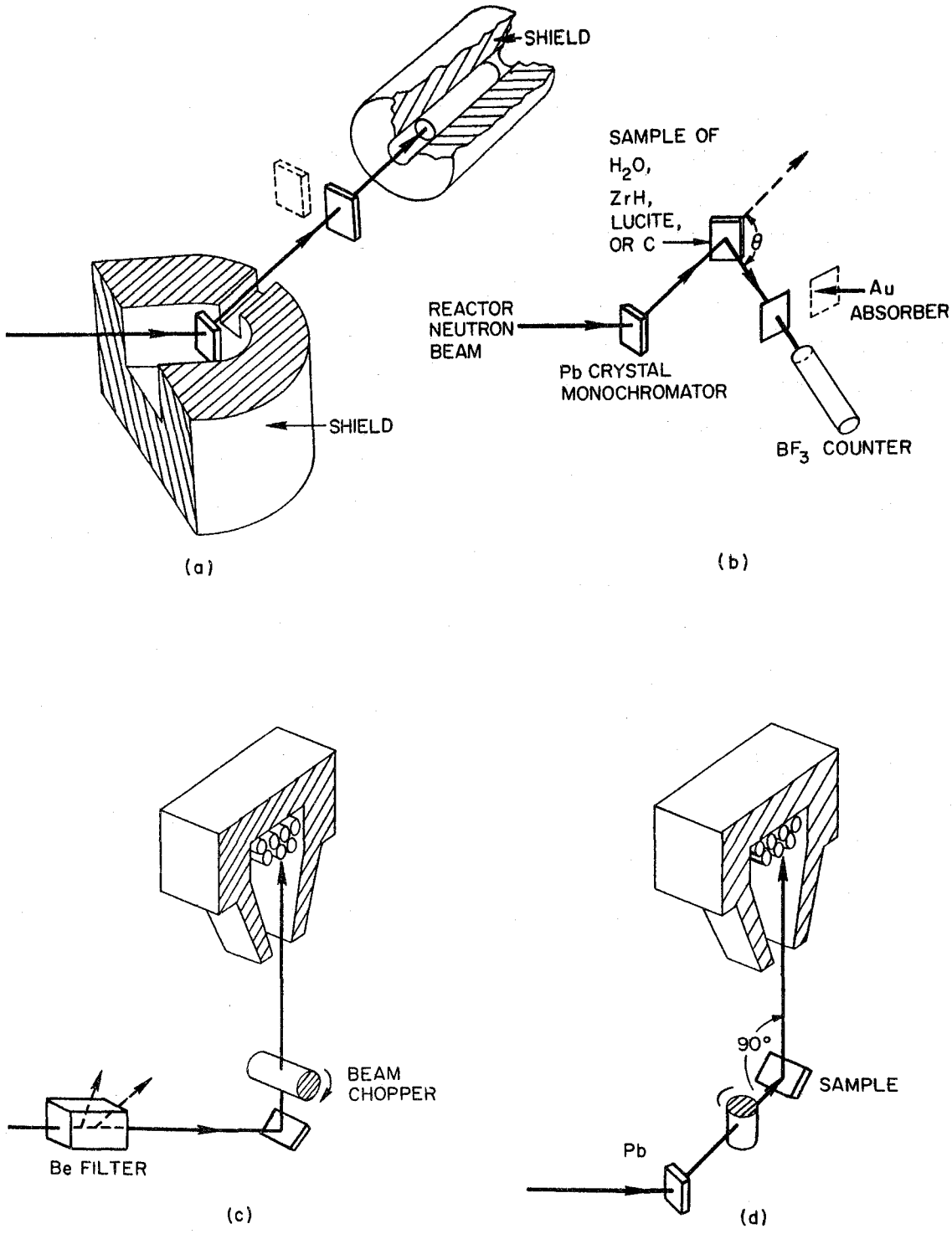

Fig. 1--Schematic representation of four types of neutron-beam measurements of neutron thermal inelastic scattering: (a) total transmission cross-section using crystal monochromator; (b) angular and energy distributions of singly scattered neutrons; (c) energy distribution by time-of-flight with incident cold neutrons; (d) energy distribution with incident monoenergetic epithermal neutrons.

samples. In Figure 1d is shown apparatus for similarly analyzing the scattered spectrum but with monoenergetic incident neutrons from a crystal spectrometer, as in 1b. Experiments of the last two types, 1c and 1d will be reported on in the next paper by W. L. Whittemore. Let us then consider here experiments 1a and 1b.

TOTAL SCATTERING CROSS SECTION

In his classic treatment of neutron slowing-down, Fermi derived the curve shown in Figure 2 on the assumption that hydrogen behaves as an isotropically-bound harmonic oscillator. The cross section exhibits minima followed by a sharp rise at multiples of $h\nu$, representing threshholds for excitation of the oscillator to higher states. This curve would not be expected to apply accurately to water, but there is reason to expect it to be applicable to the case of zirconium hydride because of its structure. The zirconium atoms are in a face-centered cubic lattice, and it is seen that the hydrogen atom lies at the center of a tetrahedron of zirconium atoms, isotropically bound and separated from its hydrogen neighbors. It therefore lies in an isotropic potential well and should behave as an independent harmonic oscillator. The experimentally determined cross section, illustrated in Figure 3 does in fact closely resemble the Fermi curve, with the expected difference that the minima are less sharp than the cusps predicted by the theoretical model. This slight broadening is somewhat greater than the instrumental resolution of the crystal spectrometer which V. L. Sailor and his collaborators at Brookhaven Laboratory made available for the measurements. A larger component is the Doppler broadening resulting from thermal vibrations of the zirconium lattice. Using the zirconium mass and the sample temperature, correction for this effect has been included in the dashed theoretical curve of Figure 3. Total cross section measurements on another hydride MgH_2 show, in Figure 4, some anomalies indicating the presence of discrete vibrational levels, but not as clearly resolved as for zirconium hydride. This is understandable from the structure, which for magnesium hydride is of a layer type for which bonding is not isotropic but relatively

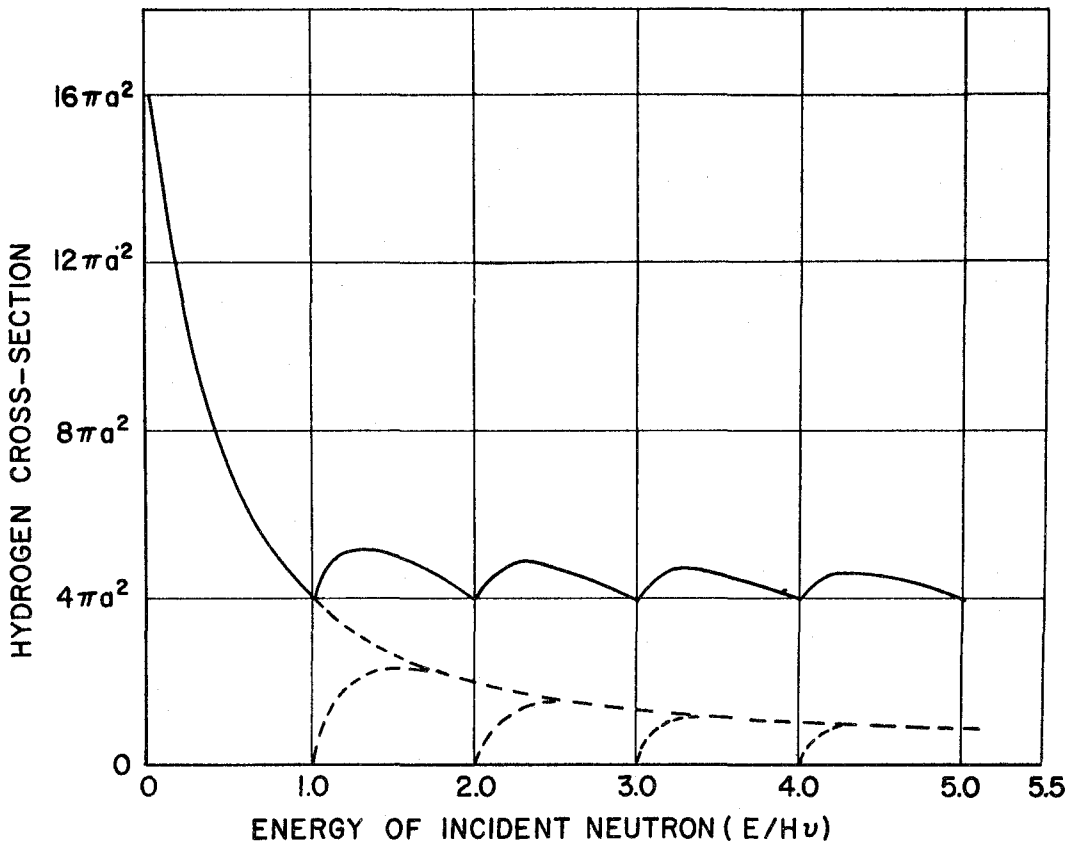

Fig. 2--Theoretical neutron cross-section of bound proton, with frequency ν of isotropic harmonic oscillation.

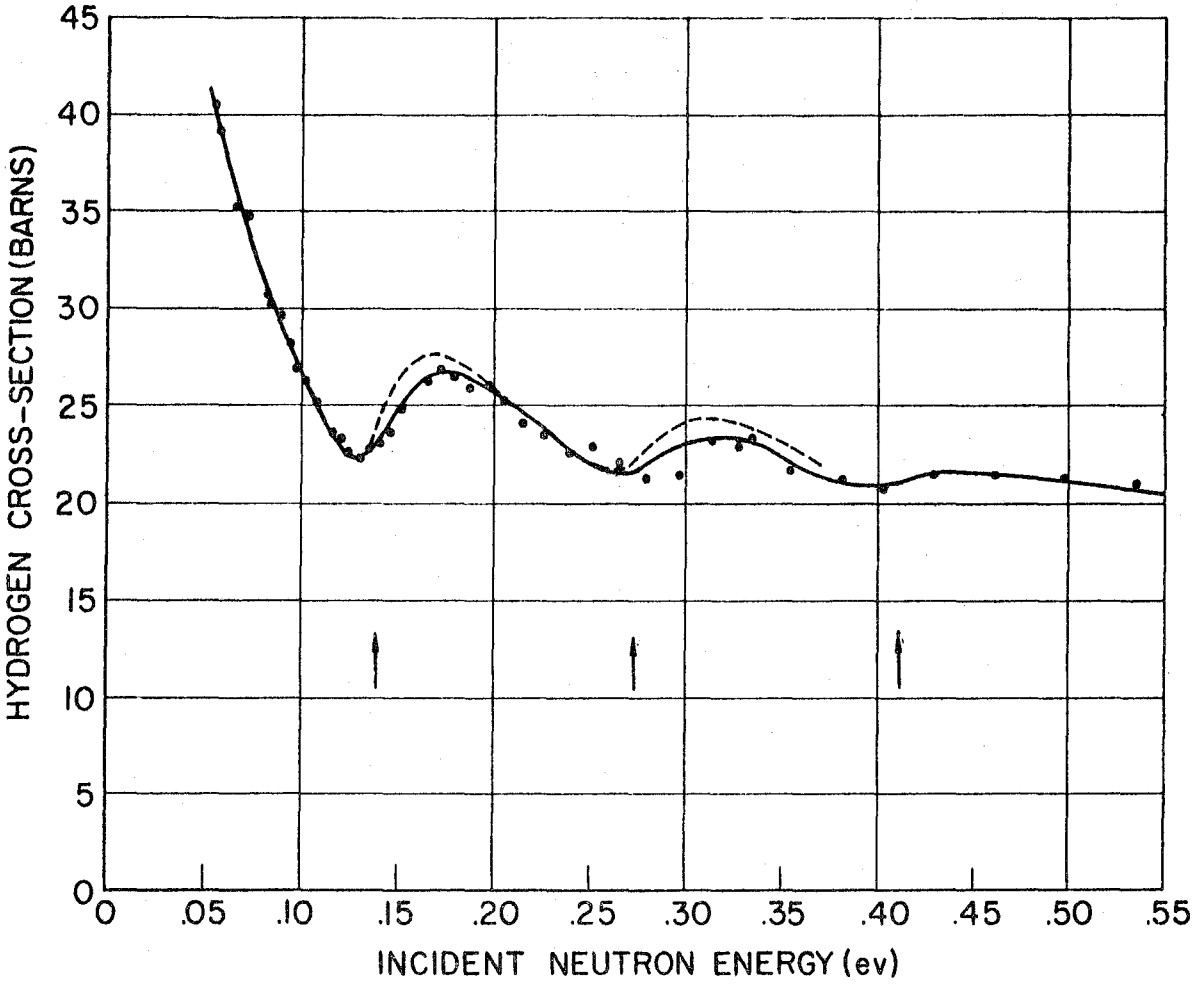

Fig. 3--The solid curve gives the total neutron cross-section of hydrogen in zirconium hydride ($ZrH_{1.5}$) obtained from total cross-section of $ZrH_{1.5}$ by subtracting constant cross-section of zirconium. Arrows indicate excitation levels for H vibrations in Zr lattice. The Fermi theoretical curve corrected for Doppler broadening has been fitted to the above data with $h\nu = 0.137$ ev and agrees exactly with the experimental curve except as shown by the dashed curve.

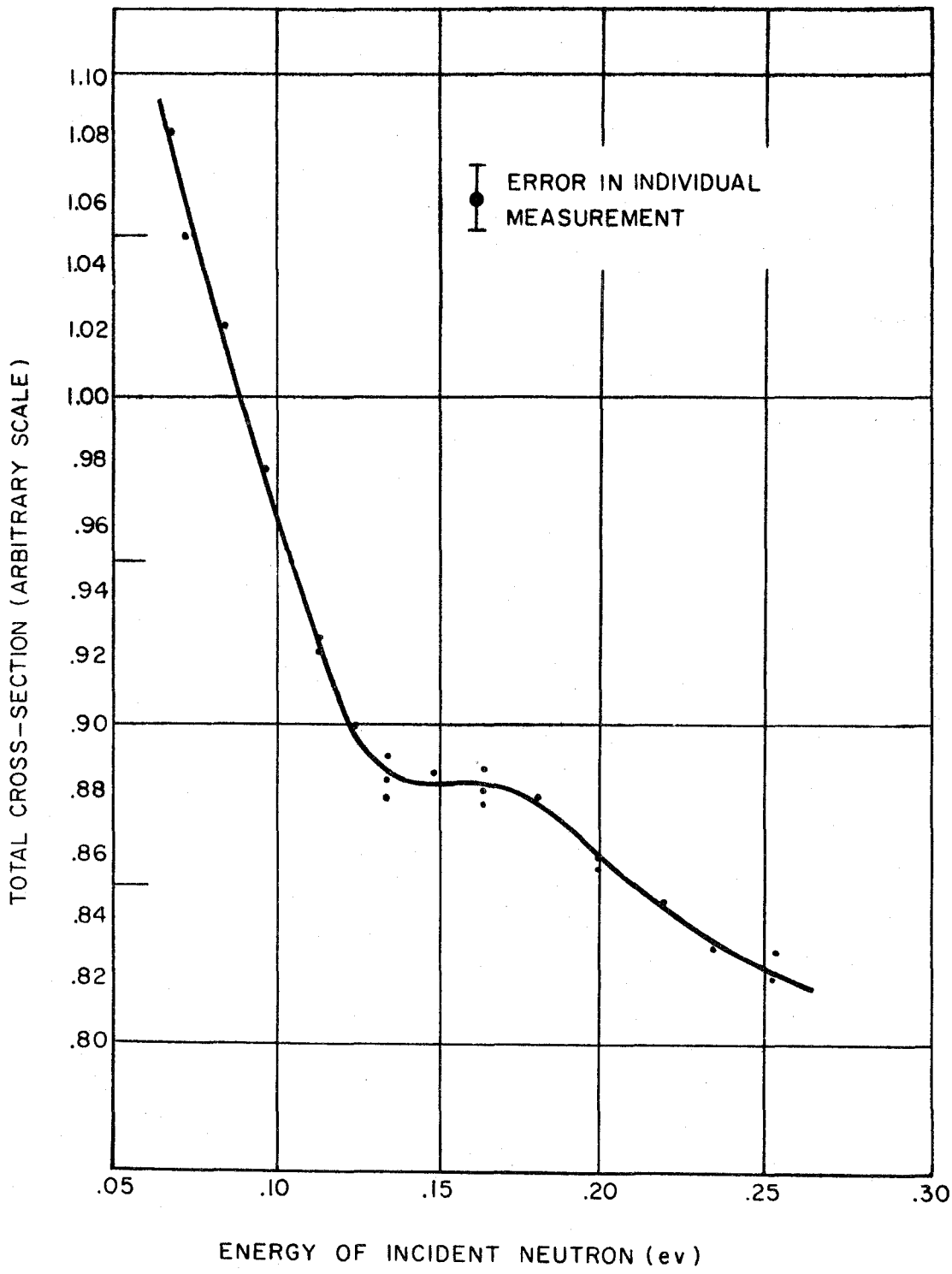

Fig. 4--Total neutron cross-section for magnesium hydride (MgH_2). Anomaly between 0.12 and 0.2 ev indicates partly resolved excitation level for H vibrations in Mg lattice.

stronger within the layer than between adjacent layers. This should give a cross section representing a superposition of Fermi curves and therefore exhibiting less pronounced maxima and minima. For comparative purposes the H_2O total cross section was measured by the same methods, but, as expected from the variety of possible excitation states, shows no resolvable anomalies.

ENERGY LOSS CROSS SECTION

In the type of measurements indicated in Figure 1b, the objective is to determine the quantity $\xi\sigma$, where ξ is the logarithmic energy decrement $\ln E_0/\bar{E}$ and σ is the scattering cross section. Since both are functions of the scattering angle θ, measurements of ξ and σ must be made separately for each angle and the product integrated over all angles to determine an average value, $\overline{\xi\sigma}$. The quantity actually measured as $\bar{E}$ differs slightly from the conventional definition, in that it is the energy corresponding to the average transmission through a 1/v absorber, rather than the true average of energies of neutrons in the beam, but the difference is not great and vanishes in the high-energy limit. Figure 5 shows, for neutrons of incident energies 0.057, 0.086, 0.117, the average energy after scattering at various angles from thin samples of zirconium hydride, lucite plastic and water. Within this energy range, the three materials differ markedly, zirconium hydride showing very little moderating effect as compared with water, and plastic intermediate between these extremes. In Figure 6 is shown a representative case of the differential scattering cross section vs. angle, as given by the angular variation of the scattered intensity from a constant monoenergetic beam. The distribution is of course peaked in the forward direction. If data of Figures 5 and 6 are now multiplied together to integrate $\int \xi\ \sigma \sin\theta\, d\theta$ over all angles, the average values $\overline{\xi\sigma}$ as shown in Figure 7 are obtained. Also shown for comparison are three theoretical curves representing the cases of hypothetical free hydrogen at $0^{\circ}K$ and $300^{\circ}K$ and a theoretical model for water, as proposed by Nelkin. Again it is seen that in this energy range zirconium hydride

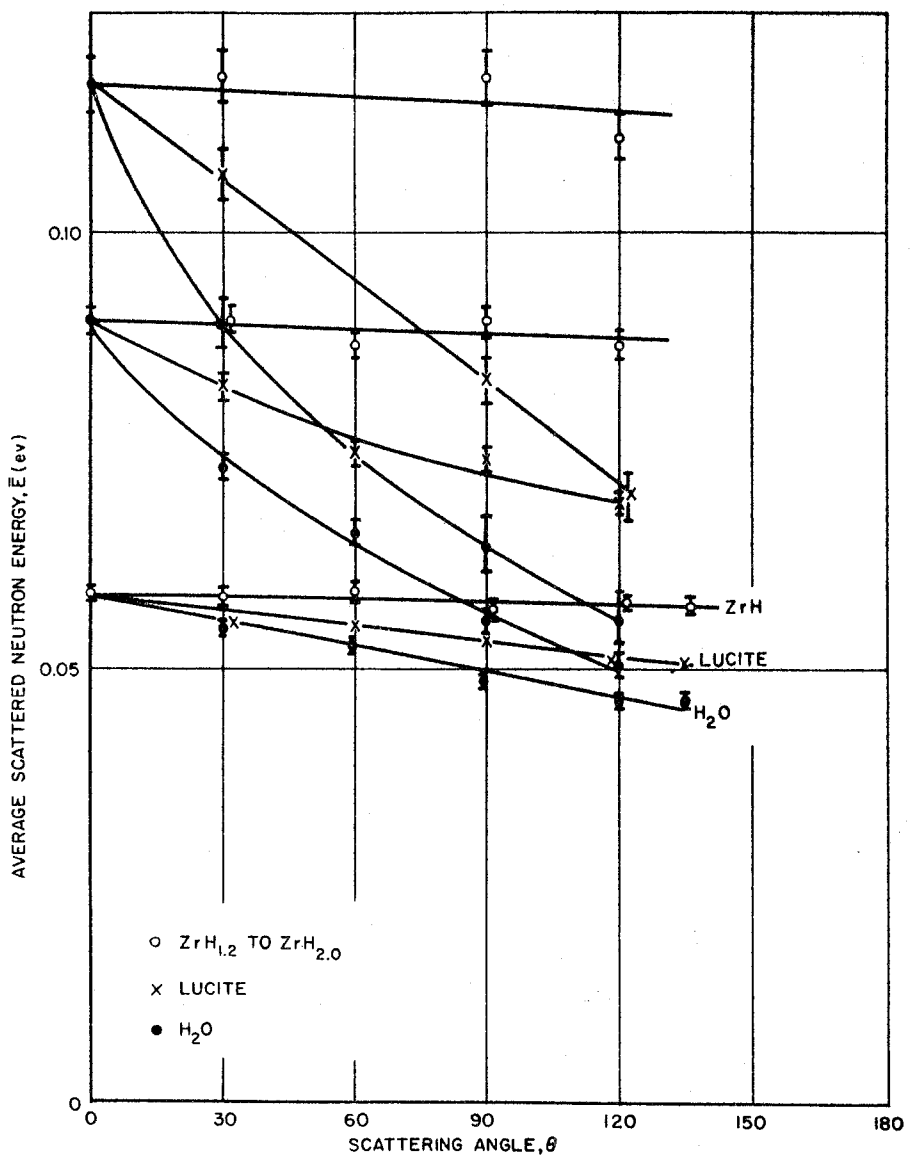

Fig. 5--Neutron scattering from hydrogen in different states of binding. Points indicate average energy after single scattering, as measured by transmission through Au, for incident (0° angle) and scattered neutrons.

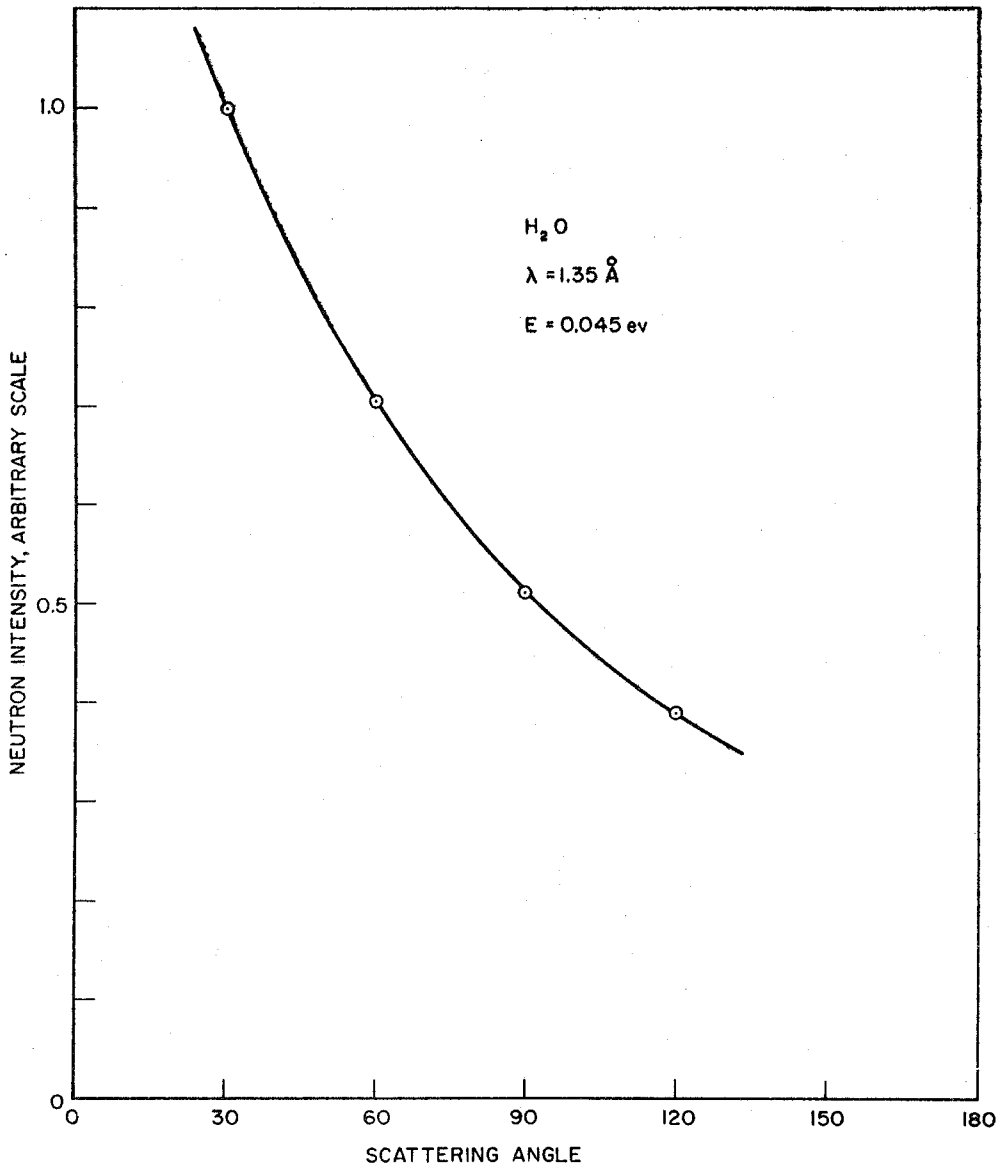

Fig. 6--Angular distribution of neutrons of 0.045-ev incident energy scattered from thin H_2O target.

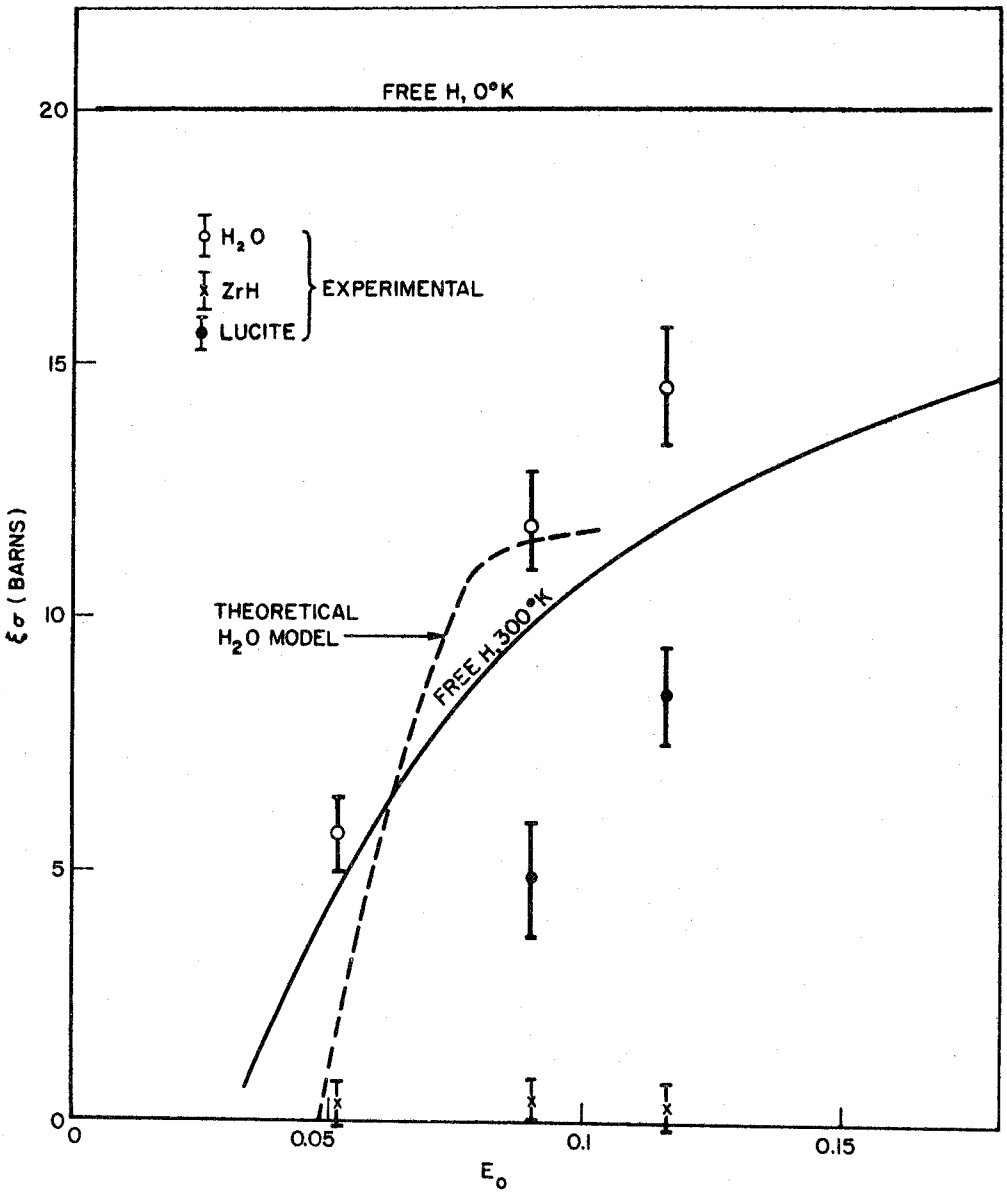

Fig. 7--Neutron scattering from hydrogenous moderators, showing values of $\xi\sigma$ as determined from Figs. 5 and 6 for ZrH and H_2O compared with computed values for free H gas and for theoretical model of H_2O.

has negligible moderating effect, and lucite is substantially below the value for free hydrogen.

Similar measurements have been extended to higher energies in Figures 8 and 9, where Figure 9 represents measurement only at the single-scattering angle of 80 degrees and Figure gives the average values of $\xi\sigma$ obtained by integration over all angles. The theoretical curves for the cases of free hydrogen and for Nelkin's water model have been so computed that the values of $\xi\sigma$ given are those which would be measured by use of a 1/v absorber and are therefore directly comparable to experimental data. The water data contain substantial corrections for multiple scattering effects, particularly in the energy range above 0.1 ev. The effect of multiple scattering is always to increase the measured value of ξ and to decrease the forward peaking of the angular distribution, both of which tend toward higher values of the average value $\overline{\xi\sigma}$. By using samples of almost zero thickness, we can eliminate the multiple scattering, but unfortunately eliminate at the same time any useful data. Intensity limitations require samples with transmission 90 percent or lower. With the inclusion of corrections, however, the behavior of water in the higher energy range continues to agree fairly well with theory. For zirconium hydride, as the neutron energy reaches the threshhold of 0.130 ev for excitation of hydrogen vibrational levels, both ξ and σ rise abruptly to a peak, then decrease until energy reaches the threshhold 0.260 for excitation of the second level. The solid curve shown is computed on the basis of a theoetical model of zirconium hydride as an isotropic harmonic oscillator, but with the resonance Doppler broadened by thermal lattice vibrations of the zirconium. Although the only parameter adjusted is the choice of 0.130 ev as the energy level, both the shape and height of the curves agree quite satisfactorily with experimental data.

GRAPHITE MEASUREMENTS

The scattering processes in graphite, beryllium, and other moderators differ from those in hydrogenous materials in several ways which make the thermalization process experimentally more difficult to

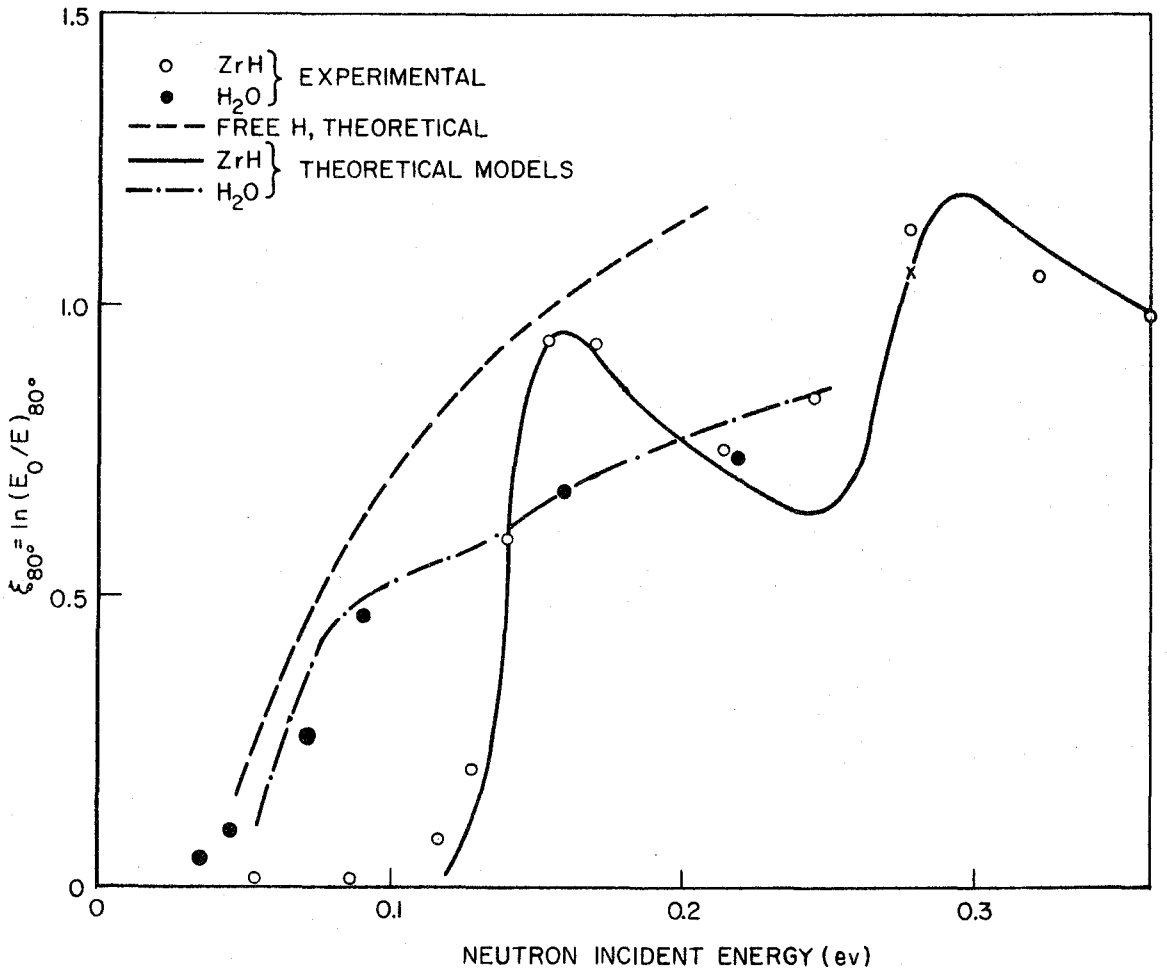

Fig. 8--Neutron inelastic scattering from H_2O and $ZrH_{1.5}$. Average energies E_0 and $\bar{E}$ of monoenergetic incident neutrons and neutrons scattered at 80° angle were measured by transmission through Au. Solid curves are fitted by choice of only one parameter.

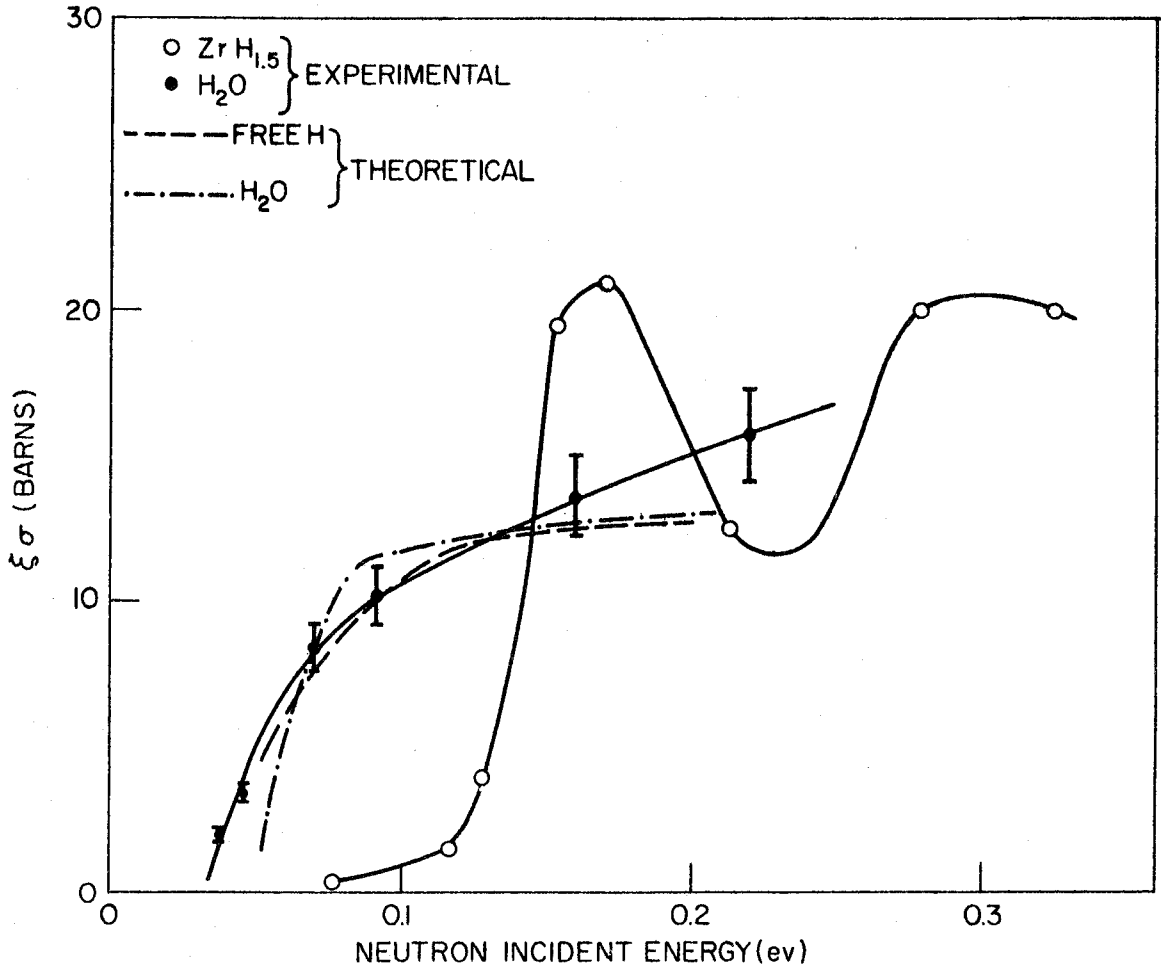

Fig. 9--Logarithmic energy decrement $\xi\sigma$ for neutron inelastic scattering from H_2O and $ZrH_{1.5}$ obtained by averaging over all scattering-angle data as shown in Fig. 8

study. First, because of the greater mass of the scattering atoms, the fractional energy loss in a single collision is small compared to the case of hydrogen, which has mass about equal to the neutron. Second, in contrast to hydrogen, there is a large degree of coherence in scattering, such that most scattering events are by elastic or Bragg diffraction which involves no energy exchange and also is concentrated into sharp peaks of intensity in the Bragg directions, which are determined by the crystal structure. The angular distribution is the familiar neutron diffraction pattern, which is shown in Figure 10 for graphite. At each scattering angle there is a mixture of elasticly and inelasticly scattered neutrons, with elastic predominating strongly in the diffraction peaks. Both ξ and σ are therefore strongly dependent on the exact scattering angle. Fortunately, however, the increases in one can be shown to compensate exactly for the decreases of the other, such that the product $\xi\,\sigma$ varies smoothly. As long as both quantities are measured on exactly the same angular distribution, this product varies smoothly. Also indicated on Figure 10 are the values of ξ measured at several angles. The points of measurement have been chosen to be those of lowest differential scattering cross section, σ, since these are the points at which the observed ξ has its largest values and can be measured with greatest accuracy. Figure 12 shows the resulting values of $\xi\,\sigma$ plotted against angle. Integration of $\xi\,\sigma \sin\theta$ over all angles is then carried out as before, using the known value of the total scattering cross section to normalize the arbitrary scale of σ measurements and obtain the average $\xi\,\sigma$ value. Figure 12 shows ξ for three different energies, compared with the constant value 0.158 characteristic of hypothetical free carbon at 0°K and also an approximation to the expected curve for free carbon at 300°K. It is seen that in the case of graphite the effects of binding reduce the energy decrement per collision to a value substantially lower than that for free carbon. It is expected that these measurements and those on hydrogenous materials will be pursued further and reported with more detailed theoretical interpretation in the coming Geneva conference. Measurements using time-of-flight analysis of the scattered neutron spectrum, as referred to in Figure 1, are reported in the next paper by W. L. Whittemore.

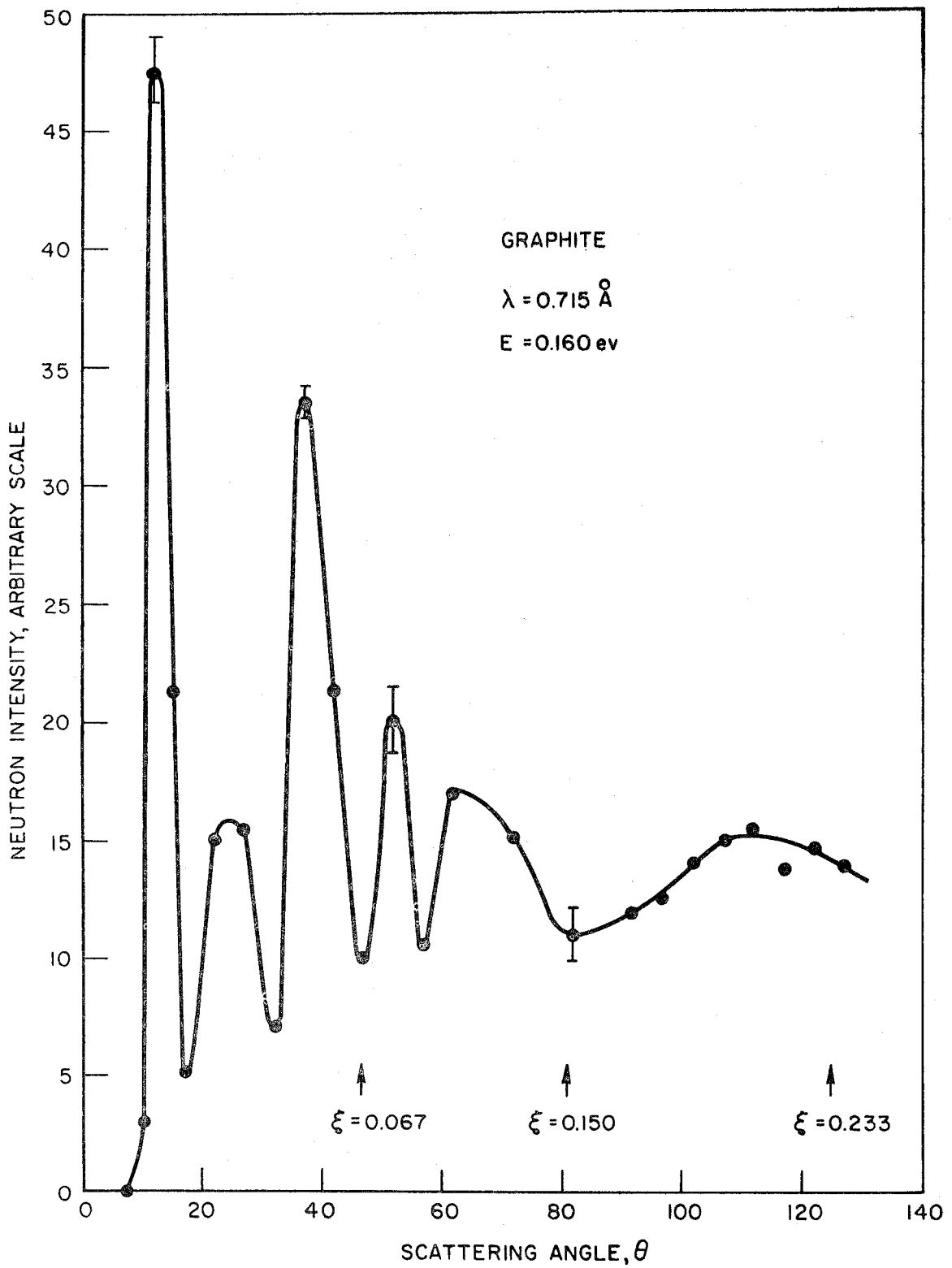

Fig. 10--Angular distribution of neutrons scattered from polycrystalline graphite. Values of ξ and angles at which measured are indicated; λ = 0.71Å, E = 0.160 ev for incident neutrons.

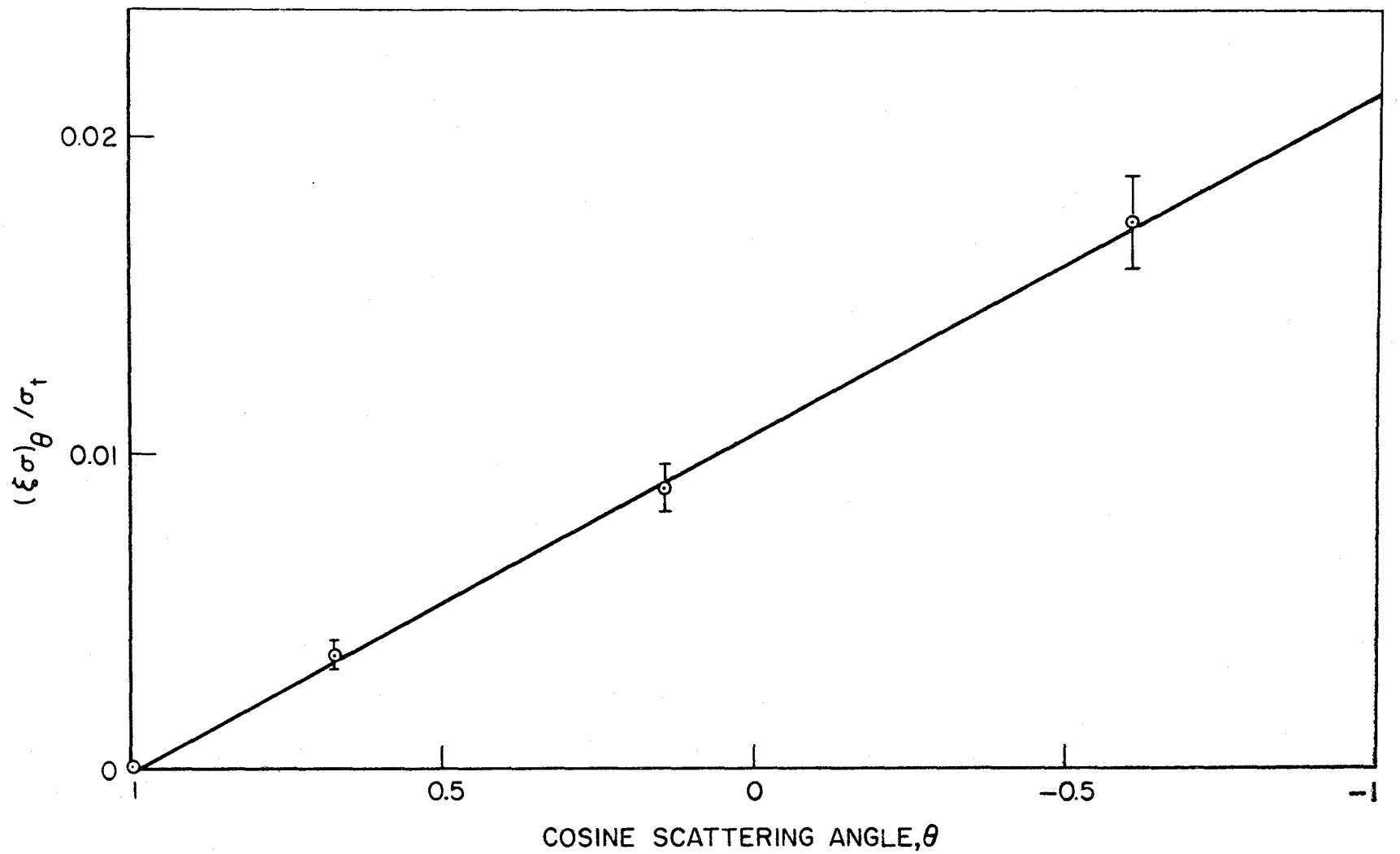

Fig. 11--Angular dependence of differential slowing-down cross-section as derived from the data of Fig. 10; $\lambda = 0.71$ A, E = 0.160 ev

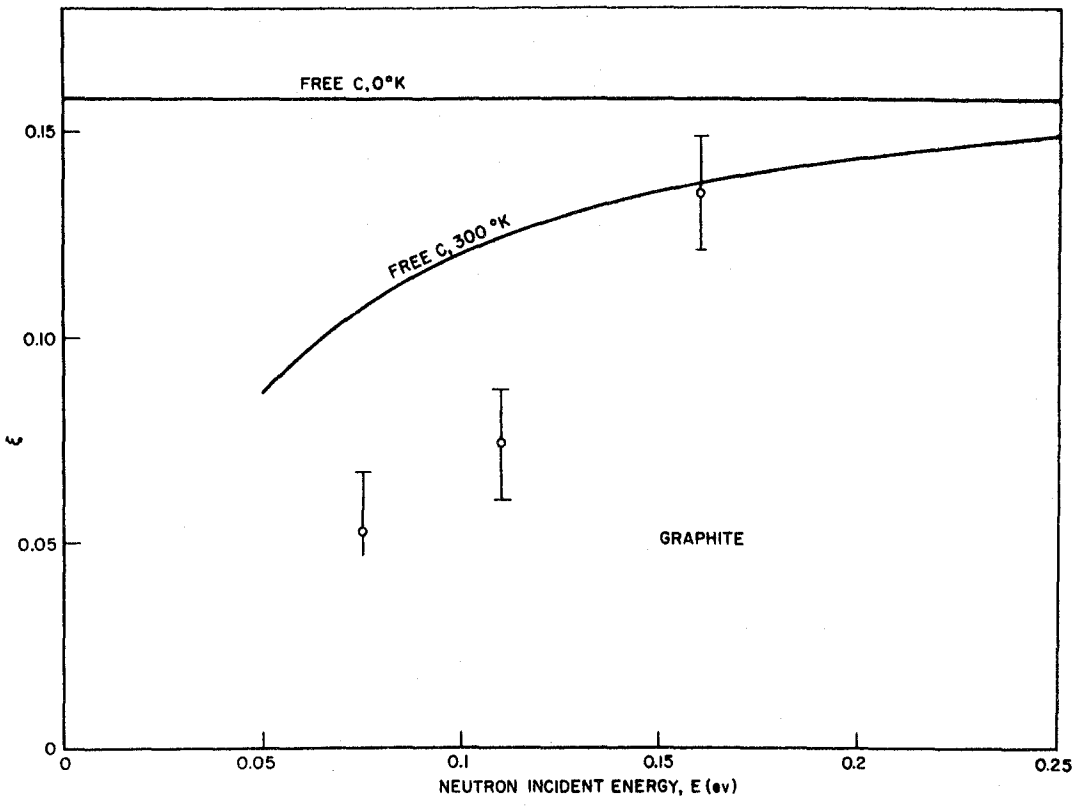

Fig. 12--Average logarithmic energy decrement ξ as function of incident energy for neutrons scattered from graphite, as compared with theoretical free C.

Paper III-C

A STUDY USING TIME-OF-FLIGHT TECHNIQUES OF THE THERMAL INELASTIC SCATTERING OF NEUTRONS

W. L. Whittemore
John Jay Hopkins Laboratory

A Study Using Time-of-Flight Techniques of the Thermal Inelastic Scattering of Neutrons

William L. Whittemore*
John Jay Hopkins Laboratory
San Diego, California

Abstract

In order to make a complete calculation of the thermalization of neutrons, one needs a detailed notion of the interaction between the neutron and the system of atoms in the moderating substance. As part of our investigation of the thermalization process, we have studied by neutron time-of-flight techniques the energy spectrum of neutrons scattered at 90 degrees by several materials, including zirconium hydride, water, and carbon. We have made two types of these measurements in which the significant difference is the energy of the incident neutron.

On the one hand, we permitted a beam of very slow neutrons to scatter from the sample. Since these neutrons will gain energy from the scattering substance, the resulting energy spectrum of these scattered neutrons reflects directly the spectrum of vibrations of the scattering substance. By studying these spectra one can deduce information needed to evaluate the moderation properties of such materials. In particular, we can study the effect of changes in the hydrogen concentration, impurities in the lattice, and temperature on the bound levels of hydrogen in zirconium hydride.

The other type of measurements was made with a somewhat higher energy (0.1 - 0.2 ev) for the incident neutron. In this case, the energy spectrum of the scattered beam shows directly the change in energy of the scattered neutron. The results of this type of measurement are intimately related to those discussed above and display directly the interaction needed for understanding the thermalization process. Results obtained by this study will be presented for liquid and solid water and other substances.

*Guest scientist at Brookhaven National Laboratory.

A Study Using Time-of-Flight Techniques of the Thermal Inelastic Scattering of Neutrons

Early in our investigation of the moderation properties of various hydrogenous materials, it became clear that several of the pertinent features could be best investigated by time-of-flight techniques. So far, we have used two different time-of-flight techniques in which the principal difference is the energy of the incident neutron. In the first case, the incident energy was 0.004 ev, selected by a cold beryllium filter. In the second case, the incident neutron beam is selected by a crystal monochromator and gives selected energies in the region 0.05 to 0.15 ev. For each of these cases, the energy spectrum for neutrons scattered through 90° gives considerable information about the thermalization process.

Consider first the case where the incident energy is about 0.004 ev. These experiments were carried out with the cooperation of the Brookhaven slow chopper group. We will confine our treatment here to some aspects of zirconium hydride.

We have already reported some results[1] concerning the energy of the

1) Phys. Rev. 108, 1092 (1957).

Einstein level. These results were obtained by examining in detail the time-of-flight spectrum of neutrons scattered at 90° by a sample of zirconium hydride. A typical spectrum is given in Fig. 1 where the sharp peak at channel 17 is due to interaction with hydrogen atoms in the first Einstein level. The results reported above were obtained by studying the relative area under the "optical" peak as it changed with the temperature of the sample. By relating this change to the Boltzmann population of the Einstein level, we determined the Einstein level to be 0.130 ± 0.005 ev. We report now some additional information obtained by studying the additional details of this Einstein level. For the practical purposes of thermalization one needs to know whether the energy of the level

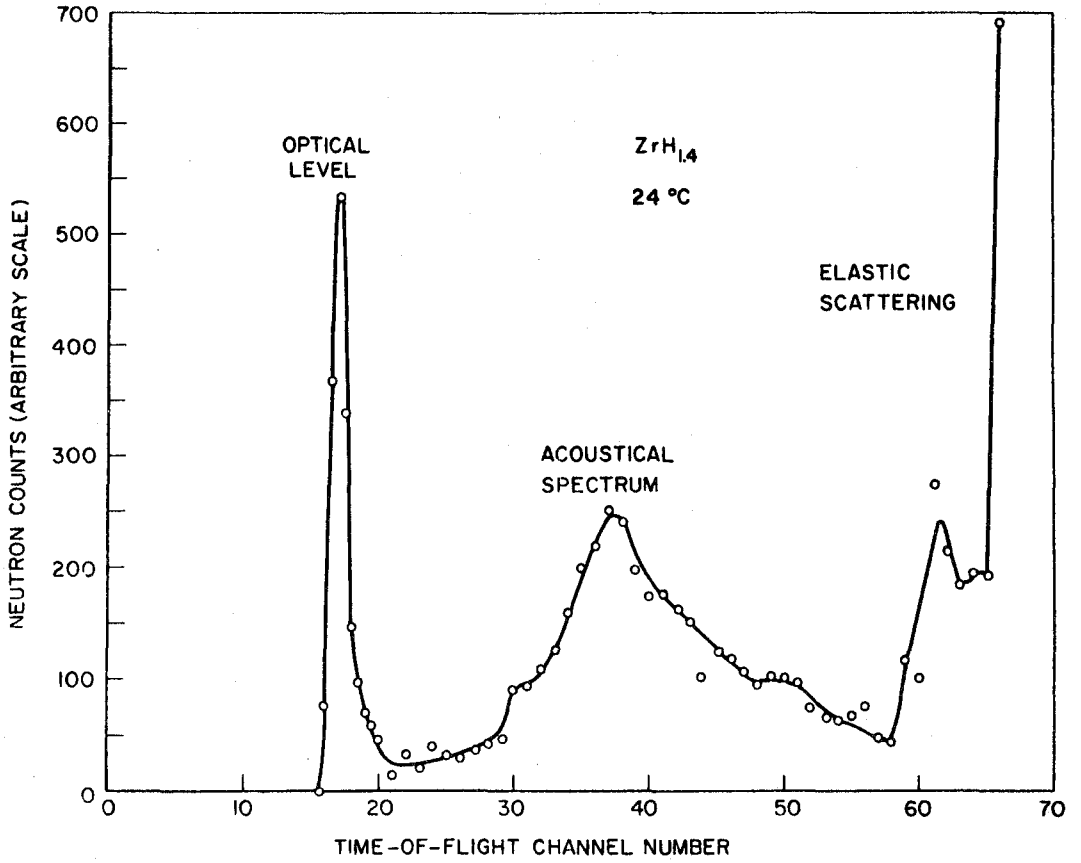

Fig. 1. Time-of Flight Distribution for Neutrons of Average Initial Energy 0.004 ev after Scattering at 90° Angle from $ZrH_{1.5}$

or its shape changes 1) with the concentration of hydrogen, 2) with the temperature of zirconium hydride, 3) or with the presence of heavy atoms in the lattice of zirconium hydride.

A study by the above technique of the Einstein level shows that the energy of the level and the width at half maximum remains unchanged when the concentration of hydrogen in the zirconium hydride is varied from 1.2 to 1.9 hydrogen atoms per zirconium atom. Furthermore, the study reported previously[1] involved the change of temperature from room temperature to 400°C. In this range of temperatures the peak of the distribution did not change, indicating no change of energy of the Einstein level. In this experiment the width at one half maximum increases with temperature, nearly as predicted by a simple perfect gas model of the zirconium lattice. The appropriate Doppler broadening computed for this lattice is sufficient to explain the width of distribution at all temperatures studied. The addition of uranium to the polycrystalline sample to make an alloy with zirconium hydride could be expected to change the characteristics of the Einstein level. This feature was studied by adding about 7% by weight of uranium to $ZrH_{1.5}$. The $UZrH_{1.5}$ alloy was studied at room temperature and 200°C. The shape and location of the peak for the Einstein level remained the same as for the sample of zirconium hydride. This showed that the distortion of the lattice caused by the uranium atoms had no effect on the Einstein level. All of these results above lead naturally to a very simple model of the hydrogen oscillator in the zirconium hydride system. It seems

reasonable and quite sufficient to picture each hydrogen atom as surrounded by a tetrahedron of zirconium atoms. With the addition of more hydrogen to the zirconium hydride system the additional hydrogen atoms simply enter empty tetrahedrons with very little influence on the hydrogen already present.

The second type of measurement was made by taking a beam of neutrons from a crystal spectrometer and allowing them to scatter at 90° into a detector placed 160 cms away. By interrupting the beam periodically one can study the time-of-flight distribution of the scattered neutrons. From this time-of-flight distribution one can easily compute the energy spectrum of the scattered neutrons. Using this technique we are presently investigating several hydrogenous materials and also certain other substances pertinent to a thermalization study. Fig. 2 shows a time-of-flight distribution for 0.07 ev neutrons scattered at 90° from a sample of water with a transmission of 0.83. When this time-of-flight distribution is transferred to an energy distribution one obtains curve 2 in Fig. 3. (In this figure we also see the energy spectrum of the incident neutrons shown as curve 4. This spectrum is obtained in two independent ways 1) by the scattering at 90° from a thin vanadium sample and 2) by the time-of-flight distribution obtained by placing a detector in the unscattered beam at a distance of 160 centimeters. These two spectra agree rather well.) The effects of multiple scattering on the data are of considerable importance. A thicker water sample with a transmission of 0.65 was used to give curve 1. Since the difference between curve 1 and 2 is rather slight one can deduce from these as a first approximation to the single scattering the result shown in curve 3. From a comparison of curves 3 and 4 one can see the effect of thermalization in single scattering from an array of water molecules. In the first place, the peak of energy distribution of the scattered neutrons is displaced to lower energies, mainly explained as a recoil effect. The width of this displaced distribution is approximately explained as

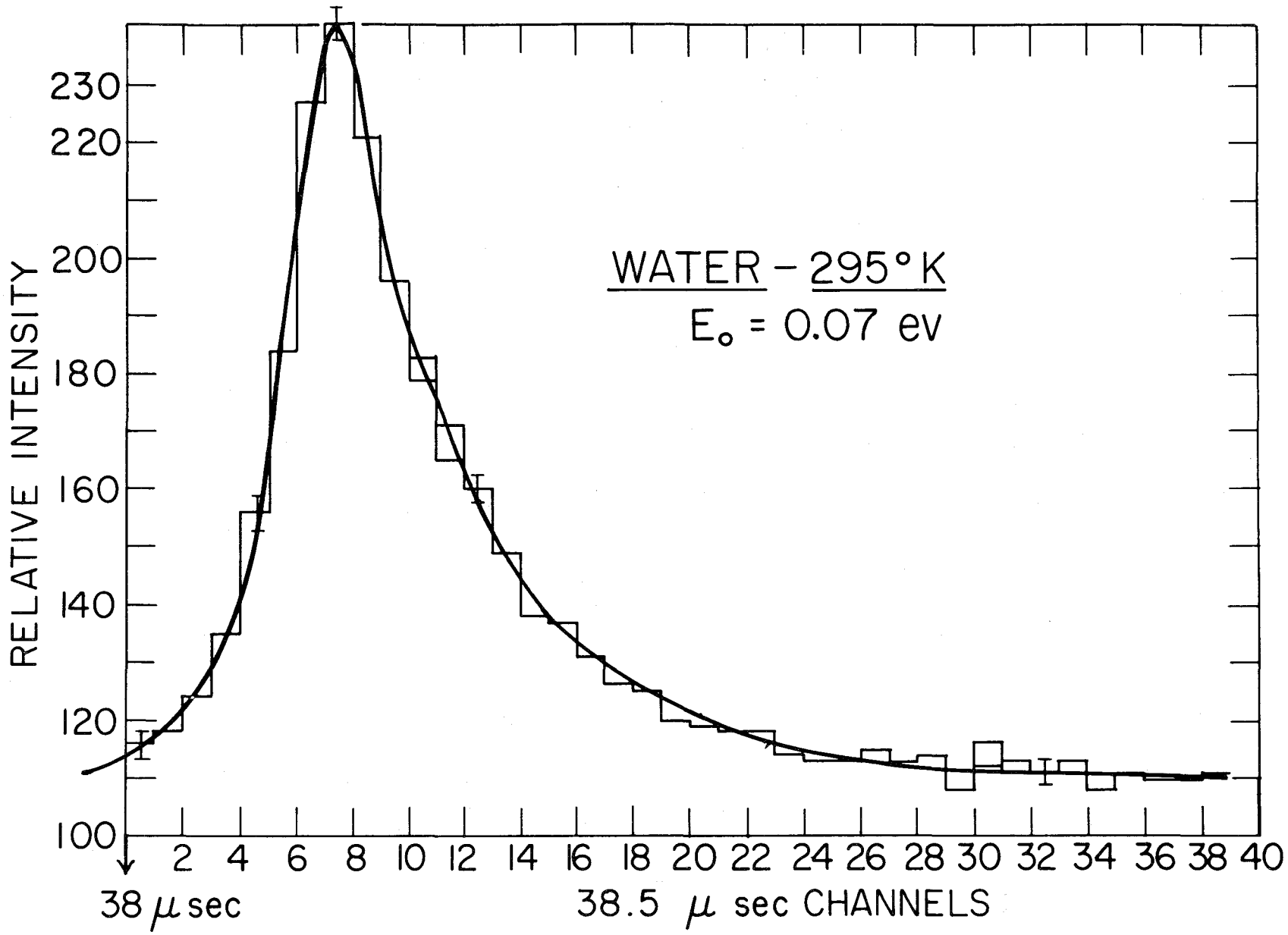

Fig. 2. Time-of-Flight Distribution for Neutrons of Average Initial Energy 0.07 ev after Scattering at 90° Angle from H_2O

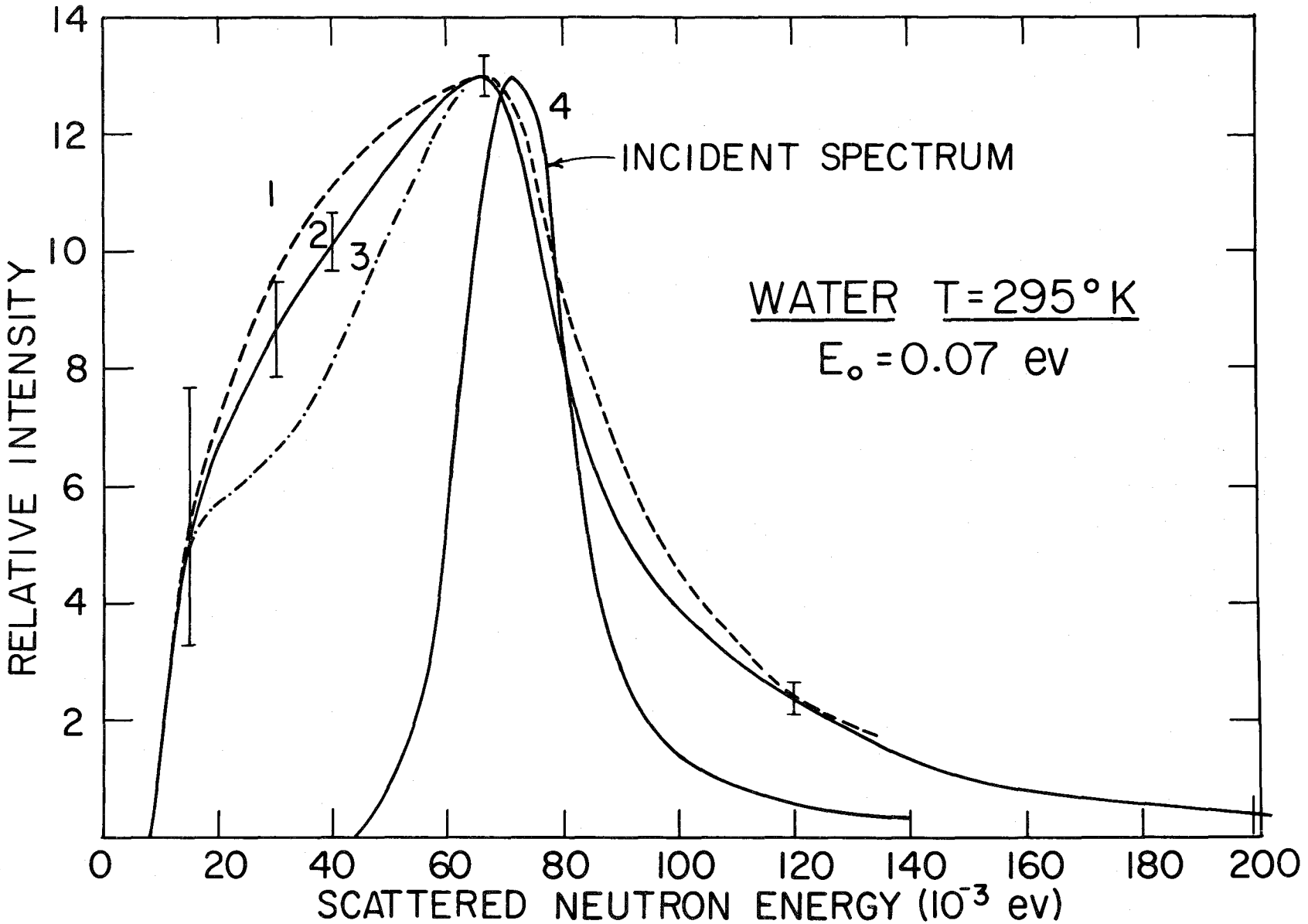

Fig. 3. Energy Distribution of Neutrons of Average Incident Energy 0.07 ev after Scattering at 90° Angle from H_2O. Curves 1 and 2 are for two sample thicknesses having a transmission of T = .65 and 0.83, respectively. Curve 3 is an approximation to the single scattering distribution. Curve 4 is the incident spectrum

being due to the Doppler broadening caused by the water molecules. In addition there is a broad band of neutrons displaced to considerably lower energy. This group of neutrons is probably due to the excitation of the hindered rotations already studied by Brockhouse.[2]

To visualize the thermalization caused by water in single scattering it is helpful to present the results shown in Fig. 4 where the area under the curve for incident neutrons is made equal to that for neutrons scattered from a thin sample of water. A computation of the logarithmic decrement $\xi = \ln E_0/E$ for this case gives $\xi \sim 0.3$, in agreement with the values obtained in the preceding paper by very different means. The results for that case were obtained by studying the average transmission of the scattered neutrons in an absorber having a 1/v dependence, whereas in the present experiment, the exact energy spectrum for the scattered neutrons is examined.

A further point of interest in the study of the thermalization of neutrons by water is obtained by studying the spectrum of neutrons scattered by solid water (ice). Fig. 5 shows the spectra obtained for a sample of ice having a transmission of 0.65, curve 1, and for a sample having transmission of 0.80, curve 2. It is clear in this case that there is a significant difference in the amount of multiple scattering, as revealed by curve 1 and 2. An estimate based on this difference for the effect of multiple scattering has been applied to the results and a first approximation to the single scattering curve for ice is shown in curve 4. From this curve for ice it is clear that the same recoil effects which were observed for water also are present for ice, giving rise to a displaced peak. However, the width of this displaced curve is much reduced compared to that for water. Furthermore, the hindered rotational level giving rise to the group of neutrons at about thermal energy is considerably sharper than in the case of water. This would seem to indicate that the broad

2) B. N. Brockhouse, Supplemento del Nuovo Cimento - "The Proceedings of the Varenna Conference on the Condensed State of Simple Systems".

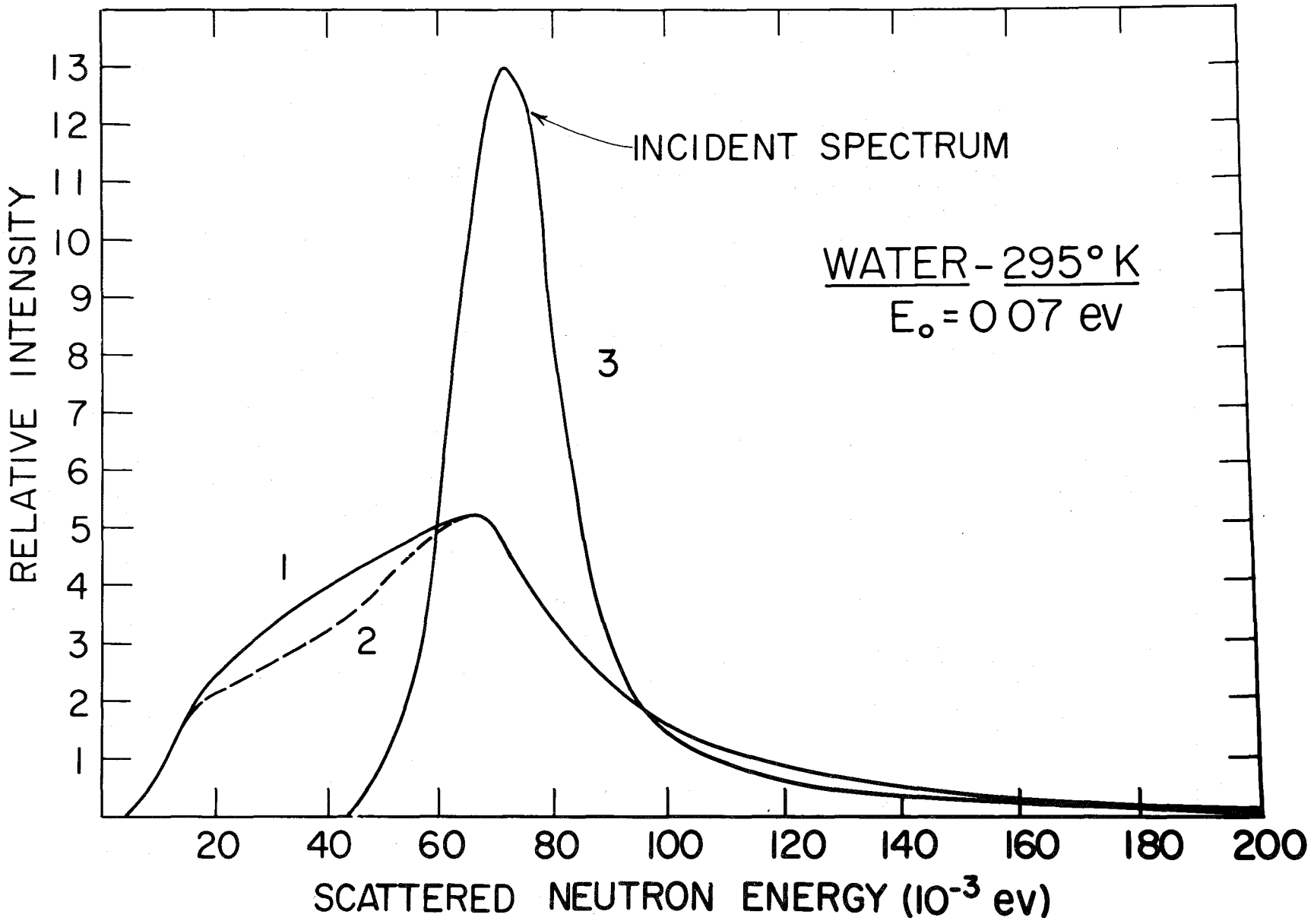

Fig. 4. Energy Distribution of Neutrons of Average Incident Energy 0.07 ev after Scattering at 90° Angle from H_2O, Normalized to the Incident Spectrum

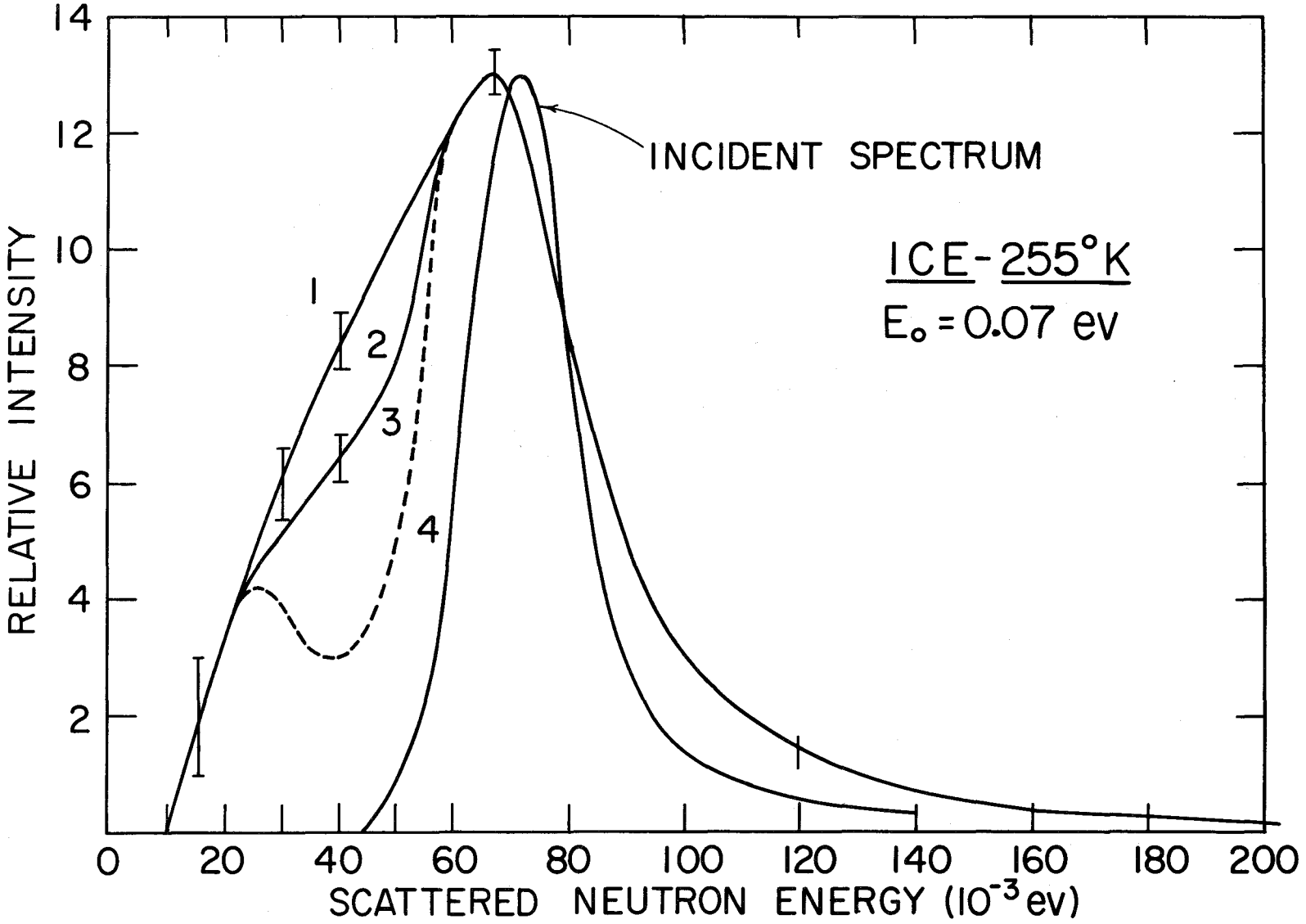

Fig. 5. Energy Distribution of Neutrons of Average Incident Energy 0.07 ev after Scattering at 90° Angle from Ice. Curves 1 and 2 are for two sample Thicknesses having a transmission of T = 0.60 and 0.80, respectively. Curve 3 is an approximation to the single scattering distribution.

distribution of levels effective in moderation by water are to a great extent reduced for the ice specimen. Fig. 6 shows the spectra for ice and water drawn on the same scale and normalized to the same peak value. These results are presented for the thin water and thin ice samples, each having a transmission of about 0.80. Also shown for comparison purposes is the distribution expected for a perfect gas composed of particles having a mass of 18.

The present technique for the investigation of thermalization can be used effectively to compare the thermalization effects expected with different moderator materials. Some reactor experimenters prefer to use in the place of one moderating substance a substitute material chosen to have more desirable properties as far as ease of experimenting is concerned. In particular, polyethylene is sometimes used in place of water. By using the time-of-flight technique we can easily show whether the detailed processes involved in the two moderating materials are sufficiently similar to make this a good approximation. Fig. 7 shows the spectrum (curve 2) we have obtained for a thin (T = 0.8) specimen of polyethylene. Curve 1 is the spectrum for a thick (T = 0.6) specimen of polyethylene. It is surprising to find curve 1 and 2 so similar, since multiple scattering should be present, particularly in the thicker sample and should act to make the curves different in the low energy region. Since the curves are not different within the statistics one must conclude that for single scattering, the scattered neutron has a broad energy distribution. However, this point is being investigated further. From the results which are presented here, the spectra from water and polyethylene are very similar and so should give similar results in critical or subcritical assemblies.

As an example of non-hydrogenous materials used for moderators, we have

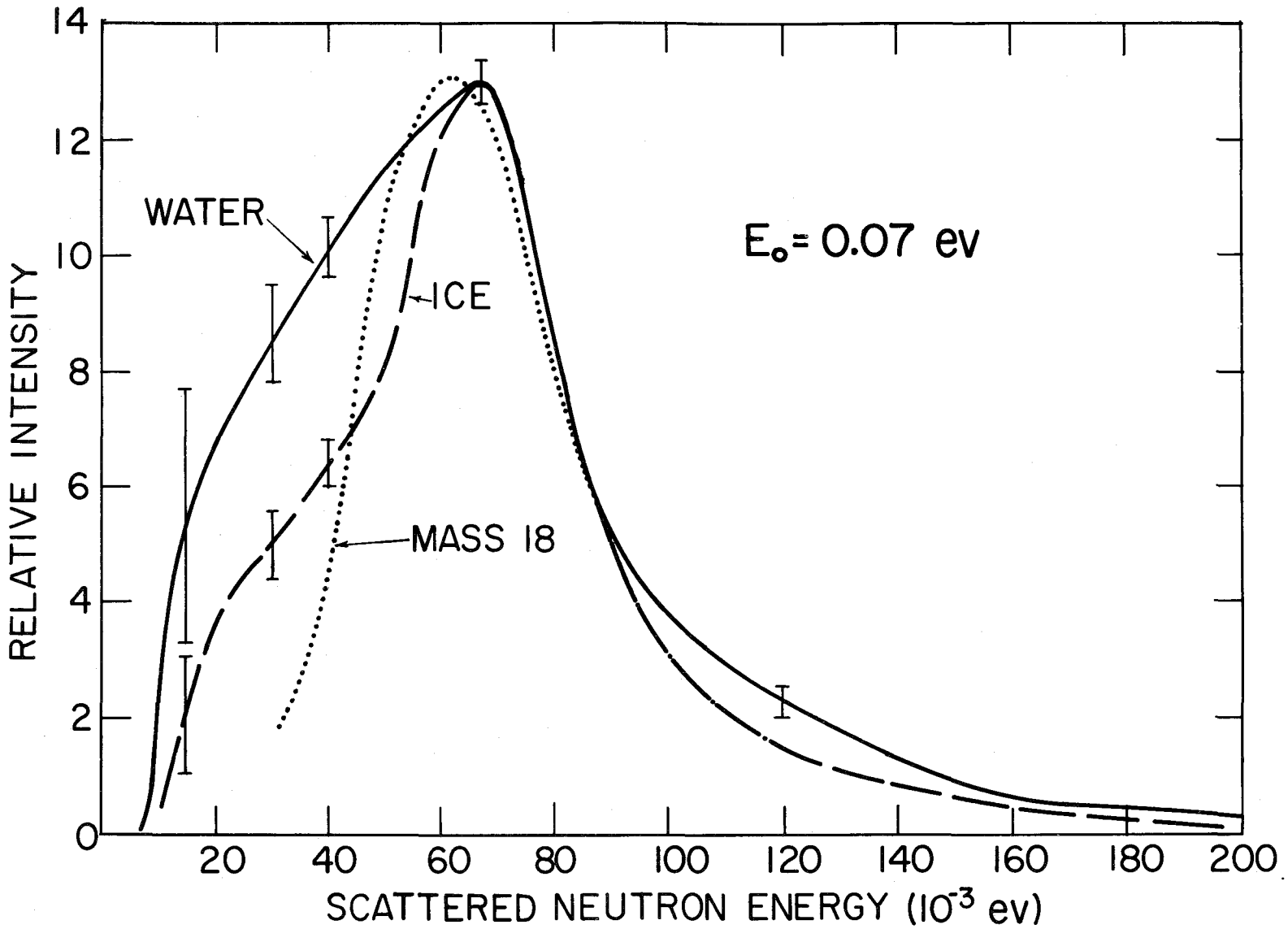

Fig. 6. Energy Distribution of Neutrons of Average Incident Energy 0.07 ev after Scattering at 90° Angle from Ice and Water. The expected curve for a simple gas with mass 18 is also shown.

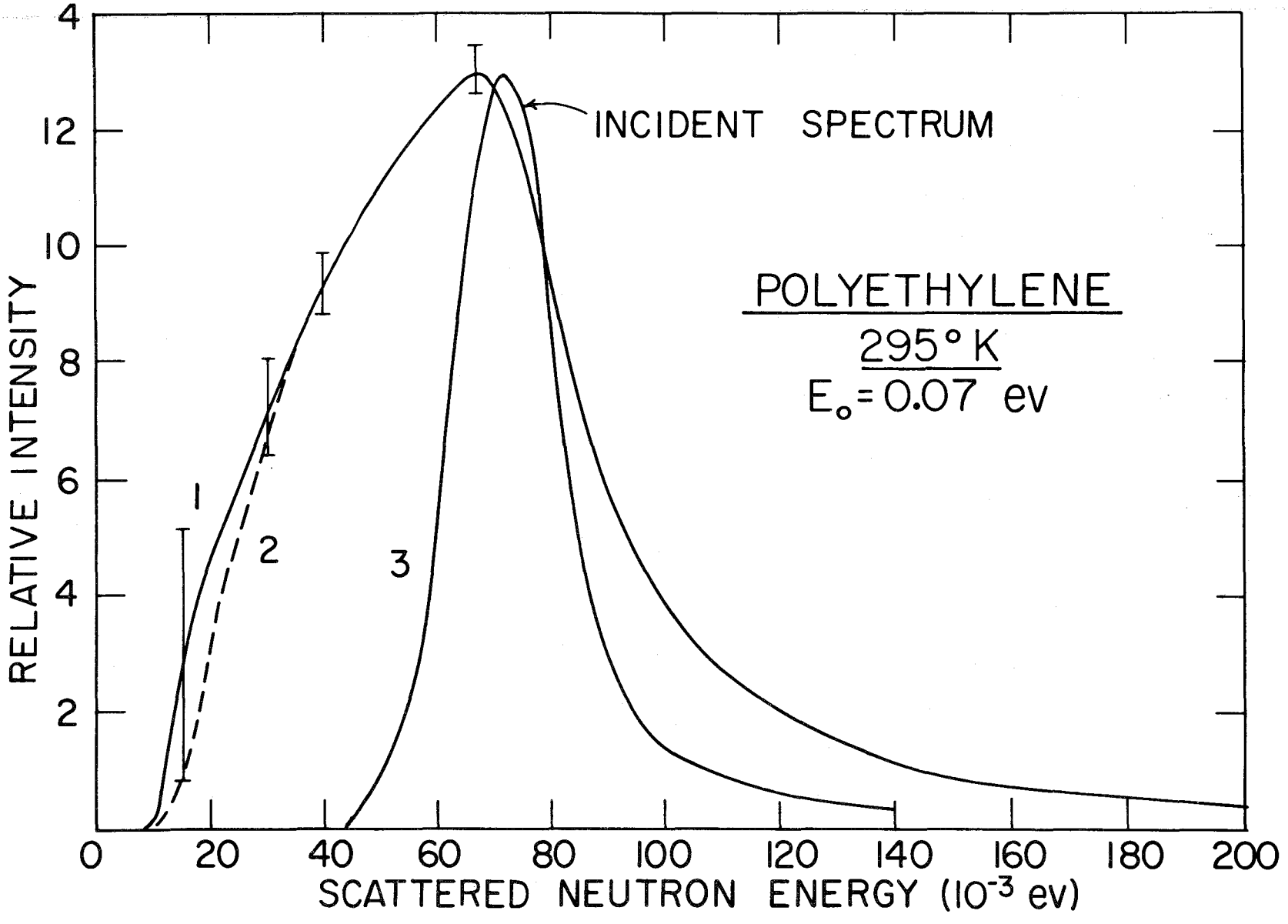

Fig. 7. Energy Distribution of Neutrons of Average Incident Energy 0.07 ev after Scattering at 90° Angle from Polyethylene. Curves 1 and 2 are for two sample thicknesses having a transmission of 0.6 and 0.8, respectively.

chosen graphite. Fig. 8 shows the spectrum obtained from a thin specimen of graphite for the scattering at 90°. For this particular experiment, the maximum experimental resolution was used. The incident spectrum here is considerably sharper than that used for preceding experiments and is important for the present experiment. One can see that the main group of scattered neutrons has the same energy as the incident beam. However, neutrons have been added by phonon interactions with the crystal to the wings on both the high and low energy side of the elastic peak. It is clear, with reference to Fig. 8 that there are more neutrons scattered to the low energy side, resulting in an over all decrease in the average energy of the scattered neutrons.

The above material is of a preliminary nature since the experiment has just begun and improvements have been made which will allow a much better signal-to-noise ratio. With this improved arrangement, the question of multiple scattering which always arises in this type of experiment can be examined with much more care. At this time it seems certain that there is a significant difference between the neutron interaction in ice and in water. Further measurements are necessary but it also appears that the neutron interaction with polyethylene and with water is very similar as far as the thermalization process is concerned though the exact details of the interaction are different.

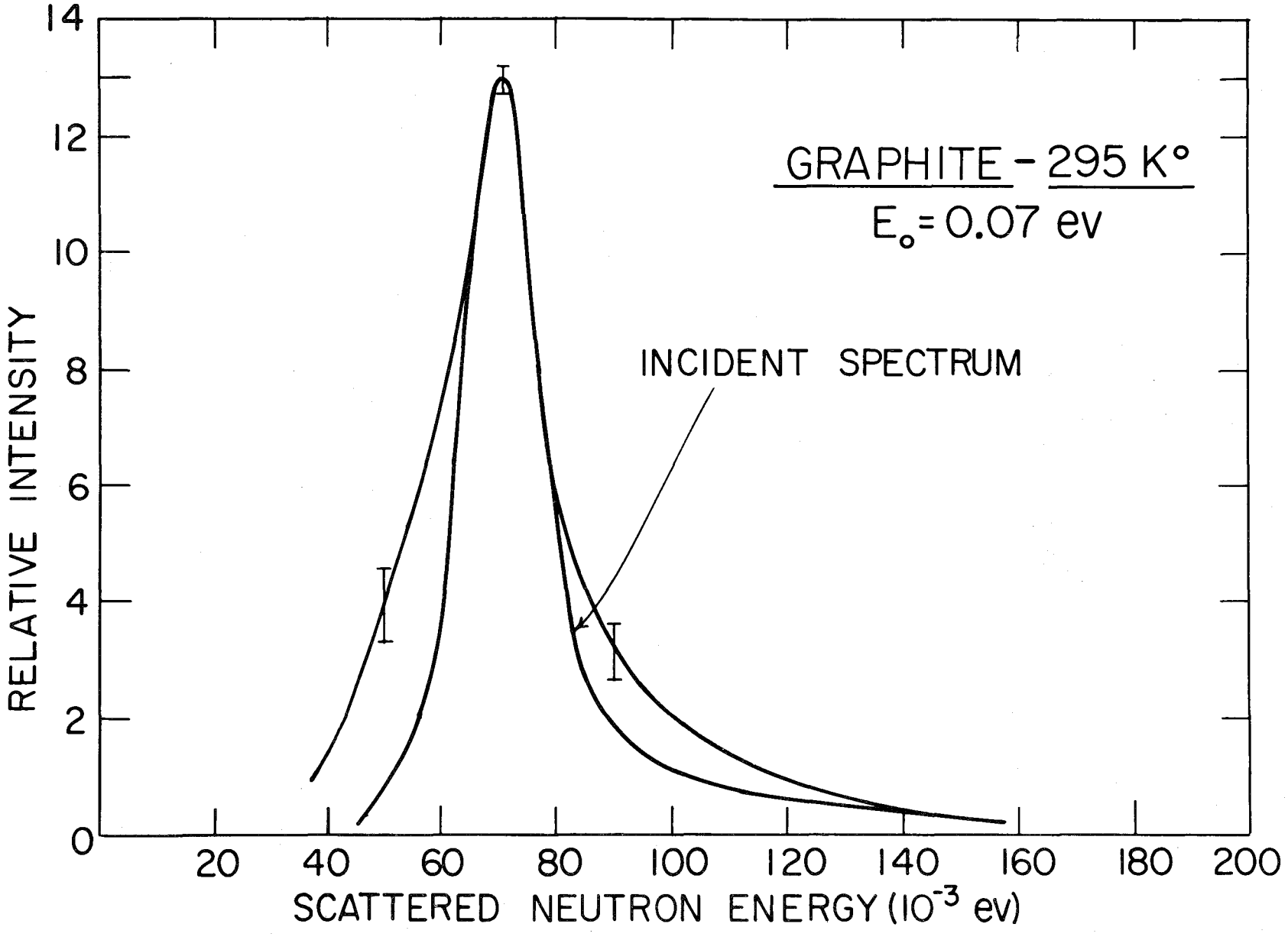

Fig. 8. Energy Distribution of Neutrons of Average Incident Energy 0.07 ev after Scattering at 90° Angle from a Sample of Polycrystalline Graphite. Also shown is the incident spectrum.

Session IV: LOW ENERGY SPECTRA IN HETEROGENEOUS MEDIA

Paper IV-A

NEUTRON THERMALIZATION CALCULATIONS FOR A HETEROGENEOUS LATTICE CONSISTING OF RODS OF URANIUM AND PLUTONIUM FUEL IN WATER

P. Greebler
General Electric Company

Neutron Thermalization Calculations for a Heterogeneous Lattice Consisting of Rods of Uranium and Plutonium Fuel in Water

Paul Greebler
General Electric Company
San Jose, California

Abstract

Calculated temperature and steam void coefficients of reactivity are highly sensitive to the techniques employed to obtain thermal cross sections, especially with the presence of a strongly non-1/v absorber such as Pu^{239}. Thermal neutron spectra are calculated for a heterogeneous lattice of a low enrichment boiling water reactor. Using blackness theory, equivalent homogeneous, mono-energetic cross sections for the lattice are computed at closely spaced energy intervals over the thermal energy range. The energy distribution of the thermal neutron flux is then obtained using both the Wigner-Wilkins and the Wilkins thermalization equations. Calculations are made with the fuel elements assumed to contain only U^{235} and U^{238} yielding almost pure 1/v absorption, and also for the case of appreciable Pu^{239} present in addition to the uranium, resulting in a significant departure from 1/v absorption. Sensitivity of the calculated spectrum to the effective mass of the hydrogen is tested by allowing wide variations of the $\xi\sigma_s$ values for water at low energies in several applications of the Wilkins equation. Variations in the thermal-neutron spectra resulting from the choice of the thermalization equation (Wigner-Wilkins or Wilkins), from changing $\xi\sigma_s$, or as a result of plutonium buildup are evaluated in terms of isotopic and total cross sections averaged over the spectrum in each case.

NEUTRON THERMALIZATION CALCULATIONS
FOR A HETEROGENEOUS LATTICE CONTAINING
URANIUM AND PLUTONIUM FUEL IN WATER

I. INTRODUCTION

Plutonium buildup in a low enrichment, uranium fueled thermal reactor affects many of the core nuclear properties, including power distribution, excess reactivity that must be held down by control rods, and the temperature and void coefficients of reactivity. In order to correctly evaluate these effects, the thermal cross sections for the fuel and other reactor materials must be averaged over the thermal spectrum. Simplified formulas for spectral hardening (1), based upon the evaluation of an effective temperature for averaging cross sections over a Maxwell-Boltzman distribution, are available for reactor cores whose absorption cross sections vary inversely with neutron velocity (1/v absorption). These relationships do not apply, however, with appreciable plutonium in the core, since the Pu-239 resonance peaked at 0.29 e.v. tends to soften the spectrum, opposing the spectral hardening of the 1/v-absorption.

Thermalization studies were made on a low enrichment, boiling water reactor as one phase of a program to determine the effect of plutonium buildup on the void and temperature coefficients of reactivity. The heterogeneous lattice, shown in Figure 1, consisted of closely-spaced uranium oxide fuel rods with an initial 1.5 percent U-235 enrichment in water. Thermal neutron spectra were evaluated as a function of plutonium concentration in the fuel, of steam void volume in the water, and of water temperature. The Wigner-Wilkins thermalization equation (2), in conjunction with the IBM 650 code DONATE (3), was used to obtain the thermal spectra for cross section averaging.

Figure 1.

Section of Lattice

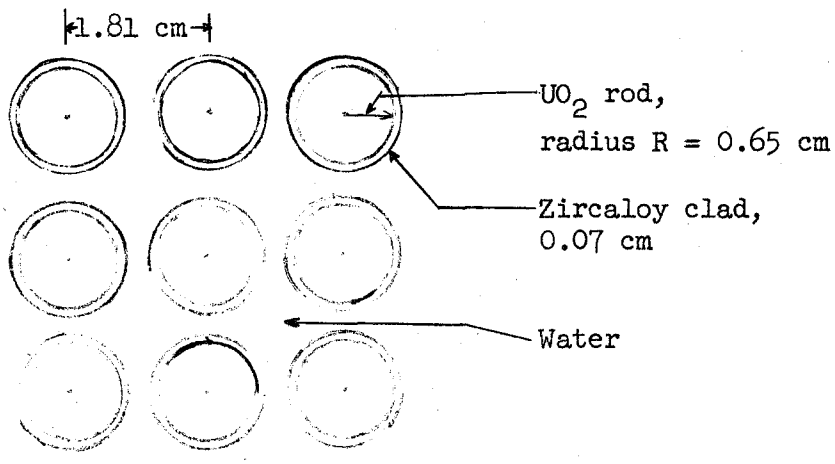

The Wigner-Wilkins thermalization model, which assumes that the neutrons suffer scattering collisions only with a monatomic hydrogen gas, does not describe the actual physical situation in water. Additional studies were made to determine the sensitivity of the calculated spectra to the thermalization model used. Spectra were obtained with the Wilkins thermalization equation (4,5,6), using an IBM 653 code WILKIE (7), and compared with the Wigner-Wilkins spectra. Investigations also were made of the sensitivity of the calculated spectra to the assumed energy variation of the effective mass of hydrogen bound in water; and of the sensitivity of the spectra to the self-shielding of the fuel rods in the heterogeneous lattice. Various spectra obtained from these studies are shown and compared in Section III. In the following section, the techniques used to evaluate the fuel self-shielding factors for the thermalization calculations are described.

II. FUEL SELF-SHIELDING

For a heterogeneous lattice, the thermal cross sections must be flux-averaged both spectrally and spatially. The usual procedure consists of an evaluation of the spectral hardening for an equivalent homogeneous medium, followed by a calculation of the spatial flux distribution using the hardened cross sections. Since the spectral and the spatial flux distributions are not completely separable, fuel self-shielding factors were calculated and applied to the cross sections used in the determination of the Wigner-Wilkins or Wilkins spectra. (Failure to taken into account the self-shielding leads to an over-estimation of the spectral hardening by the 1/v absorption and also the flux depression in the neighborhood of the 0.29 e.v. Pu-239 resonance, shown in Figure 6 and discussed in Section IIID.)

Monoenergetic cross sections for each thermal spectrum evaluation were calculated at approximately 100 energy points over the thermal energy range. At each energy point, a fuel self-shielding factor f was computed from a neutron current balance on the outer surface of the rod. For an isotropic flux on the rod surface, the expression for f is simply

$$f = \frac{\beta}{2\Sigma_a R} \tag{1}$$

where f is the ratio of the average flux in the rod to the flux on the surface of the rod, Σ_a and R are respectively the fuel absorption cross section and the radius of the fuel rod, and β is the blackness of the fuel rod (8) (the probability that a neutron incident on the rod will be captured before it emerges). A good approximation for β is given by the expression

$$\beta = 1 - e^{-2\Sigma_a R} \tag{2}$$

The exponential term in equation (2) is just the tranmission probability, $1-\beta$. The approximation is valid except for very black rods ($\Sigma_a R$ large) with appreciable scattering cross sections. For this case, however, f is nearly $1/2\Sigma_a R$ and is relatively insensitive to errors in the transmission probability as given by the exponential term of equation (2).

Flux-weighting factors E_f and E_w for the fuel and water regions respectively are evaluated from the self-shielding factor f and the water:fuel volume ratio v, using the relationships

$$E_w = \frac{1 + v}{f + v}$$

(3)

$$E_f = fE_w$$

The E factor for each region is simply the ratio of the average flux in that region to the average flux in the cell consisting of a single fuel rod and its share of the surrounding water. The flux-weighting factor for the zirconium fuel clad, E_c, was taken as unity. The equivalent homogeneous cross sections at each energy point were obtained simply by multiplying the fuel, water, and clad cross sections by their respective flux-weighting factors and averaging over the cell volume.

Flux-weighting factors obtained from equations (3), using (1) and (2), were compared with those obtained from the P_3 spherical harmonic approximation of transport theory. Several cases covering a typical range of values v, R, and Σ_a for a tight lattice were considered. (Σ_s for a low enrichment fuel does not vary appreciably with energy or from one case to another.) As indicated by the comparative E_f values shown in Table I below, flux-weighting factors for tight lattices obtained by this relatively simple calculation agreed closely with those calculated by the P_3 method. For lattice configurations more complicated than that considered here, the flux-weighting factors may be obtained from Crowther's multi-region current balance technique (9), which carries out the required calculation with considerably less computer time than is required for a P_3 calculation.

TABLE I

Comparison of E_f Values Otbained from Equation (3) and the P_3 Method

v	Σ_s-cm^{-1}	Σ_a-cm^{-1}	R-cm	E_f Equation (3)	E_f P_3 Method
1.3	.374	.1624	0.635	.943	.943
1.3	.374	.3227	0.635	.890	.887
1.5	.369	.2160	0.762	.906	.903
1.5	.365	.0860	1.067	.946	.951
1.8	.374	.3436	0.635	.869	.873
2.2	.374	.3555	0.635	.857	.863
2.534	.365	.1515	1.067	.892	.901

III. CALCULATED SPECTRA

A. Comparison of Wilkins and Wigner-Wilkins Spectra

Figures 2a and 2b show thermal spectra calculated from the Wilkins and the Wigner-Wilkins thermalization equations. Spectra in Figure 2a are for a lattice with the fuel containing appreciable plutonium, while those in Figure 2b are for a lattice containing fresh uranium fuel*. Isotopic fuel composition data, in addition to water-to-fuel ratio and the density and temperature of the water are listed in the upper left portion of each figure containing thermal spectra. Cross sections and related nuclear parameters averaged over each thermal spectrum are shown in the upper right corner of each figure. Thermal flux, plotted as the ordinate of the spectral curves, has been normalized in each case to a slowing down density of unity at 0.75 e.v. (i.e., $\int_0^{0.75} \Sigma_a \phi dE = 1$).

*U-235, U-238, and Pu-239 are the only isotopes considered in the two fuel compositions used to compute the spectra shown in this paper. Fission products and the higher plutonium isotopes, which would be included in the spectrum evaluation for a specific problem, have been omitted here since these minor fuel constituents do not contribute significantly to the general features of the spectrum.

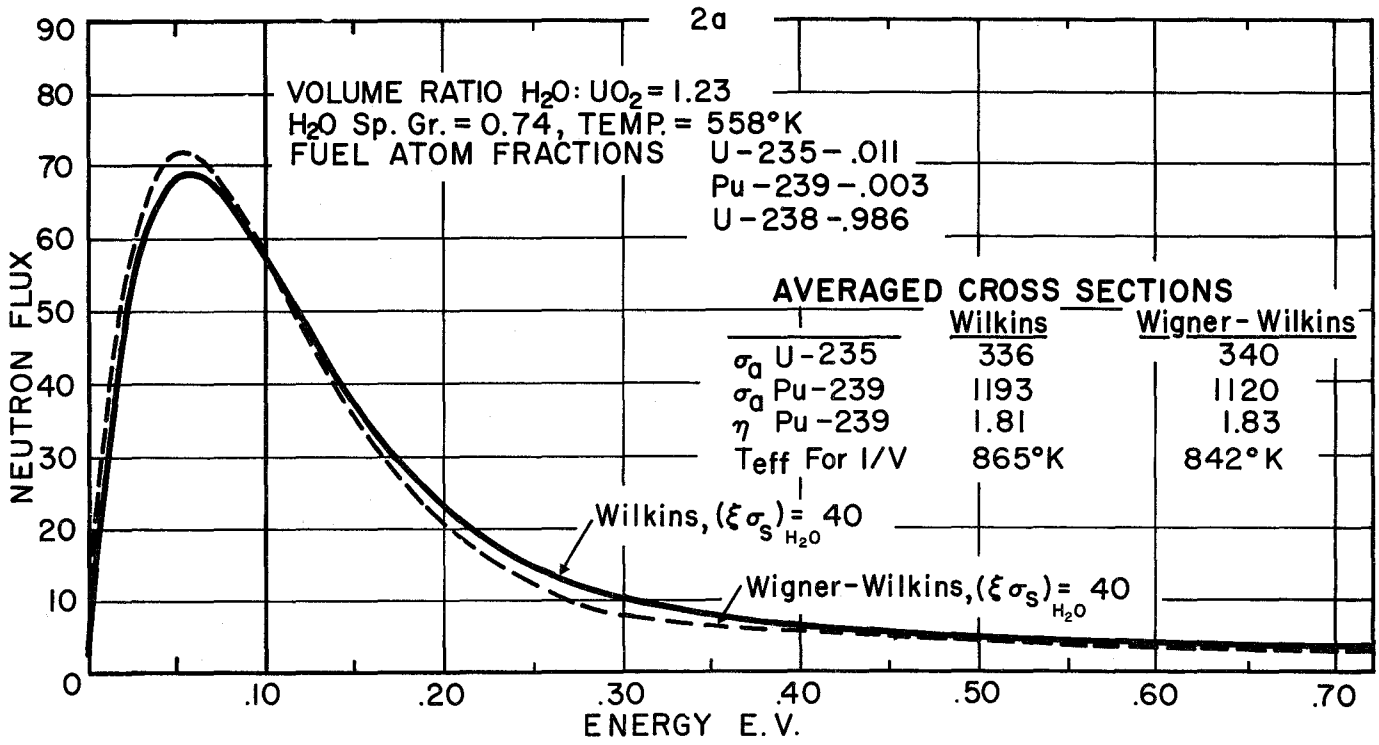

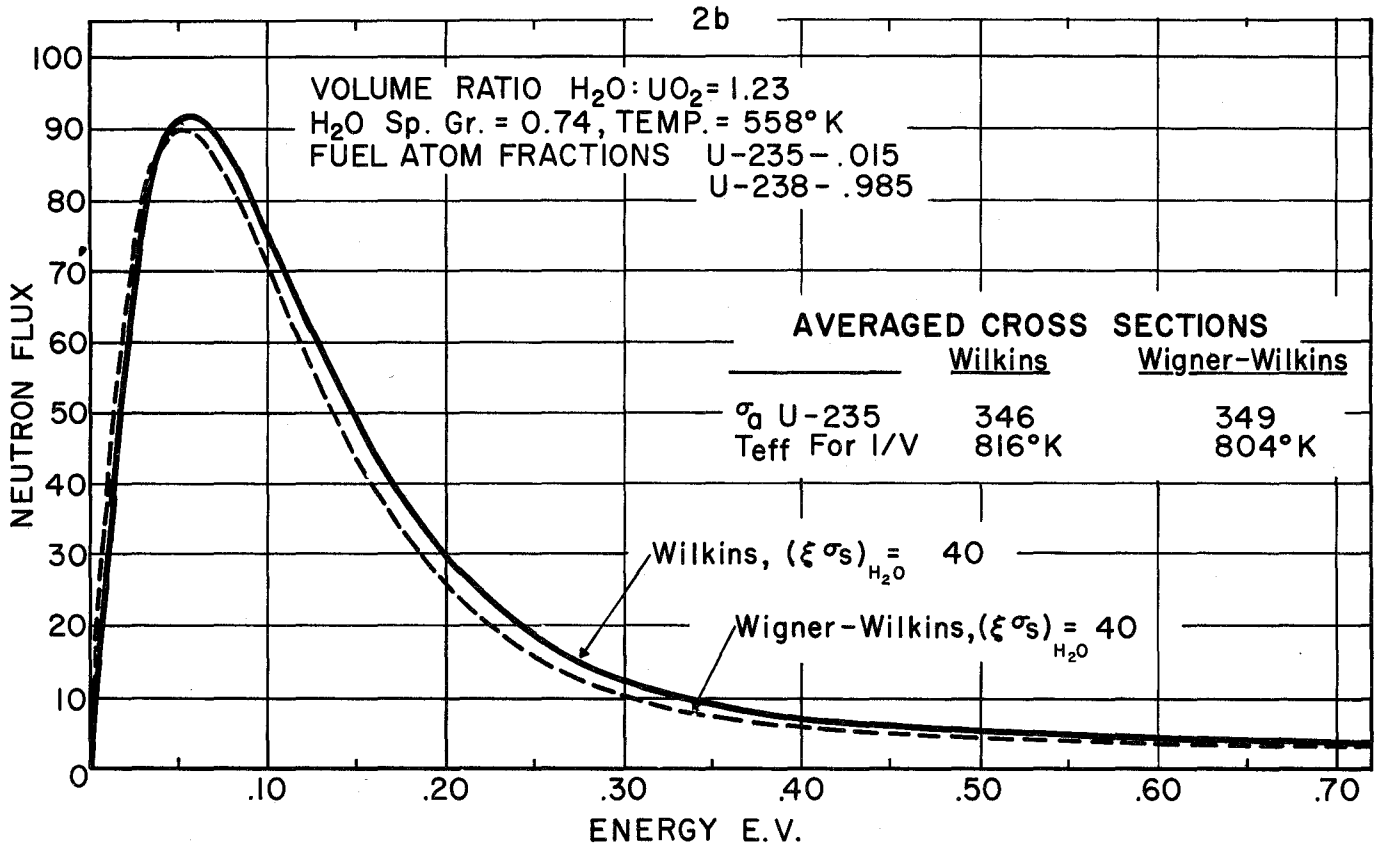

FIGURES 2a AND 2b. COMPARISON OF WILKINS AND WIGNER-WILKINS THERMAL SPECTRA FOR BURNED CORE CONTAINING PLUTONIUM (2a) AND FRESH CORE (2b).

The normalized Wilkins spectrum in Figures 2a and 2b is harder than the corresponding Wigner-Wilkins spectrum (i.e., the Wilkins flux is larger at high energies and smaller at low energies). Pu-239 in the fuel (Figure 2a) accentuates the difference. With a longer neutron residence time in the region of the 0.29 e.v. resonance for the Wilkins scattering kernel, resonance capture is increased. In the normalized spectra, the increased resonance capture is manifested by a higher flux in the neighborhood of the resonance and a depressed flux at energies below the resonance.

A distinguishing feature between the Wilkins and the Wigner-Wilkins spectra is the sharper transition of the Wigner-Wilkins flux from the 1/E region to that of the Maxwellian distribution of neutron population. A comparison by Amster(10) between calculated Wigner-Wilkins spectra and experimental spectra obtained by Poole (11) for boric acid in water indicated that the transition of the Wigner-Wilkins flux from 1/E to Maxwellian was too sharp. Figure 2c shows Poole's experimental spectral data fitted respectively by Amster's Wigner-Wilkins spectrum and by a Wilkins spectrum calculated with the WILKIE code. It appears that the Wilkins spectrum yields a better fit of the experimental values than does the Wigner-Wilkins spectrum, indicating that the Wilkins equation provides the more suitable model for neutron thermalization in water-moderated assemblies. Experimental spectral data with Pu-239, or other isotopes containing low energy resonances*, in water would be desirable and probably would provide more definite evidence in favor of one or the other of the thermalization equations.

The effect of the difference between the two thermal spectra on cross sections averaged over the spectra is shown in Figures 2a and 2b. For U-235, which is predominately a 1/v absorber, the harder Wilkins spectrum results only in a slightly lower averaged absorption cross section. For Pu-239, which is not a 1/v absorber at the moderator temperature considered (558°K), the Wilkins spectrum results in an appreciably increased absorption cross section. (At room temperature, where the effect of the Pu-239 resonance at 0.29 ev on the thermal flux distribution is less important, the spectral dependence of the Pu-239 cross section would be expected to exhibit a behavior characteristic of a 1/v absorber.) The sharp transition of the Wigner-Wilkins flux from the 1/E region to the Maxwellian neutron distribution occurs in the neighborhood of the 0.29 e.v. resonance, for the temperature considered in the spectral evaluation. This effect amplifies the increase of the Wilkins averaged Pu-239 cross section over the Wigner-Wilkins value. The η value for Pu-239 shown in Figure 2a is slightly lower for the harder Wilkins spectrum, since the fission cross section does not increase as rapidly as the absorption cross section with increasing energy as the 0.29 e.v. resonance is approached from the low energy side.

*Cadmium, samarium and europium would be suitable materials for this purpose.

The value "T_{eff} for 1/v" listed for each spectrum is the effective hardened temperature for a 1/v absorber (i.e., the temperature associated with a Maxwellian distribution which would yield the same averaged absorption cross section for a 1/v absorber as the actual spectrum obtained). Since the cross sections were flux-averaged over the energy range 0 to 0.75 e.v., the T_{eff} values are slightly higher than would be obtained if the thermal cutoff were chosen at a lower energy. T_{eff} for the Wilkins spectrum is slightly greater in each case than that for the corresponding Wigner-Wilkins spectrum. T_{eff} for either spectra is higher for the burned fuel containing plutonium than for the fresh fuel, since the burned fuel has a 40 percent higher absorption cross section. The difference of T_{eff} values, however, is considerably less than would be realized if the 40 percent additional absorption were entirely of the 1/v type. The Pu-239 resonance absorption, which causes appreciable flux depression to occur at higher energies than for 1/v absorption, contributes a spectrum softening effect opposing the spectrum hardening of the 1/v absorption.

B. Sensitivity of Calculated Spectra to the Assumed Spectral Variation of the Effective Mass of Hydrogen

Figure 3a shows three different spectral variations of $\xi\sigma_s$ for water, corresponding with three different spectral variations of the effective mass of hydrogen bound in water*. Case II is a constant $\xi\sigma_s$ for water, equal to 40 barns. The upper $\xi\sigma_s$ curve, Case I, is derived from experimentally measured scattering cross sections (12) and transport cross sections calculated by Zweifel and Petrie (13) for water, assuming that the average scattering angle for the neutron is related to the effective mass, as in the case of simple elastic scattering. The lower curve, Case III, was calculated by assuming the effective mass of hydrogen to be 18 a.m.u. below .04 e.v., with a sharp transition to a mass of one between .04 and .08 e.v.

Figure 3b and 3c show the progressive hardening of the Wilkins spectrum as the low energy $\xi\sigma_s$ for water decreases from Case I to Case III. The hardening is especially pronounced for the assumed $\xi\sigma_s$ variation of Case III. As listed on the figures, the spectral hardening results in lower absorption cross sections for U-235, but higher absorption cross sections with lower η for Pu-239.

*The term ξ does not have quite the same physical significance as in the slowing down energy region, but it bears the same relationship to the moderator-to-neutron nuclear mass ratio m. For the Wilkins equation, $\xi \approx 2/m$.

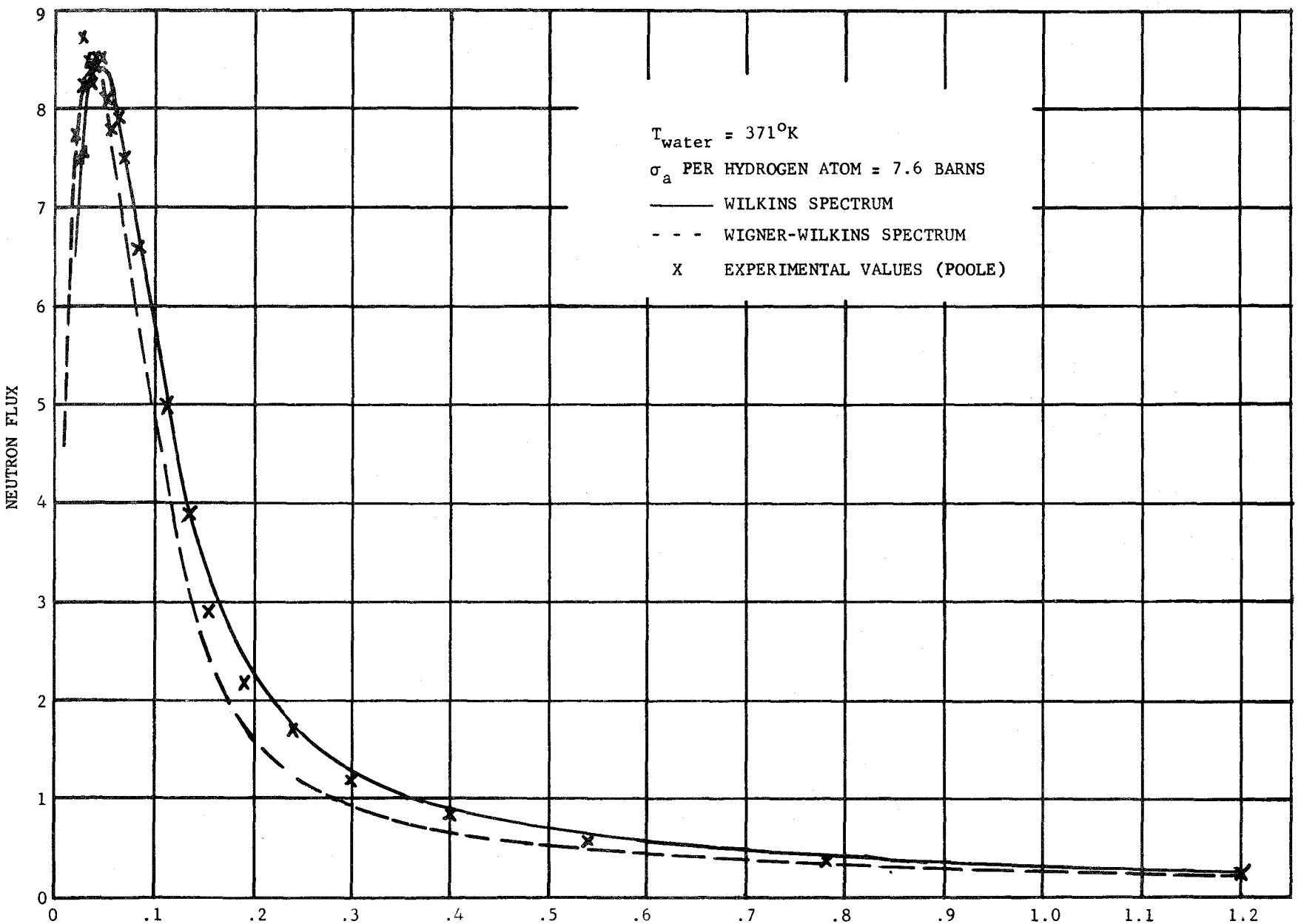

FIGURE 2c. COMPARISON OF POOLE'S EXPERIMENTAL SPECTRUM WITH CALCULATED SPECTRA.

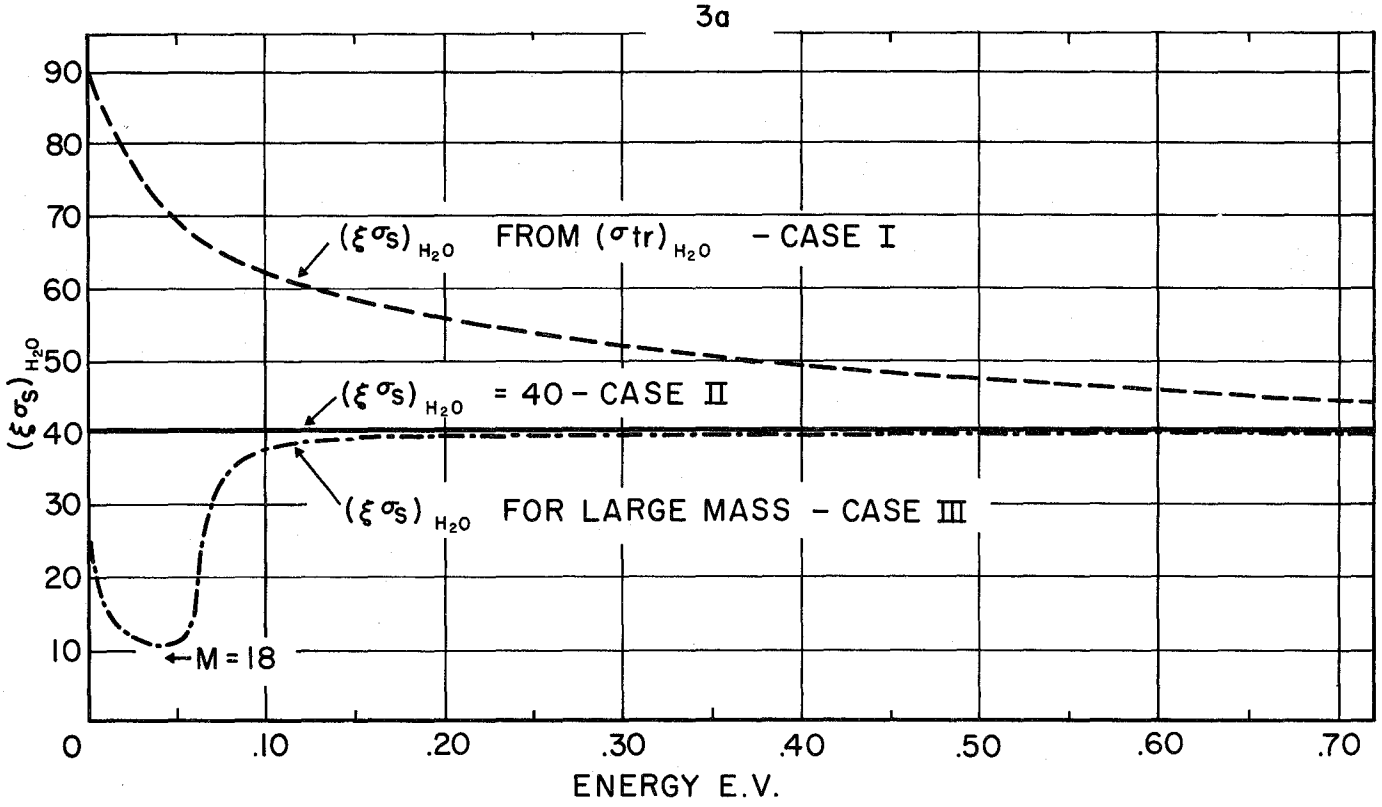

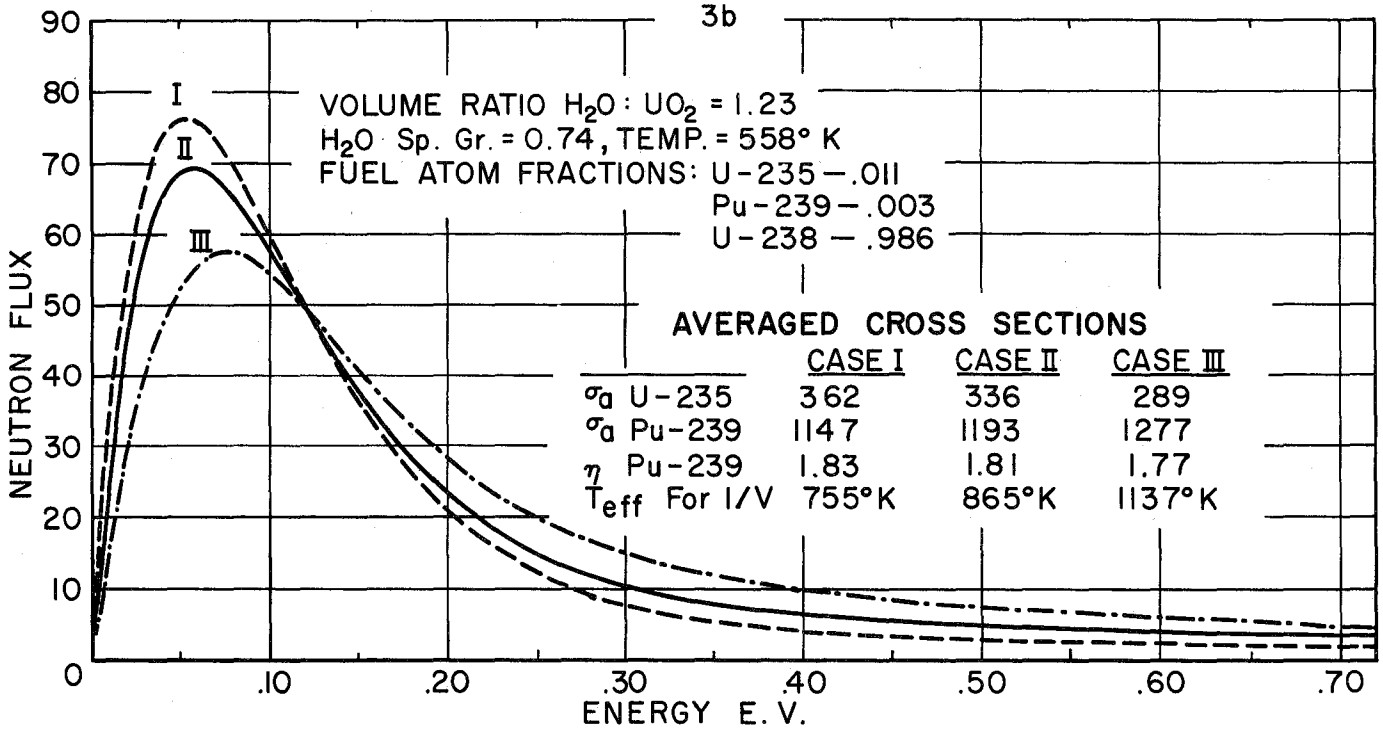

FIGURE 3a AND 3b. WILKINS SPECTRA FOR DIFFERENT $(\xi\sigma_s)_{H_2O}$ VARIATIONS WITH ENERGY (BURNED CORE CONTAINING PLUTONIUM).

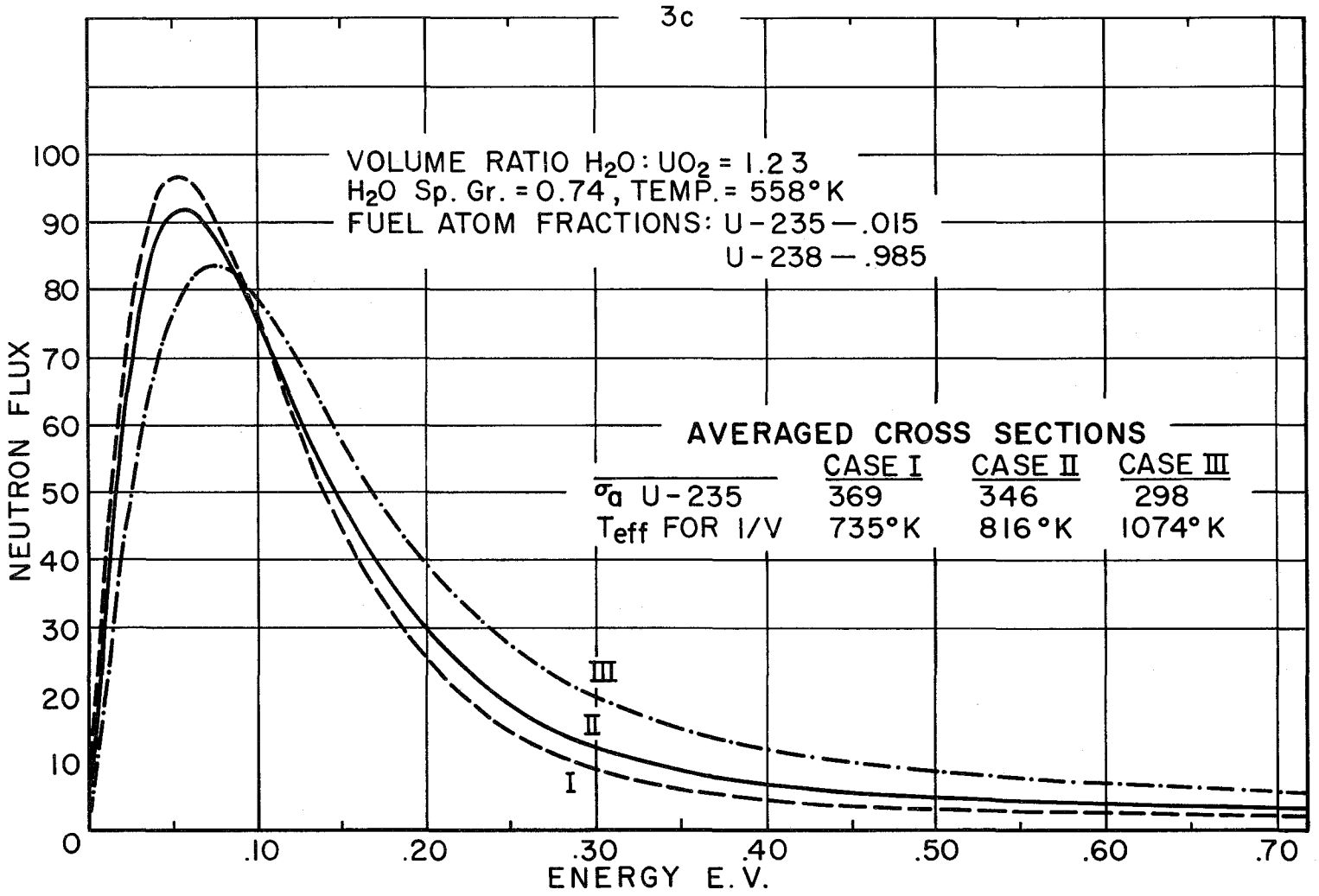

FIGURE 3c. WILKINS SPECTRA FOR DIFFERENT $(\xi\sigma_s)_{H_2O}$ VARIATIONS WITH ENERGY (FRESH CORE). SEE FIGURE 3a FOR $(\xi\sigma_s)_{H_2O}$ CURVES CORRESPONDING WITH CURVES I, II, AND III.

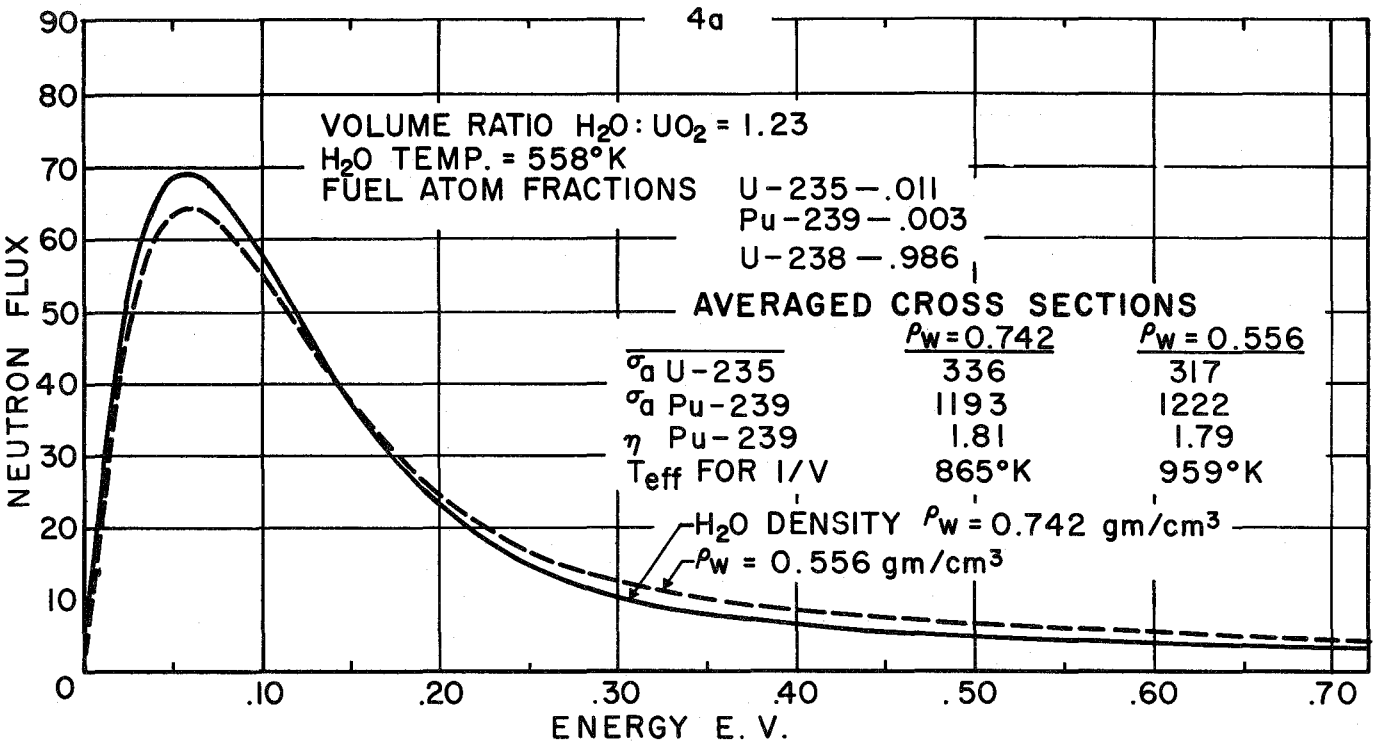

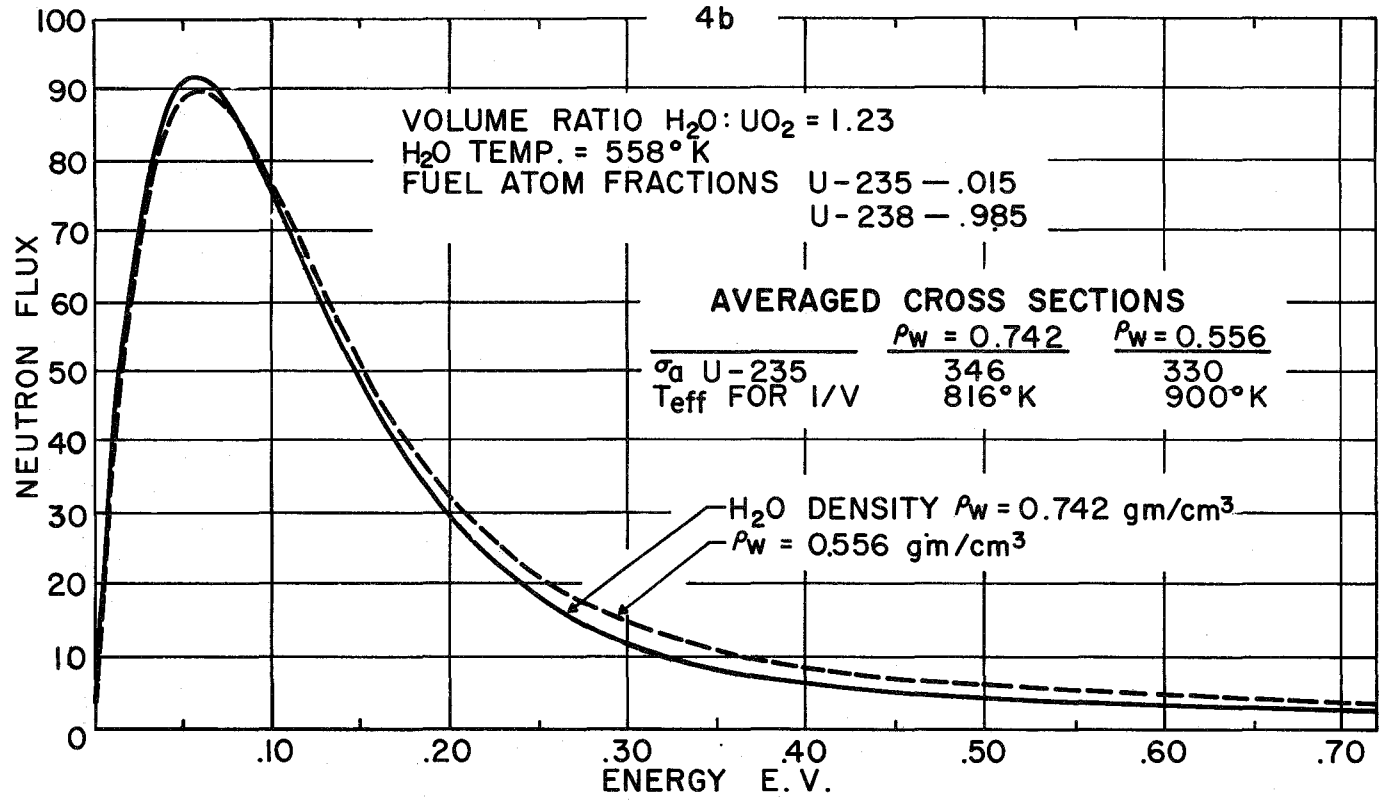

FIGURE 4. SPECTRUM HARDENING DUE TO VOIDS (STEAM) IN THE WATER FOR BURNED CORE CONTAINING PLUTONIUM (4a) AND FRESH CORE (4b). WILKINS SPECTRUM WITH $(\xi \sigma_s)_{H_2O}$ = 40 BARNS FOR ALL FOUR CASES.

C. Spectral Hardening Due to Decreased Water Density

Figures 4a and 4b show the hardening of the Wilkins spectrum resulting from a 25 percent reduction of the density of the water. This effect is especially important for a boiling water reactor, since the water density varies as it flows through the core due to the buildup of steam voids. Figure 4b, containing the spectra for the fuel with plutonium, is of interest for a consideration of the void or temperature coefficients of reactivity in a low enrichment reactor.

D. Sensitivity of Calculated Spectra to the Fuel Self-Shielding

Calculation of fuel self-shielding factors was discussed in Section II. Figure 5 shows the effect of neglecting the fuel self-shielding of the heterogeneous lattice in determining the cross sections to be used for the evaluation of the Wilkins spectrum. Setting the flux-weighting factors E_f and E_w equal to unity hardens the calculated spectrum slightly, with resultant lowering of the averaged U-235 absorption cross section and raising of the Pu-239 cross section. For a more highly self-shielded configuration, the spectrum hardening error resulting from neglect of the self-shielding would be more severe.

IV. CONCLUSIONS

Low enrichment fuel lattices at moderately high temperatures containing appreciable plutonium are more sensitive to the thermalization techniques used to obtain thermal cross sections than lattices in which the non-1/v absorption is negligibly small. The Wilkins spectrum yields considerably higher averaged absorption and fission cross sections, with a smaller η, for Pu-239 than the corresponding Wigner-Wilkins spectrum. Appreciable increase of the effective hydrogen mass at low energies significantly hardens the Wilkins spectrum, with resultant increase of the averaged Pu-239 absorption and fission cross sections and lowering of the U-235 (and other 1/v-type) cross sections. Comparison of Poole's experimental data with calculated Wilkins and Wigner-Wilkins spectra suggests that the Wilkins equation provides a more satisfactory thermalization technique. More experimental spectral data, preferably with Pu-239 in water*, is required to establish the correct thermalization model.

Calculated spectra for heterogeneous lattices are influenced by the self-shielding of the fuel, the sensitivity being dependent upon the degree of self-shielding for a specific configuration. For a relatively simple lattice geometry, accurate self-shielding factors can be obtained from extremely simple mathematical relationships, such that the numerical procedures for a spectrum evaluation are not rendered long and complicated by inclusion of the self-shielding.

---

*See footnote, page 7.

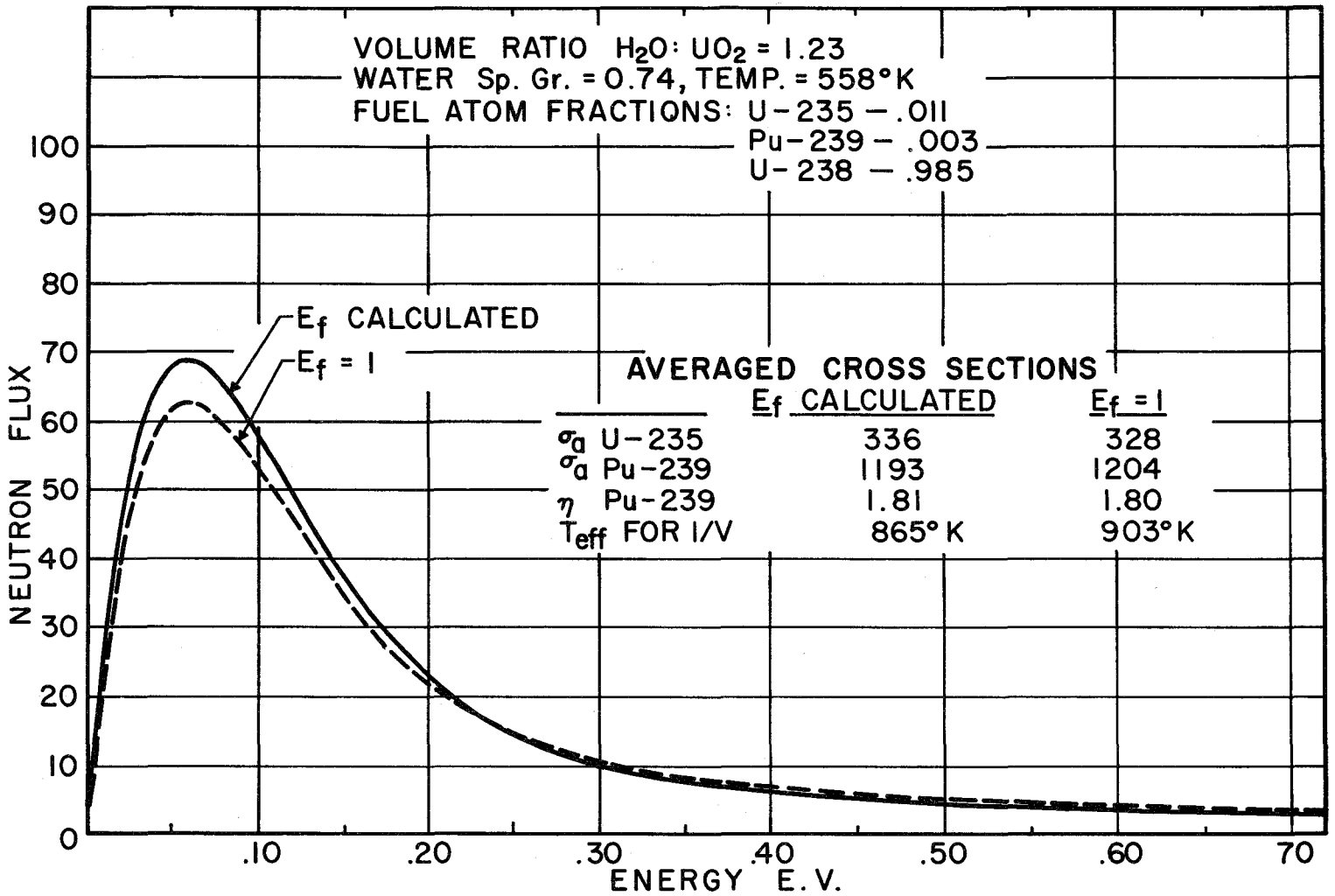

FIGURE 5. HARDENING OF CALCULATED WILKINS SPECTRUM, $(\xi \sigma_s)_{H_2O}$ = 40 BARNS, DUE TO NEGLECT OF FUEL SHELF SHIELDING (BURNED CORE CONTAINING Pu-239).

V. REFERENCES

1. R. W. Deutsch, Nucleonics, Vol 15, p. 48 (1957), (Describes method based on the work of K. Cohen.)

2. E. P. Wigner and J. E. Wilkins, Jr., AECD-2275, (September 1944).

3. H. Amster and R. Suarez, WAPD-PM-45, May 1956.

4. J. E. Wilkins, Jr., CP-2481 (1944), (Declassified).

5. H. Hurwitz, Jr., M. S. Nelkin, and G. J. Habetler, Nuclear Science and Engineering, Vol 1, p. 280 (1958).

6. E. R. Cohen, Nuclear Science and Engineering, Vol 2, p. 227 (1957).

7. C. Ehlers and G. Keirns, Thermalization Code for Wilkins Equation and Heterogeneous Lattice Developed at Vallecitos Atomic Laboratory, Pleasanton, California.

8. G. W. Stuart, Nuclear Science and Engineering, Vol 2, p. 617, (1957).

9. R. L. Crowther, "Multiregion Cell Calculations by Use of the Method of Multiple Collisions", to be presented at the American Nuclear Society Annual Meeting in Los Angeles, California, June 2-5, 1958.

10. H. J. Amster, Nuclear Science and Engineering, Vol 2, p. 394 (1957).

11. M. J. Poole, J. Nuclear Energy, Vol 5, p. 325 (1957).

12. D. J. Hughes and J. A. Harvey, BNL-325 (1955).

13. P. F. Zweifel and C. D. Petrie, KAPL-1469 (January 1956).

Paul Greebler/W. H. Harker/J. M. Harriman
Engineering Physics Operation
300 - 188

cjt

Paper IV-B

THE INFLUENCE OF NON-1/v ABSORBERS ON REACTOR PARAMETERS

T. J. Krieger M. L. Storm
P. F. Zweifel D. M. Keaveney
Knolls Atomic Power Laboratory

The Influence of Non-1/v Absorbers on Reactor Parameters

T. J. Krieger M. L. Storm
P. F. Zweifel* D. M. Keaveney

Knolls Atomic Power Laboratory
Schenectady, New York

Abstract

The development of the SOFOCATE code for the IBM-704 computer has greatly facilitated the calculation of thermal spectra and associated average cross-sections in assemblies containing non-1/v absorbers. The code is particularly useful when isotopes with low-lying resonances (< 2ev), e.g., Eu, Pu^{239}, are present, since by extending the "thermal" range to include these resonances, it is possible to analyze their effects in a more accurate and convenient way than has heretofore been available. This expedient has been employed in the analysis of the comparative xenon poisoning of U^{235}- and Pu^{239}-fueled assemblies, and also in the calculation of the influence of Eu on the temperature defect of a reactor. Results of the former study show that, because of the favorable competition of the 0.3 ev Pu fission resonance relative to the Xe captures, the control invested in overcoming peak xenon is greater in a U^{235} assembly than in the comparable Pu^{239} assembly. In the latter problem, the change in the temperature defect of a reactor upon addition of Eu is found to be dependent on the degree of spectral hardening. This dependence is directly attributable to the 0.4 ev Eu resonances. In both problems, the thermal cutoff energy in the SOFOCATE calculations was chosen to be 1.0 ev, which has the effect of yielding lower values for the various cross-sections than those usually used.

*Speaker.

The Influence of Non-1/v Absorbers on Reactor Parameters - D.M. Keaveney, T.J. Krieger, M.L. Storm, P.F. Zweifel

The availability of the SOFOCATE code[1] which solves the Wigner-Wilkins equation for moderation by hydrogen and arbitrary variation of absorption cross-section with energy has made it possible to study in detail the effect of non-1/v absorbers on reactor operation. In particular, two such absorbers have been studied in some detail at KAPL. They are europium which was studied as a possible burnable poison in the hope that the temperature defect of the reactor would thereby be decreased, and plutonium whose use as a fuel has been studied in the hope that xenon defect could be reduced.

In Figure I, the absorption cross-section of Eu and U^{235} are plotted. (The curve labeled Eu* is for a fictitious element whose cross-section is identical with that of Eu, except that the resonance at 0.5 ev is absent.) Note that the Eu cross-section falls off more rapidly with increasing energy than does the fuel cross-section. Thus, an increase in neutron temperature should lead to an increased thermal utilization $f \approx \frac{1}{1 + \Sigma_{Eu}/\Sigma_{fuel}}$, which should tend to compensate the negative reactivity effect associated with the decrease in water density. From Figure 2, where we plot $\bar{\sigma}_{aEu}/\bar{\sigma}_{aU235}$ as a function of $\beta\gamma = \Sigma_a/\xi\Sigma_s$ for two temperatures, it can be seen that below a β of around 0.2 this does occur, but as the spectrum hardens, $\beta\gamma > 0.2$, the effect of the Eu resonance is to reverse this effect. (The bars refer to cross-sections averaged over the Wigner-Wilkins spectrum corresponding to the given values of kT and $\beta\gamma$. The averages were performed on the SOFOCATE code). The dashed curves give $\bar{\sigma}_{aZr}/\bar{\sigma}_{aU235}$ for the same temperatures in order to display the effect which might be expected from a typical 1/v absorber.

In Figure 3, we see that in the case of Eu* for all $\beta\gamma$, the thermal utilization is lower at kT = 0.025 than at kT = 0.047, which demonstrates clearly that the cross-over in Figure 2 is due to the effect of the resonance.

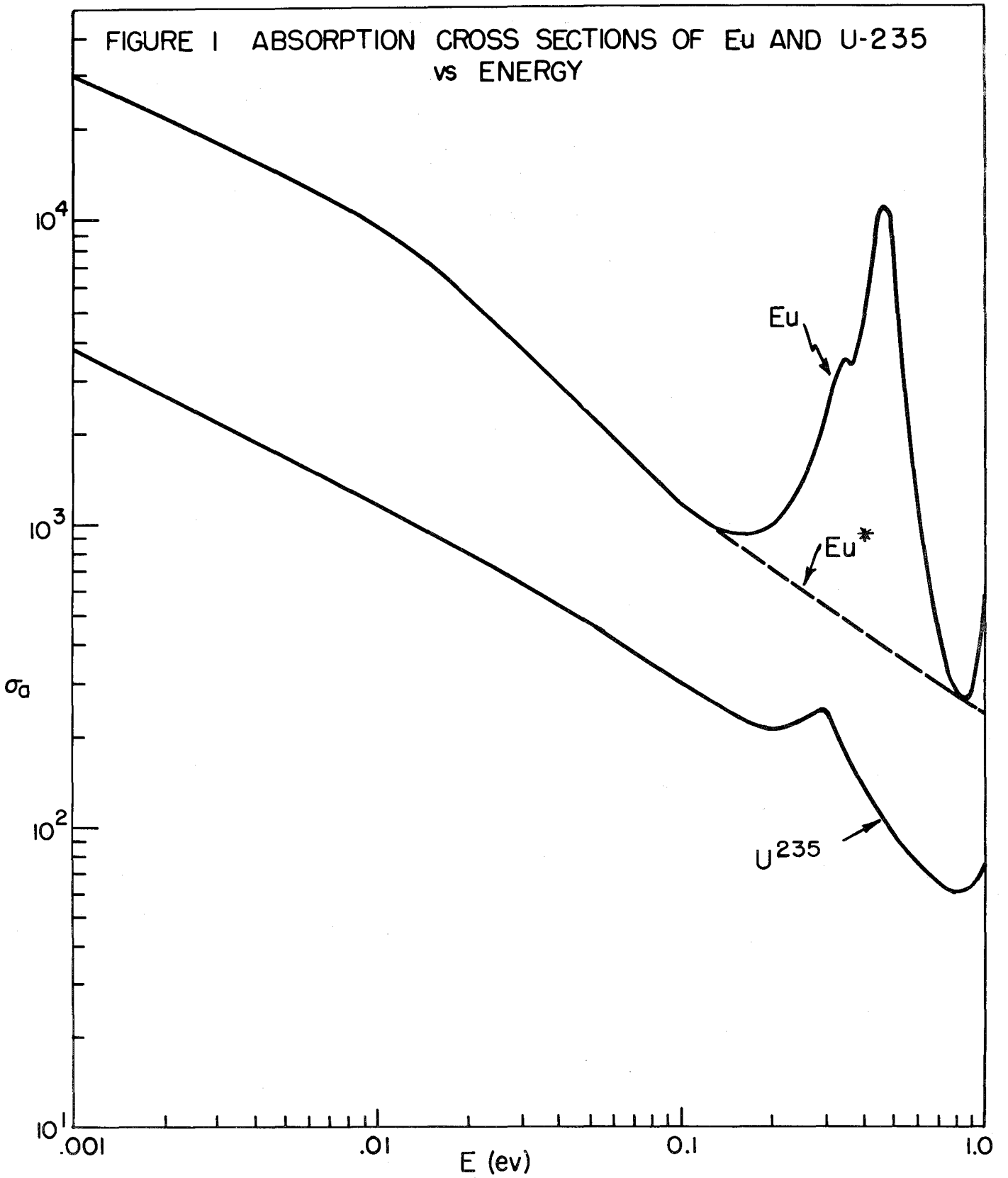
FIGURE I ABSORPTION CROSS SECTIONS OF Eu AND U-235 vs ENERGY
10^4
10^3
10^2
10^1
σ_a
Eu
Eu*
U^{235}
.001
.01
0.1
1.0
E (ev)

From this, it appears that Eu will perform the described function of reducing Δk_T only for reactors with low $\beta\gamma$ (which means cores not too black). However, the situation could undoubtedly be improved by self-shielding the Eu in order to decrease the effect of the resonance, but such calculations have not yet been performed.

In the second portion of this work, a number of comparative calculations of critical mass, temperature defect, and xenon reactivity defect for Pu^{239}-and U^{235}-fueled reactors are presented. First, it should be remembered that Pu^{239} has a large resonance at around 0.3 ev, (see Figure 4 for the cross-sections of Pu^{239} and U^{235}), which tends to "catch" the neutrons before they arrive at the xenon resonance, whose peak is down at .065 ev. For this reason, the effect of xenon should be much less in a Pu reactor than a U reactor.

The calculations performed on the IBM 704 by means of the SOFOCATE code, have borne out this conjecture. In the following table the results of the calculations are summarized.

Description	K_{eff} Peak, Hot	Clean, Hot	Clean, Cold
100% Pu + H_2O	.9999	1.1944	1.1326
75% Pu, 25% U + H_2O	1.0002		1.1706
50% Pu, 50% U + H_2O	1.0000		1.1932
25% Pu, 75% U + H_2O	1.0001		1.2243
100% U + H_2O	.9991	1.2665	1.2891
17.58 kg U + 1:1 Zr-H_2O	.9998	1.2566	1.3439
7.40 kg Pu + 1:1 Zr-H_2O	.9992	1.1801	1.2137
52.74 kg U) 157 g B^{10}) + 1:1 Zr-H_2O	1.0000		1.1620
20.94 kg Pu) 148 g B^{10}) + 1:1 Zr-H_2O	1.0002		1.0604

The results show that the Pu fueled reactors require a considerably smaller critical mass (ν = 2.88 for Pu^{239} compared to 2.5 for U^{235}) and, in addition, the xenon reactivity swings are much smaller.

The spectrum, as calculated on SOFOCATE, shows a dip at 0.3 ev, as might be expected. In Figure 5, are shown the spectra calculated on SOFOCATE.

Other features of Pu reactors such as safety, endurance, control rod effectiveness, and general power plant features will be studied in the future since the preliminary results appear favorable.

---

[1] H. Amster, R. Suarez, WAPD-TM-39, 1-26, January ~~1951~~. 1957

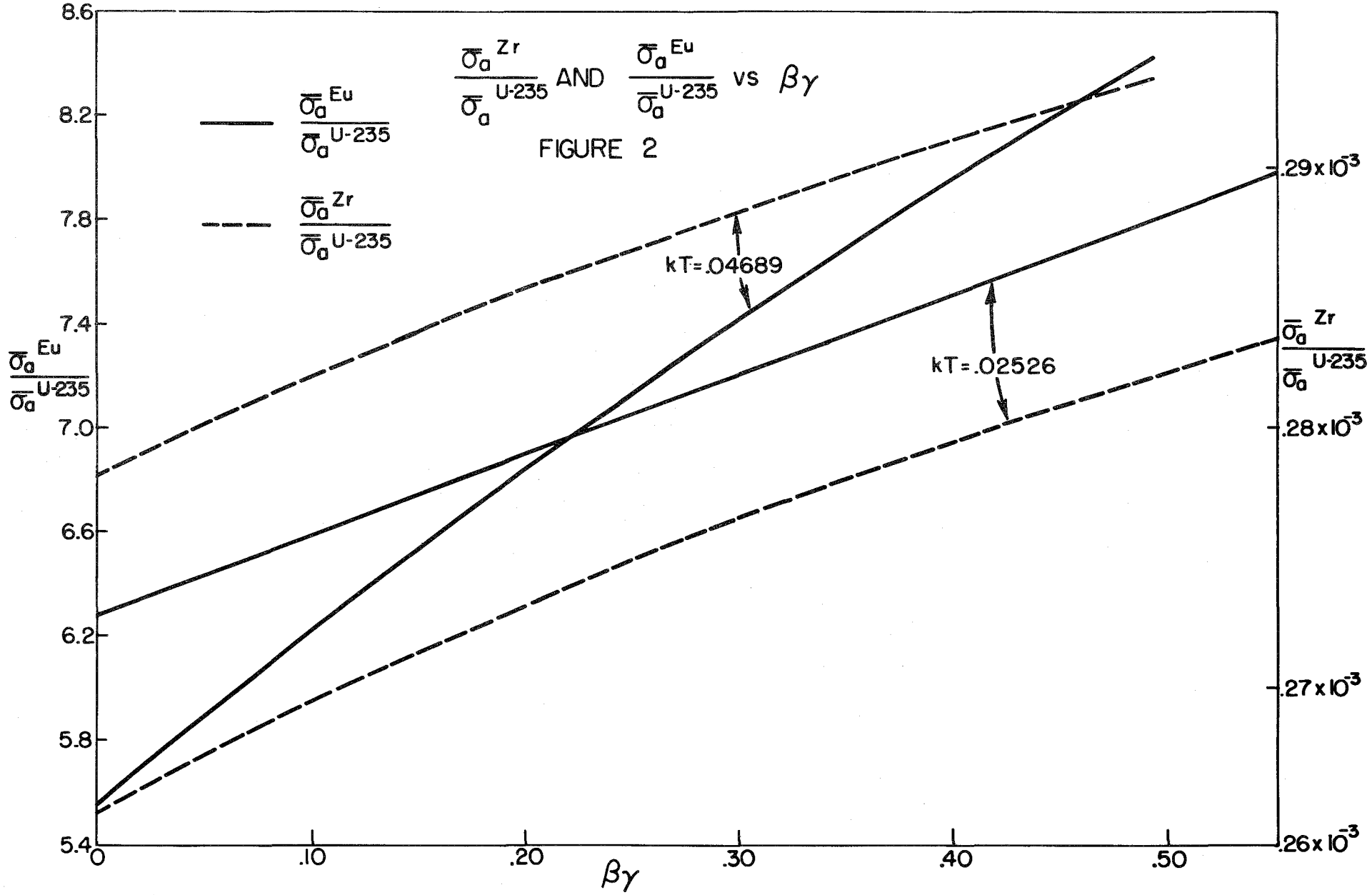
$\frac{\bar{\sigma}_a^{Zr}}{\bar{\sigma}_a^{U\text{-}235}}$ AND $\frac{\bar{\sigma}_a^{Eu}}{\bar{\sigma}_a^{U\text{-}235}}$ vs $\beta\gamma$
$\frac{\bar{\sigma}_a^{Eu}}{\bar{\sigma}_a^{U\text{-}235}}$
$\frac{\bar{\sigma}_a^{Zr}}{\bar{\sigma}_a^{U\text{-}235}}$
kT=.04689
kT=.02526
8.6
8.2
7.8
7.4
7.0
6.6
6.2
5.8
5.4
0
.10
.20
.30
.40
.50
$\beta\gamma$
$.29 \times 10^{-3}$
$.28 \times 10^{-3}$
$.27 \times 10^{-3}$
$.26 \times 10^{-3}$

FIGURE 2

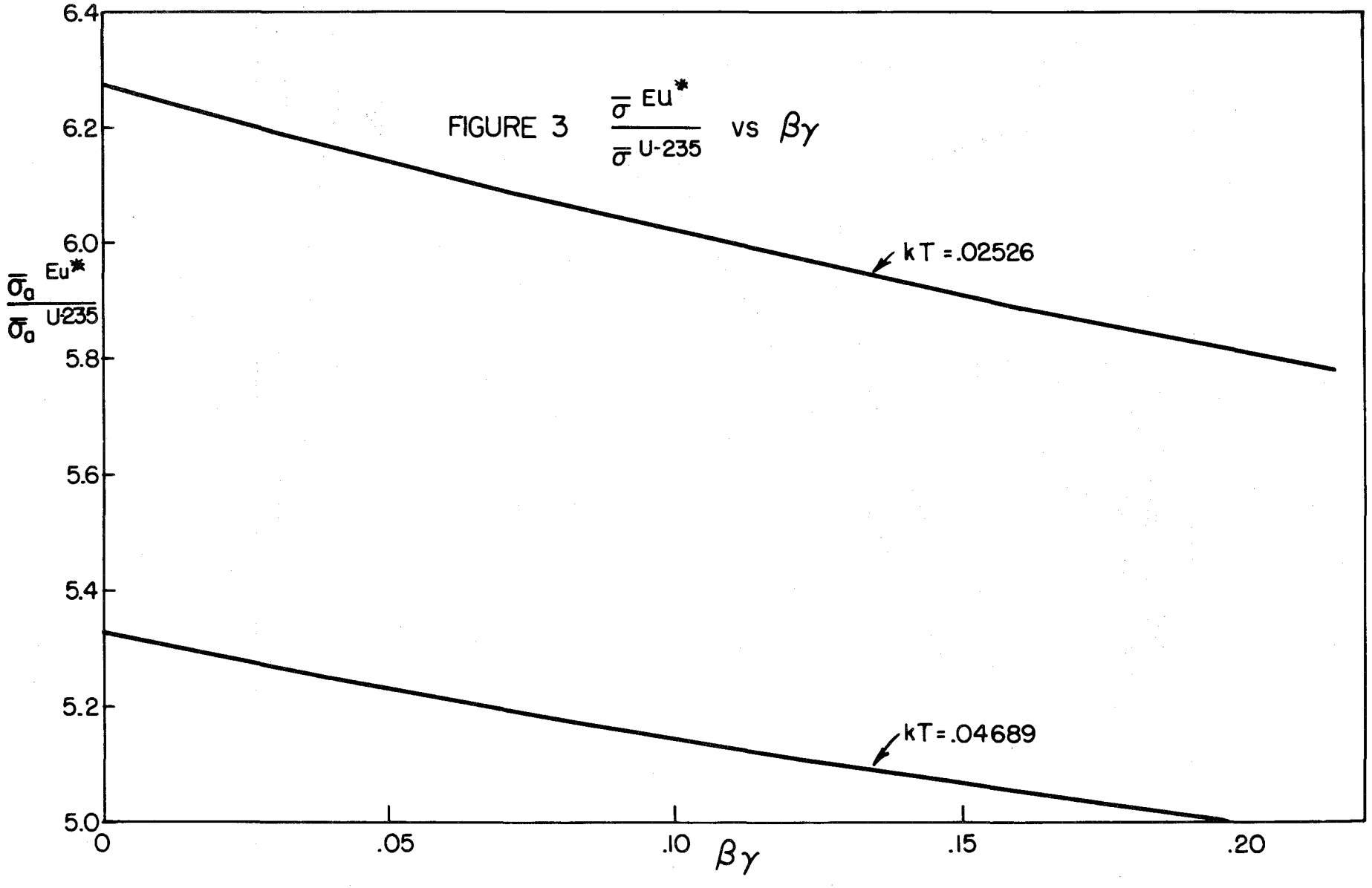

FIGURE 3 $\frac{\bar{\sigma}\ \text{Eu}^*}{\bar{\sigma}\ \text{U-235}}$ vs $\beta\gamma$

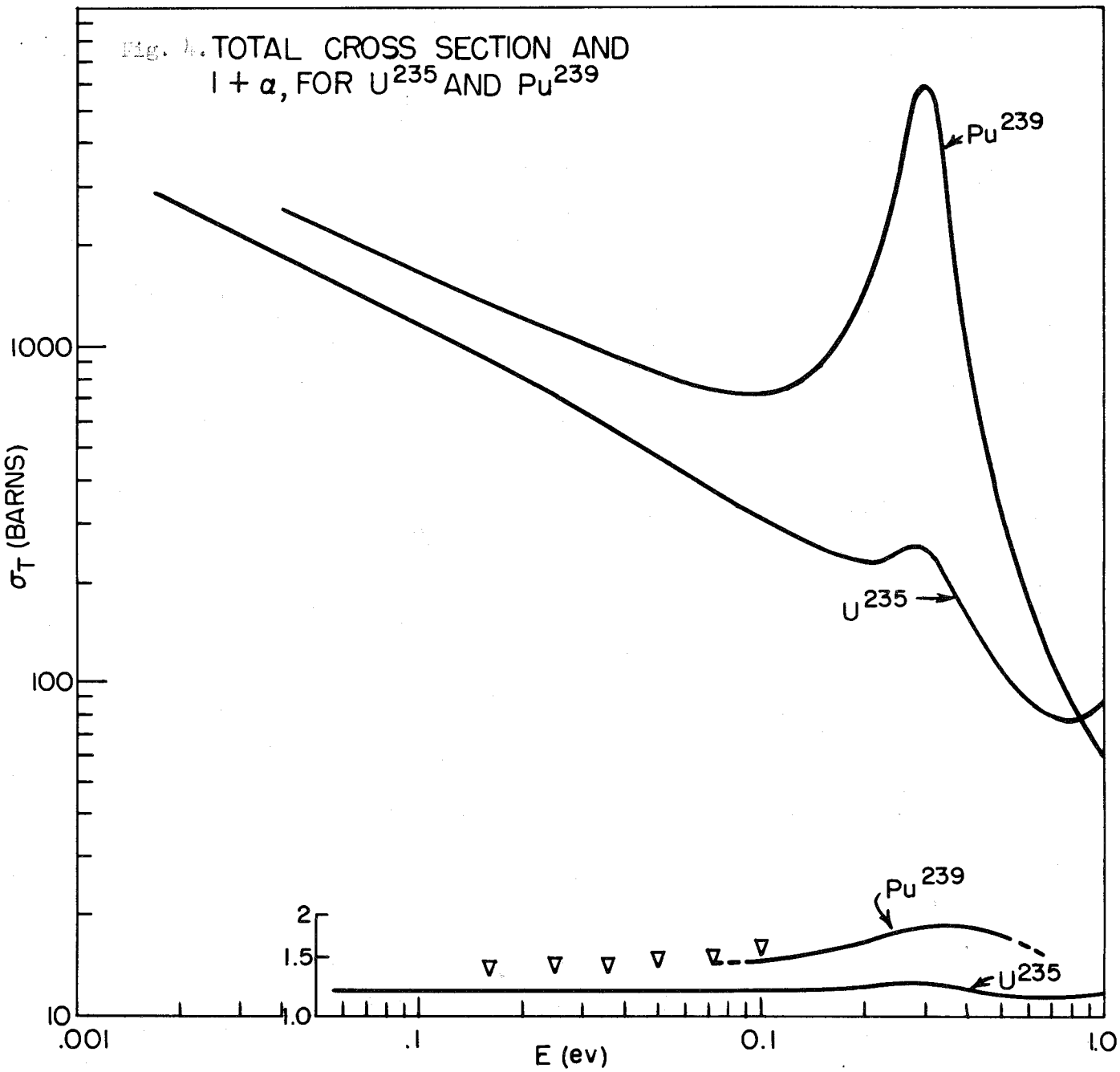
Fig. 4. TOTAL CROSS SECTION AND
1 + α, FOR U235 AND Pu239
Pu239
U235
1000
100
10
σT (BARNS)
2
1.5
1.0
Pu239
U235
.001
.1
0.1
1.0
E (ev)

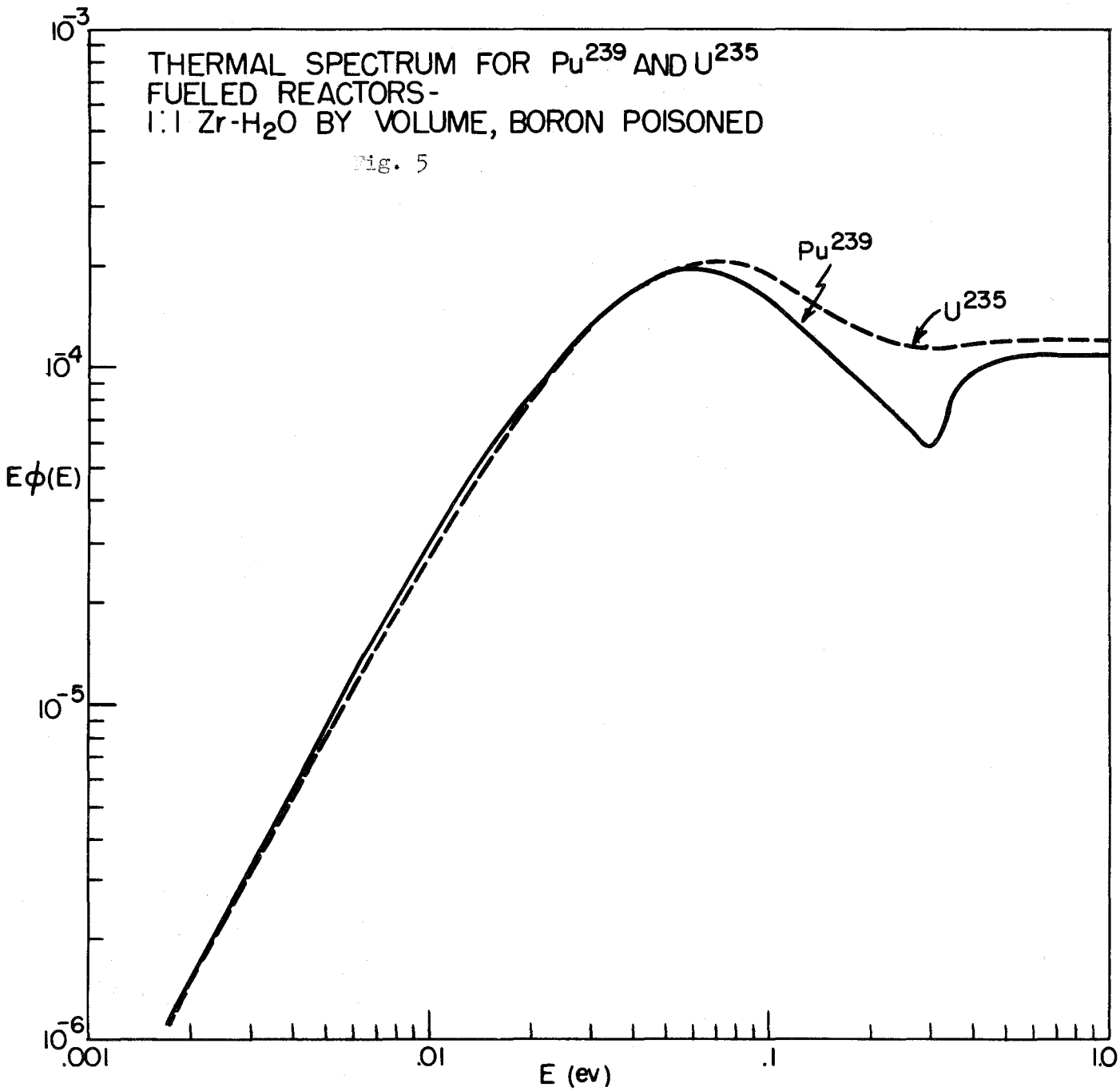
THERMAL SPECTRUM FOR Pu239 AND U235
FUELED REACTORS-
1:1 Zr-H2O BY VOLUME, BORON POISONED
Pu239
U235
10-3
10-4
10-5
10-6
Eφ(E)
.001
.01
.1
1.0
E (ev)

Fig. 5

Paper IV-C

MEASUREMENT OF NEUTRON SPECTRA IN REACTORS

M. J. Poole
Atomic Energy Research Establishment

Measurement of Neutron Spectra in Reactors

M. J. Poole
Atomic Energy Research Establishment
Harwell, Didcot, Berkshire
ENGLAND

Abstract

A method has been developed for the prediction of neutron spectra in reactors by exciting a sub-critical assembly with a pulsed source, and performing a neutron time-of-flight experiment on a beam extracted from this assembly.

Results obtained by this method are presented and compared with results obtained by more conventional means.

Measurement of Neutron Spectra in Reactors

M. J. Poole
United Kingdom Atomic Energy Authority
Harwell, England

1. Principle of Experiment

The basis of the spectrum determination is just an ordinary time-of-flight neutron spectrometer using a pulsed source. Figure 1 shows the set up. A section of the system to be investigated is placed around the target of the Harwell linac, a beam extracted from a definite point by means of a carefully designed collimator and neutrons counted at the end of a 12m flight path using a bank of BF_3 counters feeding into a set of timing gates. The effective pulse length for spectrum determination is now set by the relaxation time of the system rather than the properties of the accelerator - in fact the most useful pulse from the accelerator is that which puts most neutrons into the system. With a 12m path this restricts the method to systems with $\tau_{1/2} \sim 300$ μsec or less - i.e., to water moderated systems. A spectrometer is being built using a 60m path, which will extend the permissible τ to 1 msec. The systems amenable to the method will then be

(a) Practically all water moderated systems.

(b) Highly undermoderated systems using any moderator, including the intermediate systems.

(c) Some D_2O moderated systems,

but <u>not</u>

(d) Thermal graphite Be or D_2O moderated systems.

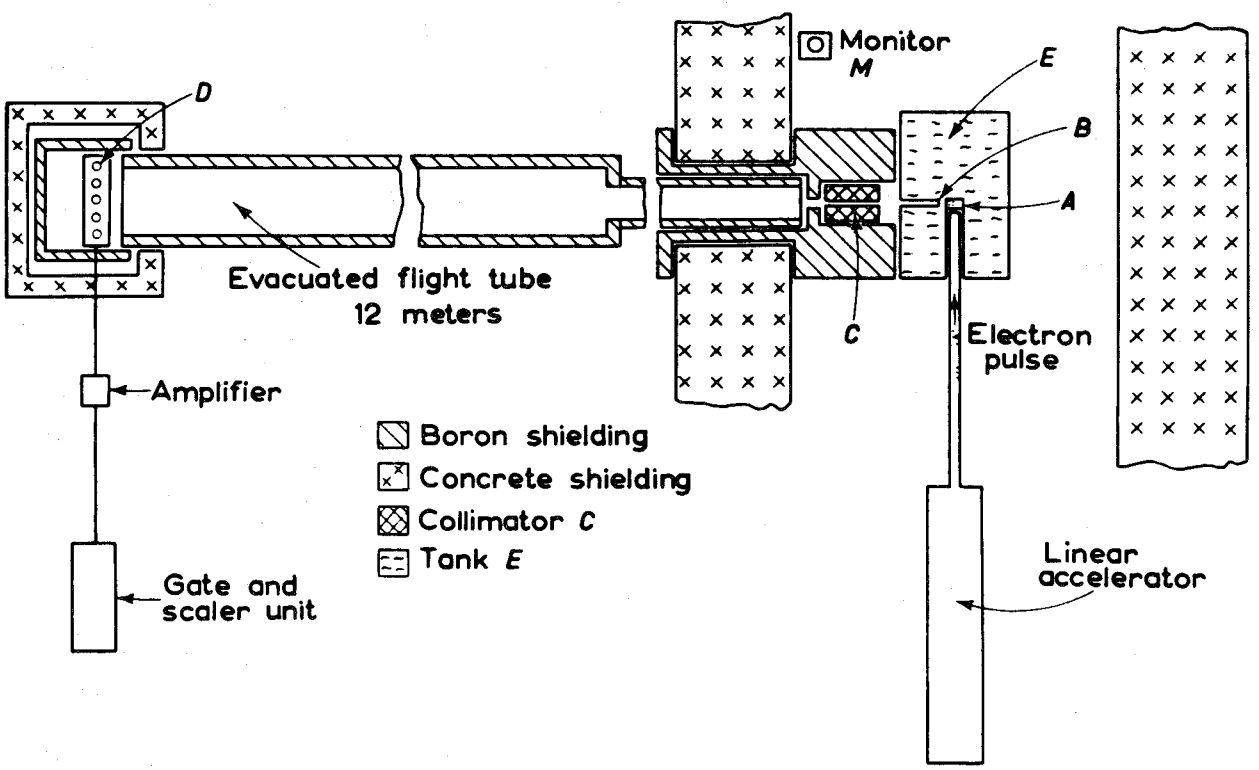
Monitor
M
E
B
A
D
Evacuated flight tube
12 meters
C
Electron
pulse
Amplifier
Boron shielding
Concrete shielding
Collimator C
Tank E
Gate and
scaler unit
Linear
accelerator

Fig. 1

2. Comparison with Other Methods

One may ask why use a method with such a severe limitation, and this question is best answered by looking at some of the other methods available.

(a) Integral measurements, such as fission chamber work of Campbell and Freemantle. This type of method has the advantage of quickness and relatively simple apparatus. However, the characterisation of the spectrum is dependent on knowing what the spectral shape is and difficulties are likely to arise as soon as the spectrum begins to depart from the accepted shape. However the integral methods are still probably the most widely used method of spectrum characterisation.

(b) Chopper. There is no doubt that much better resulutions can be obtained by the use of a chopper to measure the spectrum in a beam from an assembly continuously irradiated with neutrons. The major disadvantage of this is the activation induced in the fuel. If measurements are wanted up to ~ 10 eV energy and if neutrons are only to be taken from a reasonably small area in the assembly (e.g., .3 x 3 cm in graphite, .1 x 1 cm in water) then a flux $\sim 10^{10}$ n/cm^2/sec is required, and this flux is irradiating the uranium the whole time and not just when the chopper is open. Nevertheless a chopper has been built at Harwell (by M. S. Coates) to measure spectra in graphite systems which can only be attacked this way. This chopper uses a flight path 6m long and can give pulses down to ~ 8 μsec.

Resolution of Chopper

E	.025 eV	.3 eV	1 eV	10 eV	100 eV
$\Delta E/E$	1/20	1/17	1/9 or 1/25	1/8	1/2.5

(c) Spiral selector. This type of monochromator has not much been used. A recent paper in Atomnya Energya 5 2. 1958 describes the measurement of the spectrum in the thermal column of a power station reactor by this method. Typical resolutions are:

E	.025 eV	.5 eV
$\Delta E/E$	0.1	0.16

A disadvantage of the method is that only one energy can be registered at a time, which will offset comparatively large transmission.

(d) Other methods - very little reported using crystal spectrometer etc.

4. Problems of Beam Extraction

The success of any beam method is critically dependent on extracting a representative beam of neutrons from the assembly. This may be considered in two parts, firstly how big a lattice is needed to set up a spectrum characteristic of that lattice, and secondly, how do we get a spectrum in the beam that is the same as that in the lattice.

To satisfy the first condition it is necessary that leakage of neutrons be relatively small at all points in the lattice. Now the neutron balance condition says that, for neutrons in an energy interval E to (E + dE)

$$\left(\Sigma_a(E) + \Sigma_s(E) - D(E)\nabla^2\right) \phi(E,\underset{\sim}{r}) = \int_0^\infty \Sigma_s(E' \rightarrow E)\phi(E',\underset{\sim}{r})dE'$$

where the L.H.S. terms all result in loss of neutrons from the interval and the $\int$ on the R.H.S. gives the gain of neutrons in the interval. This shows that

(a) if only general features of the spectrum are of interest then it is sufficient that $\frac{D(E)\nabla^2\phi}{\phi} << \Sigma_a(E) + \Sigma_s(E)$ at all energies, which is easily satisfied,

(b) if the detailed effect of Σ_a on the spectrum is to be investigated, as is usually the case, then it is necessary that $\frac{D(E)\nabla^2\phi}{\phi} << \Sigma_a(E)$.

The value of $\frac{D(E)\nabla^2\phi}{\phi}$ must be calculated from the exact flux distribution; for a point source in systems ~45 cm x 45 cm x 45 cm it has values a few times the geometric buckling B_g^2. Some values are given in the table (flux distribution calculated from age theory).

System	$\frac{z}{a}$	$-\frac{\nabla^2\phi}{\phi}$	$-B_g^2(B_m^2)$	$-\frac{\nabla^2\phi}{\phi} - B_m^2$	$\frac{1}{L^2}$
Pure water	0	0.033 cm^{-2}			
a=b=c=45 cm	$\frac{1}{6}$	0.021 cm^{-2}	0.0185 cm^{-2}		0.12 cm^{-2}
	$\frac{1}{3}$	0.007 cm^{-2}			
Boric acid solution	0	0.042 cm^{-2}			
	$\frac{1}{6}$	0.035 cm^{-2}	0.0185 cm^{-2}		1.2 cm^{-2}
	$\frac{1}{3}$	0.007 cm^{-2}			
Lattice 1.85" pitch 1.2" rod dia. 1.6 Co water mod.	0	0.03 cm^{-2}		0.026 cm^{-2}	
$B_m^2 = 0.04\ cm^2$	$\frac{1}{6}$	0.026 cm^{-2}	0.185 cm^{-2}	0.027 cm^{-2}	0.35 cm^{-2}
$L^2 = 2.8\ cm^2$	$\frac{1}{3}$	0.015 cm^{-2}			

At higher energies only the rough relation $\Sigma_a + \Sigma_s >> \frac{D\nabla^2\phi}{\phi}$ holds, whereas at low energies the more severe restriction is at least approximately true. Furthermore the spectrum in the beam is not necessarily the same as that in the system. This arises from the non isotropic nature of the flux wherever there is a gradient. In a homogeneous system the simple diffusion theory expression for this is good enough

$$I(E) \propto \phi(E,0) - \lambda_t(E) \left.\frac{\partial\phi(E,Z)}{\partial x}\right|_{z=0}$$

where I(E) is the spectral distribution in the beam (z is the beam direction).

However in a close packed lattice where the gradient cannot be considered approximately constant over a distance of λ_t, then this method is not applicable, and the only solution so far found - and this only a partial solution - has been to measure at a series of angles.

Earlier experiments at two angles (along and across the rod direction) have shown that the spectra do differ. Measurement at four angles has so far only been accomplished in one lattice (2.2" spacing) and only in the moderator, but in this case no variation with angle was detected. A further cause of false spectra is disturbance of the system by the introduction of probes. For this reason the probes used are kept as small as possible ($\sim$ 1 cm dia) and also in future flux plots will be performed before any experiment is carried out.

Results

Most results are already reported in Geneva paper P/10 and in J. Nuclear Energy 1957 5. These include measurements in boric acid solutions and in

water moderated lattices. An interesting feature of the boric acid solutions has always been the relatively good agreement with Amster solutions of the Wigner-Wilkins equation (SOFOCATE code) (Fig. 2). That the difference between the two curves cannot be due to poor resolution has been shown by interposing a 1 mil layer of Cd metal in the beam and making a transmission experiment. The results of this agree completely with a transmission curve calculated using the BNL 325 cross-section data. Typical results in the moderator and fuel of a lattice are shown in Figs. 3 and 4.

These results have been analyzed in terms of a three-parameter spectrum, Eo, λ, μ. Agreement with integral measurements for λ is reasonable, even though the detailed spectrum shape differs from that assumed in the transition region. Although scatter in values for μ is large there is distinct correlation between λ and μ.

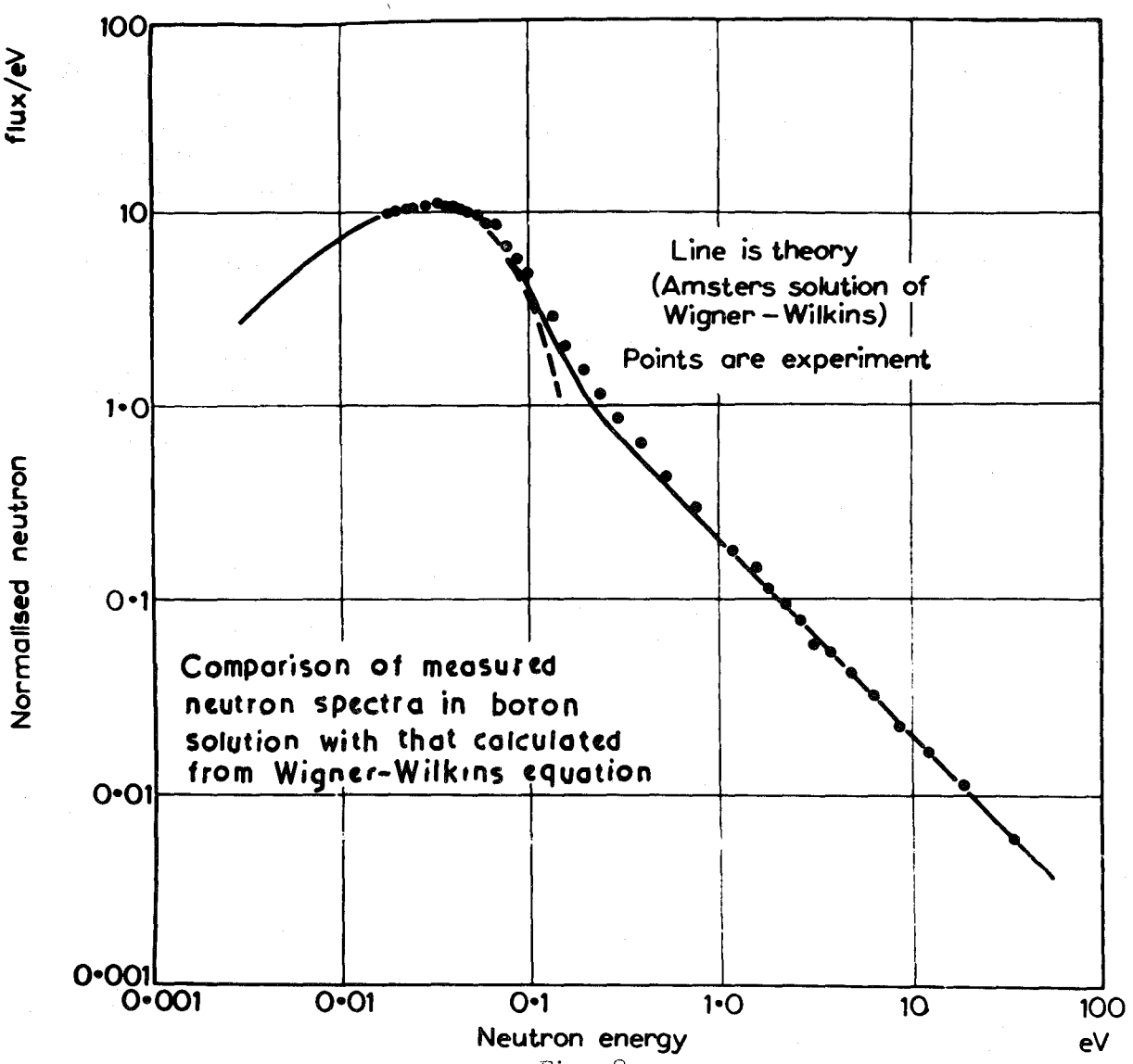
100
10
1·0
0·1
0·01
0·001
flux/eV
Normalised neutron
Line is theory
(Amsters solution of
Wigner – Wilkins)
Points are experiment
Comparison of measured
neutron spectra in boron
solution with that calculated
from Wigner-Wilkins equation
0·001
0·01
0·1
1·0
10
100
Neutron energy
eV

Fig. 2

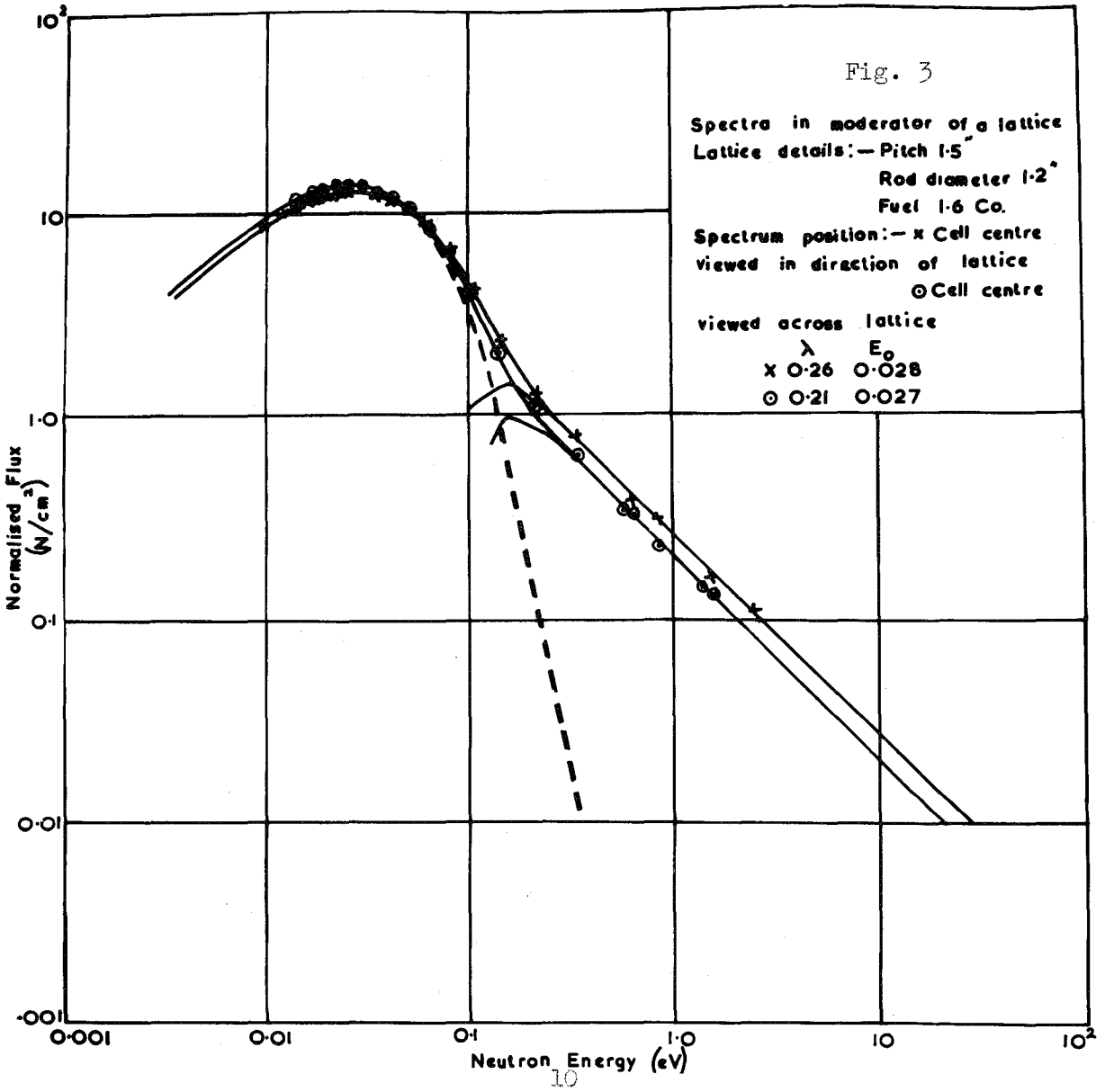
Fig. 3
Spectra in moderator of a lattice
Lattice details:— Pitch 1·5"
Rod diameter 1·2"
Fuel 1·6 Co.
Spectrum position:— x Cell centre
viewed in direction of lattice
⊙ Cell centre
viewed across lattice
λ E₀
x 0·26 0·028
⊙ 0·21 0·027
Normalised Flux (N/cm²)
Neutron Energy (eV)
10²
10
1·0
0·1
0·01
·001
0·001
0·01
0·1
1·0
10
10²
10

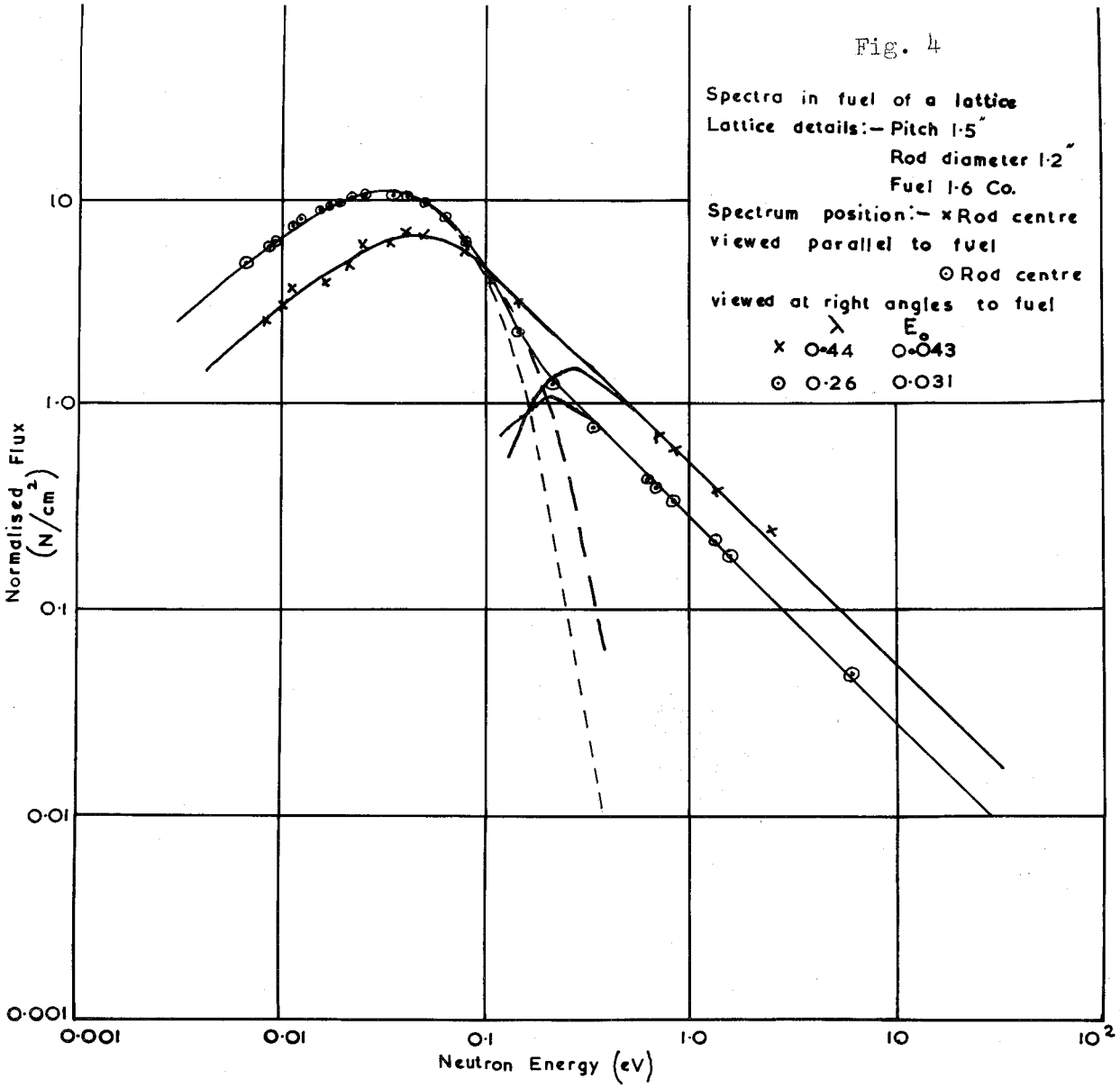
Fig. 4
Spectra in fuel of a lattice
Lattice details:– Pitch 1·5"
Rod diameter 1·2"
Fuel 1·6 Co.
Spectrum position:– × Rod centre viewed parallel to fuel
⊙ Rod centre viewed at right angles to fuel
λ E₀
× 0·44 0·043
⊙ 0·26 0·031
Normalised Flux (N/cm²)
10
1·0
0·1
0·01
0·001
0·001
0·01
0·1
1·0
10
10²
Neutron Energy (eV)

Paper IV-D

LOW ENERGY SPECTRA MEASUREMENTS

R. E. Slovacek R. S. Stone
Knolls Atomic Power Laboratory

Low Energy Spectra Measurements

R. E. Slovacek R. S. Stone*
Knolls Atomic Power Laboratory**
Schenectady, New York

Abstract

Thermal neutron spectra have been measured using the slow chopper time-of-flight technique. Spectra were obtained over an energy range from 10^{-2} to 10 ev for pure water and for a nearly homogeneous subcritical assembly where the ratio of the thermal absorption to the high energy scattering cross section was approximately 0.3. For each medium, spectra were measured at 298°K and 586°K.

The technique of measuring spectra in a subcritical assembly at elevated temperatures with a slow chopper will be presented. The advantages and limitations of this method will be discussed. In addition, the various corrections that have been applied to the data will be discussed.

The experimental results will be presented and compared with results of calculations using the SOFOCATE code. The agreement between theory and experiment is excellent for the multiplying media. On the basis of this agreement, one concludes that chemical binding effects in light water play a negligible role in determining the equilibrium neutron spectrum in water assemblies.

---

*Present address, General Atomic, San Diego, California
**Operated by the General Electric Company for the United States Atomic Energy Commission.

Paper to be Presented at the Conference on Neutron Thermalization
at
Gatlinburg, Tennessee, on April 28, 29, and 30, 1958

LOW ENERGY SPECTRA MEASUREMENTS

by

R. E. Slovacek and R. S. Stone*
Knolls Atomic Power Laboratory, Schenectady, N.Y.**

The thermal neutron spectrum in a finite medium with absorption present is of considerable interest both practically for reactor design, and theoretically for understanding neutron thermalization.

The early Wigner-Wilkins[1] calculations on the steady state spectrum in an infinite homogenous medium with 1/v absorption have been extended by Amster and Suarez[2] permitting one to calculate the spectrum in a finite medium with non 1/v or arbitrary absorption. These calculations neglected the hydrogen binding effects.

Spectrum measurements were undertaken to determine the magnitude of these binding effects on neutron spectra. Using a pulsed neutron technique, Poole[3] has obtained spectra measurements in homogenous light water solutions with various boron concentrations. His measurements ranged from room temperature to about 90°C for solutions whose ratio of $\Sigma_a/\xi\Sigma_s$, varied from .02 to .34. In general, his spectra are in good agreement with SOFOCATE calculations[4] except for a consistent deviation in the joining region between the hardened thermal spectra and the slowing down region.

In the present series of measurements, the slow chopper technique was used to measure the spectrum for a medium with non 1/v absorber over a wider temperature range (298°K to 586°K). Measurements were also obtained for a larger ratio of $\Sigma_a/\xi\Sigma_s$.

---

* Present address, General Atomic, San Diego, California.

**Operated by the General Electric Company for the United States Atomic Energy Commission.

EXPERIMENTAL ARRANGEMENT

The slow chopper technique for measuring spectra was described in detail by the authors.[5] The apparatus is shown schematically in Figure 1. The Thermal Test Reactor serves as a source of thermal neutrons to excite an enriched uranium fission plate located in the reactor thermal column. The thermal neutron flux at operating power is about 10^{10} neuts/cm^2-sec incident on the plate. The high energy neutrons resulting from fission in this plate are transmitted through the pressure vessel wall easier than the thermal neutrons and excite the subcritical assembly which is located in the rear end of the vessel.

Figure 2 shows an end-on view of the pressure vessel in the thermal column during a phase of its installation. The empty rack for holding the subcritical assembly components is seen inside the vessel. The subcritical assembly is 16 inches long and 10 inches in diameter. A reentrant hole 2 inches in diameter penetrates the forward end of the assembly to a depth of 8 inches. The hole is filled with a thin walled He tank to provide a method of extracting a neutron beam from the bottom of the hole with a small perturbation to the medium. The beam leaves the high pressure region through an 0.030" stainless steel high pressure rupture disk and is collimated by a one-meter long boron carbide collimator assembly.

The emergent beam is chopped by the rotating flat plate shutter shown in Figure 3. The 2 inch high rotor plate stack consists of 1/16 inch borated phenolic resin plates and 1/16 inch aluminum "window frames" serve as plate spacers. This plate stack was capped with borated phenolic resin to form the rotor cylinder which is 6 inches in diameter and 6 inches long. A shrunk fit thin walled stainless steel shell provides mechanical support for the rotor. Because the spectra investigated

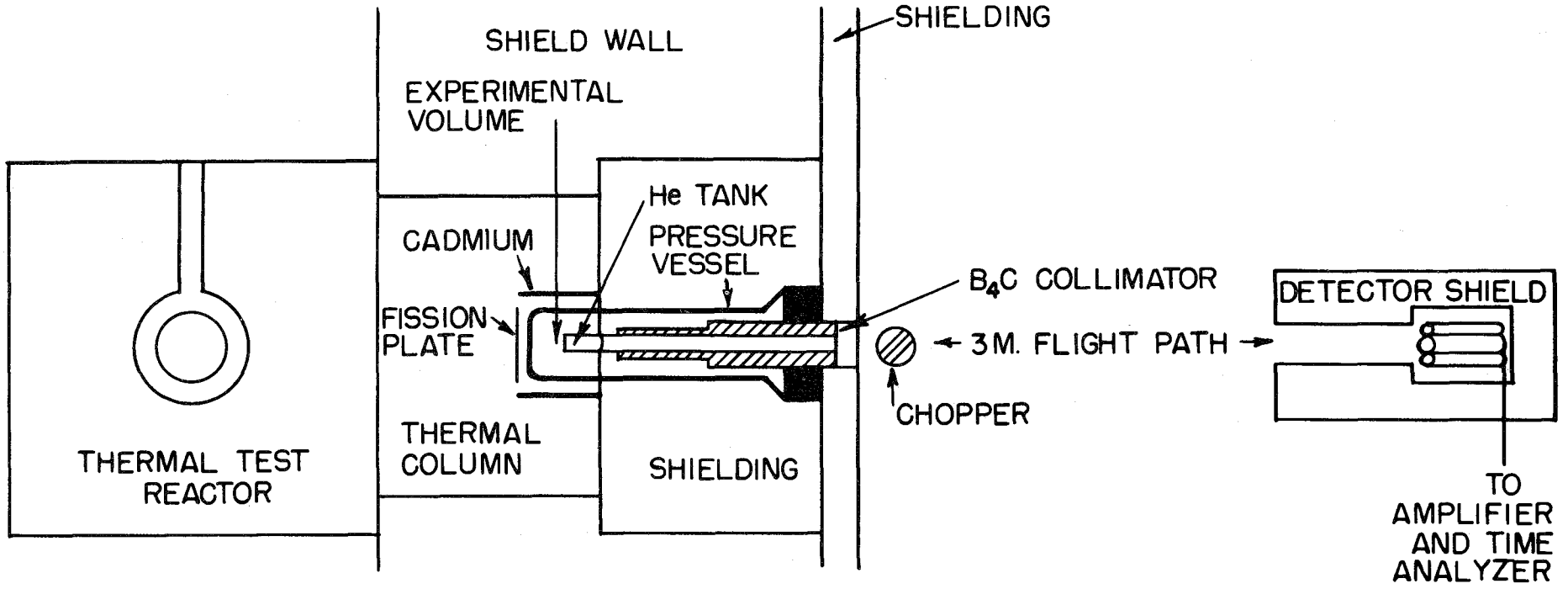

FIGURE I
EXPERIMENTAL ARRANGEMENT

KS-19578
UNCLASSIFIED

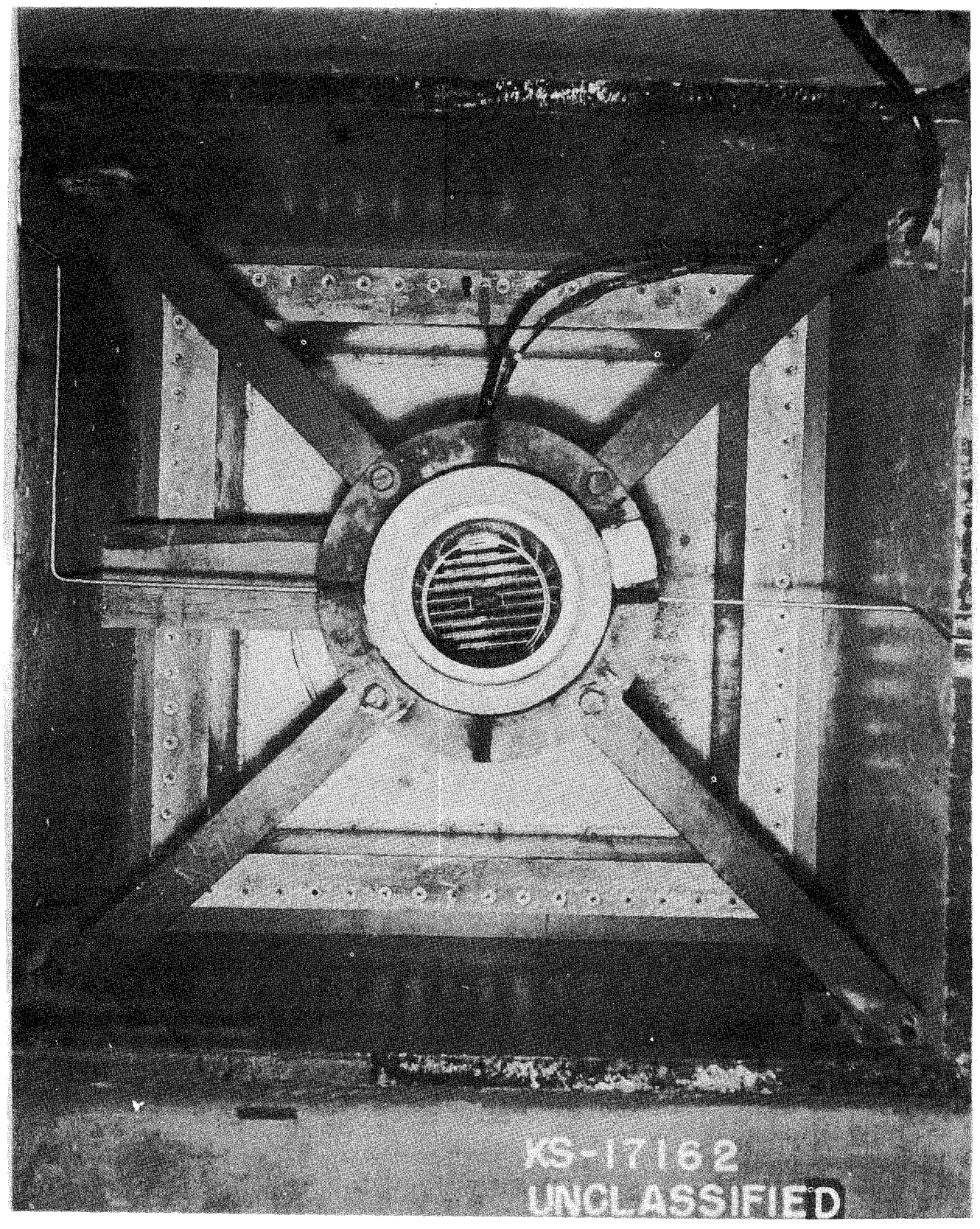

Fig. 2

TOP

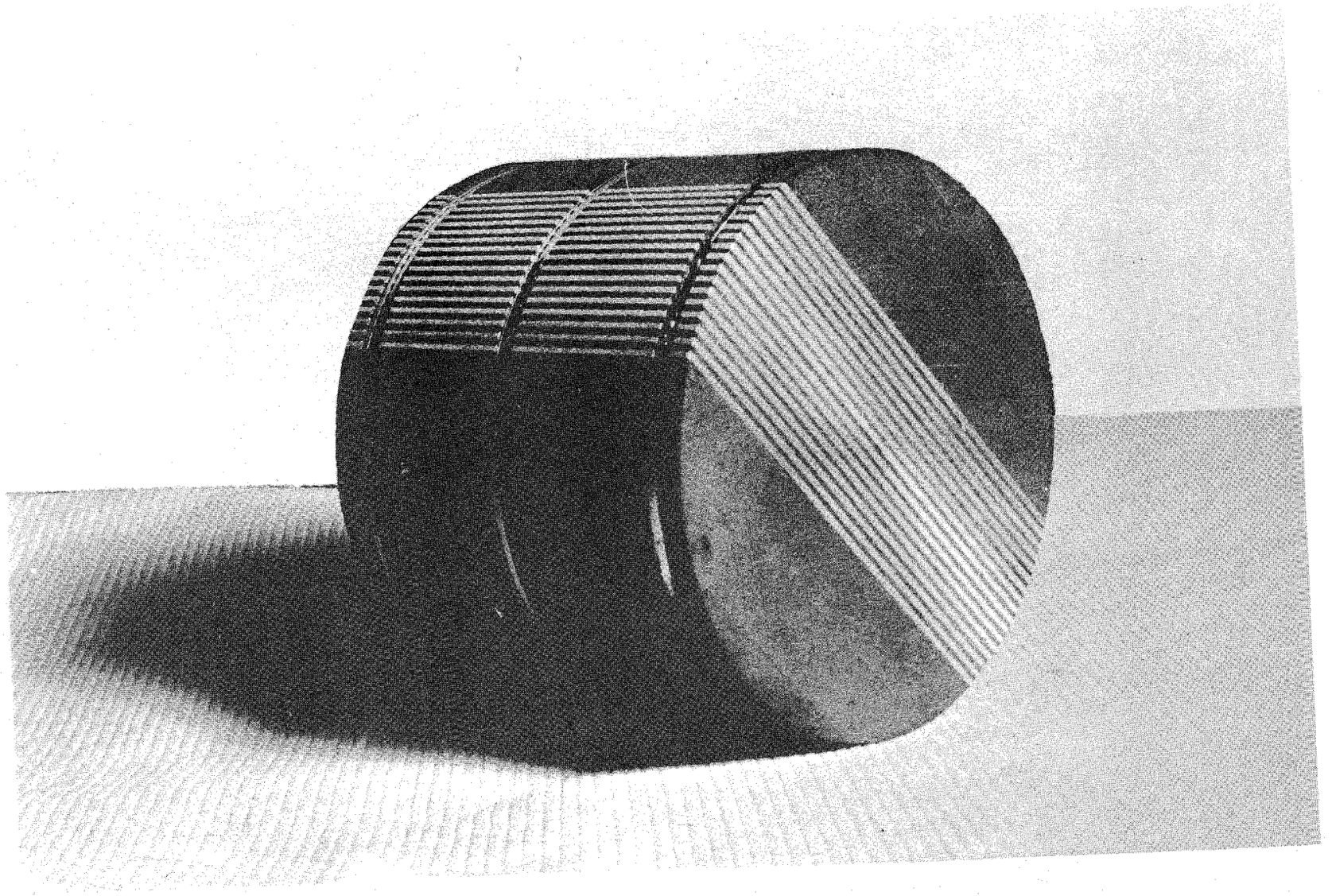

ROTOR CONSTRUCTION

KS-15526
UNCLASSIFIED

Fig. 5

contain a large number of high energy neutrons, a hydrogenous compound was used to provide a large removal cross-section at high energies.

After a flight path of 3 meters, the chopped neutron beam was detected by an array of five proportional counters. These counters were filled with $B^{10}F_3$ to one atmosphere. The counter assembly was housed in a large borated paraffin shield.

The counter pulses were amplified and recorded as to time of arrival after the neutron burst from the chopper. Figure 4 is a picture of the 256 channel time analyzer.[6] Circuits and power supply are completely transistorized and the analyzer has a ferrite core memory. Channel widths from 2.5 to 80 usecs are available. For the present measurements, 40 usec channel widths were used. Figure 5 shows the display of the information stored in the memory for three different spectra.

The channelizer was gated on by a pulse from the rotating shutter. The arrival of this pulse was adjusted so that a counter signal corresponding to an infinite velocity neutron would be recorded at the beginning of time channel 129. The system parameters were adjusted so that the flight time of a cutoff neutron was less than one half the time between bursts. Since the rotor construction is symmetric about a plane passed through the center of its plate stack, the time dependent background due to transmission through the shutter will also be symmetric about flight time zero. One can therefore obtain signal counting rates corrected for background by reflecting the data about channel 129 and subtracting. Information stored in each of the 256 channels can be printed out on IBM cards and then processed further for corrections to obtain the flux per electron volt as a function of energy.

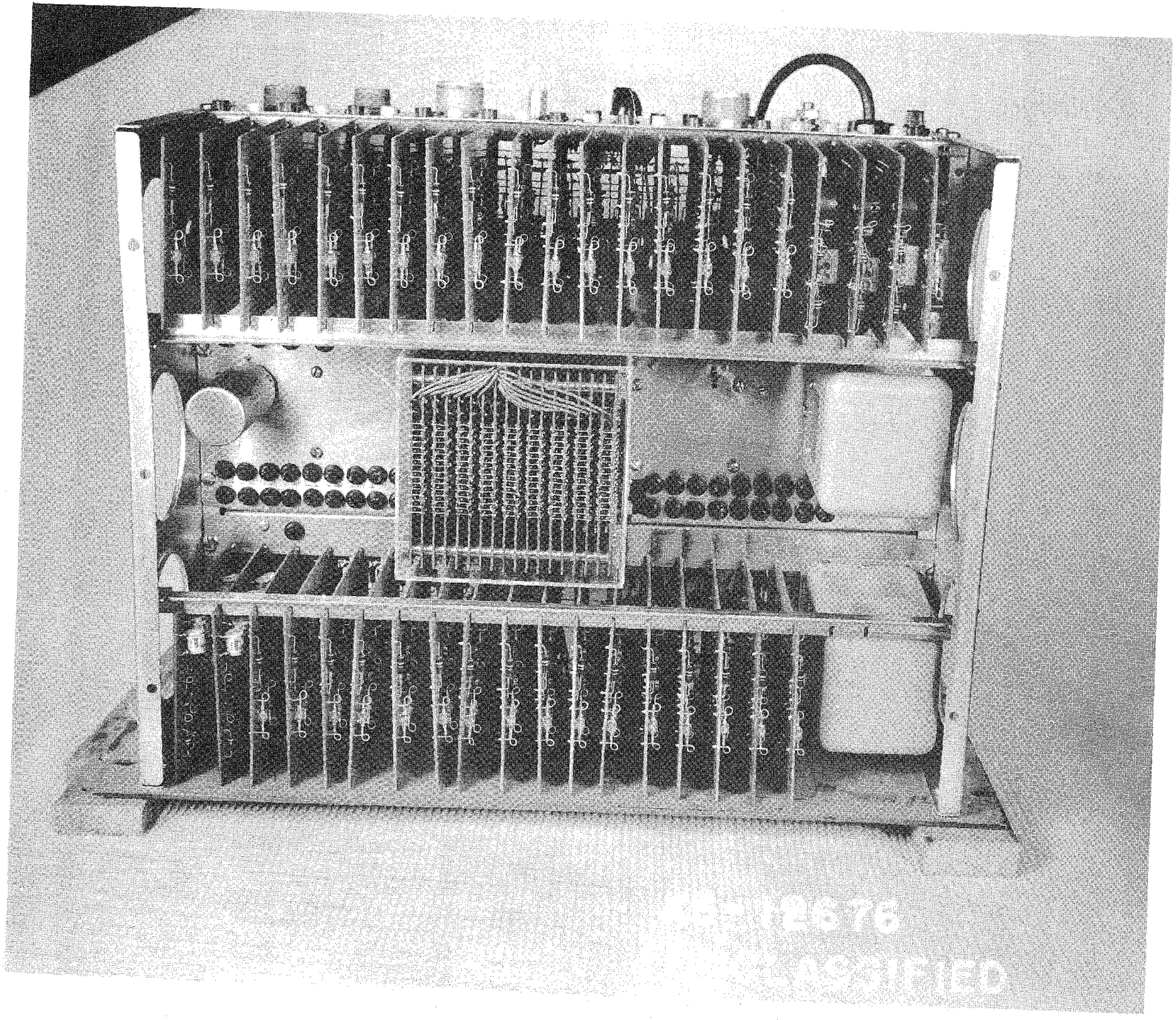

Fig. 4

FIGURE 5
DISPLAY OF ANALYZER OUTPUT

WATER
586°K

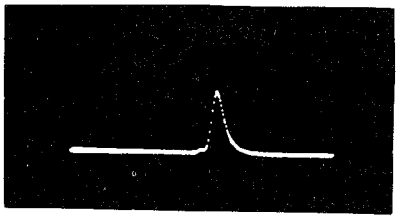

MULTIPLYING MEDIUM I
586°K
$\Sigma_a(.051) = 0.138\ cm^{-1}$
$\frac{\Sigma_a}{\xi \Sigma_s} = 0.30$

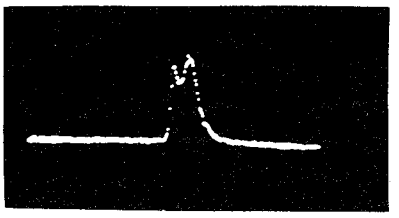

MULTIPLYING MEDIUM II
586°K
$\Sigma_a(.051) = 0.\cancel{406}\ .290\ cm^{-1}$
$\frac{\Sigma_a}{\xi \Sigma_s} = 0.56$

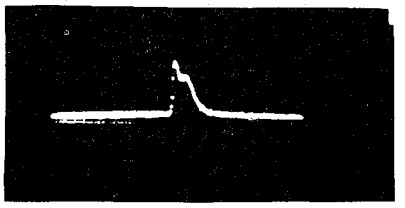

The experimental data are corrected for several effects. These include effects such as the attenuation of the beam by materials between the source and detector, the dynamic transmission of a flat plate shutter, the counter detection efficiency, the resolution of the system, and, finally, the flux gradient in the source region.

The total cross-sections of such materials as iron, aluminum, and air are well known and the correction for the beam attenuation can easily be made. This amounts to a correction that is about 20% greater at 10^{-2} ev than it is at 1 ev.

The realtive dyanmic transmission for a rotating flat plate shutter is given by

$$\tau(\beta) = 1 - 8/3\,\beta^2 \qquad 0 \leq \beta \leq 1/4$$

$$\tau(\beta) = 8/3\,\beta^2 - 8\beta + \frac{16}{3}\sqrt{\beta} \qquad 1/4 \leq \beta \leq 1$$

where $\beta \equiv v_{co}/v$ (the ratio of the minimum neutron velocity transmitted by the shutter to the neutron velocity under consideration). This correction is 35% greater at 10^{-2} ev that it is at 1 ev.

The counter efficiency as a function of energy can be calculated using the boron cross section. A correction for the change of the mean counting center on the flight path length amounts to 1.3% at 10^{-2} ev and 0.25% at 1 ev.

A correction for the resolution of the spectrometer should be applied particularly where the spectrum is rapidly varying. For our symmetric resolution function, this correction involves the even moments of the resolution function and the even derivatives of the output data. In the case of the pure water spectra, where the counting rate increases sharply between the dE/E region and the thermal

region of the spectrum, the resolution correction was as large as 20%. In the case of the subcritical assembly, this correction was as high as 6%.

The neutron beam current and the neutron flux are related by the relation,

$$J_{+}(E) = \phi_0(E) - \lambda_T(E) \left.\frac{d\phi}{dz}\right|_0$$

One can measure the flux gradient in the source region and calculate the transport mean free path to determine this correction to the measured beam current to obtain the flux at the source. This correction is about 15 to 20% greater at 10^{-2} ev for all sources than it is at 1 ev.

The chopper technique for measuring spectra in subcritical assemblies has some inherent disadvantages when compared to the pulsed neutron source technique. The source intensity is much less than that available with pulsed sources. The radioactivity built up in the assembly is considerably greater in the steady state case. In the pulsed technique, one can locate the spectrum source in the region where the flux gradient is zero. The buckling can also be easily calculated in the case of the pulse source technique.

In the pulsed technique, the slowing down and thermal neutron diffusion times tend to broaden the pulse. This results in an uncertainty in the timing of the neutron flight time for neutrons of various energies. Thus, spectra in media using moderators other than hydrogen could not be feasibly measured with the pulsed technique. The pulsed method would also not be suitable for media with any appreciable multiplication because of the long decay time of the source. This uncertainty in flight time usually requires a much longer flight path to attain the same resolution as the chopper technique.

SOURCE DATA

Figure 6 contains the description of the various media that were used in the spectrum investigations. Spectra were obtained in pure water $\left(\frac{\Sigma a(.025\ ev)}{\xi \Sigma_s (1\ ev)} \approx 0.016\right)$ and for two subcritical assemblies with $\frac{\Sigma_a}{\xi \Sigma_s} \approx 0.29$ and 0.54. In each case, measurements were obtained at room temperature and at about 600°F.

For the case of the subcritical assemblies $\Sigma a >> DB^2$ and the measured spectrum should well represent the spectrum in an infinite medium of this absorption with a small leakagecorrection. In the case of water, Σa is not large compared to DB^2 for all energies of interest, and the measured spectrum will depend strongly on the leakage.

The lateral surface of the cylindrical source region was bounded by a 1 1/4 inch thick steel pressure vessel wall which was covered by a 2 inch layer of thermal lagging and Cd sheet. Since the buckling would be difficult to calculate under the existing source and boundary conditions, measurements of the radial and axial flux traverses about the center of the beam source region were made.

These measurements indicated that the perturbation of the reentrant hole on the axial gradient was found to be less than 3%. Bare and Cd covered measurements indicated the thermal and epi cadmium flux distribution differed by less than 6% in the beam source region. The flux was found to be represented to a good approximation by the function $\phi(E, r, z) = \phi_0(E)\, e^{-\gamma z} J_0(\alpha r)$. The buckling will then be given by $B^2 = \alpha^2 - \gamma^2$.

Figure 6 lists the measured values of α, γ, and B^2 with their estimated errors. The values of α and γ were obtained from a least squares fit for a distance of three thermal diffusion lengths about the source center.

SOURCE DATA

Medium	T °K	Eo ev	σ cm^{-1}	γ cm^{-1}	B^2 cm^{-2}	$D(Eo)B^2$ cm^{-1}	$\Sigma_{a(Eo)}$ cm^{-1}	$D(1ev)B^2$	Σ_a
H_2O	298	.0257	i (0.172±.020)	.166±.001	-.057 ±.010	-.0064	.0220	-.033	.00
H_2O	586	.0505	.112±.010	.098±.001	.003 ±.002	.0007	.0115	.0025	.00
Matrix I	298	.0257	.093±.006	.056±.001	.0055±.0011	.0011	.193	.0056	.03
Matrix I	586	.0505	.056±.004	.036±.001	.0018±.0014	.0007	.138	.0024	.03
Matrix II	298	.0257	.107±.007	.062±.002	.0077±.0015	.0010	.406	.0066	.06
Matrix II	586	.0505	.063±.005	.053±.002	.0011±.0007	.0003	.290	.0012	.06

Fig. 6

The magnitude of the measured buckling was used to determine the leakage correction DB^2, which was added to the absorption cross section in calculating the spectra with the SOFOCATE code. As a consequence of the bare and Cd covered activations in the subcritical assembly, the variation of the leakage correction was taken to be the same as the variation of D with energy. The axial flux measurement was also used in relating the measured beam current to the flux in the source region.

In the case of pure water, Σa is not large compared to DB^2. Therefore, the calculated spectrum will be very sensitive to the variation of both Σa and DB^2 with energy. Since the buckling as a function of energy could not be obtained, no leakage correction was applied to the absorption cross sections in calculating the spectrum in water.

EXPERIMENTAL RESULTS

The measured results appear in Figures 7 through 12 where the calculated spectra appear as solid curves. The dashed line is the dE/E spectrum above 1 ev that is assumed in the calculations. In these figures, the crosses are the measured values of the flux with the vertical extent of the cross indicating the probable error in the relative flux as determined from the counting statistics for each channel. The data presented here were obtained with $\Delta E/E = 1/1$ at 3.8 ev.

As the fuel density increased, the slowing down spectra in the region from about 0.3 ev to 5 ev appear to deviate more from dE/E. A least squares fit to the function dE/E^x was made in this region and the experimental data were all normalized to give a slowing down flux of 1 neutron/cm^2-sec at 1 ev in each case. Figure 13 shows the results of the least squares fit.

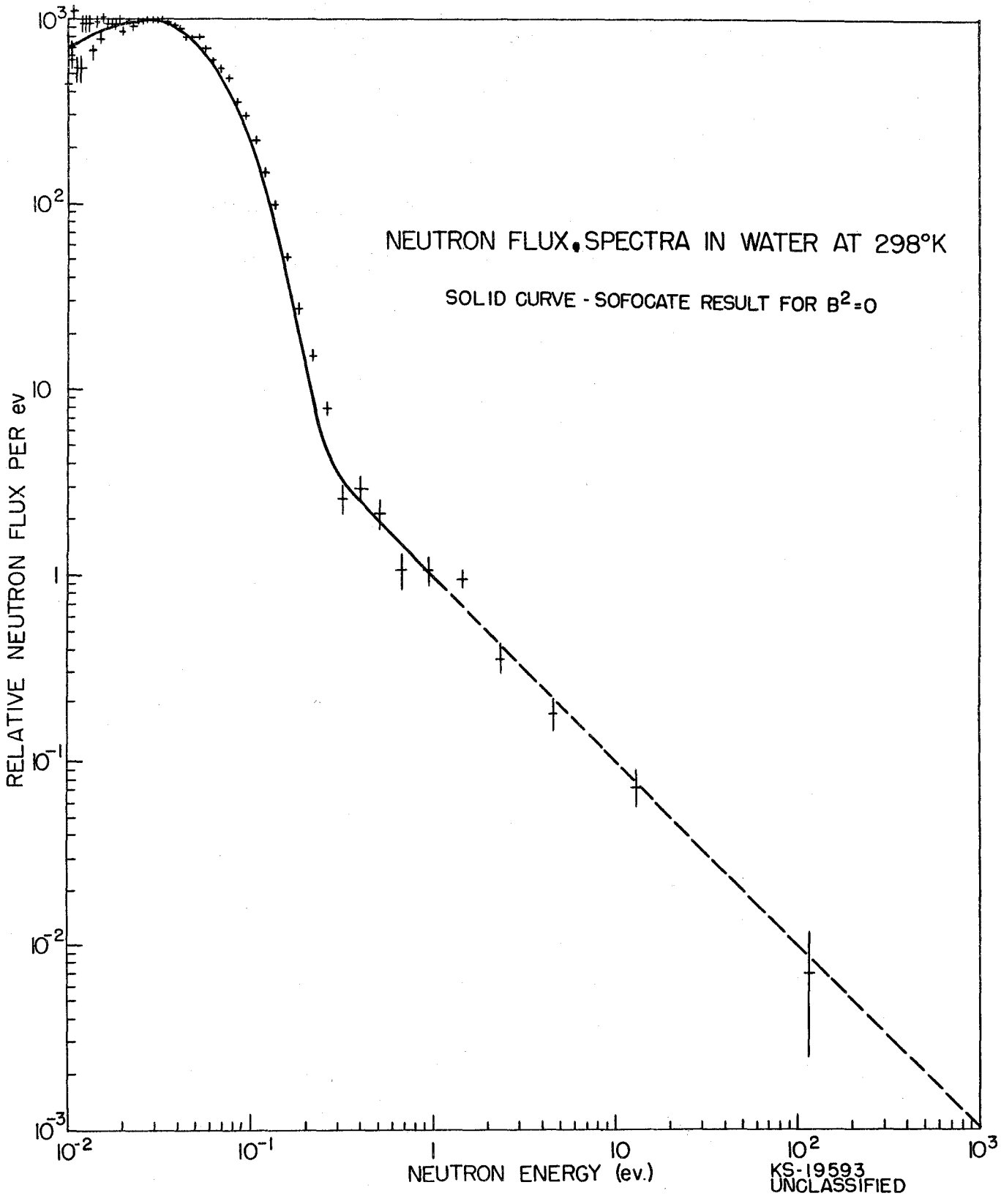
NEUTRON FLUX SPECTRA IN WATER AT 298°K
SOLID CURVE - SOFOCATE RESULT FOR $B^2=0$
RELATIVE NEUTRON FLUX PER ev
NEUTRON ENERGY (ev.)
10^3
10^2
10
1
10^{-1}
10^{-2}
10^{-3}
10^{-2}
10^{-1}
1
10
10^2
10^3
KS-19593
UNCLASSIFIED

Fig. 7

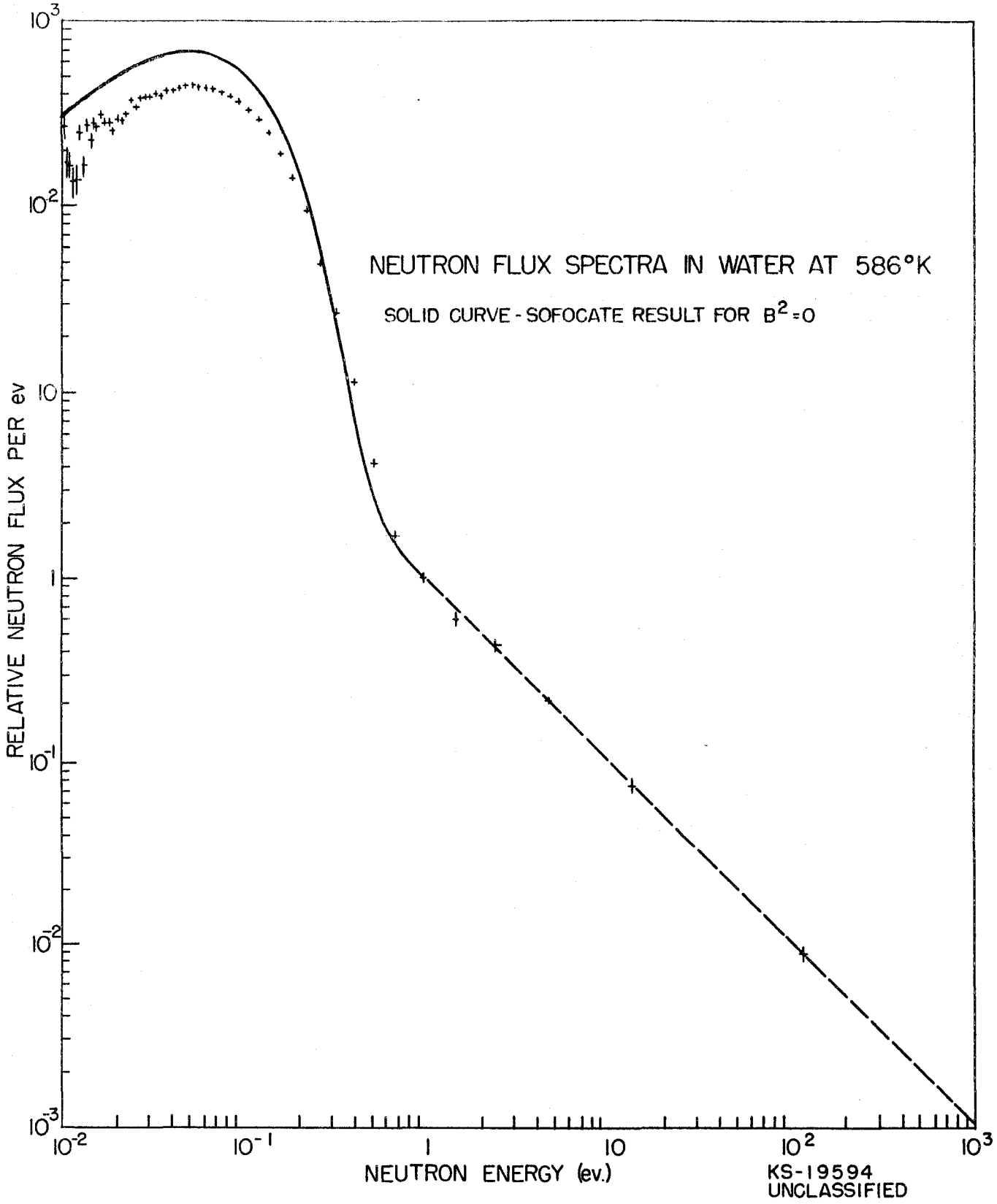
NEUTRON FLUX SPECTRA IN WATER AT 586°K
SOLID CURVE - SOFOCATE RESULT FOR $B^2=0$
RELATIVE NEUTRON FLUX PER ev
NEUTRON ENERGY (ev.)
10^3
10^2
10
1
10^{-1}
10^{-2}
10^{-3}
10^{-2}
10^{-1}
1
10
10^2
10^3
KS-19594
UNCLASSIFIED

Fig. 8

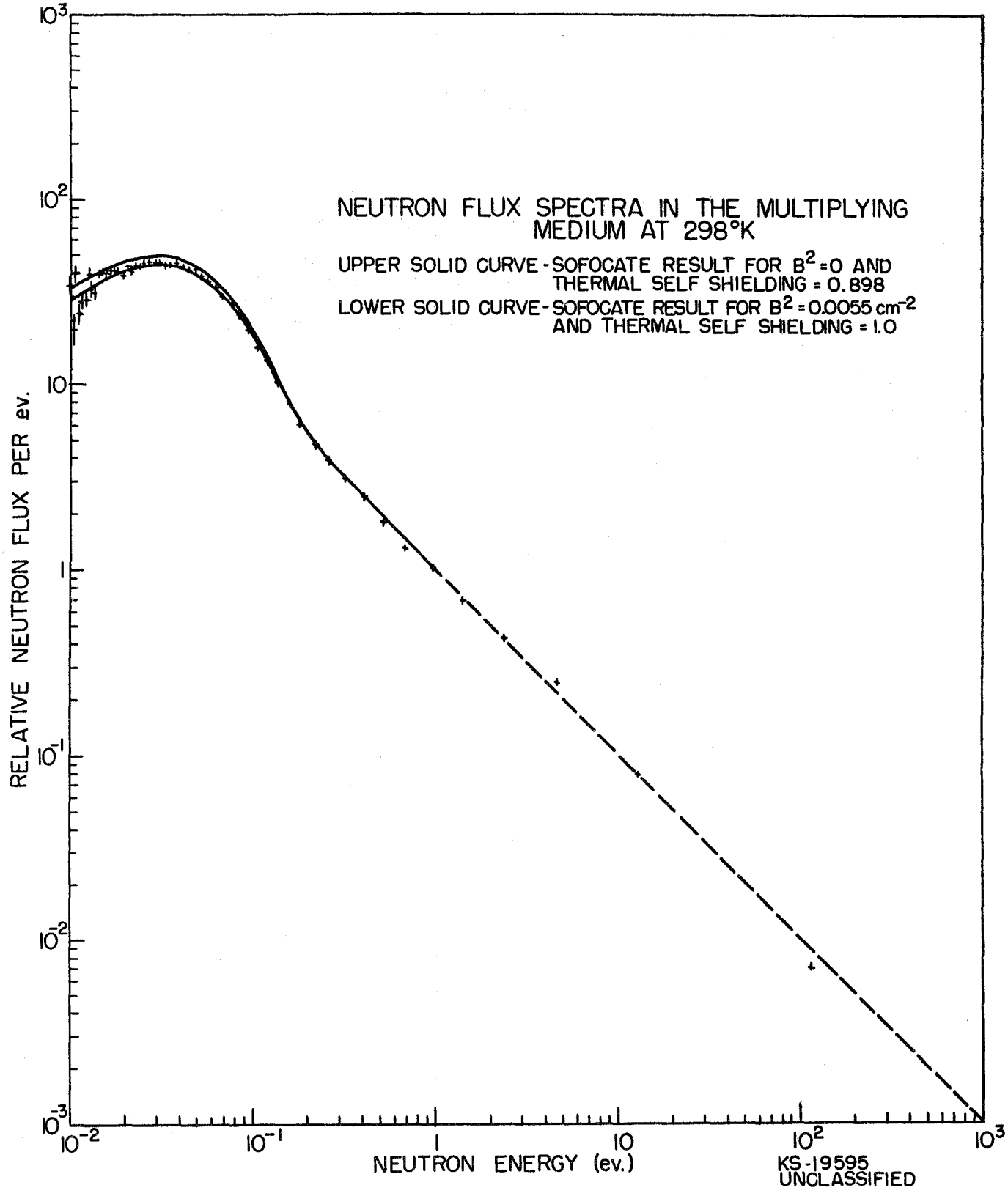
NEUTRON FLUX SPECTRA IN THE MULTIPLYING MEDIUM AT 298°K
UPPER SOLID CURVE - SOFOCATE RESULT FOR B2 = 0 AND THERMAL SELF SHIELDING = 0.898
LOWER SOLID CURVE - SOFOCATE RESULT FOR B2 = 0.0055 cm-2 AND THERMAL SELF SHIELDING = 1.0
RELATIVE NEUTRON FLUX PER ev.
NEUTRON ENERGY (ev.)
KS-19595
UNCLASSIFIED

Fig. 9

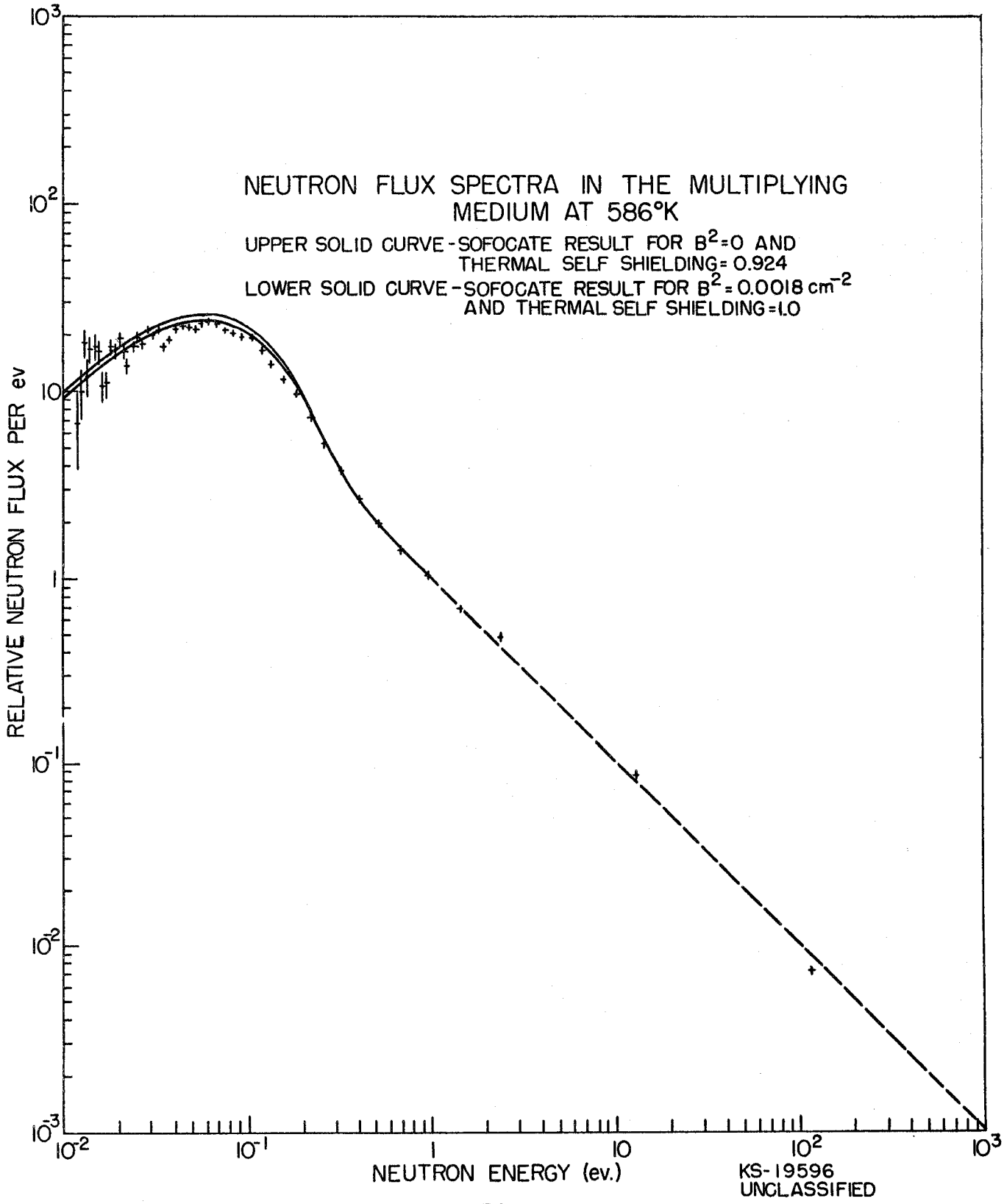
NEUTRON FLUX SPECTRA IN THE MULTIPLYING MEDIUM AT 586°K
UPPER SOLID CURVE - SOFOCATE RESULT FOR B2=0 AND THERMAL SELF SHIELDING= 0.924
LOWER SOLID CURVE - SOFOCATE RESULT FOR B2= 0.0018 cm-2 AND THERMAL SELF SHIELDING=1.0
RELATIVE NEUTRON FLUX PER ev
NEUTRON ENERGY (ev.)
KS-19596
UNCLASSIFIED

Fig. 10

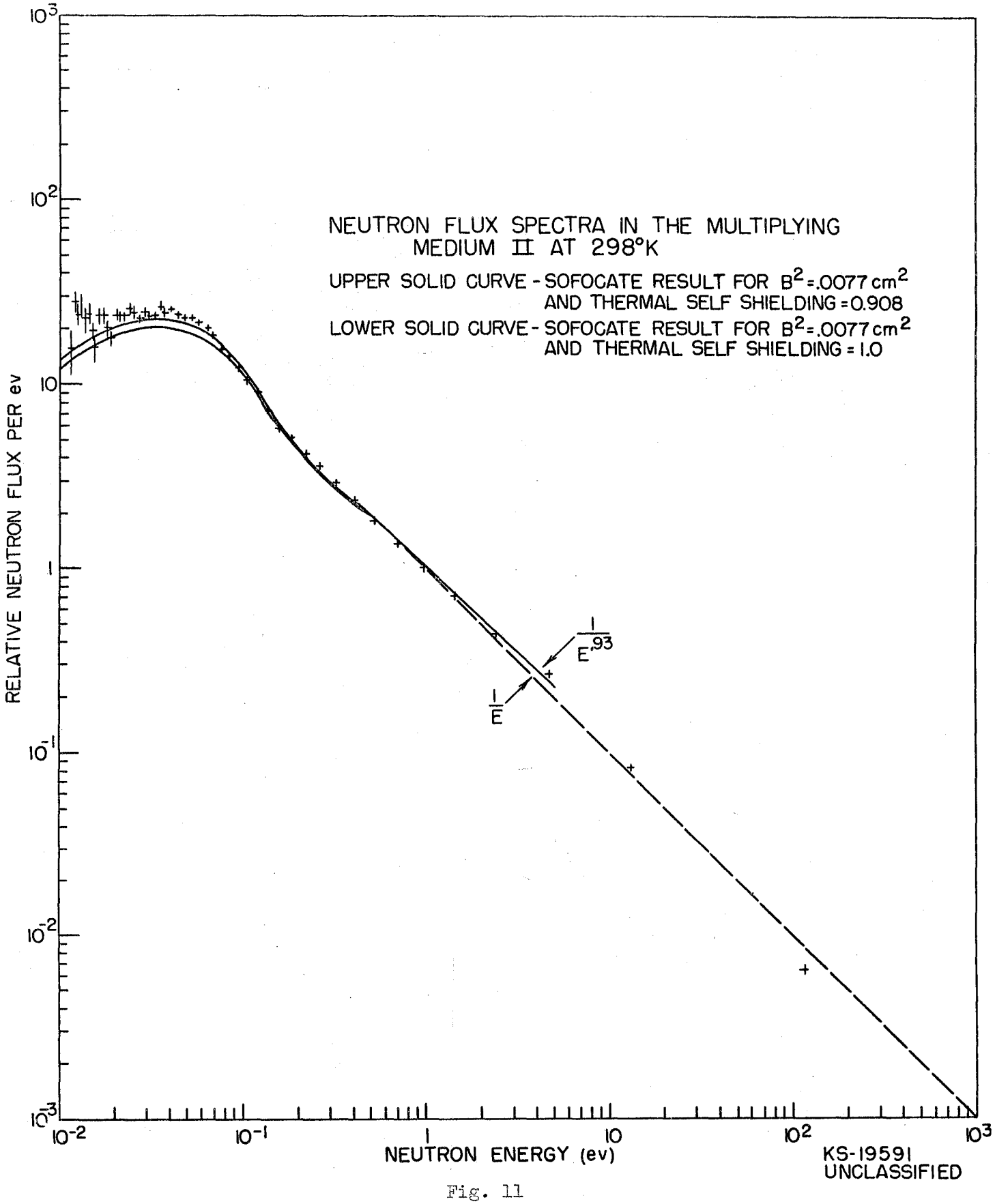
NEUTRON FLUX SPECTRA IN THE MULTIPLYING MEDIUM II AT 298°K
UPPER SOLID CURVE - SOFOCATE RESULT FOR B² = .0077 cm² AND THERMAL SELF SHIELDING = 0.908
LOWER SOLID CURVE - SOFOCATE RESULT FOR B² = .0077 cm² AND THERMAL SELF SHIELDING = 1.0
RELATIVE NEUTRON FLUX PER ev
NEUTRON ENERGY (ev)
1/E^.93
1/E
KS-19591
UNCLASSIFIED

Fig. 11

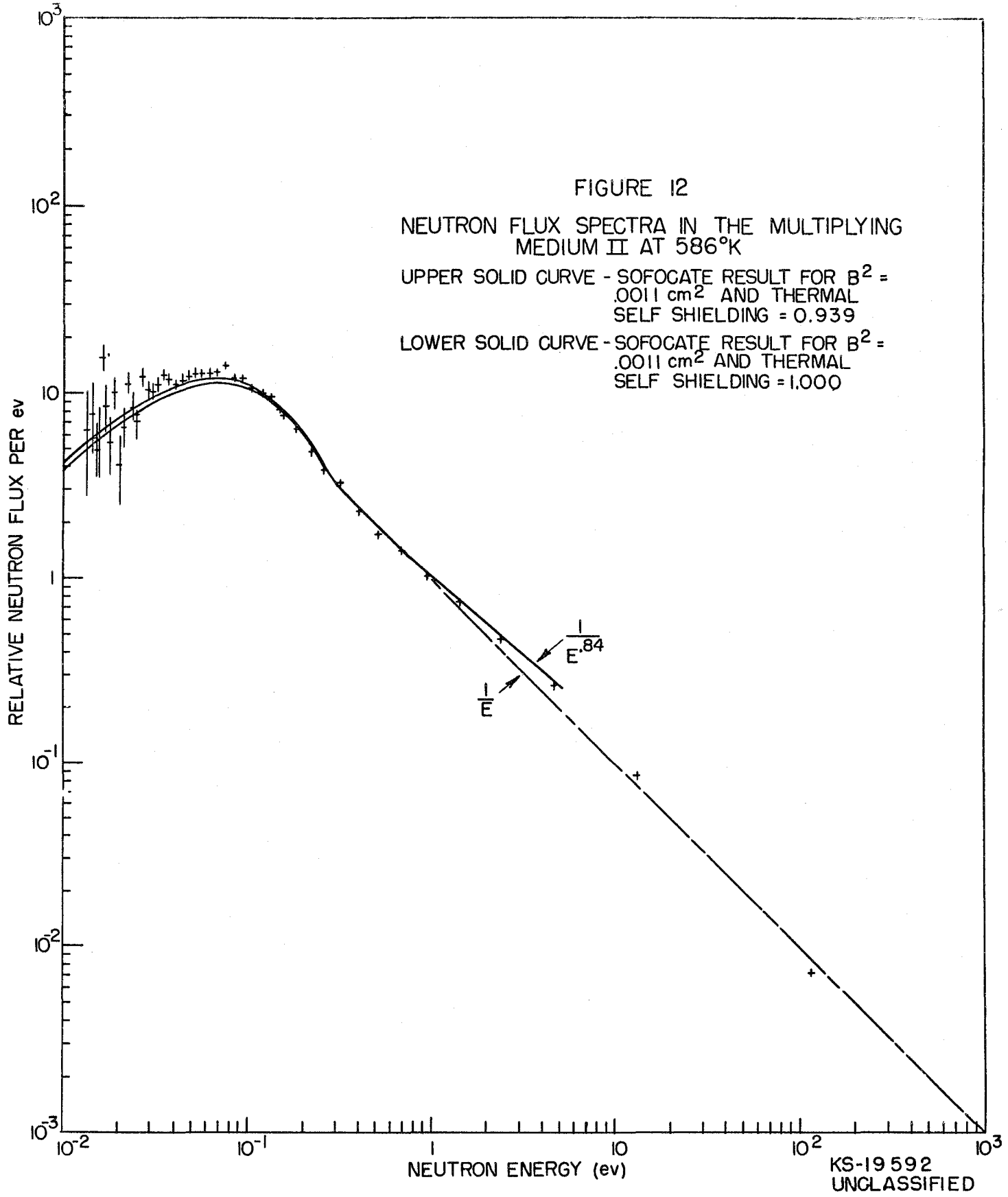
FIGURE 12
NEUTRON FLUX SPECTRA IN THE MULTIPLYING MEDIUM II AT 586°K
UPPER SOLID CURVE - SOFOCATE RESULT FOR B^2 = .0011 cm^2 AND THERMAL SELF SHIELDING = 0.939
LOWER SOLID CURVE - SOFOCATE RESULT FOR B^2 = .0011 cm^2 AND THERMAL SELF SHIELDING = 1.000
$\frac{1}{E^{.84}}$
$\frac{1}{E}$
RELATIVE NEUTRON FLUX PER ev
NEUTRON ENERGY (ev)
10^3
10^2
10
1
10^{-1}
10^{-2}
10^{-3}
10^{-2}
10^{-1}
1
10
10^2
10^3
KS-19592
UNCLASSIFIED

Least Squares $\frac{\sigma_{\perp}}{E^X}$ Fit From $E_1 \leq E \leq 4.7$ ev.

Source	T °K	E_1 ev.	X
Matrix I	298	.265	.97
Matrix I	586	.405	.96
Matrix II	298	.265	.93
Matrix II	586	.405	.84

Figure 13

COMPARISON OF THEORY WITH EXPERIMENT

Spectra were calculated for each source medium using the SOFOCATE code.[2] Calculations were performed for moderator temperatures corresponding to the measured temperatures used in the spectrum measurements, namely 298°K and 586°K.

Included in the code is the leakage term DB^2 to correct Σa in a finite medium. For the hot and cold matrix cases, the appropriate measured value of B^2 was used in the calculations. Since $\Sigma a\ (Eo) >> DB^2$ for the multiplying media, this corresponds to a small correction (~1%) to the spectra and the calculated spectra will be insensitive to errors in the measurements of $B^2(E)$. In addition, the calculation treats only an equivalent homogenous assembly having the same average composition as the heterogeneous experimental assembly. This approximation is good over most of the energy range except below 0.2 ev where self shielding effects would tend to reduce the effective homogeneous Σa value obtained from the material composition. A self shielding factor was determined for the mean fuel Σa corresponding to the hardened spectrum using Bohl's results for a repeating slab array.[7] The self shielding factors, which were then applied through the thermal range in calculations, are indicated on the plotted results.

In the case of pure water, Σa is not large compared to DB^2 over the entire energy range of interest. The calculated spectrum will then be very sensitive to $B^2(E)$ as well as $D(E)$. For the particular water source used, it is quite likely that the fast leakage is different from the thermal leakage. Since the measurement of $B^2(E)$ was not available, the thermal leakage correction was not made to Σa in the pure water cases.

The room temperature water spectra are shown in Figure 7. The good agreement between the measured spectrum in a finite medium and the infinite medium calculated spectrum is probably fortuitous. From Figure 6, it is seen that the leakage effect at 0.025 ev could be appreciable (~30%). The leakage effect at 1 ev is even greater. The water spectra at 586°K is shown in Figure 8. Here the measured thermal flux seems to be low by 50%. This is probably accounted for by the difference between the thermal leakage and fast leakage effects. The shape of the measured hot and cold water spectra in the joining energy region exhibit no large discrepancies from the calculated infinite medium spectra.

Figure 9 shows the room temperature spectra in the multiplying medium I. The lower solid curve is the calculated spectrum assuming a self shielding factor of 1.0. The upper curve is for a self shielding factor of 0.898. Above the thermal energy region, the agreement is excellent. In the thermal region, the measured points lie between the two calculated curves. Apparently, an average self shielding factor is not adequate to describe the effect and perhaps one should use an energy dependent correction here. No significant deviations due to chemical binding effects appear in the measured spectrum.

Figure 10 shows the spectra in the multiplying medium I at 586°K. The agreement is not as good as in the room temperature case, but it is still good. Again, the shape of the curve above the thermal energy range is in excellent agreement with calculations.

Figure 11 shows the spectra in the multiplying medium II at room temperature. The data appear to deviate significantly above the dE/E spectrum above 0.5 ev. The

SOFOCATE code now indicates an appreciable dip in the spectrum at around 0.3 ev below the slowing down spectrum extended back down to lower energies. The measured points do not appear to follow this dip. In the "thermal" region, the measured SPECTRA seems to be consistently higher than the calculated spectra.

Figure 12 shows the spectra in the multiplying medium II at 586°K. The deviation from dE/E is greater as expected and the discrepancy in the thermal region is about the same as the previous case.

It is planned to extend the calculations in two ways. The upper limit on the SOFOCATE calculation will be increased to 5 ev to include the U^{235} resonance effects of the slowing down spectra. The self shielding factor as a function of energy will be included in the code to see if the deviation in the thermal region can be accounted for.

The general agreement over the entire energy range of interest is consistent with Poole's results.[3,4] However, Poole's results indicated a consistent deviation in the joining region between the slowing down spectra and the "hardened" thermal spectra. The present results indicate no deviations in this region. It is to be noted that the count rate increases sharply in this region and that the resolution correction for our equipment can be as large as 20% in the case of water and 6% in the case of the matrix. Higher resolution would tend to reduce the correction and thus the uncertainty associated with the measured point. Since Poole did not indicate making a resolution correction, his discrepancies in this region may be explained in part as being due to resolution effects.

A comparison between the measured and calculated spectra can be made by using each spectrum to calculate the average cross section of a 1/v absorber for the overlapping energy range, 0.01 to 1.0 ev. One can form the ratio

$$\left(\frac{\bar{\sigma}}{\sigma_o}\right) = \frac{E_o^{1/2} \int_{.01}^{1} E^{-1/2} \; \phi(E) \; dE}{\int_{.01}^{1} \phi(E) \; dE}$$

where σ_o is the cross section at $E_o = 0.0252$ ev. Figure 14 contains the results of these calculations and the estimated errors of this ratio. The error in the ratio using the measured spectrum is based on counting statistics, the error in the energy calibration and the error in the transmission correction for materials in the beam. The error in the ratio using the calculated spectrum is based on the uncertainties in the composition cross sections and on the errors in the measured temperatures of the media.

As indicated from the plotted results, the agreement between the experimental value and the calculated value is good in each case to within about 4% or better.

CONCLUSIONS

Chemical binding effects on the spectra in water moderated reactors appear to be extremely small. Consequently, spectra as calculated by the SOFOCATE code should be quite accurate for media with $\Sigma_a/\xi\Sigma_s \approx 0.6$. The average cross sections that are used in reactor calculations obtained with the code should be good to within 4%.

REFERENCES

1. Wigner, E. P. and J. E. Wilkins, Jr., "Effect of the Temperature of the Moderator on the Velocity Distribution of Neutrons with Numerical Calculations for H as Moderator," AECD-2275 (1944).

2. Amster, H. and R. Suzrez, "The Calculation of Thermal Constants Averaged over a Wigner-Wilkins Flux Spectrum: Description of the SOFOCATE Code," WAPD-TM-39 (1957).

3. Poole, M. J., "Measurements of Neutron Spectra in Moderators and Reactor Lattices-I Aqueous Moderators," Journal of Nuclear Energy, Vol. 5, Nos 3/4 (1957).

4. Amster, H. J., "The Wigner-Wilkins Calculated Thermal Neutron Spectra Compared with Measurements in a Water Moderator," Nuclear Science and Engineering, Vol. 3, p. 394 (1957).

5. Stone, R. S. and R. E. Slovacek, "Reactor Spectrum Measurements using a Neutron Time-of-Flight Spectrometer," KAPL-1499 (1956).

6. Wade, E. J. and D. S. Davidson, "Transistorized Time of Flight Analyzer with Ferrite Core Memory," IRE Convention Record (March, 1957).

7. Bohl, L. S., "Application of the Variational Method to the Calculation of Flux Ratios in Repeating Slab Arrays," KAPL-M-LSB-2 (1957).

AVERAGE $1/v$ CROSS SECTIONS

$$\left(\frac{\bar{\sigma}}{\sigma_o}\right) = \frac{E_o^{1/2} \int_{.01}^{1} E^{-1/2}\, \phi(E)dE}{\int_{.01}^{1} \phi(E)\, dE}$$

Source	T °K	$\Sigma_a(E_T)$ cm^{-1}	Σs cm^{-1}	$\beta\gamma$	$\left(\frac{\bar{\sigma}}{\sigma_o}\right)_{exp.}$	$\left(\frac{\bar{\sigma}}{\sigma_o}\right)_{cal.}$
MATRIX I	298	.193	.667	.289	.565±.004	.587±.009
MATRIX I	586	.138	.461	.298	.458±.006	.479±.006
MATRIX II	298	.406	.747	.543	.500±.002	.489±.009
MATRIX II	586	.290	.518	.559	.419±.003	.413±.006

Figure 14

Paper IV-E

MEASUREMENT OF LOW ENERGY NEUTRON SPECTRA USING A PULSED NEUTRON SOURCE

J. R. Beyster
General Atomic

Measurement of Low Energy Neutron Spectra Using a Pulsed Neutron Source

J. R. Beyster
General Atomic
San Diego, California

Abstract

A program of measurements of low energy neutron spectra in moderators and typical sections of reactor cores is being planned to begin at General Atomic this summer. This work will use the new high current 30 Mev electron linear accelerator to produce a very intense pulsed neutron source. The initial measurements of spectra will be done on hydrogen moderated systems both poisoned and unpoisoned. The characteristics of the linear accelerator and supporting facilities will be described. The general features of the experimental program will be discussed and the two experimental techniques to be used in performing the spectral measurements will be outlined.

Measurement of Low Energy Neutron Spectra Using a Pulsed Neutron Source

By

R. S. Stone - J. R. Beyster

INTRODUCTION

Clearly, one of the most outstanding problems remaining in the field of reactor physics is that of understanding neutron thermalization. Not only must one acquire an understanding of the fundamental physics of how slow neutrons interact with a nucleus, but proven techniques for using these fundamental data to make reliable predictions of reactor behavior must continue to be developed. Unfortunately at this point in time, our ability to predict energy spectra in the thermal neutron range is limited to the calculations for the infinite homogeneous system. This limitation is imposed partly by the complexity of many physical systems, the complexity of the mathematics required to describe these systems, the lack of accurately measured fundamental constants needed in the mathematical analysis, and more important, the lack of definitive experiments which can serve to check theoretical predictions and point the direction for further exploration.

A year ago it seemed to us that an integrated experimental and theoretical program should be started which would have as its objectives the extension of our present knowledge on neutron thermalization and the development of generally applicable techniques for predicting these spectra. In part, to provide a versatile experimental facility for this work and in part, to satisfy other research needs of the laboratory, a high current traveling wave electric linear accelerator was purchased by General Atomic and is in the final stages of testing at the Applied Radiation Corporation in Walnut Creek, California.

II. ACCELERATOR AND FACILITIES

The characteristics of the General Atomic linear accelerator will be as follows: variable energy from 2 to 32.5 Mev; peak currents of about 0.3 amperes; pulse width variable from 0.5 microseconds to 15 microseconds, and repetition rates variable from 7.5 pulses per second to 720 pulses per second. The electron energy for maximum efficiency is about 18 Mev at which energy 5 Kw of beam power will be delivered.

Slide 1 is a line drawing of the accelerator indicating the major components. The injector for the accelerator is a high current version of the Stanford pulsed anode injector. A klystron cavity bunches the beam and phases it properly for injection into the first section of wave guide. Two VA820 klystrons will supply 5 MW peak power to the two 6' sections of wave guide used for accelerating the electrons. The machine has been designed so that it can be easily expanded, when our program requires, by adding higher peak power klystrons, more sections of wave guide, or increased average power capability.

Slide 2 is a plan view of the buildings we have erected to house our accelerator in San Diego. The accelerator is located at one end of the earth-shielded underground vault. The experimental set up area where the various assemblies will be constructed is separated by a thick concrete block wall from the accelerator room. The accelerator room will be able to hold additional sections of accelerator and will also house various switching magnets to be used for piping the beam to the targets. Water cooled vacuum plumbing must be used throughout the entire accelerator and target systems. Initially, we will place our neutron target at the intersection of the first two drift tubes which lead to a large outdoor area for the detector stations for time-of-flight experiments. The underground building is located about 100 feet from the General Atomic critical facility and it is planned to pipe the electron beam to this area for use with critical or nearly critical assemblies. The first neutron target will be water cooled bismuth to minimize the radiation hazard in handling the source after continued use. The accelerator control building is unshielded and provides area for the accelerator console, accelerator power distribution system, and the experimental electronics required for the research programs on the machine.

III. RESEARCH PROGRAMS

A research program of major importance on our linear accelerator will be the study of thermal spectra which we will conduct with the support of the AEC Division of Reactor Development. First let us briefly review the experimental techniques available for these investigations.

Existing Experimental Techniques

In recent years, two time-of-flight techniques have been developed for the detailed study of low energy neutron spectra and the dependence of these spectra on temperature, composition, and geometry of reactor cores.

Poole[1] at Harwell has developed a method using a pulsed accelerator as a source of neutrons. With this technique, a series of thermal spectrum measurements have been made on light water moderated, boron loaded assemblies. These data have been compared with spectra calculated by Amster[2] using a formalism developed by Wigner and Wilkins[3]. In general, these comparisons are extremely good. However, there may be some discrepancy in the range from 0.1 to 0.3 electron volts where the slowing down spectrum joins the thermal or low energy spectrum. In this region, Poole's data consistently indicate a relatively higher flux than the Wigner-Wilkins theory would predict.

A second method of measuring spectra has been developed by Stone and Slovacek[4]. This method utilizes a mechanical shutter to chop a neutron beam which is emerging from a subcritical assembly of the desired composition. The assembly is excited by fast neutrons derived from a fission plate mounted in a reactor thermal column.

In their studies of pure water and of nearly homogeneous light water moderated multiplying assemblies, the spectra obtained by Stone and Slovacek do not evidence the discrepancy noted by Amster in Poole's experiments. There are, however, experimental uncertainties associated with the lack of homogeniety in the multiplying assemblies and in the effects of thermal leakage associated with the non-multiplying assemblies.

Initial Investigations

Initially, our interest in the program will be devoted to the study of homogeneous light water moderated assemblies with varying amounts of 1/v absorber added in the form of boric oxide. This type of assembly best satisfies the conditions outlined by Wigner and Wilkins in their thermal spectrum calculations.

The neutron spectrum emergent from a source tube inserted in this assembly will be measured by the method outlined by Poole and also by the method outlined by Stone and Slovacek. In this way, any systematic error that may be inherent to either method will be isolated.

A flexible experimental arrangement for these investigations has been designed so that all geometrical factors which might conceivably affect the measured neutron spectra can be varied. For example, assembly tank size and shielding and neutron source location can be altered drastically.

In the pulsed source method, the linear accelerator will irradiate an experimental assembly with a burst of fast neutrons, these neutrons will be slowed down and will establish a fundamental mode distribution. Neutrons emitted in the solid angle subtended by the BF_3 detector bank at the end of the source tube will be detected with a time delay after the fast burst. If the flight path is sufficiently long so that the neutron flight time is long compared to the neutron slowing down time in the medium, then the delay time between fast burst and neutron detection provides a measure of neutron energy. If one counts the number of neutrons as a function of time of arrival at the detector and makes corrections for relative detector efficiency as a function of energy, one can then obtain a measure of the spectral distribution of neutrons at the bottom of the source tube.

In the chopper experiment, the linear accelerator will be pulsed at a high repetition rate to provide a maximum average neutron flux in the experimental assembly. The same source tube and detector will be used; however, a neutron chopper will be inserted between the exit aperture of the source tube and the detector and will be run asynchronously with the accelerator. Present thinking indicates that we might be able to use the same flight path as with the pulsed source method. Neutron energies in this series of experiments will be determined from a measurement of the time required for a neutron to traverse the distance from the shutter to the detector. After making corrections for energy dependent shutter transmission and detector efficiency, one can obtain a measure of the neutron spectrum at the source point within the medium.

Direction of Future Experiments

The experiments just discussed should establish the validity and compatability of the two experimental techniques developed to date. Once this is done, there are a number of interesting experiments that will be undertaken.

Perhaps one of the more interesting is a study of the time dependence of the establishment of the thermal neutron spectra in a moderating medium. We feel that it should be possible to perform this experiment by using a combination of the two experimental methods previously outlined. If we use a graphite system, then the slowing down time is sufficiently long so that our instrumentation will be able to detect the growth of the thermal spectra after a fast burst. For this experiment, the rotating shutter will

be operated in phase synchronism with the accelerator. A fast neutron burst can be introduced into the assembly and after a predetermined time, the neutron shutter will be opened. The spectrum of neutrons transmitted by the shutter at this time can be determined by the time of flight technique.

If there exists a range in time after the burst where the observed spectrum varies slowly with time, then it should be possible to obtain a large increase in counting efficiency by operating the machine and chopper synchronously. We calculate that for some experiments one can gain between a factor of two and ten in intensity by this new method. This is an important point when we consider the large cost of obtaining increased intensity by building larger accelerators.

Another problem that we plan to investigate experimentally is the spectral variations at interfaces between different media and also between media at different temperatures. This general problem has only recently been attacked theoretically by Kottwitz at Hanford and is worthy of much careful experimental study, since these situations are characteristic of many encountered in actual reactor design.

IV. CONCLUSION

Clearly, experimental and theoretical work on neutron spectra and the effect of spectra on reactor behavior is still in its infancy. At General Atomic, we feel that a fundamental investigation of these subjects will provide definitive experiments to check the theoretical work that has been done. The development of newer experimental techniques promises to provide a firm base for further theoretical work and basic understanding of reactor processes.

References

[1] Poole, M. J. - NUCLEAR ENERGY, Vol. 5, p 325 (1957)

[2] Amster, H. J. - NUCLEAR SCIENCE AND ENGINEERING, Vol. 2, p 394 (1957)

[3] Wigner, E. P. and Wilkins, J. E. Jr. - AECD 2275

[4] Stone, R. S. and Slovacek, R. E. - KAPL 1499

ORNL-2739
Physics and Mathematics
TID-4500 (14th ed. Rev.)

INTERNAL DISTRIBUTION

1. Biology Library
2. Health Physics Library
3-5. Central Research Library
6. Reactor Experimental Engineering Library
7-63. Laboratory Records
64. Laboratory Records, ORNL, R.C.
65. A. M. Weinberg
66. E. P. Blizard
67. R. R. Coveyou
68. R. A. Charpie
69-78. L. Dresner
79. W. K. Ergen
80. W. H. Jordan
81. G. Leibfried
82. A. Simon
83-84. W. Hafele
85. F. C. Maienschein
86. G. deSaussure
87. E. G. Silver
88. R. W. Peelle
89. W. Zobel
90. R. Gwin
91. D. Magnuson
92. A. D. Callihan
93. C. Preskitt
94. E. Halbert
95. F. S. Alsmiller
96. J. L. Fowler
97. J. A. Harvey
98. F. L. Keller
99. C. D. Zerby
100. D. K. Trubey
101. S. K. Penny
102. E. Guth
103. W. E. Kinney
104. M. E. LaVerne
105. J. G. Sullivan
106. J. H. Marable
107. R. B. Murray
108. T. A. Welton
109. S. H. Hanauer
110. J. T. Thomas
111. R. L. Macklin
112. P. Kasten
113. S. Jaye
114. W. Nestor
115. M. J. Skinner
116. A. M. Perry
117. C. P. Keim
118. P. M. Reyling
119. ORNL - Y-12 Technical Library Document Reference Section

EXTERNAL DISTRIBUTION

120. Division of Research and Development, AEC, ORO
121-129. Brookhaven National Laboratory (Attn: Sophie Oleksa, N. Corngold, I. Kaplan, H. Kouts, W. L. Whittemore, I. Pelah, H. Palevsky, C. Eisenhauser, and D. J. Hughes)
130. University of California Radiation Laboratory, Berkeley (Attn: H. L. Reynolds)
131-133. General Electric, Richland (Attn: E. D. Clayton, H. Neumann, and P. Gast)
134-135. General Electric, Schenectady (Attn: K. Cohen and H. Hurwitz)
136. General Electric, Cincinnati (Attn: J. W. Morfitt)
137. General Electric, San Jose (Attn: P. Greebler)
138. Babcox and Wilcox Company (Attn: M. C. Edlund)
139-142. Knolls Atomic Power Laboratory (Attn: F. J. Habetler, T. M. Snyder, T. Krieger, and R. Slovacek)
143-144. Westinghouse Electric Corporation, Pittsburgh (Attn: A. F. Henry and S. Krasik)
145-150. General Atomic, San Diego (Attn: M. Nelkin, A. McReynolds, L. W. Nordheim, F. Adler, J. Sampson, and D. Stone)
151. Phillips Petroleum Company, Idaho Falls (Attn: W. F. Nyer)

152-154. Los Alamos Scientific Laboratory (Attn: H. Paxton, J. Griffin, and G. Bell)
155-156. U.S. Atomic Energy Commission, Washington (Attn: R. Radowsky and I. F. Zartman)
157-162. Argonne National Laboratory (Attn: B. I. Spinrad, F. W. Thalgott, R. Avery, C. N. Kelbar, D. Shaftman, and H. Greenspan)
163. Princeton University (Attn: E. P. Wigner)
164-165. Nuclear Development Corporation of America (Attn: H. Goldstein and J. E. Wilkins, Jr.)
166. Jet Propulsion Laboratory (Attn: R. V. Meghreblian)
167. New York University (Attn: R. D. Richtmyer)
168-782. Given distribution as shown in TID-4500 (14th ed.) under Physics and Mathematics Category (75 copies - OTS)